Interconnected Systems with Stochastic Communication

Decomposition Methods for Analysis and Synthesis

Vom Promotionsausschuss der
Technischen Universität Hamburg

zur Erlangung des akademischen Grades

Doktor-Ingenieur (Dr.-Ing.)

genehmigte Dissertation (Monografie)

von
Christian Hespe

aus
Buchholz i.d.N.

2025

Erster Gutachter
Prof. Dr. Herbert Werner
Institut für Regelungstechnik
Technische Universität Hamburg

Zweiter Gutachter
Prof. Dr. Paolo Massioni
Ampère Laboratory – CNRS
INSA Lyon, Frankreich

Vorsitzender des Prüfungsausschusses
Prof. Dr.-Ing. Gerhard Bauch
Institut für Nachrichtentechnik
Technische Universität Hamburg

Tag der mündlichen Prüfung: 20.05.2025

doi: https://doi.org/10.15480/882.15421
isbn: 978-3-8439-5631-4
https://orcid.org/0000-0001-5772-9044

Acknowledgements

The present thesis is the product of four years of work at the Institute of Control Systems at Hamburg University of Technology, made possible by the support and encouragement of many colleagues and friends. First and foremost, I am grateful to my Ph.D. advisor Prof. Dr. Herbert Werner for guiding me throughout the process and introducing me to his way of doing research. I thoroughly enjoyed the weekly seminars and frequent workshops – especially during the maths-heavy sections of the books we read – and honour the academic freedom I was given to pursue my ideas. My sincere thanks go to Torsten Lüthje, Gerald Gläser, and Steffen Rehders for their support during my Bachelor's and Master's studies, and sparking my interest in hobby electronics. Moreover, I would like to acknowledge the late Prof. Dr. Karl Kießwetter, whose role in founding the Talentförderung Mathematik e.V. provided me with an early appreciation for the beauty and rigour of mathematical problem-solving.

My four years at the institute were greatly enriched by colleagues to whom I am deeply thankful, not only for their professional support but also for the personal connections we shared. I owe special thanks to Adwait for our lively puzzle exchanges and the many fascinating conversations we had, not just about control theory but also mathematics in general, and Philipp for the conferences and trips we experienced together. Furthermore, I would like to acknowledge the invaluable help that Patrick provided with organizational matters and teaching responsibilities, and the enjoyment that Lennart and Jannis brought to our years of shared teaching. Dirk deserves a shout-out for his eagerness in electronic tinkering and very helpful suggestions while preparing my own circuits, and I appreciate how Bindu, Prima, Shuyuan, and Henrique were always keen to help whenever asked – thank you!

I am especially grateful to my friends and family who supported me throughout my Ph.D. Thank you to Denise, Swantje, Philipp, Fabian, and Felix for proofreading my thesis and providing me with incredibly helpful suggestions, and Freddi for bolstering my creativity through his numerous ideas. Thank you also to Rike for her relentless support, honest opinions, and constant encouragement during the preparation for my defence. Even more so, I would like to express my deepest gratitude towards my parents Christiane and Heinz-Dieter, who have stood behind me at all times and provided me with the basis to follow my ideas. Their way of critical thinking and attention to detail has formed the foundation for my studies and Ph.D. Moreover, I am thankful to my brother Steffen for his support and knowing I can always count on him. Finally, I would like to wholeheartedly thank my grandparents Heinrich and Marianne for their honest and unbroken interest in my work, inspiring me in a way only they could have. You all made this thesis come to what it is!

Summary

In the context of control for structured large-scale dynamic systems such as spatially-interconnected or multiagent systems, reducing complexity is essential for the development of viable solutions. For this reason, such control problems are generally approached in a structure-exploiting distributed fashion that relies on information exchange between subsystems, *e.g.* through a wireless communication network. However, despite the inherently random nature of communication networks, the majority of existing approaches treats the resulting interconnection in an idealized and deterministic manner, potentially jeopardizing the stability and performance of the closed loop. Hence, the focus of this dissertation is on studying and developing control schemes that remain applicable to structured large-scale systems while taking random packet dropouts into account.

A central contribution of the thesis is its extension of the decomposable systems framework from linear time-invariant to stochastically switched systems, giving rise to decomposable Markov jump linear systems which capture both the interconnection structure of the dynamic system and the probability distribution of the communication links. Importantly, these systems facilitate the decoupling of their corresponding analysis conditions. Under the assumption that all packet dropouts are independent and identically Bernoulli distributed with homogeneous probability, this results in a scalable linear matrix inequality based mean-square stability test. Similarly, we obtain scalable upper bounds on the H_2- and H_∞-norm that are applicable to arbitrarily large networks and stay valid if the interconnection topology is uncertain or time-varying. In consequence, the approach can be used to synthesize distributed state- and output-feedback controllers which are tuned with respect to the loss distribution and are empirically demonstrated to partially compensate for the performance degradation incurred due to the stochastic switching.

Subsequently, the thesis investigates how the above assumptions can be relaxed while retaining the essential scalability property. By applying tools from robust control, namely linear fractional transformations and the full block S-procedure, the conditions are first extended to allow for uncertain transmission probabilities, before an alternative decomposition is employed to cover heterogeneous packet loss distributions. Moreover, a geometric argument is invoked to prove that the stability and performance analysis is robust to small spatio-temporal dependencies between the transmission links, and therefore encompassing a wide range of probability distributions.

Finally, it is examined how communication dropouts interact with aperiodic sampling that is introduced by using event-triggered control schemes. In particular, a discussion around different architectures demonstrates that the indispensable controller-side buffer induces temporal dependencies and inhomogeneities even if the underlying loss process is entirely independent and homogeneous. As such, the previously derived analysis and synthesis techniques become inapplicable.

Contents

1 Introduction

Over the past decades, technological advances have led to an ever-growing prevalence of structured large-scale control systems. In particular, this includes the class of interconnected systems (IS), which are dynamic systems composed of small-scale subsystems. IS take a variety of shapes: the subsystems can be dynamically coupled as for spatially-interconnected systems (D'Andrea & Dullerud, 2003) or coupled only through their mission, as is typically the case in multiagent systems (MAS) (Mesbahi & Egerstedt, 2010); the interconnection structure can be constant or time-varying; the subsystems can be linear or nonlinear, homogeneous or heterogeneous. Examples of the first kind are spatially discretized distributed-parameter systems that are described by partial differential equations, *e.g.* for temperature or vibration control (Schug & Werner, 2017), the latter on the other hand are obtained among others for cooperative multi-vehicle systems (Ren & Beard, 2008).

One of the most significant challenges in controlling large-scale systems is their intrinsic complexity. Featuring a high dynamic order and many inputs and outputs, such systems are often placed beyond the limits of classical monolithic control approaches. Instead, distributed and decentralized schemes as illustrated in Fig. 1.1 become the methods of choice. In contrast to centralized techniques, these architectures possess local subsystem controllers rather than a global entity that controls the entire system simultaneously, facilitating the decomposition of complexity into smaller components (Langbort et al., 2004). However, whereas decentralized controllers are exclusively linked to their respective subsystem, distributed controllers are additionally coupled among each other, thereby allowing for greater flexibility and potentially superior performance. A fundamental issue for distributed schemes is hence the exchange of information across the subsystems and their associated controllers. In many instances, this necessitates the establishment of a communication network between the controllers in either broadcast or peer-to-peer fashion, although remote sensing is a viable option for certain scenarios (Fax & Murray, 2004).

The core issue of scalability in IS goes beyond the controller implementation, but needs to be considered already in the analysis and synthesis phase. Applied naively, standard techniques result in a quadratic or worse growth in computational complexity

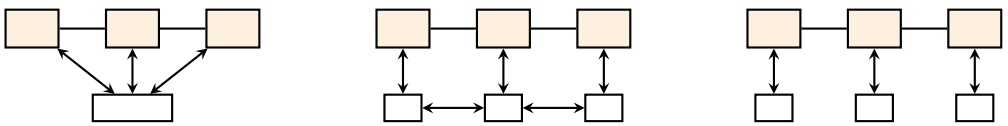

(a) Centralized (b) Distributed (c) Decentralized

Figure 1.1.: Comparison between centralized, distributed, and decentralized control

with respect to the number of subsystems (Massioni & Verhaegen, 2009), and, as to be seen in Chapter 3, some cases are even subject to an exponential growth because of the curse of dimensionality. For this reason, the last decades have brought countless specialized approaches for large-scale networked systems, some general and some for specific scenarios, see *e.g.* the books by Bullo (2018) and Mesbahi and Egerstedt (2010). The most important concepts are reviewed in the following.

1.1. Control of Large-Scale Interconnected Systems

As outlined above, the information exchange between subsystems and controllers plays a central role in the context of large-scale IS. Nonetheless, most approaches neglect this essential process in its entirety, simply assuming that information is available throughout the system instantly and without alteration. The section is therefore split in two: First, we discuss the idealized scenario *without* detrimental communication effects, before considering approaches that take network deficiencies into account.

1.1.1. The Idealized Case

A classic and widely applicable problem for homogeneous IS with integral action is to reach subsystem consensus. Starting from arbitrary initial conditions, the task is to drive the subsystems into agreement, *i.e.* to ensure that either their states or outputs converge to a common point (Tsitsiklis et al., 1986). One particular instance of this is the *first-order consensus problem*, in which all subsystems are described by dynamically-decoupled linear first-order integrators. The problem can be solved in a distributed manner by applying a localized averaging algorithm: Introducing an interconnection topology between the subsystems in form of a mathematical graph, each subsystem exchanges its opinion (or in system theoretical terms its state) with its local neighbourhood, *i.e.* other subsystems it is directly adjacent to, and updates its opinion to adhere closer to the neighbourhood average. Most commonly, the averaging step is performed as an arithmetic mean, in which case it is possible to prove convergence for both continuous-time (Olfati-Saber & Murray, 2003) and discrete-time (Olfati-Saber et al., 2007) algorithms by application of facts from algebraic graph theory. However, there also exist nonlinear updating schemes, *e.g.* choosing the local extremum as in maximum consensus (Nakamura et al., 2018), gradient flows that achieve finite-time convergence (Cortés, 2006), or multiagent flocking based on artificial potential fields (Leonard & Fiorelli, 2001; Olfati-Saber, 2006), which are advantageous in specific scenarios but more difficult to analyse than linear average consensus.

Despite its simplicity, the consensus problem forms a basic building block for many applications in distributed control (Murray, 2007). An immediate example are formation control tasks for which groups of agents have to be brought into a prespecified spatial configuration. Depending on the requirements, the resulting solution can either be cooperative as discussed in (Olfati-Saber et al., 2007), placing the higher-order agent dynamics directly in the networked feedback loop, or decoupled in the sense of the information flow filter presented by Fax and Murray (2004), combining the interconnected consensus algorithm with agent-level reference tracking controllers. Additional examples include trajectory generation for possibly nonlinear vehicle models (Cortés

& Egerstedt, 2017), distributed state estimation and filtering (Olfati-Saber, 2005), and distributed optimization algorithms (Sundararajan et al., 2020; Tsitsiklis et al., 1986).

In contrast to the first-order consensus problem, the analysis of cooperative control schemes involving higher-order subsystem dynamics is more complex. Approached naively, the whole IS has to be analysed at once, leading to an at least quadratic growth in complexity and thus intractability for sufficiently large systems. The issue can be alleviated by adopting the methodology put forth by Pecora and Carroll (1998) for the synchronization of coupled oscillators. They show that the problem can be cast equivalently as the stability of a collection of decoupled *transverse modes*, which have the same size as a single oscillator. Similarly, Fax and Murray (2004) demonstrate that *modal subsystems*, *i.e.* decoupled subsystem models that are scaled by the eigenvalues of the interconnection topology, can be employed to analyse the convergence of cooperative formation control tasks. In both instances, the techniques transform an initially large and monolithic system analysis problem into multiple small and, crucially, decoupled problems, resulting in a *linear* growth in complexity with respect to the number of subsystems and hence a significant improvement compared to any direct analysis. Moreover, in many cases the complexity can be further reduced by adopting a robust problem formulation, rendering the analysis independent of the number of subsystems (Pilz et al., 2009). A graphical variant of such a robust scheme has already been reported in the initial work of Pecora and Carroll (1998).

Originally presented for linear (or linearized) IS with constant topology and static interconnections, the approaches of Fax and Murray (2004) and Pecora and Carroll (1998) can be generalized to broader classes of systems. For example, Pilz et al. (2009) apply the technique to linear IS with uncertain or switching topologies, Seyboth et al. (2012) present an extension for linear parameter-varying subsystems, and Popov and Werner (2012) consider interconnections with transmission delays. Conversely, the methods above rely on the graph Laplacian to represent the interconnection topology in the system dynamics and are thus only applicable in specific circumstances, *e.g.* dynamically decoupled MAS with relative sensing but not spatially-interconnected systems as considered by D'Andrea and Dullerud (2003).

As such, other techniques suitable for generic IS have been developed. First and foremost, there are the approaches of Fang and Antsaklis (2008) and Langbort et al. (2004) that are based on explicitly modelling the edge-wise interconnections between subsystems. Since these approaches do not take advantage of the network topology, they are straightforward to apply to heterogeneous subsystems and non-ideal interconnections but scale with the number of communication links, which is typically significantly larger than the number of subsystems for well-connected graphs. In contrast, the framework of *decomposable systems* proposed by Massioni and Verhaegen (2009, 2010) is a direct extension of Fax and Murray's (2004) decoupling technique to general IS. Despite replacing the graph Laplacian with a generic diagonalizable pattern matrix, they demonstrate that decoupling into modal subsystems remains viable, maintaining a linear growth in complexity with respect to the number of subsystems. Furthermore, Massioni and Verhaegen (2009) broaden the scope of the analysis problem, moving from pure stabilization to H_2- or H_∞-optimal controller synthesis. However, the powerful structure-based decomposition comes at the cost of a reduced flexibility, limiting its direct application to homogeneous subsystems with ideal interconnections. In order to consider heterogeneous subsystems (Hoffmann et al., 2014; Massioni, 2014), linear

parameter-varying dynamics (Hoffmann et al., 2013), or uncertain interconnections (Eichler et al., 2013), it is therefore necessary to employ an indirect multiplier-based decomposition.

1.1.2. Stochastic Communication Deficiencies

In order to implement the schemes discussed above in practice, it is crucial to exchange information between neighbouring subsystems and their controllers in a scalable and flexible manner. Therefore, the choice often falls on wireless communication networks since they can be established in an *ad hoc* fashion and require no physical interaction, featuring reduced setup and maintenance cost compared to their wired analogues, especially if the scenario under consideration involves dynamically decoupled MAS (Goldsmith, 2012). However, wireless communication is inherently of random nature and providing hard bounds on transmission delays or guaranteeing a successful transmission of specific pieces of information hence impossible. For example, multipath propagation may lead to fading of the received signal such that even the use of error correcting codes cannot ensure all data is received as intended (Lee & Messerschmitt, 2002; Tse & Viswanath, 2005). An overview of specific considerations for *ad hoc* wireless communication networks can be found in Chapter 16 of Goldsmith (2012).

As such, instead of studying IS in isolation without accounting for the exchange of information, it becomes necessary to jointly analyse both aspects at once. This leads to the introduction of cyber-physical networks which combine *physical* dynamical systems with *virtual* communication networks. A few of the approaches discussed above for the idealized case already include features from both control and communication in their analysis or can be readily extended to do so. For example, Olfati-Saber and Murray (2004) and Ren and Beard (2005) examine first-order consensus problems with switching interconnection topologies, which Pilz et al. (2009) extend to formation control problems in general MAS. In addition, Olfati-Saber and Murray (2004), Popov and Werner (2012), and Eichler et al. (2013) supplement the analysis to include transmission delays, the former being limited to constant and uniform delays and the latter two allowing for time-varying and heterogeneous delays throughout the network.

All these approaches take a worst-case perspective on the transmission effects which ignores the intrinsic randomness of wireless communication and may hence lead to excessive conservatism. Instead, sharper results can be obtained by including a stochastic communication model into the analysis as done among others by Schenato et al. (2007) and Seiler and Sengupta (2005) for digital dropout channels, *i.e.* information is either received as intended or lost entirely, and Elia (2005) and Molinari et al. (2021) for analog fading channels that act as a multiplicative uncertainty on the transmitted signals. Since digital transmission of information dominates modern communication networks (Lee & Messerschmitt, 2002), analog channels are given no further attention in the remainder of this thesis. Furthermore, transmission delays are neglected in the following as the time required for information to propagate between subsystems is typically much smaller than the sampling period of the control system. An exception to this rule are underwater acoustic modems which operate at the speed of sound, limiting the extent of transmission links to a few tens of meters before the delay becomes significant (Sendra et al., 2016).

While Schenato et al. (2007) and Seiler and Sengupta (2005) consider monolithic systems and centralized controllers, respectively, there are other approaches that cover IS. The first examples concern the average consensus problem: Hatano and Mesbahi (2005) investigate under which conditions sampled first-order integrators converge if information transmitted on different links is lost independently and with identical Bernoulli distribution, which Fagnani and Zampieri (2008, 2009) augment by loss-compensation strategies and Patterson et al. (2010) derive convergence rates for. Generalizations to random graphs with global (as opposed to local to each individual link) Markov chain based switching are subsequently presented by Matei et al. (2008) and Zhang and Tian (2009), and Tahbaz-Salehi and Jadbabaie (2008) study the convergence of first-order averaging algorithms with stochastic switching that is independent and homogeneous in time. Different from these purely analytic approaches, Wu and Shi (2012) propose a linear matrix inequality (LMI)-based condition for convergence in mean-square that builds on a closed-form expression for the second moment of the switched graph Laplacian. However, in contrast to the previous methods, their condition scales quadratically with the number of subsystems and is therefore limited to moderately sized IS.

Just like in the lossless case presented above, extending the discussion beyond first-order algorithms towards general IS requires careful consideration to preserve scalability. Note in particular that stochastic communication effects can perturb the intrinsic structure of the interconnection topology, impeding decomposition or decoupling even if the underlying nominal system allows for a scalable analysis. For this reason, network models of varying levels of fidelity are employed in the literature, ranging from highly structured models with immediate decoupling to generic switching laws.

In the simplest scenario, studied by Zhang et al. (2017) and Zheng et al. (2019) with Bernoulli distributed loss and Xu et al. (2020) for Markov chain based switching, it is assumed that the losses are identical throughout the network, *i.e.* all communication links either fail or succeed unanimously. Under this premise, the interconnection structure is preserved at all times, thereby rendering known decoupling techniques readily applicable. Conversely, however, this scenario has little practical relevance since transmission failures in wireless networks are typically isolated to individual links and *not* synchronous (Goldsmith, 2012). A natural next step is therefore to employ the network model of Hatano and Mesbahi (2005) for general IS, imposing that transmissions across different edges occur independently but with identical distribution. Even though the interconnections are switching randomly, which prevents decomposing the system as in the lossless case, Pan et al. (2017) provide a scalable design criterion for stabilizing state-feedback controllers under the hypothesis of a bounded number of consecutively dropped packets. Furthermore, Halder et al. (2022) propose an extension that includes a scalable H_∞-norm bound which they employ for suboptimal controller synthesis.

By means of its identical packet loss distribution across the transmission links, the preceding scenario still features a homogeneous structure throughout the network. On the contrary, the model considered by Zhang and Tian (2012) allows for heterogeneous loss probabilities, further complicating the derivation of appropriate decoupling techniques. In order to retain scalability, their analysis is hence restricted to MAS that are connected via directed tree graphs since this implies that the system can be permuted into a block-triangular shape. As an alternative, Zheng et al. (2019) and Xu et al. (2020) suggest formulating the system in terms of the edge Laplacian (Zelazo & Mesbahi, 2011) instead of the commonly employed vertex-based variant, but the resulting LMI-based

convergence condition is unsuitable for large-scale systems as its dimension grows quadratically with the number of subsystems. Moreover, a scalable analysis for a specific consensus protocol is presented by Ma et al. (2020). Contrasting all previous methods, the approach is limited to *mean* stability instead of the stronger *mean-square* stability.

In view of the wireless communication model described by Goldsmith (2012) and Tse and Viswanath (2005), even the final scenario discussed above serves only as an approximation of physical reality. One particular aspect of this is discussed by Chen et al. (2021): The assumption of statistical independence of the information loss between transmission links. Instead of modelling individual stochastic processes, they consider a single Markov chain that controls the switching for the entire graph, thereby allowing for arbitrary spatio-temporal dependencies within the network. This idea is iterated upon in subsequent work of Ballam et al. (2022, 2023), who extend the approach beyond stabilizability to cover H_2 performance analysis and dynamic controller synthesis. However, all of these results are subject to an exponential worst-case growth in complexity with respect to the number of subsystems and are therefore inapplicable for large-scale IS. Zhang et al. (2024), on the other hand, focus on an entirely different issue. While all previous approaches discussed in this section presume homogeneous subsystem models, they analyse the convergence of heterogeneous MAS for a specific dynamic consensus protocol under the assumption of stochastically independent and identically Bernoulli distributed packet loss.

Finally, Fagnani and Zampieri (2009) are not the only authors to have studied methods for counteracting the adverse effects of stochastic transmission failures. In fact any optimal controller synthesis procedure which incorporates packet loss, *e.g.* those presented by Ballam et al. (2022) and Halder et al. (2022), may be considered to fall into this category in a general sense. Further proposals along these lines are to interpolate between previously stored information and the most recently received data (Datar et al., 2018) and to extrapolate from past neighbour behaviour in the absence of updates (Mirali & Werner, 2020), both of which are able to improve the convergence speed of first-order consensus problems. On the other hand, there exist event-triggered control schemes, a class of algorithms designed to update the control signal only when necessary, thus reducing the transmission frequency (Heemels et al., 2012). In the context of IS with stochastic communication effects, such schemes have been studied by Li et al. (2014) and Viel et al. (2022), any potential benefit on the transmission probability due to the reduced network load (see Goldsmith, 2012) is however neglected.

1.2. Scope and Contributions

The present dissertation addresses the problem of analysing and designing *large-scale* IS subject to stochastic communication dropouts. For all results that are to be discussed, scalability with respect to the network size is therefore of utmost importance. However, as outlined in the previous section, this requirement is at odds with the use of comprehensive and realistic packet loss models. As its main contribution, this thesis hence proposes a flexible framework that moves the necessary compromise towards higher-fidelity stochastic models and allows analysing large IS even for networks with heterogeneous distributions and spatio-temporal stochastic dependencies.

The aforementioned framework is based on a novel extension of the concept of decomposable systems to Markov jump linear systems (MJLS). Similar to most methods based on decomposability, the approach is limited to IS consisting of linear time-invariant subsystems with homogeneous dynamics but encompasses the first-order consensus problem and formation control tasks as special cases. In addition to stability and convergence analysis, the framework enables efficient calculation of H_2- and H_∞-norm bounds and consequently distributed optimal controller synthesis. Moreover, even though most results in this thesis are given in a form specialized for dynamically decoupled MAS with fixed structure, many remain valid for general IS and time-varying patterns. Different from the deterministic case, the essential scalability of the framework does however come at the cost of conservatism.

In summary, the main contributions of this dissertation are as follows:

- Decomposable MJLS are introduced as a general modelling framework for IS with stochastically switching topology. A core feature of the approach is that the pattern matrix only has to be diagonalizable in terms of its first two moments rather than simultaneously for every instance, and that this property can be established analytically for Laplacian patterns with homogeneous but non-identical Bernoulli packet loss (Lemmas 3.3 and 3.4). In consequence, we obtain Theorem 3.6 as an LMI-based sufficient stability test which relies only on the spectrum boundary of the nominal Laplacian and is therefore independent of the number of subsystems. Furthermore, Theorems 3.11 and 3.13 present scalable conditions for calculating upper bounds on the H_2- and H_∞-norm of decomposable MJLS. A subset of these results has previously appeared in (Hespe, Saadabadi et al., 2024).

- Analogous to the deterministic case considered by Pilz et al. (2009), the above results (except for the H_∞-norm bound) are shown to cover systems with uncertain and time-varying nominal topology (Theorems 6.5 and 6.6). As a prerequisite, the thesis proposes a scalable sufficient condition for mean-square stability (Theorem 6.2) and an upper bound on the H_2-norm (Theorem 6.3) for switched MJLS with deterministic switching. This builds upon the techniques presented in (Hespe & Werner, 2023a).

- The scalable analysis conditions are employed to synthesize distributed static state-feedback (Theorems 4.1 and 4.2) and dynamic output-feedback (Theorems 4.3 and 4.4) controllers that are suboptimal with respect to the closed-loop H_2 and H_∞-norm, respectively. When tuned to specific loss probabilities, these controllers can partially offset the impact of packet loss on performance, even in scenarios beyond their original design parameters. This is illustrated through empirical testing on a physically-motivated network model which has been implemented in the WiMAS simulation library (see Appendix A). The H_2 synthesis and empirical demonstration have been pre-published in (Hespe et al., 2023).

- In order to extend the analysis towards heterogeneous packet loss distributions, an alternative decomposition is developed based on a linear fractional transformation of the system and its network model. Applying the technique to dynamically decoupled MAS, we arrive at Theorem 5.3 as a scalable condition for robust stability and Theorems 5.4 and 5.5 for bounds on the H_2- and H_∞-norm. Moreover,

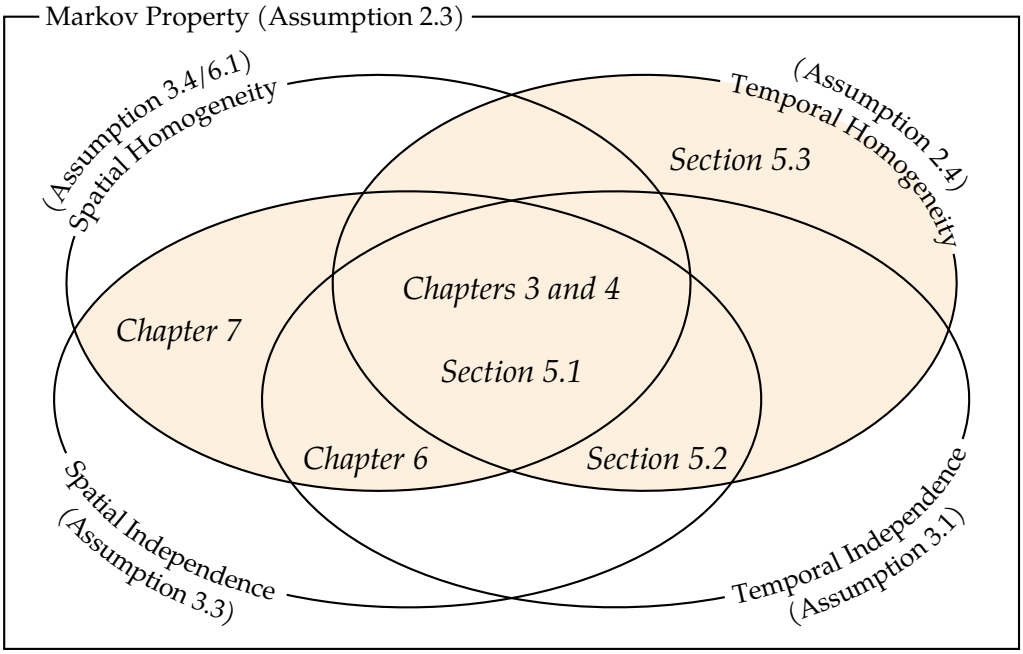

Figure 1.2.: Venn diagram of the modelling assumptions used throughout the thesis. The presented methods apply to models within the filled sets and labels within subsets indicate that the respective chapters and sections deal with the specified combination of assumptions. The unlabeled subsets are not explicitly considered in this dissertation.

Theorem 5.13 and Corollary 5.14 prove that the results remain valid if small spatio-temporal dependencies are present. The core statements have previously been published in (Hespe, Datar & Werner, 2024; Hespe & Werner, 2023b).

- Lastly, the thesis discusses challenges that arise for event-triggered control schemes on unreliable communication networks. In particular, it is demonstrated that the aperiodic sampling introduces stochastic dependencies and time variations even if transmission failures are independent and homogeneous, rendering techniques developed for periodic sampling inapplicable.

1.3. Network Modelling Assumptions Throughout the Thesis

The thesis consists of eight chapters, which can be grouped according to the assumptions they make about the stochastic packet loss of the underlying communication network. A Venn diagram of the resulting categorization is shown in Fig. 1.2.

Aside from the introduction in Chapter 1 and the closing remarks of Chapter 8, the only passage that does not appear in the figure is Chapter 2. In addition to providing necessary background material on graph theory and linear IS, it presents the essential framework of decomposable MJLS that forms the basis for the analysis techniques which are developed in the remainder of the dissertation.

Chapter 3 introduces the basic packet loss model of the thesis, the *homogeneous Bernoulli* model. Its results on the stability and performance analysis of decomposable MJLS are

derived under the assumption of spatio-temporal independence and homogeneity, *i.e.* all random variables are independent and identically distributed. The same loss model is furthermore employed for distributed controller synthesis in Chapter 4.

These assumptions are relaxed in multiple steps in the course of Chapter 5. While Section 5.1 considers the same restrictions as before but with uncertain probability, Section 5.2 includes spatially heterogeneous distributions (leading to the *heterogeneous Bernoulli* model), and Section 5.3 adds spatio-temporal dependencies. Nonetheless, the analysis conditions presented remain scalable with respect to the number of subsystems.

On the other hand, Chapter 6 addresses the assumption of temporal homogeneity since the time-varying nominal topology induces variations in the packet loss distribution. Similarly, the event-triggered sampling of Chapter 7 implies that the switching process of the closed-loop system is subject to temporal dependencies and varying in distribution, even if the underlying transmission failures are independent and homogeneous.

1.4. Essential Notation

Before proceeding to the main text, it is necessary to clarify some fundamental notation about sets and specific aspects of linear algebra. As such, let $\mathbb{N} := \{1, 2, 3, ...\}$ denote the set of natural numbers starting at 1, and correspondingly $\mathbb{N}_0 := \mathbb{N} \cup \{0\}$. Furthermore, $\mathbb{R}$, $\mathbb{R}^n$, and $\mathbb{R}^{m\times n}$ are the field of real numbers, the real n-dimensional vector space, and the set of real $m \times n$ matrices, respectively. All three sets are equipped with a norm, given by the absolute value $|x|$ in the scalar case, the Euclidean norm $\|x\|^2 := x^\top x$ for the vector space, and the induced 2-norm $\|M\| := \sup_{\|x\|=1} \|Mx\|$ for matrices. Moreover, the notation $|\mathcal{M}|$ is also used to indicate the cardinality of the set $\mathcal{M}$. Note that we distinguish between strict and non-strict subset relations, *i.e.* $\mathcal{M}_1 \subset \mathcal{M}_2$ means that $\mathcal{M}_1$ is a proper subset of $\mathcal{M}_2$, while $\mathcal{M}_1 \subseteq \mathcal{M}_2$ is used if $\mathcal{M}_1$ and $\mathcal{M}_2$ can be equal. Lastly, $\mathcal{M}_1 \times \mathcal{M}_2$ denotes the Cartesian product of the sets $\mathcal{M}_1$ and $\mathcal{M}_2$.

In terms of linear algebra, we use I_n to denote the $n \times n$ identity matrix and $\mathbf{1}_n$ is the n-dimensional vector of all ones, where the subscripts are sometimes dropped if the size is obvious from context. The symbols $M^\top$, M^{-1}, and $M^{-\top}$ are employed to indicate the transpose, inverse, and inverse transpose matrix operators. In addition to the standard matrix product $M_1 M_2$, we routinely utilize the Kronecker product $M_1 \otimes M_2$, see Section 2.2.2. Furthermore, for a sequence of matrices of arbitrary size, $\mathrm{diag}(M_1, M_2, ..., M_n)$ denotes their block-diagonal concatenation. Some extra notation is introduced specifically for symmetric matrices. For example, the symbol $*$ is used in large matrix expressions to indicate entries that can be deduced from symmetry. Moreover, the relation $M \succ (\succeq)\ 0$ means that the symmetric matrix M is positive (semi-)definite, and analogously $M \prec (\preceq)\ 0$ indicates negative (semi-)definiteness. Based on these relations, we establish a partial ordering on symmetric matrices by defining $M_1 \prec M_2$ as equivalent to $M_1 - M_2 \prec 0$ and similarly $M_1 \preceq M_2$ with its non-strict analogue $M_1 - M_2 \preceq 0$. Finally, we use $\mathbb{E}[X]$ and $\mathrm{Var}[X]$ to denote the *element-wise* expectation and variance of matrix-valued random variables X, respectively.

Interconnected Systems with Stochastic Packet Loss

2

Interconnected systems (IS) are a versatile but broad class of dynamic systems featuring different characteristics depending on the precise type of system under consideration. As the first step, it is therefore necessary to introduce the terminology and notation around the systems studied in this dissertation, which is the purpose of the current chapter.

2.1. Capturing Interconnection Topologies Using Graphs

In general terms, IS are aggregated dynamic systems consisting of multiple separated yet interacting subsystems. Typically, interactions between subsystems are not spanning the entire system but are restricted to local neighbourhoods. As an example, consider the IS shown in Fig. 2.1. The system consists of $N = 6$ subsystems $\mathcal{T}_i$ featuring both uni- (*e.g.* $\mathcal{T}_1$ to $\mathcal{T}_2$) and bidirectional (*e.g.* between $\mathcal{T}_4$ and $\mathcal{T}_5$) interactions as well as subsystems that only interact indirectly through other subsystems (*e.g.* $\mathcal{T}_3$ and $\mathcal{T}_6$). Depending on the type of IS, these subsystem interactions might be a coupling in the subsystem dynamics or an exchange of information through sensing or active communication. In either case, an arrow pointing from $\mathcal{T}_i$ to $\mathcal{T}_j$ is to be read as 'subsystem $\mathcal{T}_i$ is influencing subsystem $\mathcal{T}_j$'.

2.1.1. Elements of Graph Theory

The natural abstraction for modelling interactions between subsystems are mathematical graphs. We therefore provide a summary of the relevant definitions and results in the following. For a comprehensive overview of graph theory, see Diestel (2017) and Mesbahi and Egerstedt (2010).

A *graph* is defined as a pair $\mathcal{G} := (\mathcal{V}, \mathcal{E})$ of sets such that $\mathcal{E} \subset \mathcal{V} \times \mathcal{V}$. We refer to $\mathcal{V}$ as the *vertex set* and its elements are called *vertices* or *nodes*, and $\mathcal{E}$ is the *edge set*

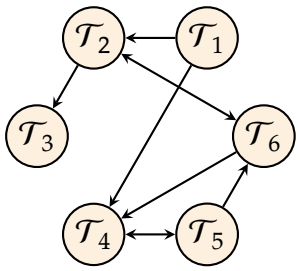

Figure 2.1.: Interaction between subsystems

and its elements are the *edges* or *links* of $\mathcal{G}$. The number of vertices of $\mathcal{G}$ is denoted as $N := |\mathcal{V}|$ and $m := |\mathcal{E}|$ is used for the number of edges. This thesis defines the vertex set as $\mathcal{V} := \{1, 2, \dots, N\}$ and assumes no vertex shares an edge with itself, *i.e.* $(i, i) \notin \mathcal{E}$ for all $i \in \mathcal{V}$. Furthermore, each edge is considered to have a fixed direction and the elements of $\mathcal{E}$ are therefore ordered pairs. As such, the edge $(i, j) \in \mathcal{E}$ is read as pointing from vertex j to vertex i, with j referred to as its tail and i being the head. In the literature, graphs with ordered pairs as edges are often called *directed* graphs in contrast to just graph. However, this dissertation does not make this distinction explicit since all graphs are considered to feature directed edges. Instead, we call a graph *undirected* if $(i, j) \in \mathcal{E}$ implies $(j, i) \in \mathcal{E}$. Note that even for an undirected graph, each edge is an ordered pair of vertices.

For each vertex $i \in \mathcal{V}$, define the set $\mathcal{N}_i^- := \{j \in \mathcal{V} \mid (i, j) \in \mathcal{E}\}$, *i.e.* all vertices with an edge ending at vertex i, as the *in-neighbourhood* and its cardinality as the *in-degree* $d_i^- := |\mathcal{N}_i^-|$. Analogously, the set $\mathcal{N}_i^+ := \{j \in \mathcal{V} \mid (j, i) \in \mathcal{E}\}$ and its cardinality $d_i^+ := |\mathcal{N}_i^+|$ are the *out-neighbourhood* and *out-degree* of vertex i. If $d_i^- = d_i^+$ holds for all vertices i, the graph is called *balanced*. For undirected graphs, we have $\mathcal{N}_i^- = \mathcal{N}_i^+$ and $d_i^- = d_i^+$ for all vertices i. Therefore, every undirected graph is balanced, and we use $\mathcal{N}_i$ and d_i without superscript when referring to the neighbourhood and degree. A useful operation we take advantage of later is the graph transpose. It describes the graph obtained by reversing all edges, *i.e.* for a graph $\mathcal{G}$, its transpose is obtained as $\mathcal{G}^\top = (\mathcal{V}, \mathcal{E}^\top)$ with the new edge set $\mathcal{E}^\top := \{(i, j) \in \mathcal{V} \times \mathcal{V} \mid (j, i) \in \mathcal{E}\}$.

A sequence of vertices $v_1, v_2, \dots, v_n$ with $v_i \in \mathcal{V}$ is called a *path* on $\mathcal{G}$ if every pair of consecutive vertices from the sequence is an edge of $\mathcal{G}$, that is, $(v_{i+1}, v_i) \in \mathcal{E}$ holds for all $i \in \{1, \dots, n-1\}$. If for every pair of distinct vertices $i, j \in \mathcal{V}$ there exist paths connecting the two vertices in both directions, the graph is said to be *strongly connected*. For undirected graphs, this property is simply called *connected*.

2.1.2. Algebraic Representations of Graphs

For our dynamic modelling, we rely on an alternative representation of graphs in terms of real matrices and their spectrum. Most relevant in the context of this dissertation is the *Laplacian* $L(\mathcal{G}) \in \mathbb{R}^{N \times N}$, defined element-wise as

$$L_{ij}(\mathcal{G}) := \begin{cases} -1 & \text{if } i \neq j \text{ and } j \in \mathcal{N}_i^-, \\ 0 & \text{if } i \neq j \text{ and } j \notin \mathcal{N}_i^-, \\ d_i^- & \text{if } i = j. \end{cases}$$

If the graph $\mathcal{G}$ is clear from context, we sometimes drop the argument and refer to the Laplacian as simply L.

Note that the row sum of the Laplacian is equal to 0 for all rows. This implies that the Laplacian is a singular matrix since the agreement vector $\mathbf{1}_N$ is mapped into the origin. More specifically, denoting the eigenvalues of $L(\mathcal{G})$ by $\lambda_1, \dots, \lambda_N$, they take the form

$$0 = \lambda_1 \leq \operatorname{Re} \lambda_2 \leq \cdots \leq \operatorname{Re} \lambda_N,$$

and the eigenvector corresponding to $\lambda_1 = 0$ is $\mathbf{1}_N$ (Mesbahi & Egerstedt, 2010). In case $\mathcal{G}$ is undirected, the Laplacian is a symmetric matrix and its eigenvalues are real. Furthermore, we obtain the following bounds on its eigenvalues:

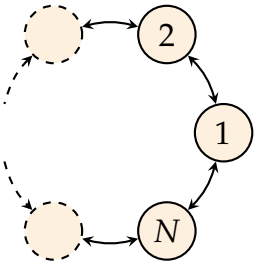

$$L\left(\mathcal{G}_5^\circ\right) = \begin{bmatrix} 2 & -1 & 0 & 0 & -1 \\ -1 & 2 & -1 & 0 & 0 \\ 0 & -1 & 2 & -1 & 0 \\ 0 & 0 & -1 & 2 & -1 \\ -1 & 0 & 0 & -1 & 2 \end{bmatrix}$$

Figure 2.2.: Visual representation and Laplacian of the circular graphs $\mathcal{G}_N^\circ$

Proposition 2.1.: Laplacian Eigenvalue Bounds

Let $\mathcal{G}$ be an undirected graph. Then the following eigenvalue bounds hold:

i) $\lambda_2 > 0$ *if and only if $\mathcal{G}$ is connected.* (*Mesbahi & Egerstedt, 2010, Theorem 2.8*)

ii) $\lambda_N \geq 1 + \max_{i \in \mathcal{V}} d_i \geq 2$ *if $\mathcal{E}$ is not empty.* (*Grone & Merris, 1994, Corollary 2*)

iii) $\lambda_N \leq 2 \max_{i \in \mathcal{V}} d_i$. (*Gershgorin discs, Horn & Johnson, 2017, Theorem 6.1.1*)

The second relevant matrix is the *incidence matrix* $\Psi(\mathcal{G}) \in \mathbb{R}^{N \times \tilde{m}}$. Each of its columns corresponds to a single edge $(i, j) \in \mathcal{E}$, where the ith entry of that column is 1, the jth is -1 and all others entries are 0. If both (i, j) and (j, i) are in $\mathcal{E}$, an arbitrary choice of direction is made, and only one of the two edges is included as a column in the incidence matrix (Mesbahi & Egerstedt, 2010). This implies that $\tilde{m}$, the number of columns of the incidence matrix, satisfies $m/2 \leq \tilde{m} \leq m$. An important fact for undirected graphs is that the Laplacian can be factored into the incidence matrix as

$$L(\mathcal{G}) = \Psi(\mathcal{G})\Psi(\mathcal{G})^\top. \tag{2.1}$$

Finally, we introduce two families of graphs that will be employed in examples throughout this dissertation:

Example 2.1.: Undirected Circular Graphs $\mathcal{G}_N^\circ$

Fig. 2.2 shows a visual representation of the circular graphs $\mathcal{G}_N^\circ$, where N is the number of vertices in the graph. All these graphs are undirected and connected, and we have $m = 2N$ (recall that each bidirectional arrow corresponds to two edges). The figure also shows the Laplacian of $\mathcal{G}_5^\circ$, and its (non-unique) incidence matrix is given by

$$\Psi\left(\mathcal{G}_5^\circ\right) = \begin{bmatrix} 1 & 0 & 0 & 0 & -1 \\ -1 & 1 & 0 & 0 & 0 \\ 0 & -1 & 1 & 0 & 0 \\ 0 & 0 & -1 & 1 & 0 \\ 0 & 0 & 0 & -1 & 1 \end{bmatrix}.$$

Note that the Laplacian is symmetric as the graphs are undirected.

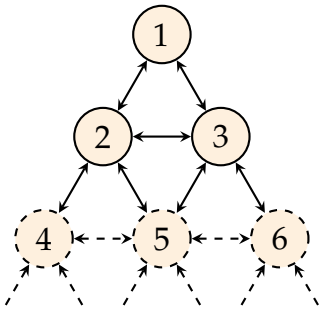

$$L\left(\mathcal{G}_3^{\triangle}\right) = \begin{bmatrix} 2 & -1 & -1 & 0 & 0 & 0 \\ -1 & 4 & -1 & -1 & -1 & 0 \\ -1 & -1 & 4 & 0 & -1 & -1 \\ 0 & -1 & 0 & 2 & -1 & 0 \\ 0 & -1 & -1 & -1 & 4 & -1 \\ 0 & 0 & -1 & 0 & -1 & 2 \end{bmatrix}$$

Figure 2.3.: Visual representation and Laplacian of the triangular grid graphs $\mathcal{G}_h^{\triangle}$

Example 2.2.: Triangular Grid Graphs $\mathcal{G}_h^{\triangle}$

Fig. 2.3 visualizes the family of triangular grid graphs $\mathcal{G}_h^{\triangle}$, where h is the number of rows of the grid. For $\mathcal{G}_h^{\triangle}$, we have $N = \frac{h}{2}(h+1)$ vertices and $m = 3h(h-1)$ edges, and all members of the family are undirected and connected. The Laplacian of $\mathcal{G}_3^{\triangle}$ is shown in Fig. 2.3 next to the visual representation.

2.2. Linear Models for Interconnected Systems

Having introduced the model for the interconnection topology, we continue with the dynamic part of modelling IS and discuss how graph and system theory are combined for this purpose. Therefore, we use this section to revisit important definitions and ideas from existing literature that apply to idealized circumstances, *i.e.* systems without packet loss.

Since the majority of modern controllers are digital and based on sampled-data control systems (Chen & Francis, 1995), this dissertation exclusively considers discrete-time models. Furthermore, the underlying subsystem dynamics and interaction rules are assumed to be linear and time-invariant. Ignoring any detrimental network effects, this leads to a linear time-invariant (LTI) description of the overall IS, which is given by

$$\begin{aligned} \xi_{k+1} &= \mathcal{A}\xi_k + \mathcal{B}w_k \\ z_k &= C\xi_k + \mathcal{D}w_k \end{aligned} \tag{2.2}$$

with initial condition ξ_0. All three signals are compound signals taking the form

$$\begin{aligned} \xi_k &= \left[(\xi_k^1)^\top \quad (\xi_k^2)^\top \quad \dots \quad (\xi_k^N)^\top\right]^\top \in \mathbb{R}^{Nn_\xi}, \\ w_k &= \left[(w_k^1)^\top \quad (w_k^2)^\top \quad \dots \quad (w_k^N)^\top\right]^\top \in \mathbb{R}^{Nn_w}, \\ z_k &= \left[(z_k^1)^\top \quad (z_k^2)^\top \quad \dots \quad (z_k^N)^\top\right]^\top \in \mathbb{R}^{Nn_z}, \end{aligned}$$

where $\xi_k^i \in \mathbb{R}^{n_\xi}$, $w_k^i \in \mathbb{R}^{n_w}$, and $z_k^i \in \mathbb{R}^{n_z}$ are the dynamic state and the performance in- and output of subsystem $i \in \mathcal{V}$, respectively. Note that each subsystem is uniquely associated with a single vertex of the underlying graph. The terms $\mathcal{A}$, $\mathcal{B}$, C, and $\mathcal{D}$ are matrices of compatible dimension that capture the behaviour of the IS as a whole, not of individual subsystems.

The first important property of LTI systems we consider is asymptotic stability in the sense of Lyapunov, which is defined in the following way:

Definition 2.1.: Asymptotic Stability (Hespanha, 2009)

The LTI system (2.2) is *asymptotically stable* if ξ_k is uniformly bounded for all $k \in \mathbb{N}_0$ and

$$\lim_{k\to\infty} \xi_k = 0$$

for all initial conditions ξ_0 and with $w \equiv 0$.

In the following, we will often refer to asymptotic stability as just *stability*. Note that this definition of stability is independent of the input-output properties of the system but solely based on the homogeneous system $\xi_{k+1} = \mathcal{A}\xi_k$. One way to test for stability of discrete-time LTI systems is by solving the Lyapunov matrix inequality given below:

Theorem 2.2.: Lyapunov Matrix Inequality (Hespanha, 2009)

The LTI system (2.2) *is asymptotically stable if and only if there exists an* $\mathcal{X} \succ 0$ *such that*

$$\mathcal{A}^\top \mathcal{X} \mathcal{A} \prec \mathcal{X} \tag{2.3}$$

holds.

The stability test in Theorem 2.2 is based on the feasibility of a linear matrix inequality (LMI), which can be posed as a semidefinite program (SDP) and thus be solved effectively (Boyd et al., 1994).

2.2.1. Consensus Problems

For many problems in the context of IS, asymptotic stability is too strict to describe the desired properties of the system accurately, and marginal stability has to be considered instead. This becomes apparent in the following example:

Example 2.3.: First-Order Consensus

Consider a system of N decoupled integrators, each described by the difference equation

$$x_{k+1}^i = x_k^i + u_k^i,$$

that are interconnected according to a fixed graph. At their inputs, all integrators apply a distributed *consensus protocol* (*cf*. Olfati-Saber et al., 2007), which in this case is given by

$$u_k^i = \kappa \sum_{j\in\mathcal{N}_i^-} \left(x_k^j - x_k^i\right),$$

i.e. all integrators apply the average deviation from their neighbours' state as a correction term with gain $\kappa > 0$. As described in Mesbahi and Egerstedt (2010), naturally occurring examples for this kind of system are resistor-capacitor circuits and distributed agreement algorithms. Combining the integrators and the

consensus protocol into a single equation, we obtain

$$x_{k+1} = (I_N - \kappa L)x_k \tag{2.4}$$

with the Laplacian L of the underlying graph.

Observe that $\mathbf{1}_N$ is an eigenvector of $I_N - \kappa L$ with eigenvalue 1 since it is the eigenvector of L corresponding to $\lambda_1 = 0$. As such, any vector in the *agreement space* $\left\{\alpha\mathbf{1}_N \,\middle|\, \alpha \in \mathbb{R}\right\}$, *i.e.* the subspace spanned by $\mathbf{1}_N$, is an equilibrium of the system and thus the system cannot be asymptotically stable. However, the system is guaranteed to converge to the agreement space, provided that the underlying interconnection graph is strongly connected and that the gain κ is sufficiently small (Olfati-Saber et al., 2007, Theorem 2). This means that the subsystems will eventually reach agreement, or *consensus*, motivating the definition below:

Definition 2.2.: Asymptotic Consensus (Olfati-Saber et al., 2007)
The LTI system (2.2) is said to reach *asymptotic consensus* if it is converging to the agreement space asymptotically for $w \equiv 0$, *i.e.* its state satisfies

$$\xi_k^1 = \xi_k^2 = \xi_k^N$$

in the limit of $k \to \infty$.

A useful operator in the context of consensus problems is the projection onto the *dis*agreement space, *i.e.* the orthogonal complement of the agreement space. It is given by the matrix

$$\Pi \coloneqq I_N - \frac{1}{N}\mathbf{1}_N\mathbf{1}_N^\top \tag{2.5}$$

and has rank $N-1$. Using the projection, the convergence condition from Definition 2.2 can alternatively be formulated as

$$\lim_{k\to\infty}\left(\Pi \otimes I_{n_\xi}\right)\xi_k = 0. \tag{2.6}$$

Therefore, reaching consensus is akin to asymptotic stability on the disagreement space.

2.2.2. Facts About the Kronecker Product

In (2.6), the *Kronecker product* of matrices has been employed to increase the dimension of the projection operator to match the internal structure of the composite state ξ_k. Since the Kronecker product is an essential tool in the context of IS, this section is introducing its most important properties. An in-depth discussion of the Kronecker product and its applications is given by Steeb (1991).

The Kronecker product of two matrices $A \in \mathbb{R}^{m\times n}$ and $B \in \mathbb{R}^{p\times q}$ is defined as

$$A \otimes B \coloneqq \begin{bmatrix} a_{11}B & a_{12}B & \cdots & a_{1n}B \\ a_{21}B & a_{22}B & \cdots & a_{2n}B \\ \vdots & \vdots & \ddots & \vdots \\ a_{m1}B & a_{m2}B & \cdots & a_{mn}B \end{bmatrix}$$

and has dimension $(mp) \times (nq)$. The product is distributive, *i.e.* we have

$$(A + B) \otimes (C + D) = A \otimes C + A \otimes D + B \otimes C + B \otimes D$$

and $(\lambda A) \otimes B = \lambda(A \otimes B) = A \otimes (\lambda B)$ with appropriately sized matrices A, B, C, and D, and a scalar λ. Furthermore, the Kronecker product is associative, such that $A \otimes (B \otimes C) = (A \otimes B) \otimes C$ holds. However, similar to other matrix products, it is not commutative.

For expressions that contain both the Kronecker and standard matrix product, there are two helpful identities. Specifically, such mixed products can be regrouped if the involved matrices are of appropriate dimension:

Lemma 2.3.: Mixed Product Identities (Steeb, 1991)

For appropriately sized matrices $A_1, A_2, \dots, A_d$ and $B_1, B_2, \dots, B_d$, the Kronecker product satisfies the mixed-product identities

$$(A_1 \otimes A_2 \otimes \cdots \otimes A_d)(B_1 \otimes B_2 \otimes \cdots \otimes B_d) = (A_1 B_1) \otimes (A_2 B_2) \otimes \cdots \otimes (A_d B_d)$$

and

$$(A_1 A_2 \cdots A_d) \otimes (B_1 B_2 \cdots B_d) = (A_1 \otimes B_1)(A_2 \otimes B_2) \cdots (A_d \otimes B_d).$$

In the special case of $d = 2$, the identities from Lemma 2.3 are equivalent. Moreover, for matrices $A \in \mathbb{R}^{m \times n}$ and $B \in \mathbb{R}^{p \times q}$, the commutation property

$$(A \otimes I_p)(I_n \otimes B) = A \otimes B = (I_m \otimes B)(A \otimes I_q)$$

results as a corollary. Another important feature of the Kronecker product is that many matrix functions distribute over its factors (Steeb, 1991). For example, the transpose of a Kronecker product can be computed as the transpose of each factor, *i.e.* $(A \otimes B)^\top = A^\top \otimes B^\top$. Additional functions that are relevant in the context of this dissertation are the trace and determinant, where for square matrices $A \in \mathbb{R}^{m \times m}$ and $B \in \mathbb{R}^{p \times p}$, we have

$$\operatorname{tr}(A \otimes B) = (\operatorname{tr} A)(\operatorname{tr} B) \qquad \text{and} \qquad \det(A \otimes B) = (\det A)^p (\det B)^m. \tag{2.7}$$

Finally, if A and B are non-singular, the inverse of the product is guaranteed to exist and obtained as $(A \otimes B)^{-1} = A^{-1} \otimes B^{-1}$ (Steeb, 1991).

2.2.3. Decomposable Systems

The central issue when working with IS of many subsystems is their scale. Even though each individual subsystem may have only a few states, the collective size can render system analysis and controller synthesis intractable. For example, since X is a symmetric matrix in the stability condition of Theorem 2.2, the number of variables grows quadratically with N, resulting in computational problems for exceedingly large IS. We therefore have to rely on approaches that take advantage of the structural properties of the system in order to reduce the computational complexity.

One such approach that forms the basis for much of the work in this dissertation is to utilize the spectral decomposition of the interconnection topology in order to decouple the interconnected subsystems. Originally developed by Pecora and Carroll (1998)

and Fax and Murray (2004) to study the synchronization of oscillators and stability of vehicle formations, respectively, this method was later extended into the framework of *decomposable systems* by Massioni and Verhaegen (2009), covering not only stability but also system performance. In that framework, a matrix M is called *decomposable* with respect to a pattern S if there exist two matrices M_d and M_c such that $M = I_N \otimes M_\mathrm{d} + S \otimes M_\mathrm{c}$, which are termed *decoupled* and *coupled* components. Moreover, an LTI system is called *decomposable* if all matrices of its state-space representation are decomposable with respect to the same pattern matrix, *i.e.* if there exist matrices $\mathcal{A}_\mathrm{d}$ and $\mathcal{A}_\mathrm{c}$ such that

$$\mathcal{A} = I_N \otimes \mathcal{A}_\mathrm{d} + S \otimes \mathcal{A}_\mathrm{c}$$

for unforced systems and analogously for $\mathcal{B}$, $\mathcal{C}$, and $\mathcal{D}$ if the system has inputs and outputs.

Example 2.3.: First-Order Consensus, (started on page 15)
The first-order consensus problem with update equation

$$x_{k+1} = (I_N - \kappa L)x_k \qquad \text{(2.4, restated)}$$

can be posed in the form of a decomposable system by taking the Laplacian as pattern matrix, *i.e.* $S = L$, and setting $\mathcal{A}_\mathrm{d} = 1$ and $\mathcal{A}_\mathrm{c} = -\kappa$ for the decoupled and coupled component, respectively.

The power of imposing such a structure onto the system matrices stems from the commutation property of the Kronecker product that has been introduced below Lemma 2.3. Assuming that the pattern matrix is diagonalizable, that is, that there exists a non-singular matrix $U \in \mathbb{R}^{N\times N}$ such that $U^{-1}SU = \Lambda$ with diagonal Λ, the transformation U will in turn also block-diagonalize any decomposable matrix $M \in \mathbb{R}^{nN\times nN}$ as

$$\begin{aligned}(U \otimes I_n)^{-1} M (U \otimes I_n) &= (U \otimes I_n)^{-1}(I_N \otimes M_\mathrm{d} + S \otimes M_\mathrm{c})(U \otimes I_n) \\ &= I_N \otimes M_\mathrm{d} + (U^{-1}SU) \otimes M_\mathrm{c} \\ &= I_N \otimes M_\mathrm{d} + \Lambda \otimes M_\mathrm{c}.\end{aligned}$$

Note that the Kronecker product is used to match the internal structure of the system matrices in similar fashion to (2.6). Since this operation is routinely needed for decomposable systems, we introduce the shorthand notation $M_{(d)} \coloneqq M \otimes I_d$. By applying the diagonalizing transformation to the state of an LTI system, we obtain a simplified stability condition. Similar results were previously proposed by Fax and Murray (2004) and Pecora and Carroll (1998) for continuous-time systems.

Theorem 2.4.: Massioni and Verhaegen (2009)

Assume that S is a diagonalizable matrix. Then the LTI system

$$\xi_{k+1} = (I_N \otimes \mathcal{A}_\mathrm{d} + S \otimes \mathcal{A}_\mathrm{c})\xi_k$$

is asymptotically stable if and only if all systems

$$\hat{\xi}^i_{k+1} = (\mathcal{A}_\mathrm{d} + \lambda_i \mathcal{A}_\mathrm{c})\hat{\xi}^i_k \qquad (2.8)$$

with $i \in \{1, \dots, N\}$ are asymptotically stable, where λ_i are the eigenvalues of S.

Theorem 2.4 demonstrates that we can reason about the stability of the IS by analysing a set of *N smaller* systems, which have the state dimension of a single subsystem. Note, however, that the individual systems in (2.8) are *not* equal to the subsystems of the IS. For this reason, they were termed *modal subsystems* by Massioni and Verhaegen (2009). The advantage lies in the scalability of the approach: While the number of optimization variables scales quadratically with N when analysing the IS as a whole using Theorem 2.2, the complexity is reduced to scale linearly if we analyse the modal subsystems.

In addition to the stability analysis result presented in Theorem 2.4, the decomposable systems framework is flexible enough to cover also H_2 and H_∞ performance analysis as well as suboptimal synthesis of distributed output-feedback controllers with respect to these norms. Moreover, it is possible to generalize the approach to systems with more than one pattern matrix, *i.e.*

$$\mathcal{A} = \sum_{i=1}^{n} S_i \otimes \mathcal{A}_i$$

for some positive integer n. This, however, requires that all pattern matrices S_i are simultaneously diagonalizable (Massioni & Verhaegen, 2009).

2.3. Modelling Loss of Information in Wireless Networks

Modelling interconnection topologies of IS as constant graphs as described in Section 2.1 is a powerful tool for capturing the system structure, but does not allow to express the unreliable nature of communication networks. This section is therefore introducing a network model that is able to represent stochastic effects induced by packet loss.

Only one specific type of interconnection is studied in detail in this dissertation: Wireless broadcast networks. Especially for multiagent systems (MAS) with mobile agents, establishing a wireless communication network for exchange of information offers great flexibility and is therefore an attractive solution. For this reason, there exists a broad range of literature on networked MAS, for example the books by Bullo (2018) and Mesbahi and Egerstedt (2010). However, due to physical effects like thermal noise and fading (Goldsmith, 2012; Tse & Viswanath, 2005), but also aspects of the communication protocol such as correlations in medium access control (Lee & Messerschmitt, 2002), wireless communication networks are inherently unreliable and are failing randomly. Even though there are means to mitigate part of the problem, *e.g.* by tuning the communication channel or through forward error correcting codes, the exchange of information through a wireless communication channel needs to be analysed in a probabilistic fashion.

Before introducing a model for the communication network, a few simplifying assumptions are required. Most importantly, we assume that the communication is packet based, *i.e.* information is transmitted in discrete bunches, not as a continuous stream. Furthermore, it is assumed that sufficient measures for error detection and correction have been implemented. We therefore consider every packet to be either received in full without errors or corrupted information, or to be lost entirely. Moreover, we assume that the time required for transmitting packets is small compared to the time between the transmission of packets and can thus be neglected, such that the transmissions are received instantaneously and without delay. The final assumption is that the transmissions

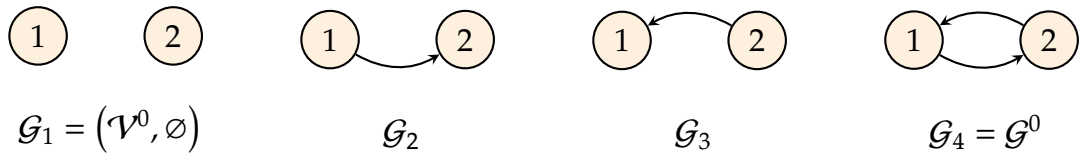

Figure 2.4.: Family of subgraphs for the complete graph with two vertices

are occurring in regular, evenly spaced intervals and are synchronized throughout the communication network. More restrictive assumptions will be required in the following chapters of this dissertation.

Out of all of these assumptions, the requirement for synchronized transmissions is the most restrictive, because it requires synchronized clocks on all transmitters and thus subsystems. In contrast, packet-based protocols with regular transmissions are the natural counterpart to discrete-time control systems as introduced in Section 2.2. Furthermore, the speed of propagation is typically very large in wireless communication networks (close to the speed of light or speed of sound for radio or acoustic communication, respectively, see Sendra et al., 2016; Tse & Viswanath, 2005), such that the transmission times are dominated by the processing time in the transmitter and receiver.

Because wireless networks are typically modelled in a probabilistic fashion, we have to augment our system model by a stochastic component. First and foremost, we introduce the *nominal graph* $\mathcal{G}^0 = (\mathcal{V}^0, \mathcal{E}^0)$ as the topology of the communication network in case all transmissions are successful. In case of broadcast communication, $\mathcal{G}^0$ is the complete graph, but other graphs can be chosen if a localized exchange of information is desired. However, due to the effects described above, any combination of edges could potentially fail to transmit, such that the actual communication topology is switched randomly between subgraphs $\mathcal{G}_i = (\mathcal{V}^0, \mathcal{E}_i)$ of $\mathcal{G}^0$ with $\mathcal{E}_i \subseteq \mathcal{E}^0$. As demonstrated in Fig. 2.4 for the complete graph with two vertices, there exist 2^m unique $\mathcal{G}_i$, including the graph without edges and $\mathcal{G}^0$ itself, such that we can index the subgraphs by $i \in \mathcal{K} := \{1, \dots, 2^m\}$. Furthermore, the assumption of synchronized and periodic transmissions ensures that the switching can be described as a *sequence* of values out of $\mathcal{K}$, in contrast to requiring a switching function defined on $\mathbb{R}$. Therefore, we introduce a discrete-time stochastic process $\{\sigma_k\}$ taking values in $\mathcal{K}$ for all $k \in \mathbb{N}_0$ that, together with the subgraphs $\mathcal{G}_i$, defines the graph process $\left\{\mathcal{G}_{\sigma_k}\right\}$ as our stochastic packet loss model.

In general, the distribution of σ_k may not only depend on previous samples $\sigma_{k'}$ of the stochastic process but also on past positions and velocities of the transmitters and receivers and therefore the state $\xi_{k'}$ of the underlying MAS, where $0 \leq k' < k$ in both cases. However, analysing a networked MAS at this level of generality is mathematically intractable for all but very small networks. Throughout the dissertation, we will therefore impose additional assumptions on the stochastic processes as required. Most importantly, there are two standing assumptions on $\{\sigma_k\}$ that are implicitly imposed throughout the thesis if not explicitly mentioned otherwise:

Assumption 2.3.: Markov Chain (Klenke, 2013)
The stochastic process $\{\sigma_k\}$ describing the communication network satisfies the *Markov property*, *i.e.*

$$\mathbb{P}\Big(\sigma_{k+1} = j \,\Big|\, \sigma_0, \xi_0, \sigma_1, \xi_1, \dots, \sigma_k, \xi_k\Big) = \mathbb{P}\Big(\sigma_{k+1} = j \,\Big|\, \sigma_k\Big)$$

holds for all $k \in \mathbb{N}_0$ and all $j \in \mathcal{K}$. Therefore, the distribution of σ_{k+1} is uniquely determined by σ_k alone, independent of previous samples or the dynamic state ξ_k.

Assumption 2.4.: Temporal Homogeneity (Douc et al., 2018)
The Markov chain $\{\sigma_k\}$ describing the communication network is *homogeneous in time*, *i.e.* there exist $\theta_{ij}, t_i \in [0,1]$ such that

$$\mathbb{P}\Big(\sigma_{k+1} = j \,\Big|\, \sigma_k = i\Big) = \theta_{ij}$$

holds for all $k \in \mathbb{N}_0$ and $i, j \in \mathcal{K}$ with initial distribution $\mathbb{P}\Big(\sigma_0 = i\Big) = t_i$.

The probabilities θ_{ij} are called *transition probabilities*, and it follows from the definition of the probability measure $\mathbb{P}$ that $\sum_{j\in\mathcal{K}} \theta_{ij} = \sum_{j\in\mathcal{K}} t_j = 1$ for all $i \in \mathcal{K}$. Moreover, for a compact way to refer to all transition probabilities, we element-wise define the *transition probability matrix* (*TPM*) as $\Theta = \Big[\theta_{ij}\Big]$, which is a row-stochastic matrix, *i.e.* a matrix with non-negative elements and each row sums up to 1.

In contrast to the assumptions on the implementation of the communication network, Assumptions 2.3 and 2.4 cannot be enforced through suitable choice of the communication infrastructure and are motivated purely by mathematical tractability. Specifically, the assumption that the transition probabilities are independent of the dynamical state is only satisfied for systems with stationary subsystems, since the probability of a successful transmission depends on the received signal strength, which in turn follows the inverse-square law and therefore decreases with growing distance between transmitter and receiver (Tse & Viswanath, 2005). However, it is empirically justified that a packet loss model as described by the above assumptions is a reasonable approximation of reality even for wirelessly networked IS with moving subsystems such as MAS and is thus suitable to design and optimize controllers for practical scenarios. This idea is elaborated on in Section 4.3 below.

In order to map from the process $\{\sigma_k\}$ describing the entire communication network to the individual transmission links, the edges (i, j) are associated with the digits of the binary representation of σ_k. Formally, this affiliation is determined by the function $\alpha\colon \mathcal{E}^0 \to \{1, 2, \dots, m\}$ that maps every edge $(i, j) \in \mathcal{E}^0$ into a unique integer, *i.e.* unique digit. This leads to the definition of stochastic processes $\Big\{\phi_k^{ij}\Big\}$ as $\phi_k^{ij} := \beta\Big(\sigma_k - 1, \alpha(i, j)\Big) \in \{0, 1\}$, where $\beta(n, i)$ is the ith digit of the binary representation of n. In our interpretation, $\phi_k^{ij} = 1$ represents a successful transmission across the edge (i, j), while $\phi_k^{ij} = 0$ is read as a transmission failure. Accordingly, $\mathcal{E}_l$, the set of transmitting edges if $\sigma_k = l$, is given by $\mathcal{E}_l = \Big\{(i, j) \in \mathcal{E}^0 \,\Big|\, \beta\Big(l - 1, \alpha(i, j)\Big) = 1\Big\}$. An example of a graph with its edge processes $\Big\{\phi_k^{ij}\Big\}$ is visualized in Fig. 2.5.

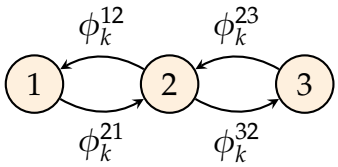

Figure 2.5.: Line graph of three vertices with edge processes $\left\{\phi_k^{ij}\right\}$

Of course, introducing the stochastic edge processes does also turn the algebraic representation of the communication graph stochastic. Most importantly, this is the case for the Laplacian $\left\{L\left(\mathcal{G}_{\sigma_k}\right)\right\}$, which now is a stochastic process given element-wise by

$$L_{ij}\left(\mathcal{G}_{\sigma_k}\right) = \begin{cases} -\phi_k^{ij} & \text{if } i \neq j \text{ and } j \in \mathcal{N}_i^-, \\ 0 & \text{if } i \neq j \text{ and } j \notin \mathcal{N}_i^-, \\ \sum\limits_{l \in \mathcal{N}_i^-} \phi_k^{il} & \text{if } i = j, \end{cases}$$

where $\mathcal{N}_i^-$ refers to the neighbourhood of vertex i in $\mathcal{G}^0$. Note that every realization of the stochastic Laplacian is guaranteed to have a row sum of zero for all rows and all $k \in \mathbb{N}_0$, implying that the zero eigenvalue with eigenvector $\mathbf{1}_N$ is preserved. For notational convenience, we define the shorthand terms $L^0 := L(\mathcal{G}^0)$ for the Laplacian of the nominal graph and $L_i := L(\mathcal{G}_i)$ with $i \in \mathcal{K}$ for the switching Laplacian, which will be used whenever the graph can be determined from context.

2.4. Markov Jump Linear Systems

While working with LTI systems is sufficient for modelling networked IS with idealized communication, they fail to capture detrimental effects of networking such as the stochastic packet loss described in the preceding section. In order to study the effects of packet loss, we therefore have to extend the class of systems under consideration from time-invariant systems to switched systems. This becomes apparent in the consensus example that was started above with idealized communication:

Example 2.4.: First-Order Consensus with Packet Loss

With the same discrete-time single integrator dynamics as in Example 2.3, running the consensus protocol over stochastic communication links leads to the distributed control law

$$u_k^i = \kappa \sum_{j \in \mathcal{N}_i^-} \phi_k^{ij}\left(x_k^j - x_k^i\right), \tag{2.9}$$

where the stochastic processes ϕ_k^{ij} determine which neighbour's information is received by subsystem i at any given time k. For the closed-loop system, this results in the stochastic difference equation

$$x_{k+1} = \left(I_N - \kappa L_{\sigma_k}\right) x_k \tag{2.10}$$

with the stochastically switching Laplacian L_{σ_k}.

A class of dynamic systems that can accommodate the stochastic difference equation (2.10) are Markov jump linear systems (MJLS), which are switched linear systems whose switching is determined by a Markov chain. In state-space form, an MJLS is described by

$$\mathcal{T}\colon \begin{cases} \xi_{k+1} = \mathcal{A}_{\sigma_k}\xi_k + \mathcal{B}_{\sigma_k}w_k, \\ z_k = \mathcal{C}_{\sigma_k}\xi_k + \mathcal{D}_{\sigma_k}w_k, \end{cases} \tag{2.11}$$

where $\sigma_k \in \mathcal{K}$ is the state of a homogeneous Markov chain (see Assumptions 2.3 and 2.4), $\mathcal{A}_i$, $\mathcal{B}_i$, $\mathcal{C}_i$, and $\mathcal{D}_i$ are known matrices of appropriate dimension for all $i \in \mathcal{K}$, and $\mathcal{K}$ is a finite set. Same as for the LTI systems in Section 2.2, $\xi_k \in \mathbb{R}^{Nn_\xi}$, $w_k \in \mathbb{R}^{Nn_w}$, and $z_k \in \mathbb{R}^{Nn_z}$ are the dynamic state and the performance in- and output, respectively. While a brief recapitulation of important definitions and results is given below, we refer to (Costa et al., 2005) for a comprehensive treatment of discrete-time MJLS.

2.4.1. Stochastic Notions of Stability

Because of the stochastic switching, asymptotic stability as described in Definition 2.1 is in many cases prohibitively strict if applied to MJLS. This effect is apparent from Example 2.4. If the entire network fails at once, *i.e.* $\sigma_k = 1$ and thus $\phi_k^{ij} = 0$ for all edges, (2.10) turns into decoupled first-order integrators. It is therefore impossible to establish asymptotic convergence in case this situation has non-zero probability to occur. On the other hand, as shown by Matei et al. (2008), mild assumptions on the distribution of $\{\sigma_k\}$ are sufficient to prove that almost all realizations of the problem converge.

The issue with the deterministic kind of asymptotic stability used above is that the knowledge about the distribution of the switching process $\{\sigma_k\}$ is disregarded. In order to obtain less conservative results, we therefore turn towards stochastic notions of stability and introduce the two most relevant definitions below:

Definition 2.5.: Stability of Markov Jump Linear Systems (Ji et al., 1991)
The MJLS $\mathcal{T}$ is

i) *almost surely asymptotically stable* if

$$\mathbb{P}\left(\lim_{k\to\infty} \xi_k = 0\right) = 1$$

for all initial conditions ξ_0, σ_0 and with $w \equiv 0$,

ii) *asymptotically mean-square stable* if

$$\lim_{k\to\infty} \mathbb{E}\left[\|\xi_k\|^2\right] = 0$$

for all initial conditions ξ_0, σ_0 and with $w \equiv 0$.

Remark. There exist other, seemingly stricter, variants of stability involving the second stochastic moment of its state, such as stochastic stability and exponential mean-square stability (Ji & Chizeck, 1990). However, for MJLS with finite $\mathcal{K}$, Ji et al. (1991) have shown that both alternatives are in fact equivalent to asymptotic mean-square stability.

From the two stochastic kinds of stability introduced in Definition 2.5, almost sure asymptotic stability is a natural extension of asymptotic stability for LTI systems (Definition 2.1) as it ensures that trajectories of the MJLS converge to the origin with probability one. However, testing for almost sure stability is a difficult problem in general, as it hinges on calculating the top Lyapunov exponent or approximations thereof (*cf*. Bolzern et al., 2004; Fang et al., 1994; Song et al., 2014). In contrast, there exists a rich theory on mean-square stability that parallels the well known stability theory for LTI systems based on quadratic Lyapunov functions and, as such, features close analogues of some important results. One particular instance is the MJLS counterpart of Theorem 2.2, the LMI condition for asymptotic stability, which is given in the theorem below:

Theorem 2.5.: MJLS Lyapunov Inequality (Costa & Fragoso, 1993)

The MJLS $\mathcal{T}$ is asymptotically mean-square stable if and only if there exist $\mathcal{X}_i \succ 0$ such that

$$\sum_{j\in\mathcal{K}} \theta_{ij}\mathcal{A}_j^\top \mathcal{X}_j \mathcal{A}_j \prec \mathcal{X}_i \tag{2.12}$$

holds for all $i \in \mathcal{K}$.

In the same way as its LTI analogue, the MJLS stability test in Theorem 2.5 can be posed as a semidefinite feasibility problem and thus be checked efficiently using existing solvers for SDPs. Importantly, as shown by Ji et al. (1991), asymptotic mean-square stability of an MJLS implies that it is also almost surely asymptotically stable, such that the desired trajectory-wise convergence is obtained. Note that the converse does not hold, *i.e*. MJLS can be almost surely asymptotically stable without being asymptotically mean-square stable (Ji et al., 1991).

Likewise, similar considerations about stochastic kinds of convergence have to be made for consensus problems over stochastic graphs. On the one hand, there exist approaches such as Fagnani and Zampieri (2009) and Zhang and Tian (2009) that study consensus in the mean-square sense, while other results are concerned with almost sure convergence to the agreement space (*cf*. Fagnani & Zampieri, 2008; Hatano & Mesbahi, 2005; Matei et al., 2008; Tahbaz-Salehi & Jadbabaie, 2008). In either variant, convergence is defined as a stochastic generalization of the deterministic condition (2.6). For the latter, all system trajectories have to converge to agreement with probability one, *i.e*.

$$\mathbb{P}\left(\lim_{k\to\infty} \Pi_{(n_\xi)}\xi_k = 0\right) = 1$$

has to hold, and the former is defined as follows:

Definition 2.6.: Mean-Square Consensus (Fagnani & Zampieri, 2009)

The MJLS $\mathcal{T}$ is said to reach *mean-square consensus* if it is asymptotically converging to the agreement space in mean-square with $w \equiv 0$, *i.e*. its state satisfies

$$\lim_{k\to\infty} \mathbb{E}\left[\left\|\Pi_{(n_\xi)}\xi_k\right\|^2\right] = 0.$$

Note that mean-square consensus and almost sure consensus can be seen as mean-square stability and almost sure stability on the disagreement space, respectively. As

such, a system is guaranteed to reach consensus almost surely if it reaches consensus in the mean-square sense (Zhang & Tian, 2009).

2.4.2. Measuring Performance with System Norms

In addition to answering the question of stability posed in the previous section, the goal of this dissertation is to study and optimize the performance of IS in the presence of stochastic packet loss. As a prerequisite, we therefore introduce two MJLS norms that are defined as generalizations of the H_2- and H_∞-norm for LTI systems. Since both of these norms are defined for the frequency domain transfer function representation of LTI systems, the extensions to MJLS have to be described in terms of their respective time-domain interpretations instead. Hence, we introduce ℓ_2^d as the set of $\mathbb{R}^d$-valued, square-summable discrete-time stochastic processes with finite norm

$$\|z\|_{\ell_2} := \sqrt{\sum_{k=0}^{\infty} \mathbb{E}\left[\|z_k\|^2\right]},$$

which simplifies to the 2-norm of square-summable sequences for deterministic signals.

The first quantity to consider is the H_2-norm, which is commonly used to model control problems of Linear-Quadratic-Gaussian type. For discrete-time LTI systems, the H_2-norm is defined as the Frobenius norm of the corresponding transfer function matrix integrated along the unit circle in the complex plane, but can analogously be calculated as the energy – *viz.* ℓ_2-norm – of the impulse response (Chen & Francis, 1995, Theorem 4.4.1). It is this second interpretation that can be extended to MJLS in a straightforward manner:

Definition 2.7.: MJLS H_2-Norm (Costa et al., 1997; do Val et al., 2002)
The H_2-norm of the mean-square stable MJLS $\mathcal{T}$ is given by

$$\|\mathcal{T}\|_{H_2} := \sqrt{\sum_{i\in\mathcal{K}} \sum_{s=1}^{Nn_w} t_i \|z^{s,i}\|_{\ell_2}^2},$$

where $z^{s,i}$ is the response of $\mathcal{T}$ to the input $w_k = e_s\delta_k$ with initial condition $\xi_0 = 0$ and $\sigma_0 = i$,

$$\delta_k := \begin{cases} 1 & \text{if } k = 0, \\ 0 & \text{else} \end{cases}$$

is the discrete-time unit impulse, and e_s is the sth canonical basis vector of $\mathbb{R}^{Nn_w}$.

Notice that while we have to calculate the expected energy of the output signal, the input w used to generate $z^{s,i}$ is deterministic, making the H_2-norm a good target for estimation using Monte-Carlo techniques.

Remark (Output Covariance Interpretation of the H_2-norm). For LTI systems, there is a 'stochastic' interpretation of the H_2-norm as the expected output power due to unit covariance white noise in addition to the 'deterministic' interpretation as the energy of the impulse response (Skogestad & Postlethwaite, 2010). Under the assumption that

the Markov chain $\{\sigma_k\}$ is ergodic (see Klenke, 2013) and that σ_0 follows its stationary distribution, a similar interpretation can be applied to MJLS (Costa et al., 2005). That is,

$$\|\mathcal{T}\|_{H_2} = \lim_{k\to\infty} \sqrt{\mathbb{E}\left[\|z_k\|^2\right]}$$

if w is zero-mean unit covariance white noise that is independent of $\{\sigma_k\}$.

Similar to the H_2-norm, the H_∞-norm is originally defined in terms of the transfer function matrix of an LTI system but is equivalently induced by the signal 2-norm as the peak energy gain of the system (Chen & Francis, 1995, Theorem 4.4.2). By extending the signal spaces to stochastic processes in ℓ_2, this time-domain interpretation generalizes to MJLS as the peak gain in the expected signal energy.

Definition 2.8.: MJLS H_∞-Norm (Costa & Marques, 1998; Seiler & Sengupta, 2003)
The H_∞-norm of the mean-square stable MJLS $\mathcal{T}$ is given by

$$\|\mathcal{T}\|_{H_\infty} := \sup_{\sigma_0\in\mathcal{K}} \sup_{0\neq w\in\ell_2^{Nn_w}} \frac{\|z\|_{\ell_2}}{\|w\|_{\ell_2}}$$

with initial condition $\xi_0 = 0$.

In the MJLS H_∞-norm as defined by Costa and Marques (1998) and Seiler and Sengupta (2003), it is not only the output signal z that is extended to the space of stochastic signals, but also the input w. This is a necessity to obtain the peak gain of the system, since the worst-case input signal w depends on the state trajectory, which is a stochastic process (Costa et al., 2005, p. 145). However, for certain scenarios, there is merit in using an adjusted definition of the norm with deterministic input signals w as done by Seiler (2001). This is discussed in detail in Section 3.4.3.

2.4.3. Decomposable Markov Jump Linear Systems

In order to benefit from the advantages of decomposable systems that were discussed in Section 2.2.3 for IS subject to stochastic packet loss, the framework has to be extended from LTI systems to MJLS. Most importantly, the stochastic switching must be integrated into the decomposable matrix structure in a way that is flexible enough to encompass the network model discussed above, but at the same time has enough structure to allow for decomposition methods to be applied.

Motivated by the stochastic difference equation (2.10) in Example 2.4, we proposed in (Hespe, Saadabadi et al., 2024) to have a mode-dependent pattern matrix S_i but to keep all other components of the decomposable matrices mode-independent. Furthermore, this model is extended by an additional mode-independent pattern matrix S^0 in order to represent interconnection patterns that do not depend on the mode in (Hespe et al., 2023). In combination, this leads to a family of matrices M_i that are structured as

$$M_i = I_N \otimes M_\mathrm{d} + S_i \otimes M_\mathrm{c} + S^0 \otimes M_\mathrm{p} \tag{2.13}$$

with M_d, M_c, and M_p being the *decoupled*, *stochastically coupled*, and *deterministically coupled* component, respectively. A *decomposable MJLS* can then be defined analogously to the LTI case of Section 2.2.3:

Definition 2.9.: Decomposable MJLS

An MJLS is called *decomposable* if all matrices of its state-space representation are decomposable with respect to the same pairs (S_i, S^0) for all modes, *i.e.* if

$$\mathcal{A}_i = I_N \otimes \mathcal{A}_\mathrm{d} + S_i \otimes \mathcal{A}_\mathrm{c} + S^0 \otimes \mathcal{A}_\mathrm{p} \tag{2.14a}$$
$$\mathcal{B}_i = I_N \otimes \mathcal{B}_\mathrm{d} + S_i \otimes \mathcal{B}_\mathrm{c} + S^0 \otimes \mathcal{B}_\mathrm{p} \tag{2.14b}$$
$$C_i = I_N \otimes C_\mathrm{d} + S_i \otimes C_\mathrm{c} + S^0 \otimes C_\mathrm{p} \tag{2.14c}$$
$$\mathcal{D}_i = I_N \otimes \mathcal{D}_\mathrm{d} + S_i \otimes \mathcal{D}_\mathrm{c} + S^0 \otimes \mathcal{D}_\mathrm{p} \tag{2.14d}$$

for all $i \in \mathcal{K}$ with suitable choice of the coupled and decoupled components.

As an example of a decomposable MJLS, consider the stochastic consensus problem introduced above:

Example 2.4.: First-Order Consensus with Packet Loss, (started on page 22)

Analogous to the deterministic case in Example 2.3, the first-order consensus problem over stochastic communication links described by

$$x_{k+1} = \left(I_N - \kappa L_{\sigma_k}\right) x_k \tag{2.10, restated}$$

can be posed in terms of a decomposable MJLS with pattern matrices $S_i = L_i$ and $S^0 = L^0$. The respective components for the coupled and decoupled parts follow as $\mathcal{A}_\mathrm{d} = 1$, $\mathcal{A}_\mathrm{c} = -\kappa$, and $\mathcal{A}_\mathrm{p} = 0$. Note that the deterministically coupled component remains unused since the only coupling between the subsystems is through the stochastic communication channel.

The system structure introduced above is not immediately compatible with the decomposition approach proposed by Massioni and Verhaegen (2009). In order to apply the decomposing transformation in the same way as in Section 2.2.3, the pattern matrices S_i and S^0 in (2.14) would have to be simultaneously diagonalizable, which, however, is generally *not* the case and would be a severe restriction on the patterns. In particular, this applies if the graph Laplacian is chosen as the pattern matrix, *e.g.* for the consensus problem in Example 2.4 (Ghadami & Shafai, 2010). Chapter 3 will therefore discuss weaker conditions than simultaneous diagonalizability of the pattern matrices that nonetheless allow decomposition methods to be applied.

2.5. Geometric Properties of Convex Sets

Having discussed all relevant system theoretic concepts in the sections above, this chapter closes by introducing a few important concepts from analytic geometry that are applied in this dissertation, especially in Chapter 5. The definitions and results stated below are taken from Rockafellar (1970).

First, we define two specific kinds of sets. A subset $\mathcal{M}$ of $\mathbb{R}^n$ is said to be an *affine set* (or *linear variety*) if $\tau x + (1-\tau)y \in \mathcal{M}$ for every pair of points $x, y \in \mathcal{M}$ and $\tau \in \mathbb{R}$. Alternatively, these are precisely those sets which can be written as $\mathcal{M} = \{x \in \mathbb{R}^n | Mx = c\}$

for some vector $c \in \mathbb{R}^d$ and matrix $M \in \mathbb{R}^{d\times n}$ (Rockafellar, 1970, Theorem 1.4). On the other hand, $\mathcal{M}$ is called *convex set* if the inclusion above holds for $\tau \in (0,1)$ instead of $\tau \in \mathbb{R}$. A specific kind of convex set is the *unit d-simplex* $\mathcal{S}_d$, which is defined as

$$\mathcal{S}_d \coloneqq \left\{ v \in \mathbb{R}^{d+1} \;\middle|\; \sum_{i=0}^{d} v_i = 1, v_i \geq 0 \right\}.$$

Corresponding to affine and convex sets, there are furthermore the *affine* and *convex hull*, which are denoted by aff $\mathcal{M}$ and conv $\mathcal{M}$, respectively. These are the unique smallest affine (or convex) set that contains $\mathcal{M}$ and are obtained as the intersection of all affine (convex) sets $\bar{\mathcal{M}}$ such that $\mathcal{M} \subseteq \bar{\mathcal{M}}$ (Rockafellar, 1970). Moreover, a point x in a convex set $\mathcal{M}$ is said to be an *extreme point* of $\mathcal{M}$ if there exist no distinct points $y, z \in \mathcal{M}$ such that $x = \tau y + (1-\tau)z$ with $\tau \in (0,1)$. The set of extreme points of $\mathcal{M}$ is denoted by $\mu(\mathcal{M}) \subseteq \mathcal{M}$.

With the usual interior, subsets $\mathcal{M} \subset \mathbb{R}^n$ only have non-empty interior if they contain an open ball in $\mathbb{R}^n$. For convex sets, it is sometimes more useful to rely on the concept of *relative interior* instead. The relative interior of a convex set $\mathcal{M}$, denoted by ri $\mathcal{M}$, is defined as the interior that results if $\mathcal{M}$ is seen as a subset of its affine hull. Correspondingly, there is the *relative boundary* of convex sets, which is the set difference between their closure and relative interior (Rockafellar, 1970, Section 6). Importantly, the relative interior (just like the affine and convex hull) distributes over the Cartesian product:

Lemma 2.6.: Hulls and Interior of Cartesian Products

Let $\mathcal{M}_1$ and $\mathcal{M}_2$ be non-empty sets. We have (Bertsekas, 2009, Problem 1.19)

$$\text{aff}(\mathcal{M}_1 \times \mathcal{M}_2) = (\text{aff}\,\mathcal{M}_1) \times (\text{aff}\,\mathcal{M}_2)$$

and

$$\text{conv}(\mathcal{M}_1 \times \mathcal{M}_2) = (\text{conv}\,\mathcal{M}_1) \times (\text{conv}\,\mathcal{M}_2).$$

Furthermore, if $\mathcal{M}_1$ and $\mathcal{M}_2$ are convex, then in addition (Bertsekas, 2009, Section 1.3)

$$\text{ri}(\mathcal{M}_1 \times \mathcal{M}_2) = (\text{ri}\,\mathcal{M}_1) \times (\text{ri}\,\mathcal{M}_2).$$

Finally, for two nested convex sets, it can be shown that the relative interior of the smaller set is contained in the relative interior of the other if it is not entirely within its boundary. This intuitive idea is formalized in the following lemma:

Lemma 2.7.: Interior Inclusion (Rockafellar, 1970, Corollary 6.5.2)

Let $\mathcal{M}_1$ be a convex set and $\mathcal{M}_2$ a convex set contained in the closure of $\mathcal{M}_1$ but not entirely within the relative boundary of $\mathcal{M}_1$. Then ri $\mathcal{M}_2 \subseteq$ ri $\mathcal{M}_1$.

Scalable Analysis of Stochastically Interconnected Linear Systems

3

With the introduction of decomposable MJLS in the previous chapter, we have found a suitable framework to model IS with stochastic packet loss. However, it has already been observed at the end of Section 2.4.3 that decoupling an IS into modal subsystems requires overly restrictive assumptions on the pattern matrices. In particular, these assumptions are violated by the Laplacian matrices L^0 and L_i, which play an important role for many problems in the realm of MAS. The goal of the current chapter is thus to develop an approach to decompose the analysis of MJLS without having to rely on simultaneous diagonalizability of all pattern matrices.

At its core, the procedure that is proposed in this chapter relies on the LMI-based formulation of stability and performance criteria for MJLS. Specifically, the mean-square stability test stems from the Lyapunov inequality (2.12) proposed by Costa and Fragoso (1993) and Ji et al. (1991), while the H_2 and H_∞ norm bounds presented in Theorems 3.11 and 3.13 are derived from matrix inequalities that were introduced in (Costa et al., 1997; do Val et al., 2002) and (Seiler & Sengupta, 2003), respectively. A key lemma on the stochastic properties of the switched graph Laplacian is furthermore inspired by work of Wu and Shi (2012), who derived a precursory statement for the special case of the consensus problem. However, for reasons of mathematical tractability, major parts of the current chapter are limited in scope to networks with independent and identically distributed packet loss. While this is generally an idealizing restriction of the communication model, it is a trade-off between model fidelity and complexity (Schenato et al., 2007), empirically justified (see Section 4.3.3), and will be revisited in Chapter 5.

The main ideas of this chapter have previously appeared in (Hespe, Saadabadi et al., 2024) but are presented here in a significantly revised form. Most importantly, system performance is discussed in terms of both the H_2- and H_∞-norm instead of being restricted to the former. Moreover, all results have been augmented by the mode-independent pattern matrix S^0 that was originally proposed in (Hespe et al., 2023), and are initially discussed for general pattern matrices S^0, S_i and later specialized to the graph Laplacian.

3.1. Decomposing Jump Linear Systems

In the original decomposable systems framework proposed by Massioni and Verhaegen (2009), the diagonalizing transformation of the pattern matrix is applied directly to the system as a state and input-output transformation, resulting in a transformed system with fully decoupled modal subsystems. An alternative perspective has been taken by Hoffmann et al. (2013) and Eichler et al. (2013) in their generalizations of the result to linear parameter-varying (LPV) systems and integral quadratic constraints, respectively.

Instead of applying the transformation to the system itself, it is suggested to take an indirect approach of decomposing the analysis conditions formulated in terms of LMIs. In this way, the decomposition can be employed without any system-theoretic considerations in a purely algebraic procedure, facilitating extensions to non-LTI systems.

Following this observation, we will study the decomposition of MJLS in terms of their analysis LMIs, starting with the condition for mean-square stability from Theorem 2.5. As a first step, note that the LMI condition (2.12) can be written as

$$\mathbb{E}\Big[\mathcal{A}_{\sigma_{k+1}}^{\top}\mathcal{X}_{\sigma_{k+1}}\mathcal{A}_{\sigma_{k+1}} \,\Big|\, \sigma_k = i\Big] \prec \mathcal{X}_i$$

for all $i \in \mathcal{K}$. After inserting the decomposable system matrix described in (2.14a) and expanding the products, observe that many terms are independent of σ_{k+1} such that they can be pulled out of the expectation. As a result, we obtain the condition

$$\begin{aligned}\big(I_N \otimes \mathcal{A}_{\mathrm{d}} + S^0 \otimes \mathcal{A}_{\mathrm{p}}\big)^{\top}\, \mathbb{E}\Big[\mathcal{X}_{\sigma_{k+1}} \,\Big|\, \sigma_k = i\Big]\big(I_N \otimes \mathcal{A}_{\mathrm{d}} + S^0 \otimes \mathcal{A}_{\mathrm{p}}\big) \\ + \big(I_N \otimes \mathcal{A}_{\mathrm{d}} + S^0 \otimes \mathcal{A}_{\mathrm{p}}\big)^{\top}\, \mathbb{E}\Big[\mathcal{X}_{\sigma_{k+1}}\big(S_{\sigma_{k+1}} \otimes \mathcal{A}_{\mathrm{c}}\big) \,\Big|\, \sigma_k = i\Big] \\ + \mathbb{E}\Big[\big(S_{\sigma_{k+1}} \otimes \mathcal{A}_{\mathrm{c}}\big)\mathcal{X}_{\sigma_{k+1}} \,\Big|\, \sigma_k = i\Big]^{\top}\big(I_N \otimes \mathcal{A}_{\mathrm{d}} + S^0 \otimes \mathcal{A}_{\mathrm{p}}\big) \\ + \mathbb{E}\Big[\big(S_{\sigma_{k+1}} \otimes \mathcal{A}_{\mathrm{c}}\big)^{\top}\mathcal{X}_{\sigma_{k+1}}\big(S_{\sigma_{k+1}} \otimes \mathcal{A}_{\mathrm{c}}\big) \,\Big|\, \sigma_k = i\Big] \prec \mathcal{X}_i,\end{aligned}$$

which can be simplified further by applying the mixed-product rule of the Kronecker product (*cf.* Lemma 2.3). Subsequently, the only expectations that have to be evaluated are $\mathbb{E}\Big[\mathcal{X}_{\sigma_{k+1}} \,\Big|\, \sigma_k = i\Big]$, $\mathbb{E}\Big[\big(S_{\sigma_{k+1}} \otimes I_{n_\xi}\big)\mathcal{X}_{\sigma_{k+1}} \,\Big|\, \sigma_k = i\Big]$, and

$$\mathbb{E}\Big[\big(S_{\sigma_{k+1}} \otimes I_{n_\xi}\big)^{\top}\mathcal{X}_{\sigma_{k+1}}\big(S_{\sigma_{k+1}} \otimes I_{n_\xi}\big) \,\Big|\, \sigma_k = i\Big] \tag{3.1}$$

for $i \in \mathcal{K}$. In principle, it is possible to calculate all of these expectations numerically by enumerating $\mathcal{K}$ since the Markov chain state-space $\mathcal{K}$ is finite. However, for the scenario that is motivating our study of decomposable MJLS, *i.e.* wirelessly networked IS that exhibit packet loss as described in Section 2.3, the cardinality of $\mathcal{K}$ grows exponentially with the number of edges in the nominal communication graph $\mathcal{G}^0$. Not only does this render the numerical evaluation of the expectations above prohibitively expensive for any IS with more than a few subsystems, but it also causes an exponential growth in the size of the resulting SDP. The reason is that there is one variable $\mathcal{X}_i$ and one LMI constraint for each $i \in \mathcal{K}$. In order to obtain a stability test that is tractable even for large-scale IS, we therefore have to apply additional simplifications.

3.1.1. Time-Independent Switching Processes

A class of MJLS for which the computational complexity of the stability test can be drastically reduced without leading to conservatism are those with switching processes $\{\sigma_k\}$ that are independent in time as described in the following assumption:

Assumption 3.1.: Independence in Time

The Markov chain $\{\sigma_k\}$ is *independent in time*, *i.e.* there exist θ_j such that $\theta_{ij} = \theta_j$ holds for all $i, j \in \mathcal{K}$, or, in other words, the TPM Θ has identical rows.

For a process $\{\sigma_k\}$ as described by Assumption 3.1, the distribution of σ_{k+1} is not merely independent of σ_k but constant for all $k \in \mathbb{N}_0$. When making Assumption 3.1, we will therefore drop the time index k when referring to an arbitrary instant of the process in order to obtain a concise notation. Furthermore, the assumption of independence implies that considering conditional expectations to test for mean-square stability is redundant and an equivalent condition to Theorem 2.5 can be posed as a single LMI:

Theorem 3.1.: Stability with Independent Switching (Costa & Fragoso, 1993)

An MJLS $\mathcal{T}$ satisfying Assumption 3.1 is asymptotically mean-square stable if and only if there exists an $\mathcal{X} \succ 0$ that solves the LMI

$$\sum_{j \in \mathcal{K}} \theta_j \mathcal{A}_j^\top \mathcal{X} \mathcal{A}_j \prec \mathcal{X}. \tag{3.2}$$

Theorem 3.1 is drastically reducing the computational effort required to verify mean-square stability since only a single matrix variable $\mathcal{X}$ and a single LMI constraint have to be considered in contrast to one of each for all $i \in \mathcal{K}$. In addition to the computational aspect, this implies that $\mathcal{X}$ is a constant weighting in the expectation that has to be evaluated instead of appearing as a random variable like in (3.1), creating the possibility to restate the stability condition in a concise form.

As a step towards this goal, we introduce a weighted generalization of the variance for matrix-valued random variables X, which we define as

$$\Xi_Q[X] \coloneqq \mathbb{E}\Big[(X - \mathbb{E}[X])^\top Q (X - \mathbb{E}[X])\Big] = \mathbb{E}[X^\top Q X] - \mathbb{E}[X]^\top Q\, \mathbb{E}[X] \tag{3.3}$$

with a constant weighting matrix $Q \succeq 0$ of compatible dimension. Note that $\Xi_Q[X]$ is equivalent to the usual variance for scalar random variables, *i.e.* $\Xi_1[X] = \mathrm{Var}[X]$ if X is scalar-valued. Furthermore, if $\Xi_Q[X]$ exists, it holds that $\Xi_Q[X] \succeq 0$ because $(X - \mathbb{E}[X])^\top Q (X - \mathbb{E}[X]) \succeq 0$ for all realizations of X. The motivation to define this generalized variance comes from the expectation of the squared pattern matrix, which, as demonstrated on the right-hand side of (3.3), can be split into two components: The variance $\Xi_Q[X]$ and the weighted square of $\mathbb{E}[X]$. Accordingly, we obtain

$$\mathbb{E}\Big[(S_\sigma \otimes I_{n_\xi})^\top \mathcal{X} (S_\sigma \otimes I_{n_\xi})\Big] = \Big(\mathbb{E}[S_\sigma] \otimes I_{n_\xi}\Big)^\top \mathcal{X} \Big(\mathbb{E}[S_\sigma] \otimes I_{n_\xi}\Big) + \Xi_{\mathcal{X}}\Big[S_\sigma \otimes I_{n_\xi}\Big],$$

which we use to reformulate the LMI (3.2) into

$$\mathbb{E}[\mathcal{A}_\sigma]^\top \mathcal{X}\, \mathbb{E}[\mathcal{A}_\sigma] + (I_N \otimes \mathcal{A}_\mathrm{c})^\top \Xi_{\mathcal{X}}\Big[S_\sigma \otimes I_{n_\xi}\Big](I_N \otimes \mathcal{A}_\mathrm{c}) \prec \mathcal{X}, \tag{3.4}$$

with the mean of the system matrix given by $\mathbb{E}[\mathcal{A}_\sigma] = I_N \otimes \mathcal{A}_\mathrm{d} + \mathbb{E}[S_\sigma] \otimes \mathcal{A}_\mathrm{c} + S^0 \otimes \mathcal{A}_\mathrm{p}$. While the concept of the *mean system* appears only as a sidenote in the current derivation, it will be taken up below in Section 3.5 in order to estimate possible conservatism in the methods described in this chapter.

3.1.2. Simultaneous Diagonalizability of Pattern Matrices

Apart from the component involving the generalized variance, condition (3.4) closely resembles the stability test of Theorem 2.2 applied to a decomposable LTI system with the two pattern matrices $\mathbb{E}[S_\sigma]$ and S^0. As such, we are restricted to decomposable MJLS for which $\mathbb{E}[S_\sigma]$ and S^0 are simultaneously diagonalizable in order to comply with the requirements discussed by Massioni and Verhaegen (2009). However, this assumption alone will in general not be sufficient to ensure that (3.4) can be decomposed since the variance $\Xi_{\mathcal{X}}[S_\sigma \otimes I_{n_\xi}]$ and expectation $\mathbb{E}[S_\sigma]$ typically cannot be diagonalized simultaneously for arbitrary $\mathcal{X}$. As one particular example, consider the special case of the consensus problem (*cf*. Example 2.4) for which Wu and Shi (2012) study a condition related to (3.4) and derive an explicit expression for $\Xi_{\mathcal{X}}[L_\sigma]$. While decomposability is not discussed by the authors, their expression does not lead to a decomposable (and thus scalable) analysis condition for unstructured Lyapunov matrices $\mathcal{X}$.

The increased difficulty in decomposing $\Xi_{\mathcal{X}}[S_\sigma \otimes I_{n_\xi}]$ compared to S^0 and $\mathbb{E}[S_\sigma]$ stems from the fact that the latter can be targeted in isolation from the Lyapunov matrix $\mathcal{X}$ due to the mixed-product rule, while $\mathcal{X}$ cannot be separated from the former in general. In order to facilitate decomposition, we therefore proceed by imposing structure onto the matrix variable $\mathcal{X}$, simplifying the variance calculations at the cost of conservatism. The idea is to mandate that $\mathcal{X}$ has a block-repeated structure, *i.e*. that $\mathcal{X}$ takes the form $\mathcal{X} = I_N \otimes Y$ for some $Y \in \mathbb{R}^{n_\xi \times n_\xi}$, since this structure is paramount to utilize the commutation property of the Kronecker product (*cf*. Section 2.2.2). With this restriction to structured matrix variables, the generalized variance can be rewritten as

$$\Xi_{\mathcal{X}}[S_\sigma \otimes I_{n_\xi}] = \Xi_{I_N \otimes Y}[S_\sigma \otimes I_{n_\xi}] = \Xi_{I_N}[S_\sigma] \otimes Y, \tag{3.5}$$

separating the variance from the Lyapunov matrix and creating the possibility to selectively apply transformations to $\Xi_{I_N}[S_\sigma]$.

Remark. Even though imposing a sparse block-repeated structure onto the matrix variable $\mathcal{X}$ might seem overly restrictive at first, similar assumptions have successfully been applied to analyse interconnected LPV systems (Hoffmann et al., 2013) and distributed first-order optimization algorithms (Sundararajan et al., 2020). Furthermore, as already discussed by Massioni and Verhaegen (2009) in their original work on decomposable systems, the distributed controller synthesis of Chapter 4 requires a related, albeit less conservative, restriction to the Lyapunov matrix regardless of the analysis conditions. In view of the simplifications achieved, the resulting conservatism is typically deemed acceptable.

Having isolated the variance term from the Lyapunov matrix, we can now apply a diagonalizing transformation to each of the coupling terms in (3.4). To successfully decompose the LMI condition in this way, the pattern matrices have to satisfy the following additional assumption:

Assumption 3.2.: Simultaneous Orthogonal Diagonalizability

There exists an orthogonal matrix U such that the terms $U^\top S^0 U$, $U^\top \mathbb{E}[S_\sigma] U$, and $U^\top \Xi_{I_N}[S_\sigma] U$ are diagonal.

Assumption 3.2 is stronger than just demanding that S^0 and $\mathbb{E}[S_\sigma]$ are simultaneously diagonalizable but does *not* imply that there exists a single transformation that diagonalizes all switched patterns S_i. Note, however, that the assumption implicitly requires S^0 and $\mathbb{E}[S_\sigma]$ to be symmetric and constrains the distribution of the switching process $\{\sigma_k\}$ in addition to the pattern pairs (S_i, S^0). Based on Assumption 3.2, we can then finally obtain a decomposed sufficient condition for mean-square stability of suitable MJLS.

Theorem 3.2.: Mean-Square Stability for Decomposable Jump Systems

A decomposable MJLS $\mathcal{T}$ satisfying Assumptions 3.1 and 3.2 is mean-square stable if there exists a $Y \succ 0$ that solves the LMIs

$$\bar{\mathcal{A}}_i^\top Y \bar{\mathcal{A}}_i + \lambda_i\Big(\Xi_{I_N}[S_\sigma]\Big)\mathcal{A}_\mathsf{c}^\top Y \mathcal{A}_\mathsf{c} \prec Y \tag{3.6}$$

for all $i \in \{1, \dots, N\}$, where $\bar{\mathcal{A}}_i = \mathcal{A}_\mathsf{d} + \lambda_i\Big(\mathbb{E}[S_\sigma]\Big)\mathcal{A}_\mathsf{c} + \lambda_i\Big(S^0\Big)\mathcal{A}_\mathsf{p}$ and $\lambda_i(M)$ denotes the ith eigenvalue of the matrix M.

Proof. First, note that $Y \succ 0$ implies $\mathcal{X} = I_N \otimes Y \succ 0$. Inserting into (3.4) and applying U from Assumption 3.2 as a congruence transformation by multiplying with $(U \otimes I_{n_\xi})^\top$ and $(U \otimes I_{n_\xi})$ from the left and right, respectively, we obtain

$$\Big(U^\top \mathbb{E}[\mathcal{A}_\sigma]U\Big)^\top \Big(I_N \otimes Y\Big)\Big(U^\top \mathbb{E}[\mathcal{A}_\sigma]U\Big) + \Big(U^\top \Xi_{I_N}[S_\sigma]U\Big) \otimes \Big(\mathcal{A}_\mathsf{c}^\top Y \mathcal{A}_\mathsf{c}\Big) \prec I_N \otimes Y$$

by the mixed-product rule and orthogonality of U. According to Assumption 3.2, this is a block-diagonal LMI with the diagonal blocks corresponding to (3.6). We conclude that $\mathcal{T}$ is mean-square stable by referring to Theorem 3.1. ■

For decomposable MJLS, Theorem 3.2 plays a role similar to that of the decomposition Theorem 2.4 of Massioni and Verhaegen (2009) in the LTI case. Instead of solving one big LMI representing the whole IS, the analysis condition is decomposed into a set of coupled but smaller LMIs. Each inequality has the size of a single subsystem, which we term *modal constraints* in analogue to the modal subsystems of Theorem 2.4. Accordingly, the number of constraints in the underlying SDP grows linearly with N, such that the result remains applicable even for very large IS.

3.2. Diagonalizing the Stochastic Laplacian

While Theorem 3.2 drastically improves the computational complexity by decomposing the analysis condition, an important issue remains to be solved before the result can be applied to specific decomposable MJLS. The problem lies in Assumption 3.2: in order to verify that a given MJLS satisfies the assumption, and thus that Theorem 3.2 is applicable, the expectation and generalized variance of S_σ have to be calculated. As outlined above, this computation may become arbitrarily expensive for switching processes $\{\sigma_k\}$ with large state-space $\mathcal{K}$, such that verifying simultaneous diagonalizability of expectation and variance may become the bottleneck in proving mean-square stability. In the current section, we will therefore consider an important special case, namely having the graph Laplacian as the pattern matrix, and provide conditions on the switching process $\{\sigma_k\}$ under which Assumption 3.2 is guaranteed to be satisfied.

3.2.1. The Heterogeneous Bernoulli Packet Loss Model

The first step in proving the simultaneous diagonalizability of expectation and variance is to derive an expression for the generalized variance of the graph Laplacian. However, with the general packet loss model described in Section 2.3, such an expression is difficult to obtain because of possible spatial dependencies between the individual edge processes $\left\{\phi_k^{ij}\right\}$. Our first additional assumption is therefore imposed to ensure that the distribution of $\{\sigma_k\}$ is such that the edge processes are spatially independent.

Assumption 3.3.: Spatial Independence of Edge Processes

The stochastic processes $\{\phi_k^{ij}\}$ and $\{\phi_k^{sr}\}$ are independent whenever $(i,j) \in \mathcal{E}^0$ and $(s,r) \in \mathcal{E}^0$ do not connect the same vertex pair, *i.e.* if $(i,j) \neq (s,r) \neq (j,i)$.

With Assumptions 3.1 and 3.3 in place, it is a natural step to consider the edge processes as individual Markov chains with state-space $\{0,1\}$ and distribution

$$\mathbb{P}\left(\phi_k^{ij} = 1\right) = p^{ij}, \qquad \mathbb{P}\left(\phi_k^{ij} = 0\right) = 1 - p^{ij},$$

where $p^{ij} \in [0,1]$ for all $(i,j) \in \mathcal{E}^0$ and $k \in \mathbb{N}_0$. This kind of stochastic process is also known as a *Bernoulli process*, which is why we call the switching of the Laplacian as described by Assumptions 3.1 and 3.3 our *heterogeneous Bernoulli packet loss model*. In particular, the model is called heterogeneous since the transmission probability varies between different communication links. This is in contrast to the *homogeneous* Bernoulli model that is introduced in Assumption 3.4 below, which imposes that the probability is identical throughout the network.

For the model at hand, it is then possible to derive an element-wise expression for the generalized variance that enables a straightforward interpretation in terms of the nominal communication graph $\mathcal{G}^0$ and the distribution of the edge processes $\left\{\phi_k^{ij}\right\}$. The result presented below is a direct consequence of (Hespe & Werner, 2023b, Lemma 3), which allows for temporal dependencies of the packet loss and therefore has to work in the more general setting of Markov chains instead of Bernoulli processes. A first version of the statement appeared in (Hespe, Saadabadi et al., 2024) under the additional hypothesis that $p^{ij} = p$ for all $(i,j) \in \mathcal{E}^0$.

Lemma 3.3.: Generalized Variance of the Laplacian

With nominal communication graph $\mathcal{G}^0$ and packet loss satisfying Assumptions 3.1 and 3.3, the generalized variance of the Laplacian is given by

$$\Xi_{I_N}\left[L(\mathcal{G}_\sigma)\right] = \mathrm{Var}\left[L(\mathcal{G}_\sigma)\right] + \mathrm{Var}\left[L(\mathcal{G}_\sigma^\top)\right].$$

Proof. Define ρ_{ij} as the elements of $\mathbb{E}[L(\mathcal{G}_\sigma)^\top L(\mathcal{G}_\sigma)]$ such that we have $\rho_{ij} = \sum_{s=1}^{N} \rho_{ij}^s$ with $\rho_{ij}^s \coloneqq \mathbb{E}[L_{si}(\mathcal{G}_\sigma) L_{sj}(\mathcal{G}_\sigma)]$ due to linearity of the expectation. By doing a five-fold case

distinction in i, j, and s, ρ_{ij}^s can be calculated as

$$\rho_{ij}^s = \begin{cases} p^{si}\,\mathbb{1}_{\mathcal{N}_s^-}(i) & \text{if } i = j \neq s, \\ \sum_{t\in\mathcal{N}_i^-}\sum_{r\in\mathcal{N}_i^-} p^{it}p^{ir} + \sum_{r\in\mathcal{N}_i^-} p^{ir}\left(1-p^{ir}\right) & \text{if } i = j = s, \\ p^{si}p^{sj}\,\mathbb{1}_{\mathcal{N}_s^-}(i)\,\mathbb{1}_{\mathcal{N}_s^-}(j) & \text{if } s \neq i \neq j \neq s, \\ -\left[\sum_{r\in\mathcal{N}_i^-} p^{ir}p^{ij} + p^{ij}\left(1-p^{ij}\right)\right]\mathbb{1}_{\mathcal{N}_i^-}(j) & \text{if } s = i \neq j, \\ -\left[\sum_{r\in\mathcal{N}_j^-} p^{ji}p^{jr} + p^{ji}\left(1-p^{ji}\right)\right]\mathbb{1}_{\mathcal{N}_j^-}(i) & \text{if } i \neq j = s, \end{cases}$$

where $\mathbb{1}_{\mathcal{M}}(x)$ denotes the set-membership indicator function

$$\mathbb{1}_{\mathcal{M}}(x) \coloneqq \begin{cases} 1 & \text{if } x \in \mathcal{M}, \\ 0 & \text{else} \end{cases}$$

for some set $\mathcal{M}$. Subtracting the expectation and summing over s, we obtain

$$\sum_{s=1}^{N}\left(\rho_{ii}^s - \mathbb{E}\left[L_{si}(\mathcal{G}_\sigma)\right]^2\right) = \sum_{r\in\mathcal{N}_i^-} p^{ir}\left(1-p^{ir}\right) + \sum_{t\in\mathcal{N}_i^+} p^{ti}\left(1-p^{ti}\right)$$

for the diagonal entries by using $\mathbb{1}_{\mathcal{N}_j^-}(i) = \mathbb{1}_{\mathcal{N}_i^+}(j)$, and

$$\sum_{s=1}^{N}\left(\rho_{ij}^s - \mathbb{E}\left[L_{si}(\mathcal{G}_\sigma)\right]\mathbb{E}\left[L_{sj}(\mathcal{G}_\sigma)\right]\right) = -p^{ij}\left(1-p^{ij}\right)\mathbb{1}_{\mathcal{N}_i^-}(j) - p^{ji}\left(1-p^{ji}\right)\mathbb{1}_{\mathcal{N}_i^+}(j)$$

for the off-diagonal ones. Noting that $\operatorname{Var}\left[\phi^{ij}\right] = p^{ij}\left(1-p^{ij}\right)$, these correspond to the element-wise variance of $L(\mathcal{G}_\sigma)$ and $L(\mathcal{G}_\sigma^\top)$, respectively. ■

Lemma 3.3 shows that the generalized variance of the switching Laplacian in the heterogeneous Bernoulli packet loss model can be calculated as the Laplacians of two weighted graphs: The nominal graph $\mathcal{G}^0$ and its transpose, each weighted with the variances of the corresponding edge processes. Note that $L(\mathcal{G}^\top) = L(\mathcal{G})^\top$ if and only if $\mathcal{G}$ is balanced since the in- and out-neighbourhoods are swapped.

A related statement extending beyond unit weights has previously been presented by Wu and Shi (2012). However, the resulting expression is not interpretable in terms of the nominal graph and the edge processes since it consists of multiple sums that assemble the variance in an element-wise fashion. Moreover, the statement is valid only for a special case of the *homogeneous* Bernoulli packet loss model to be discussed next.

3.2.2. Homogeneous Packet Loss Probabilities

Even though the heterogeneous Bernoulli packet loss model of the previous section has brought us closer to our goal of proving that the switched Laplacian fulfils Assumption 3.2, it still has to be shown that the expectation and variance of the Laplacian can be diagonalized simultaneously. However, in the decomposable systems framework, homogeneous features are preferable to heterogeneous ones because they are simpler

to accommodate. This is the case not only for the subsystem dynamics but also other components, *e.g.* the scheduling variables in the extension to LPV systems (Hoffmann et al., 2013). For this reason, we are restricting ourselves to homogeneous packet loss probabilities for the current chapter and return to the heterogeneous case in Chapter 5.

Assumption 3.4.: Homogeneous Bernoulli Packet Loss Model

In addition to Assumptions 3.1 and 3.3, the edge processes $\left\{\phi_k^{ij}\right\}$ have a homogeneous success probability, *i.e.* there exists a $p \in [0,1]$ such that $p^{ij} = p$ and thus

$$\mathbb{P}\left(\phi_k^{ij} = 1\right) = p \qquad \mathbb{P}\left(\phi_k^{ij} = 0\right) = 1 - p$$

for all $k \in \mathbb{N}_0$ and $(i,j) \in \mathcal{E}^0$.

For any fixed time $k \in \mathbb{N}_0$, the random graph $\mathcal{G}_{\sigma_k}$ resulting from Assumption 3.4 is an instance of a *reliability network* as described by Janson et al. (2000). That is, $\mathcal{G}_{\sigma_k}$ is generated by independently removing edges from a given graph (the nominal graph in our case) with probability $1 - p$. In case $\mathcal{G}^0$ is the complete graph of N vertices, we obtain the often used *Erdős–Rényi model* $\mathcal{G}(N,p)$ for random graphs, sometimes called binomial random graphs (Janson et al., 2000).

A particular feature of these networks is that the expectation and variance of their Laplacian are scaled versions of the nominal Laplacian L^0, *i.e.* we obtain $\mathbb{E}[L_\sigma] = pL^0$ and $\mathrm{Var}[L_\sigma] = p(1-p)L^0$. This is used in the next lemma to prove that Assumption 3.2 can be satisfied by choosing the Laplacian as the pattern matrix. A related result without the mode-independent pattern S^0 was shown by Hespe, Saadabadi et al. (2024).

Lemma 3.4.: Laplacian Diagonalizability

Given a nominal communication graph $\mathcal{G}^0$ and packet loss satisfying Assumption 3.4, the choice $S^0 = L^0$ and $S_i = L_i$ satisfies Assumption 3.2 if and only if $\mathcal{G}^0$ is undirected.

Proof. First, note that the existence of an orthogonal transformation that diagonalizes L^0 is equivalent to L^0 being symmetric, which is the case if and only if $\mathcal{G}^0$ is undirected. We therefore only have to show that L^0, $\mathbb{E}[L_\sigma]$, and $\Xi_{I_N}[L_\sigma]$ are simultaneously diagonalizable if the nominal Laplacian is symmetric. Since all undirected graphs are balanced, it follows that $L\left((\mathcal{G}^0)^\top\right) = L(\mathcal{G}^0)^\top = L^0$ and, from Assumption 3.4 and Lemma 3.3, that $\mathbb{E}[L_\sigma] = pL^0$ and $\Xi_{I_N}[L_\sigma] = 2p(1-p)L^0$, thus simultaneous diagonalizability is guaranteed. ■

The condition that the nominal graph $\mathcal{G}^0$ has to be undirected is limiting which kind of control problems Lemma 3.4 applies to. While undirected graphs are sufficient to implement consensus and formation control problems, other scenarios, such as leader-follower schemes, require directed communication (Olfati-Saber et al., 2007). A similar restriction is known from the extension of the decomposable systems framework to LPV systems by Hoffmann and Werner (2015b) and Hoffmann et al. (2013), where it was proposed to introduce fictitious communication channels. However, the proposed solution does not extend to the mean-square analysis above due to the variance term $\Xi_{I_N}[L_\sigma]$. Furthermore, the class of graphs considered cannot be extended to directed graphs even if the *a priori* assumption of an undirected $\mathcal{G}^0$ is waived:

Proposition 3.5.: Laplacian Commutation

The Laplacians $L(\mathcal{G})$ and $L(\mathcal{G}^\top)$ commute if and only if $L(\mathcal{G})$ is normal, i.e. *if and only if $L(\mathcal{G})L(\mathcal{G})^\top = L(\mathcal{G})^\top L(\mathcal{G})$.*

Proof. First, assume that $L(\mathcal{G})$ is normal. As shown in (Wu & Chua, 1995, Lemma 4), any normal matrix with zero row-sum does also have zero column-sum, therefore $\mathcal{G}$ is balanced and $L(\mathcal{G}^\top) = L(\mathcal{G})^\top$, which commutes with $L(\mathcal{G})$ since it is normal.

On the other hand, assume that $L(\mathcal{G})$ and $L(\mathcal{G}^\top)$ commute. We then rewrite the Laplacian matrices as $L(\mathcal{G}) = \Delta^- - A$ and $L(\mathcal{G}^\top) = \Delta^+ - A^\top$, where Δ^- and Δ^+ are the in- and out-degree matrices, *i.e.* diagonal matrices that contain the in- and out-degrees of the nodes on their diagonal, and A is the adjacency matrix of $\mathcal{G}$ (see Mesbahi & Egerstedt, 2010). Then, define $\tilde{\Delta} \coloneqq \Delta^+ - \Delta^- = L(\mathcal{G}^\top) - L(\mathcal{G})^\top$ such that

$$L(\mathcal{G})\Big(L(\mathcal{G})^\top + \tilde{\Delta}\Big) = L(\mathcal{G})L(\mathcal{G}^\top) = L(\mathcal{G}^\top)L(\mathcal{G}) = \Big(L(\mathcal{G})^\top + \tilde{\Delta}\Big)L(\mathcal{G}),$$

which is equivalent to

$$L(\mathcal{G})L(\mathcal{G})^\top - L(\mathcal{G})^\top L(\mathcal{G}) = \tilde{\Delta}L(\mathcal{G}) - L(\mathcal{G})\tilde{\Delta} = A\tilde{\Delta} - \tilde{\Delta}A = A \circ \Big(\mathbf{1}\mathbf{1}^\top\tilde{\Delta} - \tilde{\Delta}\mathbf{1}\mathbf{1}^\top\Big),$$

where $M_1 \circ M_2$ denotes the Hadamard product. Note that the left-hand side is symmetric, and therefore the right-hand side also has to be. Since $\mathbf{1}\mathbf{1}^\top\tilde{\Delta} - \tilde{\Delta}\mathbf{1}\mathbf{1}^\top$ is skew-symmetric and A has non-negative entries (and hence cannot change the sign of the off-diagonal elements), this is only possible if the right-hand side is the zero matrix. Accordingly, $L(\mathcal{G})L(\mathcal{G})^\top - L(\mathcal{G})^\top L(\mathcal{G}) = 0$, implying that $L(\mathcal{G})$ is normal. ■

Since diagonalizable matrices are simultaneously diagonalizable if and only if they commute (Horn & Johnson, 2017, Theorem 1.3.12), Proposition 3.5 shows that the above techniques only apply to graphs with normal Laplacian even if the requirement of an orthogonal diagonalizing transformation would be removed from Assumption 3.2.

3.3. Stability and Consensus with Bernoulli Packet Loss

With the groundwork laid by Theorem 3.2 and Lemma 3.4 in the previous two sections, we are now ready to state a scalable sufficient condition for mean-square stability of IS subject to homogeneous Bernoulli packet loss as described by Assumption 3.4. In its original form given by Hespe, Saadabadi et al. (2024), the result is formulated without deterministically coupled component $\mathcal{A}_\mathrm{p}$, the required extension is however minor.

Theorem 3.6.: Mean-Square Stability

A decomposable MJLS $\mathcal{T}$ with L^0 and L_σ as patterns, an undirected nominal graph $\mathcal{G}^0$, and packet loss satisfying Assumption 3.4 is mean-square stable if there exists a $Y \succ 0$ that solves the LMI

$$\bar{\mathcal{A}}_i^\top Y \bar{\mathcal{A}}_i + 2p(1-p)\lambda_i \mathcal{A}_\mathrm{c}^\top Y \mathcal{A}_\mathrm{c} \prec Y \tag{3.7}$$

for $i \in \{1, N\}$, where $\bar{\mathcal{A}}_i$ denotes $\mathcal{A}_\mathrm{d} + \lambda_i(p\mathcal{A}_\mathrm{c} + \mathcal{A}_\mathrm{p})$ and λ_i are the eigenvalues of L^0.

Proof. Inserting $S^0 = L^0$ and $S_i = L_i$ into (3.6) of Theorem 3.2 and applying Lemma 3.3, we obtain

$$M(\lambda_i) \coloneqq \bar{\mathcal{A}}_i^\top Y \bar{\mathcal{A}}_i + 2p(1-p)\lambda_i \mathcal{A}_\mathrm{c}^\top Y \mathcal{A}_\mathrm{c} \prec Y,$$

which has to be verified for all eigenvalues of L^0. Furthermore, note that $M(\lambda)$ is a quadratic polynomial in λ with matrix-valued coefficients, where the coefficient for λ^2 is $(p\mathcal{A}_\mathrm{c} + \mathcal{A}_\mathrm{p})^\top Y (p\mathcal{A}_\mathrm{c} + \mathcal{A}_\mathrm{p})$. Since this is a positive semidefinite matrix, $M(\lambda)$ is convex in λ and it is sufficient to verify $M(\lambda_1) \prec Y$ and $M(\lambda_N) \prec Y$ with the smallest and largest eigenvalue of L^0, respectively. ■

With Theorem 3.6, we now have a scalable sufficient condition to test for mean-square stability of IS that are subject to homogeneous Bernoulli packet loss. Because neither the size nor the number of variables and constraints depend on the number of subsystems, the condition can be applied to IS of arbitrary size without computational complexity issues. This is in stark contrast to the original stability condition in Theorem 3.1, for which the size of the matrix variable and constraint grows quadratically with N and, even worse, the number of sum terms needed to construct the LMI is exponential in the number of edges of the nominal communication graph. The consequence of this simplification is that the above condition is sufficient but *not* necessary, the sole cause of which is the structure of $I_N \otimes Y$ that is imposed on the Lyapunov matrix $\mathcal{X}$. Furthermore, the result is only applicable to systems satisfying Assumption 3.4 which is restrictive despite its empirical justification. Nonetheless, since it would have been intractable to obtain any kind of statement about stability of large IS with Theorem 3.1, even a conservative stability test is valuable.

A distinctive feature of Theorem 3.6 is that only partial knowledge about the nominal Laplacian, and thus the interconnection topology, is required. Instead of the whole spectrum of L^0, it is sufficient to know the lower bound $\lambda_1 = 0$ and an upper bound λ_N, which can be obtained from Proposition 2.1. At the same time, this renders the stability test robust against uncertain communication topologies: Since only the boundary of the spectrum is considered, the IS is guaranteed to be mean-square stable for all undirected $\mathcal{G}^0$ whose spectrum is upper bounded by λ_N. This highlights the conservatism of the result since knowledge about specific features of the communication graph cannot be utilized. Note, however, that with the proof above the result is robust against uncertain but constant $\mathcal{G}^0$, not time-varying ones, in contrast to similar results for IS without packet loss, *e.g.* Pilz et al. (2009). This aspect is reconsidered in Chapter 6.

3.3.1. Mean-Square Convergence on the Disagreement Space

For some distributed control problems, *e.g.* the consensus problem introduced in Section 2.2.1, asymptotic (mean-square) stability is not the relevant property to evaluate success. Typically, these are control problems in which we do not care about the absolute state of the IS but only about the states of the subsystems relative to each other, which therefore have a whole subspace of equilibria spanned by the agreement vector $\mathbf{1}_N$. Since that implies that these systems are marginally stable at best, we have to establish an alternative result focussed on reaching mean-square consensus instead of stability.

The approach we take to analyse consensus problems and other related control problems is to separate the dynamics that evolve on the agreement space $\{\alpha \mathbf{1}_N \mid \alpha \in \mathbb{R}\}$ from

those that evolve in its orthogonal complement, the disagreement space. For interconnected LTI systems without packet loss, this amounts to ignoring the modal subsystem that corresponds to $\lambda_1 = 0$ since the respective eigenvector is $\mathbf{1}_N$ (Fax & Murray, 2004). Similarly, these arguments also apply to the modal constraints in Theorem 3.2, which we exploit for the following theorem:

Theorem 3.7.: Mean-Square Consensus

A decomposable MJLS $\mathcal{T}$ with L^0 and L_σ as patterns, an undirected nominal graph $\mathcal{G}^0$, and packet loss satisfying Assumption 3.4 reaches mean-square consensus if there exists a $Y \succ 0$ that solves

$$\bar{\mathcal{A}}_i^\top Y \bar{\mathcal{A}}_i + 2p(1-p)\lambda_i \mathcal{A}_\mathsf{c}^\top Y \mathcal{A}_\mathsf{c} \prec Y \tag{3.8}$$

for $i \in \{2, N\}$, where $\bar{\mathcal{A}}_i$ denotes $\mathcal{A}_\mathsf{d} + \lambda_i(p\mathcal{A}_\mathsf{c} + \mathcal{A}_\mathsf{p})$ and λ_i are the eigenvalues of L^0.

Proof. According to Definition 2.6, we have to show that $\lim_{k\to\infty} \mathbb{E}\left[\|\Pi_{(n_\xi)}\xi_k\|^2\right] = 0$ for all initial states, where Π is the projection onto the disagreement space defined in (2.5) on page 16. As the first step, apply U, the orthogonal diagonalizing transformation of L^0, to the state as $\tilde{\xi}_k := U_{(n_\xi)}^\top \xi_k$, where we partition the transformed state as

$$\tilde{\xi}_k = \begin{bmatrix} \xi_k^{\mathrm{cg}} \\ \xi_k^{\delta} \end{bmatrix} \quad \text{conforming to our choice of} \quad U^\top = \begin{bmatrix} \mathbf{1}_N^\top/\sqrt{N} \\ \tilde{U}^\top \end{bmatrix}. \tag{3.9}$$

In contrast to the LTI case, the transformed system does not decompose into N decoupled subsystems, but we obtain

$$U_{(n_\xi)}^\top \mathcal{A}_i U_{(n_\xi)} = \begin{bmatrix} 1 & 0 \\ 0 & I_{N-1} \end{bmatrix} \otimes \mathcal{A}_\mathsf{d} + \begin{bmatrix} 0 & \frac{1}{\sqrt{N}}\mathbf{1}_N^\top L_i \tilde{U} \\ 0 & \tilde{U}^\top L_i \tilde{U} \end{bmatrix} \otimes \mathcal{A}_\mathsf{c} + \begin{bmatrix} 0 & 0 \\ 0 & \Lambda \end{bmatrix} \otimes \mathcal{A}_\mathsf{p} \tag{3.10}$$

where Λ is a diagonal matrix containing the eigenvalues λ_2 to λ_N. Furthermore, observe that Π satisfies $\Pi U = \begin{bmatrix} 0 & \tilde{U} \end{bmatrix}$ such that $\left\|\Pi_{(n_\xi)}\xi_k\right\| = \left\|\Pi_{(n_\xi)}U_{(n_\xi)}\tilde{\xi}_k\right\| = \left\|\tilde{U}_{(n_\xi)}\xi_k^\delta\right\| = \left\|\xi_k^\delta\right\|$. Since (3.10) is in upper block-triangular form, it is therefore sufficient to show that the MJLS corresponding to its bottom-right block is mean-square stable.

The issue with verifying the stability of the bottom-right subsystem using condition (3.4) lies in the generalized variance: While the expectation can be evaluated as

$$\mathbb{E}\left[\tilde{U}^\top L_\sigma \tilde{U}\right] = \tilde{U}^\top \mathbb{E}[L_\sigma]\tilde{U} = p\tilde{U}^\top L^0 \tilde{U} = p\Lambda,$$

the variance required is $\Xi_{I_N}[\tilde{U}^\top L_\sigma \tilde{U}] = \tilde{U}^\top \Xi_\Pi[L_\sigma]\tilde{U}$ because of $\tilde{U}\tilde{U}^\top = \Pi$ such that Lemma 3.3 is not applicable. However, note that because $\Xi_Q[X]$ is linear in the weight Q and $I_N = \Pi + \frac{1}{N}\mathbf{1}_N\mathbf{1}_N^\top$, we have

$$\Xi_{I_N}[L_\sigma] = \Xi_\Pi[L_\sigma] + \frac{1}{N}\Xi_{\mathbf{1}_N\mathbf{1}_N^\top}[L_\sigma] \qquad \Rightarrow \qquad \Xi_{I_N}[L_\sigma] \succeq \Xi_\Pi[L_\sigma]$$

and can therefore overestimate $\Xi_\Pi[L_\sigma]$ by $\Xi_{I_N}[L_\sigma]$. Consequently, apply Lemma 3.3 to obtain $\tilde{U}^\top \Xi_{I_N}[L_\sigma]\tilde{U} = 2p(1-p)\Lambda$. Inserting the expectation and overestimated variance into (3.4) with the structured Lyapunov matrix $\mathcal{X} = I_{N-1} \otimes Y$, we arrive at a block-diagonal LMI such that we can apply the convexity argument from the proof of Theorem 3.6 to arrive at the consensus condition above. ∎

Like the stability condition above, Theorem 3.7 imposes two LMI constraints and its single matrix variable has a size that only depends on n_ξ, the number of states for each subsystem, and importantly not the number of subsystems, such that the favourable scalability properties of Theorem 3.6 transfer. Moreover, it is sufficient to have information about the boundary of the Laplacian spectrum, this time in terms of an upper *and* a lower bound. While the upper bound on λ_N can be obtained as before from Proposition 2.1, λ_2 can be bounded from below using Cheeger's inequality (Mesbahi & Egerstedt, 2010, Section 2.4.2). As such, λ_2 is related to the smallest number of edges that have to be removed from the graph before it splits into two disconnected components.

3.3.2. A Discussion on Boundedness of the Average State

Because of the way that consensus is introduced in Definitions 2.2 and 2.6, Theorem 3.7 completely ignores the behaviour of the average subsystem state. Therefore, even though the theorem guarantees that the relative states of the subsystems asymptotically converge to 0, the behaviour of their absolute states is unknown. A desirable property would thus be that the average state is bounded.

If the graph $\mathcal{G}_i$ is balanced for all $i \in \mathcal{K}$, the first subsystem in (3.10) decouples from the other subsystems since $\mathbf{1}_N$ is both a left and right eigenvector of L_{σ_k} at all times. The behaviour of the average subsystem state is therefore described by the autonomous LTI system $\xi^{\mathrm{cg}}_{k+1} = \mathcal{A}_{\mathrm{d}}\xi^{\mathrm{cg}}_k$, *i.e.* the desired property is achieved if $\mathcal{A}_{\mathrm{d}}$ is marginally stable. On the other hand, the situation becomes more difficult if $\mathcal{G}_i$ is not guaranteed to be balanced such as in the packet loss model described by Assumption 3.4. In that case, the average state cannot be considered in isolation since the coupling through the top-right block of (3.10) persists. Instead, it is now described by the LTI system

$$\xi^{\mathrm{cg}}_{k+1} = \mathcal{A}_{\mathrm{d}}\xi^{\mathrm{cg}}_k + \tilde{w}_k \qquad \text{with} \qquad \tilde{w}_k \coloneqq \frac{1}{\sqrt{N}}\Big(\big(\mathbf{1}_N^\top L_{\sigma_k}\tilde{U}\big) \otimes \mathcal{A}_{\mathrm{c}}\Big)\xi^{\delta}_k, \tag{3.11}$$

where $\tilde{w}_k$ acts as a stochastic input disturbance.

The question is therefore whether $\mathcal{T}$ reaching consensus and marginal stability of $\mathcal{A}_{\mathrm{d}}$ are sufficient to ensure boundedness, which is formalized in Conjecture 3.8. For simplicity, we assume that $\xi^{\mathrm{cg}}_0 = 0$ and hence consider only the forced response of the systems. However, the general case can be recovered as a superposition with the free response, which is guaranteed to be bounded if $\mathcal{A}_{\mathrm{d}}$ is marginally stable.

Conjecture 3.8.: Almost Sure Boundedness of the Average State

Let the decomposable MJLS $\mathcal{T}$ with L^0 and L_σ as patterns reach mean-square consensus, $\max_i\big|\lambda_i(\mathcal{A}_{\mathrm{d}})\big| \leq 1$, all $\lambda_i(\mathcal{A}_{\mathrm{d}})$ with $\big|\lambda_i(\mathcal{A}_{\mathrm{d}})\big| = 1$ have equal algebraic and geometric multiplicity, and $\xi^{\mathrm{cg}}_0 = 0$. Then there exists a $d > 0$ such that

$$\mathbb{P}\Big(\big\|\xi^{\mathrm{cg}}_k\big\| \leq d\big\|\xi^{\delta}_0\big\| \;\; \forall\, k \in \mathbb{N}_0\Big) = 1$$

for all initial states ξ^{δ}_0.

The above result is stated in terms of a conjecture since we are only able to give a partial proof for its validity. As a first step, suppose $\tilde{w}_k$ was a deterministic signal perturbing

the LTI system (3.11) with initial state $\xi_0^{\mathrm{cg}} = 0$. Accordingly, its state trajectory is given by the forced response $\xi_k^{\mathrm{cg}} = \sum_{i=0}^{k-1} \mathcal{A}_{\mathrm{d}}^{k-i-1} \tilde{w}_i$, which leads to

$$\left\|\xi_k^{\mathrm{cg}}\right\| \leq \sum_{i=0}^{k-1} \left\|\mathcal{A}_{\mathrm{d}}^{k-i-1} \tilde{w}_i\right\| \leq \sum_{i=0}^{k-1} \left\|\mathcal{A}_{\mathrm{d}}^{k-i-1}\right\| \|\tilde{w}_i\| \leq \max_{0\leq i<k} \left\|\mathcal{A}_{\mathrm{d}}^{i}\right\| \sum_{i=0}^{k-1} \|\tilde{w}_i\| \leq \sup_{i\geq 0} \left\|\mathcal{A}_{\mathrm{d}}^{i}\right\| \sum_{i=0}^{\infty} \|\tilde{w}_i\|$$

for all $k \in \mathbb{N}$ by taking norms on both sides and applying the triangle inequality. Converting $\mathcal{A}_{\mathrm{d}}$ into its Jordan normal form, we see that $\sup_{i\geq 0} \|\mathcal{A}_{\mathrm{d}}^{i}\|$ can be determined independently for each of the Jordan blocks, which contribute finite terms if either $\lambda_i(\mathcal{A}_{\mathrm{d}}) < 1$ or $\lambda_i(\mathcal{A}_{\mathrm{d}}) = 1$ and the size of the block is one. For marginal stable $\mathcal{A}_{\mathrm{d}}$, the state is therefore bounded for all deterministic $\tilde{w}_k$ that are absolutely summable.

In order to transfer the argument to the stochastic disturbance defined in (3.11), we have to show that randomly sampled realizations of $\tilde{w}_k$ are absolutely summable with probability 1. As discussed in Section 2.4.1, asymptotic mean-square stability implies almost sure asymptotic stability and is furthermore equivalent to exponential mean-square stability. We therefore work under the unproven hypothesis that almost sure *exponential* stability follows, *i.e.* that there exist a $c > 0$ and a $\rho \in [0,1)$ such that

$$\mathbb{P}\left(\left\|\xi_k^{\delta}\right\| \leq c\rho^k \left\|\xi_0^{\delta}\right\| \ \ \forall k \in \mathbb{N}_0\right) = 1. \tag{3.12}$$

A related concept of an almost sure exponential convergence rate has been discussed by Bolzern et al. (2004). Finally, since all exponentially converging sequences are absolutely summable, the above hypothesis implies that $\tilde{w}_k$ is absolutely summable with probability 1, such that d of Conjecture 3.8 can be chosen as

$$d = \frac{c}{(1-\rho)\sqrt{N}} \sup_{i\geq 0} \left\|\mathcal{A}_{\mathrm{d}}^{i}\right\| \max_{j\in\mathcal{K}} \left\|\left(\mathbf{1}_N^{\top} L_j \tilde{U}\right) \otimes \mathcal{A}_{\mathrm{c}}\right\|.$$

The missing link in the outlined argument therefore lies in establishing (3.12) based on $\mathcal{T}$ reaching mean-square consensus.

3.3.3. Convergence of First-Order Integrators

Before widening the scope of the analysis towards performance analysis, let us apply the above results to the stochastic first-order consensus problem of Example 2.4. Since for this problem $\mathcal{A}_{\mathrm{d}} = 1$ and $\mathcal{A}_{\mathrm{c}} = -\kappa$, the LMI (3.8) turns into a scalar inequality and can be solved analytically, leading to the following general statement:

Proposition 3.9.: Mean-Square First-Order Consensus

The first-order integrators of Example 2.4 with a communication network that satisfies Assumption 3.4 reach mean-square consensus for all $p \in (0,1]$ if $\mathcal{G}^0$ is connected and

$$0 < \kappa < \frac{2}{\lambda_N} \leq \frac{1}{\max_{i\in\mathcal{V}} d_i}. \tag{3.13}$$

Proof. Inserting the first-order integrator into (3.8), we have to find a $Y > 0$ such that

$$(1 - \kappa\lambda p)^2 Y + 2p(1-p)\lambda\kappa^2 Y < Y$$

for the non-zero eigenvalues λ. Dividing by Y and subtracting 1 leads to

$$p^2\lambda^2\kappa^2 + 2p\lambda\kappa^2 < 2p\lambda\kappa + 2p^2\lambda\kappa^2 \qquad \Leftrightarrow \qquad p\kappa(p\lambda + 2) < 2p(1 + p\kappa)$$

since $\lambda, \kappa > 0$. This statement is false for $p = 0$, but is equivalent to

$$\kappa < \frac{2}{p(\lambda - 2) + 2} \tag{3.14}$$

for $p > 0$. Since $\lambda_N \geq 2$ by Proposition 2.1, the denominator satisfies

$$\max_{\lambda \in \{\lambda_2, \lambda_N\}} \sup_{p \in (0,1]} p(\lambda - 2) + 2 = \lambda_N$$

and therefore (3.14) holds under the hypothesis of the proposition. Finally, the second bound follows since $\lambda_N < 2 \max_{i \in \mathcal{V}} d_i$ by Proposition 2.1. ■

Proposition 3.9 shows that the consensus problem introduced in Example 2.4 is hardly affected by the homogeneous Bernoulli packet loss model considered here, since the convergence condition (3.13) is the same as in the deterministic case (Olfati-Saber et al., 2007). As such, stability (or, in case of the consensus problem, convergence) is not an issue if the open loop is marginally stable, and the focus should rather be on system performance. On the other hand, it is not surprising that the protocol stops working for $p = 0$, since this implies that there is almost surely no communication in the network, such that the consensus protocol cannot drive the integrators to convergence. However, the result serves only as an example for the applicability of Theorem 3.7, since stronger results under weaker assumption on the communication network have been obtained before, *e.g.* (Fagnani & Zampieri, 2008; Hatano & Mesbahi, 2005; Matei et al., 2008; Tahbaz-Salehi & Jadbabaie, 2008).

3.4. Bounding the Control Performance

In the preceding sections, it has only been discussed how to analyse mean-square stability for large IS (and in the broader sense also mean-square consensus). Our next task is therefore to apply the techniques introduced above to derive scalable conditions to upper bound the control performance of such IS, in terms of both the MJLS H_2- and H_∞-norm. The resulting performance bounds do not only provide us with an effective method to compare IS and thus study the effect of stochastic packet loss, but moreover serve as a basis for the distributed controller synthesis that is discussed in Chapter 4.

3.4.1. Analysing LQ-Type Problems with the H_2-Norm

The first performance criterion we consider is the MJLS H_2-norm, which by Definition 2.7 describes the expected energy of the impulse response. For LTI systems, it is well known that the H_2-norm can be computed from the Gramian matrices, either through solving a Lyapunov equation (Chen & Francis, 1995) or as an LMI constrained SDP (de Oliveira et al., 1999). Similarly, there exist multiple different but equivalent results to compute the MJLS H_2-norm from Costa et al. (1997) and do Val et al. (2002), both in terms of the

controllability and observability Gramian. However, the conditions for general MJLS with a time-dependent switching process $\{\sigma_k\}$ suffer from the same scalability issues for large state-spaces $\mathcal{K}$ as discussed for the mean-square stability analysis in Section 3.1. Under Assumption 3.1, *i.e.* a time-independent switching law $\{\sigma_k\}$, this can be alleviated with the formulation obtained by Fioravanti et al. (2012):

Theorem 3.10.: H_2-Norm Calculation (Fioravanti et al., 2012)

A mean-square stable MJLS $\mathcal{T}$ has H_2-norm less than $\gamma > 0$ if and only if there exist $\mathcal{X}_i > 0$ and a symmetric $\mathcal{Z}$ with $\operatorname{tr}\mathcal{Z} < \gamma^2$ that solve the LMIs

$$\sum_{j\in\mathcal{K}} \theta_{ij}\left(\mathcal{A}_j^\top \mathcal{X}_j \mathcal{A}_j + C_j^\top C_j\right) \prec \mathcal{X}_i \tag{3.15a}$$

and

$$\sum_{j\in\mathcal{K}} t_j\left(\mathcal{B}_j^\top \mathcal{X}_j \mathcal{B}_j + \mathcal{D}_j^\top \mathcal{D}_j\right) \prec \mathcal{Z} \tag{3.15b}$$

for all $i \in \mathcal{K}$. In particular, this holds with $\mathcal{X}_i = \mathcal{X} > 0$ if $\mathcal{T}$ satisfies Assumption 3.1.

Remark. Theorem 3.10 reformulates the condition of Fioravanti et al. (2012) by introducing $\mathcal{Z}$ as an auxiliary variable. Their equivalence can be established by using the fact that $M_1 \prec M_2$ implies $\operatorname{tr} M_1 < \operatorname{tr} M_2$ for symmetric M_1 and M_2 and on the other hand choosing $\mathcal{Z} = \varepsilon I + \sum_{j\in\mathcal{K}} t_j\left(\mathcal{B}_j^\top \mathcal{X}_j \mathcal{B}_j + \mathcal{D}_j^\top \mathcal{D}_j\right)$ with sufficiently small $\varepsilon > 0$.

The LMI condition (3.15) is closely related to the mean-square stability test in Theorem 3.1 such that we can apply the decomposing procedure of Section 3.1 in the same way. In particular, (3.15a) simplifies to a single LMI under Assumption 3.1 and can be rephrased as

$$\mathbb{E}[\mathcal{A}_\sigma^\top \mathcal{X} \mathcal{A}_\sigma] + \mathbb{E}[C_\sigma^\top C_\sigma] \prec \mathcal{X},$$

where the first term corresponds exactly to the stability condition in (3.4). Furthermore, we may split the second component by employing the generalized variance, resulting in

$$\mathbb{E}[C_\sigma^\top C_\sigma] = \mathbb{E}[C_\sigma]^\top \mathbb{E}[C_\sigma] + \Xi_{I_N}[S_\sigma] \otimes (C_\mathrm{c}^\top C_\mathrm{c})$$

with the simple to compute expectation of the output matrix C_σ and the unweighted generalized variance. Note that no simplifications were necessary to obtain this unweighted variance for the output matrices since, in contrast to the LMI considered in Section 3.1.2, the product does not involve the Lyapunov matrix $\mathcal{X}$. Finally, by imposing $\mathcal{X} = I_N \otimes Y$ as above, we reach the existence of $Y \succ 0$ such that

$$\mathbb{E}[\mathcal{A}_\sigma]^\top (I_N \otimes Y)\, \mathbb{E}[\mathcal{A}_\sigma] + \mathbb{E}[C_\sigma]^\top \mathbb{E}[C_\sigma] + \Xi_{I_N}[S_\sigma] \otimes \left(\mathcal{A}_\mathrm{c}^\top Y \mathcal{A}_\mathrm{c} + C_\mathrm{c}^\top C_\mathrm{c}\right) \prec I_N \otimes Y \tag{3.16}$$

as a sufficient condition for (3.15a). Referring to Assumption 3.2, this LMI can be decomposed into modal constraints as done in Theorem 3.2 for mean-square stability. Likewise, applying the same procedure to (3.15b) *without* restricting $\mathcal{Z}$ leads to a decomposable condition for the second LMI.

For ease of exposition, we present the resulting LMI condition directly for the special case where the Laplacian assumes the role of the pattern matrix. However, the approach can be extended to general pattern matrices S^0 and S_i. The original formulation of the

theorem appeared in (Hespe, Saadabadi et al., 2024) without the mode-independent pattern matrix, which was subsequently added by Hespe et al. (2023).

Theorem 3.11.: Bounded H_2-Norm (Hespe et al., 2023)

A decomposable MJLS $\mathcal{T}$ with L^0 and L_σ as patterns, an undirected nominal graph $\mathcal{G}^0$, and packet loss satisfying Assumption 3.4 is mean-square stable and has H_2-norm less than $\gamma > 0$ if there exists a $Y \succ 0$ and symmetric Z_i with $\sum_{i=1}^{N} \operatorname{tr} Z_i < \gamma^2$ that solve the LMIs

$$\bar{\mathcal{A}}_i^\top Y \bar{\mathcal{A}}_i + \bar{\mathcal{C}}_i^\top \bar{\mathcal{C}}_i + 2p(1-p)\lambda_i\left(\mathcal{A}_\mathrm{c}^\top Y \mathcal{A}_\mathrm{c} + \mathcal{C}_\mathrm{c}^\top \mathcal{C}_\mathrm{c}\right) \prec Y, \tag{3.17a}$$

$$\bar{\mathcal{B}}_i^\top Y \bar{\mathcal{B}}_i + \bar{\mathcal{D}}_i^\top \bar{\mathcal{D}}_i + 2p(1-p)\lambda_i\left(\mathcal{B}_\mathrm{c}^\top Y \mathcal{B}_\mathrm{c} + \mathcal{D}_\mathrm{c}^\top \mathcal{D}_\mathrm{c}\right) \prec Z_i \tag{3.17b}$$

for all $i \in \{1, \dots, N\}$, where λ_i are the eigenvalues of L^0, $\bar{\mathcal{A}}_i$ denotes $\mathcal{A}_\mathrm{d} + \lambda_i(p\mathcal{A}_\mathrm{c} + \mathcal{A}_\mathrm{p})$, and analogously for $\bar{\mathcal{B}}_i$, $\bar{\mathcal{C}}_i$, and $\bar{\mathcal{D}}_i$. Moreover, it is sufficient to validate (3.17a) for the smallest and largest eigenvalue of L^0.

Proof. Applying the steps outlined above to (3.15a) in combination with a congruence transformation by $U_{(n_\xi)}$, the orthogonal diagonalizing transformation of L^0, results in N decoupled LMIs of the form

$$M(\lambda_i) \coloneqq \bar{\mathcal{A}}_i^\top Y \bar{\mathcal{A}}_i + \bar{\mathcal{C}}_i^\top \bar{\mathcal{C}}_i + 2p(1-p)\lambda_i\left(\mathcal{A}_\mathrm{c}^\top Y \mathcal{A}_\mathrm{c} + \mathcal{C}_\mathrm{c}^\top \mathcal{C}_\mathrm{c}\right) \prec Y,$$

one for each of the eigenvalues of L^0. Following the arguments in the proof of Theorem 3.6, $M(\lambda)$ is a convex polynomial in λ, and it is thus sufficient to verify $M(\lambda_1) \prec Y$ and $M(\lambda_N) \prec Y$ for the smallest and largest eigenvalues, respectively.

Repeating for (3.15b), imposing structure onto $\mathcal{X}$ but *not* on $\mathcal{Z}$, we obtain

$$\begin{aligned}\left(I_N \otimes \mathcal{B}_\mathrm{d} + \Lambda \otimes (p\mathcal{B}_\mathrm{c} + \mathcal{B}_\mathrm{p})\right)^\top \left(I_N \otimes Y\right)\left(I_N \otimes \mathcal{B}_\mathrm{d} + \Lambda \otimes (p\mathcal{B}_\mathrm{c} + \mathcal{B}_\mathrm{p})\right) \\ + \left(I_N \otimes \mathcal{D}_\mathrm{d} + \Lambda \otimes (p\mathcal{D}_\mathrm{c} + \mathcal{D}_\mathrm{p})\right)^\top \left(I_N \otimes \mathcal{D}_\mathrm{d} + \Lambda \otimes (p\mathcal{D}_\mathrm{c} + \mathcal{D}_\mathrm{p})\right) \\ + 2p(1-p)\Lambda \otimes \left(\mathcal{B}_\mathrm{c}^\top Y \mathcal{B}_\mathrm{c} + \mathcal{D}_\mathrm{c}^\top \mathcal{D}_\mathrm{c}\right) \prec \tilde{\mathcal{Z}}\end{aligned}$$

with $\tilde{\mathcal{Z}} \coloneqq U_{(n_w)}^\top \mathcal{Z} U_{(n_w)}$. Note that, neglecting $\tilde{\mathcal{Z}}$, this LMI is block-diagonal. The Schur complement implies that the diagonal blocks of any negative definite matrix must be negative definite, therefore we can, without loss of generality, assume that $\tilde{\mathcal{Z}}$ is block diagonal with Z_i on the diagonal, making the LMI equivalent to (3.17b). Furthermore, the trace is invariant under orthogonal transformations such that $\operatorname{tr} \mathcal{Z} = \operatorname{tr} \tilde{\mathcal{Z}} = \sum_{i=1}^{N} \operatorname{tr} Z_i$.

It is left to show that $\mathcal{T}$ is mean-square stable. Since $\lambda_i \geq 0$ and $p \in [0,1]$, it holds that $2p(1-p)\lambda_i \geq 0$, therefore (3.17a) implies (3.7). Accordingly, $\mathcal{T}$ is mean-square stable, and we bound the H_2-norm by application of Theorem 3.10. ∎

In contrast to the stability test in Theorem 3.6, the condition for bounding the H_2-norm proposed by Theorem 3.11 does not consist of a constant number of LMI constraints and matrix variables, but both counts increase linearly with N. More importantly, however, all constraints and variables are of constant size, namely $n_\xi \times n_\xi$ and $n_w \times n_w$, respectively. Therefore, the complexity of Theorem 3.6 grows linearly with N and scales to IS with

many subsystems. Moreover, we can take advantage of the convexity of (3.17b) in λ_i by imposing that there exists a symmetric Z with $Z_i = Z$ for all $i \in \{1, \dots, N\}$. At the cost of additional conservatism in the norm bound, this assumption ensures that it is sufficient to test (3.17b) for $\lambda_1 = 0$ and λ_N instead of all Laplacian eigenvalues, such that the computational complexity is again independent of the number of subsystems. For similar reasons, Theorem 3.11 is not robust against uncertain nominal graphs $\mathcal{G}^0$ *per se*, but can be converted into a robust condition by insisting on a uniform Z. In that case, only the boundary of the Laplacian spectrum has to be known.

3.4.2. Gramian Duality and the Adjoint System

In the context of LTI systems, it is well known that the H_2-norm can equivalently be calculated from both the observability and the controllability Gramian and that it is therefore generally irrelevant if analysis procedures are formulated in terms of one or the other. However, if conservatism is introduced into the analysis, *e.g.* by imposing artificial structure onto the problem, the equivalence breaks down and the two Gramians can result in two different bounds. It may therefore be advisable to apply the analysis as a minimization over both Gramians in order to reduce the incurred conservatism.

In similar fashion, the H_2-norm of MJLS can be computed via distinct but dual SDPs (Costa et al., 2005, Section 4.4.2). On the one hand, there is the condition of Theorem 3.10 which is formulated in terms of the observability Gramian. Alternatively, do Val et al. (2002) show that $\|\mathcal{T}\|_{H_2}$ is less than γ if and only if there exist $\mathcal{Y}_i \succ 0$ and a symmetric $\mathcal{Z}$ with $\operatorname{tr} \mathcal{Z} < \gamma^2$ that solve the LMIs

$$\sum_{j \in \mathcal{K}} \theta_{ji} \left(\mathcal{A}_j \mathcal{Y}_j \mathcal{A}_j^\top + t_j \mathcal{B}_j \mathcal{B}_j^\top \right) \prec \mathcal{Y}_i \tag{3.18a}$$

and

$$\sum_{j \in \mathcal{K}} \left(\mathcal{C}_j \mathcal{Y}_j \mathcal{C}_j^\top + t_j \mathcal{D}_j \mathcal{D}_j^\top \right) \prec \mathcal{Z} \tag{3.18b}$$

for all $i \in \mathcal{K}$, which is based on the controllability Gramian. Even though the decomposition procedure proposed above is not directly applicable to these alternative LMIs, the condition can still be used to derive a dual H_2-norm bound for decomposable MJLS under two assumptions on the underlying Markov chain. The first property we have to impose is that $\{\sigma_k\}$ is *irreducible*, which means that every state can be reached from every other state of the chain (Klenke, 2013). By Theorem 7.2.1 and Corollary 7.2.3 of Douc et al. (2018), all irreducible Markov chains with finite state space $\mathcal{K}$ admit a unique *stationary distribution* π, and furthermore $\pi_i > 0$ for all $i \in \mathcal{K}$. In addition, assume that $t = \pi$, *i.e.* that σ_0 follows its stationary distribution. (See also the remark below Definition 2.7, where similar assumptions were made.)

Under these assumptions, introduce $\tilde{\mathcal{Y}}_i := {}^1\!/_{\pi_i} \mathcal{Y}_i \succ 0$ and insert into (3.18a) to obtain

$$\sum_{j \in \mathcal{K}} \pi_j \theta_{ji} \left(\mathcal{A}_j \tilde{\mathcal{Y}}_j \mathcal{A}_j^\top + \mathcal{B}_j \mathcal{B}_j^\top \right) \prec \pi_i \tilde{\mathcal{Y}}_i \qquad \Leftrightarrow \qquad \sum_{j \in \mathcal{K}} \theta^{\mathrm{r}}_{ij} \left(\mathcal{A}_j \tilde{\mathcal{Y}}_j \mathcal{A}_j^\top + \mathcal{B}_j \mathcal{B}_j^\top \right) \prec \tilde{\mathcal{Y}}_i$$

where $\theta^{\mathrm{r}}_{ij} := {}^{\pi_j}\!/_{\pi_i} \theta_{ji}$. Furthermore, (3.18b) is converted into

$$\sum_{j \in \mathcal{K}} \pi_j \left(\mathcal{C}_j \tilde{\mathcal{Y}}_j \mathcal{C}_j^\top + \mathcal{D}_j \mathcal{D}_j^\top \right) \prec \mathcal{Z}$$

in terms of the rescaled variables. Comparing with condition (3.15) of Theorem 3.10, observe that the LMIs are identical up to the substitutions

$$\mathcal{A}_i \leftrightarrow \mathcal{A}_i^\top \qquad \mathcal{B}_i \leftrightarrow \mathcal{C}_i^\top \qquad \mathcal{C}_i \leftrightarrow \mathcal{B}_i^\top \qquad \mathcal{D}_i \leftrightarrow \mathcal{D}_i^\top \qquad \theta_{ij} \leftrightarrow \theta_{ij}^{\mathrm{r}}$$

performed in either direction. In conclusion, the MJLS $\mathcal{T}$ and

$$\mathcal{T}^* \colon \begin{cases} \xi_{k+1} = \mathcal{A}_{\sigma_k^{\mathrm{r}}}^\top \xi_k + \mathcal{C}_{\sigma_k^{\mathrm{r}}}^\top w_k \\ z_k = \mathcal{B}_{\sigma_k^{\mathrm{r}}}^\top \xi_k + \mathcal{D}_{\sigma_k^{\mathrm{r}}}^\top w_k \end{cases}$$

have the same H_2-norm if $\{\sigma_k^{\mathrm{r}}\}$ has the TPM $\Theta^{\mathrm{r}} = \left[\theta_{ij}^{\mathrm{r}}\right]$ and both Markov chains follow the initial distribution π. Note that $\{\sigma_k^{\mathrm{r}}\}$ is the *reversed* Markov chain of $\{\sigma_k\}$ because of how θ_{ij}^{r} is defined (Klenke, 2013), which matches with the interpretation of the *adjoint system* as running backwards in time (Kouba & Bernstein, 2020). In particular, $\Theta = \Theta^{\mathrm{r}}$ if Assumption 3.1 is satisfied. If $\mathcal{T}$ is a decomposable MJLS satisfying Assumption 3.4, an alternative bound on its H_2-norm can therefore be obtained by applying Theorem 3.11 to $\mathcal{T}^*$, potentially improving the previously available estimate.

3.4.3. Obtaining H_∞-Norm Bounds for Input-Decoupled Systems

In the same way as for the H_2-norm in Section 3.4.1, we aim to derive conditions to bound the MJLS H_∞-norm that can be applied to arbitrarily large IS. Obtaining such a bound would allow to estimate the worst-case energy gain of these systems, paving the way to systematically analyse their robustness and, in Chapter 4 below, synthesize robust state- and output-feedback controllers.

A well known result to calculate the H_∞-norm for LTI systems is the *bounded real Lemma* (*BRL*), which equates upper bounds on the norm with the solution of an LMI constrained SDP (Gahinet & Apkarian, 1994). In the case of the MJLS H_∞-norm, an analogous result has been established by Seiler and Sengupta (2003), hinging on the feasibility of a coupled set of LMI constraints. Before stating their condition, we have to introduce a specific notion of controllability for MJLS.

Definition 3.5.: Weak Controllability (Seiler & Sengupta, 2003)
The MJLS $\mathcal{T}$ is *weakly controllable* if for all initial states (ξ_0, σ_0) and all final states $\left(\xi^{\mathrm{f}}, \sigma^{\mathrm{f}}\right)$, there exists a time $k \in \mathbb{N}_0$ and a (stochastic) input w such that

$$\mathbb{P}\left(\xi_k = \xi^{\mathrm{f}}, \sigma_k = \sigma^{\mathrm{f}}\right) > 0.$$

If an MJLS is weakly controllable according to Definition 3.5, it is ensured that the system state can be affected by disturbances. As noted by Seiler and Sengupta (2003), this property is crucial in their proof of the BRL in order to construct the worst-case input disturbance for a given MJLS and state. Accordingly, the resulting LMI condition is still sufficient for MJLS that are not weakly controllable but no longer necessary. This is in contrast to the LTI version of the BRL presented by Gahinet and Apkarian (1994), which explicitly does *not* depend on controllability of the system (see also the related discussion on controllability assumptions for dissipativity by Scherer, 2022).

In the same way as the mean-square stability test in Theorem 2.5 and the bounds for the MJLS H_2-norm by Costa et al. (1997) and do Val et al. (2002), the BRL as proposed by Seiler and Sengupta (2003) is ill-suited for systems with many modes since it requires one LMI constraint and one matrix variable for each $i \in \mathcal{K}$. We will therefore once more rely on a special case obtained by Fioravanti et al. (2012) for MJLS with switching processes $\{\sigma_k\}$ that are independent in time.

Theorem 3.12.: MJLS Bounded Real Lemma (Fioravanti et al., 2012)

Let $\gamma > 0$ be such that $\gamma^2 I - \mathcal{D}_i^\top \mathcal{D}_i \succ 0$ for all $i \in \mathcal{K}$ and let the MJLS $\mathcal{T}$ be weakly controllable. Then $\mathcal{T}$ is mean-square stable and has H_∞-norm less than γ if and only if there exist $\mathcal{X}_i \succ 0$ that solve $\mathcal{X}_i^{-1} - \mathcal{B}_i \Gamma_i \mathcal{B}_i^\top \succ 0$ and

$$\sum_{j \in \mathcal{K}} \theta_{ij} \left(\tilde{\mathcal{A}}_j^\top \left(\mathcal{X}_j^{-1} - \mathcal{B}_j \Gamma_j \mathcal{B}_j^\top \right)^{-1} \tilde{\mathcal{A}}_j + \mathcal{C}_j^\top \left(I + \mathcal{D}_j \Gamma_j \mathcal{D}_j^\top \right) \mathcal{C}_j \right) \prec \mathcal{X}_i \tag{3.19}$$

for all $i \in \mathcal{K}$, where $\tilde{\mathcal{A}}_j$ denotes $\mathcal{A}_j + \mathcal{B}_j \Gamma_j \mathcal{D}_j^\top \mathcal{C}_j$ and $\Gamma_i \coloneqq (\gamma^2 I - \mathcal{D}_i^\top \mathcal{D}_i)^{-1}$. In particular, this holds with $\mathcal{X}_i = \mathcal{X} \succ 0$ if $\mathcal{T}$ satisfies Assumption 3.1.

Remark. In their derivation, Fioravanti et al. (2012) assume $\mathcal{C}_i^\top \mathcal{D}_i = 0$ for all $i \in \mathcal{K}$ to simplify the calculations but note that this can be done without loss of generality. However, we opt not to apply this simplifying assumption for Theorem 3.12 to be explicit with the required state and output transformation. The original condition is recovered under the orthogonality assumption.

In contrast to the BRL presented by Seiler and Sengupta (2003), Theorem 3.12 is reduced to a single matrix variable if Assumption 3.1 holds and, while there are multiple matrix inequalities, only (3.19) involves taking the expectation over $\{\sigma_k\}$. Note, however, that none of the inequalities are LMIs since they contain the inverse of $\mathcal{X}$. To formulate the result as an SDP, and thus to be able to evaluate the H_∞-norm efficiently, Fioravanti et al. (2012, 2013) propose a linearization procedure that introduces $|\mathcal{K}|$ auxiliary variables, effectively negating the advantage of having only a single matrix variable. Furthermore, the reformulation does not take the expectation of the system matrices but of the auxiliary variables, such that the results on the expectation of the Laplacian that were derived in Section 3.2 would not be applicable.

With the intended application in mind, *i.e.* studying large IS, we therefore propose an alternative approach that is restricted to a specific subclass of decomposable MJLS but alleviates both of the previously mentioned issues. The key idea is to demand that the individual subsystems are only coupled through the system matrix $\mathcal{A}_i$ and output matrix $\mathcal{C}_i$, but importantly not through the input and feedthrough terms. This is formalized with the following assumption:

Assumption 3.6.: Decoupled Inputs

The decomposable MJLS $\mathcal{T}$ is *input-decoupled*, *i.e.* $\mathcal{B}_\mathrm{c} = \mathcal{B}_\mathrm{p} = 0$ and $\mathcal{D}_\mathrm{c} = \mathcal{D}_\mathrm{p} = 0$.

By enforcing Assumption 3.6, we unlock a series of important simplifications on the LMI (3.19). First and foremost, an immediate consequence is that the input and feedthrough terms of any such MJLS are mode independent and structured as $\mathcal{B}_i =$

$I_N \otimes \mathcal{B}_\mathrm{d}$ and $\mathcal{D}_i = I_N \otimes \mathcal{D}_\mathrm{d}$. Furthermore, we obtain $\Gamma_i = I_N \otimes \tilde{\Gamma}$ with $\tilde{\Gamma} \coloneqq (\gamma^2 I - \mathcal{D}_\mathrm{d}^\top \mathcal{D}_\mathrm{d})^{-1}$ because the inverse of a Kronecker product can be calculated by inverting each factor separately (*cf.* Section 2.2.2). With the structured Lyapunov matrix $\mathcal{X} = I_N \otimes Y$ that has been used before in the mean-square stability test and H_2-norm calculation, it is a consequence of the above that the two inner factors of (3.19) decouple into

$$\left(\mathcal{X}^{-1} - \mathcal{B}_j \Gamma_j \mathcal{B}_j^\top\right)^{-1} = I_N \otimes \left(Y^{-1} - \mathcal{B}_\mathrm{d} \tilde{\Gamma} \mathcal{B}_\mathrm{d}^\top\right)^{-1}$$

and

$$I_{N n_w} + \mathcal{D}_j \Gamma_j \mathcal{D}_j^\top = I_N \otimes \left(I_{n_w} + \mathcal{D}_\mathrm{d} \tilde{\Gamma} \mathcal{D}_\mathrm{d}^\top\right).$$

Accordingly, (3.19) consists of the weighted squared expectations of $\tilde{\mathcal{A}}_\sigma$ and C_σ with block diagonal weights such that we can exploit (3.5) to express the expectation analytically. Ultimately, we obtain the matrix inequality

$$\begin{aligned}\mathbb{E}[\tilde{\mathcal{A}}_\sigma]^\top \left(I_N \otimes \left(Y^{-1} - \mathcal{B}_\mathrm{d} \tilde{\Gamma} \mathcal{B}_\mathrm{d}^\top\right)^{-1}\right) \mathbb{E}[\tilde{\mathcal{A}}_\sigma] \\ + \Xi_{I_N}[S_\sigma] \otimes \left(\tilde{\mathcal{A}}_\mathrm{c}^\top \left(Y^{-1} - \mathcal{B}_\mathrm{d} \tilde{\Gamma} \mathcal{B}_\mathrm{d}^\top\right)^{-1} \tilde{\mathcal{A}}_\mathrm{c} + C_\mathrm{c}^\top \left(I + \mathcal{D}_\mathrm{d} \tilde{\Gamma} \mathcal{D}_\mathrm{d}^\top\right) C_\mathrm{c}\right) \\ + \mathbb{E}[C_\sigma]^\top \left(I_N \otimes \left(I + \mathcal{D}_\mathrm{d} \tilde{\Gamma} \mathcal{D}_\mathrm{d}^\top\right)\right) \mathbb{E}[C_\sigma] \prec I_N \otimes Y \quad (3.20)\end{aligned}$$

as a sufficient condition for (3.19), where $\tilde{\mathcal{A}}_\mathrm{c} = \mathcal{A}_\mathrm{c} + \mathcal{B}_\mathrm{d} \tilde{\Gamma} \mathcal{D}_\mathrm{d}^\top C_\mathrm{c}$. Inequality (3.20) is still nonlinear in its variables Y and γ, however, the expectation and variance of the pattern matrix are now isolated such that the decomposition techniques of Section 3.1 are applicable. For ease of exposition, we once more directly present the case of $S^0 = L^0$ and $S_i = L_i$ but emphasize that the result remains applicable to any decomposable MJLS that satisfies Assumption 3.2.

Theorem 3.13.: Bounded H_∞-Norm

A decomposable MJLS $\mathcal{T}$ fulfilling Assumption 3.6 with L^0 and L_σ as patterns, an undirected nominal graph $\mathcal{G}^0$, and packet loss satisfying Assumption 3.4 is mean-square stable and has H_∞-norm less than $\gamma > 0$ if there exists a $Y \succ 0$ that solves the LMI

$$\begin{bmatrix} \bar{\mathcal{A}}_i^\top Y \bar{\mathcal{A}}_i + \bar{\lambda}_i^2 \mathcal{A}_\mathrm{c}^\top Y \mathcal{A}_\mathrm{c} - Y & \bar{\mathcal{A}}_i^\top Y \mathcal{B}_\mathrm{d} & \bar{C}_i^\top & \bar{\lambda}_i \mathcal{A}_\mathrm{c}^\top Y \mathcal{B}_\mathrm{d} & \bar{\lambda}_i C_\mathrm{c}^\top \\ \mathcal{B}_\mathrm{d}^\top Y \bar{\mathcal{A}}_i & \mathcal{B}_\mathrm{d}^\top Y \mathcal{B}_\mathrm{d} - \gamma I & \mathcal{D}_\mathrm{d}^\top & 0 & 0 \\ \bar{C}_i & \mathcal{D}_\mathrm{d} & -\gamma I & 0 & 0 \\ \bar{\lambda}_i \mathcal{B}_\mathrm{d}^\top Y \mathcal{A}_\mathrm{c} & 0 & 0 & \mathcal{B}_\mathrm{d}^\top Y \mathcal{B}_\mathrm{d} - \gamma I & \mathcal{D}_\mathrm{d}^\top \\ \bar{\lambda}_i C_\mathrm{c} & 0 & 0 & \mathcal{D}_\mathrm{d} & -\gamma I \end{bmatrix} \prec 0 \quad (3.21)$$

for $i \in \{1, N\}$, where $\bar{\lambda}_i \coloneqq \sqrt{2p(1-p)\lambda_i}$, λ_i are the eigenvalues of L^0 and $\bar{\mathcal{A}}_i$, $\bar{C}_i$ denote $\mathcal{A}_\mathrm{d} + \lambda_i(p\mathcal{A}_\mathrm{c} + \mathcal{A}_\mathrm{p})$ and $C_\mathrm{d} + \lambda_i(pC_\mathrm{c} + C_\mathrm{p})$, respectively.

Proof. After inserting the Laplacian as pattern matrix, apply the diagonalizing transformation to (3.20) in order to obtain a set of N decoupled matrix inequalities

$$\begin{aligned}\left(\bar{\mathcal{A}}_i + \mathcal{B}_\mathrm{d}\tilde{\Gamma}\mathcal{D}_\mathrm{d}^\top\bar{\mathcal{C}}_i\right)^\top\tilde{Y}\left(\bar{\mathcal{A}}_i + \mathcal{B}_\mathrm{d}\tilde{\Gamma}\mathcal{D}_\mathrm{d}^\top\bar{\mathcal{C}}_i\right) + \bar{\mathcal{C}}_i^\top\left(I + \mathcal{D}_\mathrm{d}\tilde{\Gamma}\mathcal{D}_\mathrm{d}^\top\right)\bar{\mathcal{C}}_i \\ + 2p(1-p)\lambda_i\left(\tilde{\mathcal{A}}_\mathrm{c}^\top\tilde{Y}^{-1}\tilde{\mathcal{A}}_\mathrm{c} + \mathcal{C}_\mathrm{c}^\top\left(I + \mathcal{D}_\mathrm{d}\tilde{\Gamma}\mathcal{D}_\mathrm{d}^\top\right)\mathcal{C}_\mathrm{c}\right) \prec Y\end{aligned}$$

with $i \in \{1, \dots, N\}$, where $\tilde{Y} := \left(Y^{-1} - \mathcal{B}_\mathrm{d}\tilde{\Gamma}\mathcal{B}_\mathrm{d}^\top\right)^{-1}$. Assuming for now that $\tilde{\Gamma}$ and $\tilde{Y}$ are positive definite (which is required by Theorem 3.12), the left-hand side of the inequality is a quadratic polynomial in λ_i with matrix-valued coefficients and, following the arguments in the proof of Theorem 3.6, convex in λ_i. It is therefore sufficient to verify the inequality for λ_1 and λ_N.

By the Schur complement, the inequality above and $\tilde{Y} \succ 0$ are equivalent to

$$\begin{bmatrix} Y - \bar{\mathcal{C}}_i^\top\left(I + \mathcal{D}_\mathrm{d}\tilde{\Gamma}\mathcal{D}_\mathrm{d}^\top\right)\bar{\mathcal{C}}_i - \bar{\lambda}_i^2\mathcal{C}_\mathrm{c}^\top(I + \mathcal{D}_\mathrm{d}\tilde{\Gamma}\mathcal{D}_\mathrm{d}^\top)\mathcal{C}_\mathrm{c} & \bar{\mathcal{A}}_i^\top + \bar{\mathcal{C}}_i^\top\mathcal{D}_\mathrm{d}\tilde{\Gamma}\mathcal{B}_\mathrm{d}^\top & \bar{\lambda}_i\tilde{\mathcal{A}}_\mathrm{c}^\top \\ \bar{\mathcal{A}}_i + \mathcal{B}_\mathrm{d}\tilde{\Gamma}\mathcal{D}_\mathrm{d}^\top\bar{\mathcal{C}}_i & \tilde{Y}^{-1} & 0 \\ \bar{\lambda}_i\tilde{\mathcal{A}}_\mathrm{c} & 0 & \tilde{Y}^{-1} \end{bmatrix}$$

being positive definite. Furthermore, separating out the terms containing $\tilde{\Gamma}$ (including those contained in $\tilde{Y}^{-1}$) and applying the Schur complement with $\tilde{\Gamma} \succ 0$, we obtain

$$\begin{bmatrix} Y - \bar{\mathcal{C}}_i^\top\bar{\mathcal{C}}_i - \bar{\lambda}_i^2\mathcal{C}_\mathrm{c}^\top\mathcal{C}_\mathrm{c} & -\bar{\mathcal{C}}_i^\top\mathcal{D}_\mathrm{d} & -\bar{\lambda}_i\mathcal{C}_\mathrm{c}^\top\mathcal{D}_\mathrm{d} & \bar{\mathcal{A}}_i^\top & \bar{\lambda}_i\mathcal{A}_\mathrm{c}^\top \\ -\mathcal{D}_\mathrm{d}^\top\bar{\mathcal{C}}_i & \tilde{\Gamma}^{-1} & 0 & \mathcal{B}_\mathrm{d}^\top & 0 \\ -\bar{\lambda}_i\mathcal{D}_\mathrm{d}^\top\mathcal{C}_\mathrm{c} & 0 & \tilde{\Gamma}^{-1} & 0 & \mathcal{B}_\mathrm{d}^\top \\ \bar{\mathcal{A}}_i & \mathcal{B}_\mathrm{d} & 0 & Y^{-1} & 0 \\ \bar{\lambda}_i\mathcal{A}_\mathrm{c} & 0 & \mathcal{B}_\mathrm{d} & 0 & Y^{-1} \end{bmatrix} \succ 0,$$

which, by using the Schur complement again, can be reposed as

$$\begin{bmatrix} Y - \bar{\mathcal{A}}_i^\top Y\bar{\mathcal{A}}_i - \bar{\lambda}_i^2\mathcal{A}_\mathrm{c}^\top Y\mathcal{A}_\mathrm{c} & -\bar{\mathcal{A}}_i^\top Y\mathcal{B}_\mathrm{d} & -\bar{\lambda}_i\mathcal{A}_\mathrm{c}^\top Y\mathcal{B}_\mathrm{d} \\ -\mathcal{B}_\mathrm{d}^\top Y\bar{\mathcal{A}}_i & \gamma^2 I - \mathcal{B}_\mathrm{d}^\top Y\mathcal{B}_\mathrm{d} & 0 \\ -\bar{\lambda}_i\mathcal{B}_\mathrm{d}^\top Y\mathcal{A}_\mathrm{c} & 0 & \gamma^2 I - \mathcal{B}_\mathrm{d}^\top Y\mathcal{B}_\mathrm{d} \end{bmatrix}$$
$$- \begin{bmatrix} \bar{\mathcal{C}}_i^\top & \bar{\lambda}_i\mathcal{C}_\mathrm{c}^\top \\ \mathcal{D}_\mathrm{d}^\top & 0 \\ 0 & \mathcal{D}_\mathrm{d}^\top \end{bmatrix}\begin{bmatrix} \bar{\mathcal{C}}_i & \mathcal{D}_\mathrm{d} & 0 \\ \bar{\lambda}_i\mathcal{C}_\mathrm{c} & 0 & \mathcal{D}_\mathrm{d} \end{bmatrix} \succ 0.$$

Finally, applying the Schur complement one last time, followed by a congruence transformation of

$$\mathrm{diag}\left(\frac{1}{\sqrt{\gamma}}, \frac{1}{\sqrt{\gamma}}, \frac{1}{\sqrt{\gamma}}, -\sqrt{\gamma}, -\sqrt{\gamma}\right),$$

rescaling Y by γ, and reordering the rows and columns, we obtain (3.21). ∎

In contrast to the BRL for general MJLS with time-independent switching, the matrix inequality (3.21) is linear in both Y and γ and the bound on the H_∞-norm can thus be posed as a convex minimization problem. Moreover, the resulting SDP consists of only two variables and two LMI constraints regardless of the number of subsystems. Theorem 3.13 therefore has the same excellent scalability as previously achieved by the mean-square stability test of Theorem 3.6 and in discounted fashion also by the H_2-norm bound in Theorem 3.11.

3.4.4. An Alternative Bounded Real Lemma

An alternative BRL for MJLS that satisfy Assumption 3.1 has been proposed by Seiler (2001) and Seiler and Sengupta (2005). Similar to Theorem 3.12, their result consists of a single matrix inequality and two variables $\mathcal{X}$ and γ and yet, in contrast to the formulation by Fioravanti et al. (2012), the inequality is linear in both $\mathcal{X}$ and γ^2. As such, the alternative condition would be a prime candidate to derive an upper bound on the H_∞-norm for decomposable MJLS that do not necessarily satisfy Assumption 3.6, generalizing Theorem 3.13. However, Seiler (2001) uses a different definition for the MJLS H_∞-norm than Definition 2.8. Instead of finding the worst-case input signal over all square-summable random processes, and thus allowing w_k to depend on ξ_k, they assume that w_k is deterministic and therefore independent of the state. Accordingly, the resulting norm is a lower bound on the worst-case gain of the MJLS over all admissible signals. In fact, this issue has already been noted by Fioravanti et al. (2012), who stated that the LMI condition presented by (Seiler, 2001; Seiler & Sengupta, 2005), *i.e.*

$$\sum_{j\in\mathcal{K}} \theta_j \begin{bmatrix} \mathcal{A}_j & \mathcal{B}_j \\ C_j & \mathcal{D}_j \end{bmatrix}^\top \begin{bmatrix} \mathcal{X} & 0 \\ 0 & I \end{bmatrix} \begin{bmatrix} \mathcal{A}_j & \mathcal{B}_j \\ C_j & \mathcal{D}_j \end{bmatrix} \prec \begin{bmatrix} \mathcal{X} & 0 \\ 0 & \gamma^2 I \end{bmatrix}, \tag{3.22}$$

is a necessary condition for (3.19), but generally not sufficient. Even though this rules out using the result for robustness analysis, *i.e.* in terms of the small-gain theorem (Todorov & Fragoso, 2009, 2012), there is nonetheless merit in studying the alternative BRL if it is known that the input signal is deterministic.

In order to obtain a computationally efficient method to bound the energy gain for deterministic input signals, we strive to decouple (3.22) in the same way as Theorem 3.12. Contrasting the derivation above for general stochastic input signals, it is possible to refrain from limiting the scope to input-decoupled system but work with general decomposable MJLS, since the condition is linear in $\mathcal{X}$ and γ^2 already. To start, note that there exists a permutation matrix U that transforms the left and right factor of (3.22) as

$$U^\top \begin{bmatrix} \mathcal{A}_j & \mathcal{B}_j \\ C_j & \mathcal{D}_j \end{bmatrix} U = I_N \otimes \begin{bmatrix} \mathcal{A}_\mathrm{d} & \mathcal{B}_\mathrm{d} \\ C_\mathrm{d} & \mathcal{D}_\mathrm{d} \end{bmatrix} + S_j \otimes \begin{bmatrix} \mathcal{A}_\mathrm{c} & \mathcal{B}_\mathrm{c} \\ C_\mathrm{c} & \mathcal{D}_\mathrm{c} \end{bmatrix} + S^0 \otimes \begin{bmatrix} \mathcal{A}_\mathrm{p} & \mathcal{B}_\mathrm{p} \\ C_\mathrm{p} & \mathcal{D}_\mathrm{p} \end{bmatrix}.$$

Furthermore, under the assumption that $\mathcal{X} = I_N \otimes Y$, the same permutation matrix transforms the affine term of (3.22) as

$$U^\top \begin{bmatrix} \mathcal{X} & 0 \\ 0 & \gamma^2 I \end{bmatrix} U = I_N \otimes \begin{bmatrix} Y & 0 \\ 0 & \gamma^2 I \end{bmatrix},$$

and analogously for the inner weighting factor without γ^2. As a result, we obtain an LMI that takes the form of (3.2) with augmented left and right factors and a structured matrix variable, enabling us to apply the same steps to transform the inequality as in Section 3.1. Specialized for the case of $S_i = L_i$ and $S^0 = L^0$, this leads to a set of N decoupled LMIs

$$\begin{bmatrix} \bar{\mathcal{A}}_i & \bar{\mathcal{B}}_i \\ \bar{C}_i & \bar{\mathcal{D}}_i \end{bmatrix}^\top \begin{bmatrix} Y & 0 \\ 0 & I \end{bmatrix} \begin{bmatrix} \bar{\mathcal{A}}_i & \bar{\mathcal{B}}_i \\ \bar{C}_i & \bar{\mathcal{D}}_i \end{bmatrix} + 2p(1-p)\lambda_i \begin{bmatrix} \mathcal{A}_\mathrm{c} & \mathcal{B}_\mathrm{c} \\ C_\mathrm{c} & \mathcal{D}_\mathrm{c} \end{bmatrix}^\top \begin{bmatrix} Y & 0 \\ 0 & I \end{bmatrix} \begin{bmatrix} \mathcal{A}_\mathrm{c} & \mathcal{B}_\mathrm{c} \\ C_\mathrm{c} & \mathcal{D}_\mathrm{c} \end{bmatrix} \prec \begin{bmatrix} Y & 0 \\ 0 & \gamma^2 I \end{bmatrix}, \tag{3.23}$$

where λ_i are the eigenvalues of L^0, $\bar{\mathcal{A}}_i$ and $\bar{C}_i$ are as in Theorem 3.13, and $\bar{\mathcal{B}}_i$, $\bar{\mathcal{D}}_i$ follow analogously. Moreover, since the left-hand side is a quadratic matrix-valued polynomial

in λ_i and $Y \succ 0$, the condition is convex in λ_i, and it is thus sufficient to verify the condition for the largest and smallest eigenvalue (*cf*. the proof of Theorem 3.6). The energy gain of the decomposable MJLS $\mathcal{T}$ with undirected nominal graph $\mathcal{G}^0$ and packet loss satisfying Assumption 3.4 is therefore less than γ for deterministic input signals if there exists a $Y \succ 0$ such that (3.23) holds for $i \in \{1, N\}$.

With this alternative condition, we now have two possible approaches to bound the energy gain of decomposable MJLS that are admissible for different kinds of scenarios. On the one hand, there is Theorem 3.13 that bounds the MJLS H_∞-norm as introduced in Definition 2.8 but is invalid for systems that violate Assumption 3.6. If, on the other hand, coupled inputs are essential to model a specific IS, we can fall back to solve (3.23) which is applicable to general decomposable MJLS but results in a worst-case gain which is determined over deterministic input signals. However, since input signals w_k that stochastically depend on the state may achieve a larger energy gain, its use for robustness analysis is invalidated. Note that, while (3.23) is in general neither necessary nor sufficient for (3.19), *i.e*. it does not bound the H_∞-norm of $\mathcal{T}$ from above or below, it is a necessary condition for the existence of $Y \succ 0$ such that (3.21) holds if Assumption 3.6 is satisfied, since the conservatism in either LMI stems purely from the structured Lyapunov variable $\mathcal{X} = I_N \otimes Y$. For input-decoupled systems, bounds obtained from Theorem 3.13 are therefore always above the bound calculated from (3.23) with deterministic inputs.

3.4.5. Performance on the Disagreement Space

As discussed in Section 3.3.1, it is advantageous or even vital for some distributed control problems that the closed loop is marginally stable. However, since the H_2- and H_∞-norm are only defined for (asymptotically) stable systems and, in addition, Theorems 3.11 and 3.13 imply mean-square stability, the performance bounds derived above are not applicable for these kinds of control problems.

There are two main approaches in the literature to circumvent this issue, both based on the idea of suppressing undesired components of the system response. On one hand, there are approaches that define alternative performance criteria, most prominently the convergence rate of the subsystems to a common state (*e.g*. Bullo, 2018; Fagnani & Zampieri, 2008; Olfati-Saber et al., 2007; Sundararajan et al., 2020). In particular, this view on the IS is often taken if the system is representing a computational algorithm, such as the distributed first-order optimization methods studied by Sundararajan et al. (2020). On the other hand, it is possible to consider the system dynamics only on a specific subspace, similarly to the consensus analysis of Section 3.3.1. By applying the projection Π not only to the state ξ_k but also to the output z_k, the system is analysed with respect to the disagreement space and the marginally stable component along its orthogonal complement is suppressed. Examples for this projected system norm approach include Capone et al. (2023), Wang et al. (2013) and Zhang et al. (2021).

Since this work is relying on the system norms as performance criteria, the projected system approach is pursued in the following, *i.e*. the decomposable MJLS $\mathcal{T}$ is replaced by the projected system $\Pi_{(n_z)}\mathcal{T}$ for the purpose of analysing the H_2- and H_∞-norm. Similar to the proof of Theorem 3.7, the orthogonal matrix U that is diagonalizing the nominal Laplacian L^0 is used to transform the state, but in addition also applied at the input and

output, resulting in the transformed signals

$$\tilde{\xi}_k \coloneqq U_{(n_\xi)}^\top \xi_k \qquad \tilde{w}_k \coloneqq U_{(n_w)}^\top w_k \qquad \tilde{z}_k \coloneqq U_{(n_z)}^\top \Pi_{(n_z)} z_k$$

in terms of the state, input, and output of the original MJLS $\mathcal{T}$. Moreover, the three transformed signals are partitioned into ξ_k^{cg} & ξ_k^{δ}, w_k^{cg} & w_k^{δ}, and z_k^{cg} & z_k^{δ}, respectively, where the first component of each signal corresponds to its coordinate in the agreement space. All together, the state-space model of the transformed system is given by

$$\begin{aligned}
\begin{bmatrix} \xi_{k+1}^{\mathrm{cg}} \\ \xi_{k+1}^{\delta} \end{bmatrix} &= \begin{bmatrix} \mathcal{A}_{\mathrm{d}} & \frac{1}{\sqrt{N}}\left(\mathbf{1}_N^\top L_{\sigma_k} \tilde{U}\right) \otimes \mathcal{A}_{\mathrm{c}} \\ 0 & \tilde{\mathcal{A}}_{\sigma_k} \end{bmatrix} \begin{bmatrix} \xi_k^{\mathrm{cg}} \\ \xi_k^{\delta} \end{bmatrix} + \begin{bmatrix} \mathcal{B}_{\mathrm{d}} & \frac{1}{\sqrt{N}}\left(\mathbf{1}_N^\top L_{\sigma_k} \tilde{U}\right) \otimes \mathcal{B}_{\mathrm{c}} \\ 0 & \tilde{\mathcal{B}}_{\sigma_k} \end{bmatrix} \begin{bmatrix} w_k^{\mathrm{cg}} \\ w_k^{\delta} \end{bmatrix} \\
\begin{bmatrix} z_k^{\mathrm{cg}} \\ z_k^{\delta} \end{bmatrix} &= \begin{bmatrix} 0 & 0 \\ 0 & \tilde{\mathcal{C}}_{\sigma_k} \end{bmatrix} \begin{bmatrix} \xi_k^{\mathrm{cg}} \\ \xi_k^{\delta} \end{bmatrix} + \begin{bmatrix} 0 & 0 \\ 0 & \tilde{\mathcal{D}}_{\sigma_k} \end{bmatrix} \begin{bmatrix} w_k^{\mathrm{cg}} \\ w_k^{\delta} \end{bmatrix}
\end{aligned}$$

with

$$\tilde{\mathcal{A}}_i \coloneqq I_{N-1} \otimes \mathcal{A}_{\mathrm{d}} + \left(\tilde{U}^\top L_i \tilde{U}\right) \otimes \mathcal{A}_{\mathrm{c}} + \Lambda \otimes \mathcal{A}_{\mathrm{p}}$$

and analogously for $\tilde{\mathcal{B}}_i$, $\tilde{\mathcal{C}}_i$, and $\tilde{\mathcal{D}}_i$.

First and foremost, notice that $z_k^{\mathrm{cg}} = 0$ and thus $\left\|\Pi_{(n_z)} z_k\right\| = \left\|\tilde{z}_k\right\| = \left\|z_k^{\delta}\right\|$ for all $k \in \mathbb{N}_0$, since the Euclidean norm is invariant under orthogonal transformations. Furthermore, the input w_k^{cg} is unobservable in the output, *i.e.* with a chosen realization of the switching process $\{\sigma_k\}$ and fixed input w_k^{δ}, the response z_k^{δ} is independent of w_k^{cg}. It is therefore sufficient to analyse the reduced system

$$\begin{aligned}
\xi_{k+1}^{\delta} &= \tilde{\mathcal{A}}_{\sigma_k} \xi_k^{\delta} + \tilde{\mathcal{B}}_{\sigma_k} w_k^{\delta} \\
z_k^{\delta} &= \tilde{\mathcal{C}}_{\sigma_k} \xi_k^{\delta} + \tilde{\mathcal{D}}_{\sigma_k} w_k^{\delta}
\end{aligned}$$

in order to determine the expected output energy. Following the arguments in the proof of Theorem 3.7, this corresponds to ignoring the trivial eigenvalue $\lambda_1 = 0$ of the nominal Laplacian during analysis.

It remains to show that the w_k^{cg} component of the input can be neglected without affecting the system norm. In the H_2 case, the norm is determined as a sum over all input channels, and thus any input channel with no output response can be ignored. On the other hand, the H_∞-norm involves finding the worst-case input signal in terms of w_k^{cg} and w_k^{δ}. Because z_k^{δ} is independent of w_k^{cg}, the respective supremum is maximized for $w_k^{\mathrm{cg}} = 0$ and can thus be reduced to just w_k^{δ}. Accordingly, we arrive at a bound for the projected H_2-norm by verifying the conditions of Theorem 3.11 for $i \in \{2, \dots, N\}$, and the projected H_∞-norm can be bounded by testing Theorem 3.13 at λ_2 and λ_N.

3.5. Optimistic Norm Bounding With the Mean System

Until now, the current chapter has focused on deriving conditions that ensure mean-square stability and provide upper bounds on system norms while being computationally efficient to evaluate. Even though these bounds are conservative, they do provide worst-case estimates in situations where computing the actual norm is prohibitively expensive.

On the other hand, conditions that provide lower norm bounds commonly have limited value since the actual performance of the plant can be arbitrarily bad in comparison to the optimistic bound. Nevertheless, lower bounds play an essential role in estimating the conservatism of their corresponding upper bounds by yielding an interval for the unknown true figure of the norm. To complement the preceding derivation of upper bounds, this section is therefore providing guaranteed lower bounds on the MJLS system norms and a necessary condition for mean-square stability.

The basis for the results of this section is formed by an artificial LTI system which can be derived from the MJLS $\mathcal{T}$. More specifically, under Assumption 3.1, *i.e.* independence of the switching process $\{\sigma_k\}$ in time, the *mean system* is introduced as the LTI system

$$\bar{\mathcal{T}}: \begin{cases} \bar{\xi}_{k+1} = \mathbb{E}[\mathcal{A}_\sigma]\bar{\xi}_k + \mathbb{E}[\mathcal{B}_\sigma]\bar{w}_k \\ \bar{z}_k = \mathbb{E}[\mathcal{C}_\sigma]\bar{\xi}_k + \mathbb{E}[\mathcal{D}_\sigma]\bar{w}_k \end{cases}$$

built from the expectations of the switched MJLS state-space matrices. Because of the independence of σ_k from ξ_k, this system can be seen as propagating the expected state in time: In the autonomous case with $w \equiv 0$, taking the expectation of σ_{k+1} results in

$$\mathbb{E}[\xi_{k+1}] = \mathbb{E}[\mathcal{A}_{\sigma_k}\xi_k] = \mathbb{E}[\mathcal{A}_{\sigma_k}]\,\mathbb{E}[\xi_k],$$

giving the state update equation of the mean system without input by taking $\bar{\xi}_k = \mathbb{E}[\xi_k]$. This aspect of propagating the expectation (and variance) of the state is discussed in Section 3.2 of (Costa et al., 2005) in a more general setting without assuming independence of the switching process.

Since the MJLS $\mathcal{T}$ and its mean system $\bar{\mathcal{T}}$ are intricately linked through their state-space realizations, it is a natural question to ask how they are related in terms of their system theoretic properties. For three particular properties, namely asymptotic stability and the H_2- and H_∞-norm, this question is answered by the following proposition:

Proposition 3.14.: Mean System Bounds

Let $\mathcal{T}$ be an asymptotically mean-square stable MJLS satisfying Assumption 3.1 and $\bar{\mathcal{T}}$ be its associated mean system. Then i) $\bar{\mathcal{T}}$ is asymptotically stable, ii) $\|\bar{\mathcal{T}}\|_{H_2} \leq \|\mathcal{T}\|_{H_2}$, and iii) $\|\bar{\mathcal{T}}\|_{H_\infty} \leq \|\mathcal{T}\|_{H_\infty}$.

Remark. The definitions of the H_2- and H_∞-norm for LTI systems are not addressed in this dissertation. However, since the H_2- and H_∞-norm of MJLS are proper generalizations, they are obtained from Definitions 2.7 and 2.8 by considering the special case of an MJLS with a single mode.

Proof. The proposition hinges on the fact that $\Xi_Q[X] \succeq 0$ for all random variables X and all weights $Q \succeq 0$. The claims are proven in the order in which they appear:

i) Start from Theorem 3.1 and reformulate its LMI condition in terms of a weighted squared expectation and the generalized variance as

$$\mathbb{E}[\mathcal{A}_\sigma]^\top \mathcal{X}\, \mathbb{E}[\mathcal{A}_\sigma] + \Xi_{\mathcal{X}}[\mathcal{A}_\sigma] \prec \mathcal{X} \qquad \Rightarrow \qquad \mathbb{E}[\mathcal{A}_\sigma]^\top \mathcal{X}\, \mathbb{E}[\mathcal{A}_\sigma] \prec \mathcal{X},$$

which by Theorem 2.2 implies asymptotic stability of $\bar{\mathcal{T}}$.

ii) Let $\gamma > 0$ be such that there exist $\mathcal{X}$ and $\mathcal{Z}$ satisfying the conditions of Theorem 3.10 and therefore $\|\mathcal{T}\|_{H_2} < \gamma$. Posing (3.17) in terms of the variance, we obtain

$$\begin{aligned}\mathbb{E}[\mathcal{A}_\sigma]^\top \mathcal{X}\, \mathbb{E}[\mathcal{A}_\sigma] + \mathbb{E}[\mathcal{C}_\sigma]^\top \mathbb{E}[\mathcal{C}_\sigma] \;\; + \Xi_{\mathcal{X}}[\mathcal{A}_\sigma] + \Xi_I[\mathcal{C}_\sigma] \;\; &\prec \mathcal{X} \\ \mathbb{E}[\mathcal{B}_\sigma]^\top \mathcal{X}\, \mathbb{E}[\mathcal{B}_\sigma] \; + \mathbb{E}[\mathcal{D}_\sigma]^\top \mathbb{E}[\mathcal{D}_\sigma] + \Xi_{\mathcal{X}}[\mathcal{B}_\sigma] \; + \Xi_I[\mathcal{D}_\sigma] &\prec \mathcal{Z},\end{aligned}$$

such that $\mathcal{X}$ and $\mathcal{Z}$ also solve

$$\begin{aligned}\mathbb{E}[\mathcal{A}_\sigma]^\top \mathcal{X}\, \mathbb{E}[\mathcal{A}_\sigma] + \mathbb{E}[\mathcal{C}_\sigma]^\top \mathbb{E}[\mathcal{C}_\sigma] \;\; &\prec \mathcal{X} \\ \mathbb{E}[\mathcal{B}_\sigma]^\top \mathcal{X}\, \mathbb{E}[\mathcal{B}_\sigma] \; + \mathbb{E}[\mathcal{D}_\sigma]^\top \mathbb{E}[\mathcal{D}_\sigma] &\prec \mathcal{Z}.\end{aligned}$$

By Theorem 2 of De Caigny et al. (2010), this implies that $\|\bar{\mathcal{T}}\|_{H_2} < \gamma$, too. Since $\gamma > 0$ was arbitrary and Theorem 3.10 is necessary and sufficient, the H_2-norm of the mean system $\bar{\mathcal{T}}$ is thus smaller than any upper bound on the H_2-norm of $\mathcal{T}$.

iii) Let $\gamma > 0$ be such that there exists an $\mathcal{X}$ satisfying the conditions of Theorem 3.12 and therefore $\|\mathcal{T}\|_{H_\infty} < \gamma$. As noted by Fioravanti et al. (2012), $\mathcal{X}$ thus also solves (3.22) since it is a necessary condition for (3.19). Reformulated in terms of the squared expectation and the generalized variance, we obtain

$$\mathbb{E}\begin{bmatrix}\mathcal{A}_\sigma & \mathcal{B}_\sigma \\ \mathcal{C}_\sigma & \mathcal{D}_\sigma\end{bmatrix}^\top \underbrace{\begin{bmatrix}\mathcal{X} & 0 \\ 0 & I\end{bmatrix}}_{\tilde{\mathcal{X}}} \mathbb{E}\begin{bmatrix}\mathcal{A}_\sigma & \mathcal{B}_\sigma \\ \mathcal{C}_\sigma & \mathcal{D}_\sigma\end{bmatrix} + \Xi_{\tilde{\mathcal{X}}}\begin{bmatrix}\mathcal{A}_\sigma & \mathcal{B}_\sigma \\ \mathcal{C}_\sigma & \mathcal{D}_\sigma\end{bmatrix} \prec \begin{bmatrix}\mathcal{X} & 0 \\ 0 & \gamma^2 I\end{bmatrix},$$

which by dropping the variance term and applying a Schur complement turns into

$$\begin{bmatrix}\mathbb{E}[\mathcal{A}_\sigma]^\top \mathcal{X}\, \mathbb{E}[\mathcal{A}_\sigma] - \mathcal{X} & \mathbb{E}[\mathcal{A}_\sigma]^\top \mathcal{X}\, \mathbb{E}[\mathcal{B}_\sigma] & \mathbb{E}[\mathcal{C}_\sigma]^\top \\ \mathbb{E}[\mathcal{B}_\sigma]^\top \mathcal{X}\, \mathbb{E}[\mathcal{A}_\sigma] & \mathbb{E}[\mathcal{B}_\sigma]^\top \mathcal{X}\, \mathbb{E}[\mathcal{B}_\sigma] - \gamma^2 I & \mathbb{E}[\mathcal{D}_\sigma]^\top \\ \mathbb{E}[\mathcal{C}_\sigma] & \mathbb{E}[\mathcal{D}_\sigma] & -I\end{bmatrix} \prec 0,$$

the BRL for the mean system (Gahinet & Apkarian, 1994). The claim follows by the same arguments on γ as above. ■

According to Proposition 3.14, the mean system can be used to generate necessary conditions on the stability and performance of the corresponding MJLS. For example, the MJLS $\mathcal{T}$ cannot be mean-square stable if its corresponding mean system is unstable. This property is closely related to the well-known result that mean-square stability implies convergence of the mean state (Costa et al., 2005, Proposition 3.6).

If the MJLS being considered is decomposable, then the LTI mean system is also decomposable. More specifically, it assumes the structure

$$\mathbb{E}[\mathcal{A}_\sigma] = I_N \otimes \mathcal{A}_\mathrm{d} + \mathbb{E}[S_\sigma] \otimes \mathcal{A}_\mathrm{c} + S^0 \otimes \mathcal{A}_\mathrm{p}$$

for its system matrix, and analogously for the input, output, and feedthrough terms. Under the condition that S^0 and $\mathbb{E}[S_\sigma]$ are simultaneously diagonalizable, which is ensured by Assumption 3.2, we can therefore decouple the plant into modal subsystems as proposed by Massioni and Verhaegen (2009) and obtain a necessary condition that scales linearly in the number of subsystems. Note that, unlike the sufficient conditions in Theorems 3.6, 3.11, and 3.13, the resulting stability and performance tests cannot be reformulated to be independent of the number of variables and constraints. This is because the necessity of the conditions would be lost in the process, invalidating them as lower bounds for the MJLS.

3.6. Application Examples

Let us now discuss a few examples to demonstrate the applicability of the material considered in this chapter. For all three scenarios below, we consider groups of first-order integrator agents that are tasked with attaining consensus using a wireless network. In comparison to the integrators of Examples 2.3 and 2.4, the agents posses a disturbance input w_k^i such that we can measure their performance in terms of the H_2- and H_∞-norm.

Example 3.1.: First-Order Consensus with Inputs

The integrators of Examples 2.3 and 2.4 are augmented by a performance input w_k with unit input gain. Each agent is therefore described by the difference equation

$$x_{k+1}^i = x_k^i + u_k^i + w_k^i$$

and implements the consensus protocol (2.9). In addition, we employ the *formation error* $L^0 x_k$ as the performance output z_k, leading to the closed-loop model

$$\begin{aligned} x_{k+1} &= \left(I_N - \kappa L_{\sigma_k}\right) x_k + w_k \\ z_k &= L^0 x_k \end{aligned}$$

for the overall MAS. Note that it is essential to use the *nominal* and not the *stochastic* Laplacian for the performance output, since the formation error would otherwise vanish for small transmission probabilities $p \to 0$ even if the agents do not converge. In the same way as for Example 2.4, the first-order integrators with inputs form a decomposable MJLS with

$$\mathcal{A}_\mathrm{d} = 1, \qquad \mathcal{A}_\mathrm{c} = -\kappa, \qquad \mathcal{B}_\mathrm{d} = 1, \qquad C_\mathrm{p} = 1,$$

and all other matrices zero.

Importantly, the MJLS described in Example 3.1 is only interconnected through its system and output matrices, but *not* in its input or feedthrough terms. It is therefore input-decoupled and the H_∞-norm bound of Theorem 3.13 is applicable. Furthermore, the current chapter considers a fixed gain of $\kappa = 0.1$. Retuning the gain to improve the behaviour of the closed-loop system is approached in Section 4.3.1.

3.6.1. Conservatism of the Norm Bounds

The first scenario is a study of the conservatism incurred by Theorems 3.11 and 3.13 because of the block-repeated structure that is imposed onto the Lyapunov matrix, and is adapted from (Hespe, Saadabadi et al., 2024). For the fixed triangular grid graph $\mathcal{G}_3^\triangle$ as introduced in Example 2.2, we minimize the norm bound γ subject to the respective LMI constraints of Theorems 3.10, 3.11, and 3.13 with transmission probability p varying in the interval $[0,1]$. Furthermore, following Proposition 3.14, the mean system is used to obtain scalable lower bounds for both the H_2- and H_∞-norm. Note that we do not employ Theorem 3.12 to calculate an exact figure for the H_∞-norm since the graph has $m = 18$ edges and the MJLS thus $|\mathcal{K}| = 2^{18}$ modes, leading to an SDP with as many variables and constraints. As for all SDPs throughout the thesis, this optimization problem is

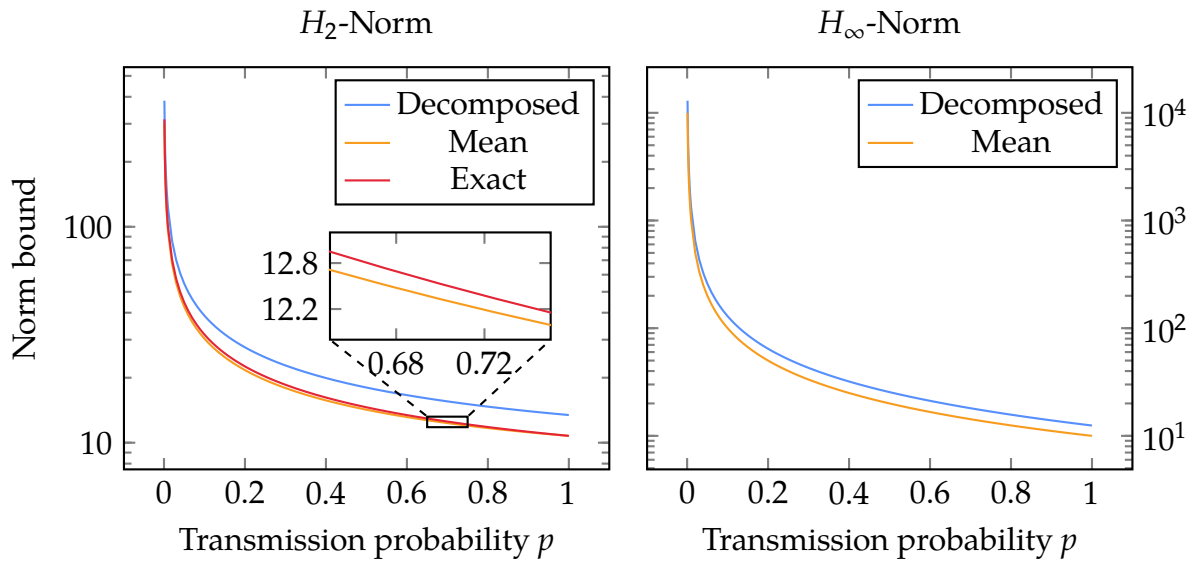

Figure 3.1.: Bounds on the H_2- and H_∞-norm of the first-order integrators with inputs for varying transmission probability p. The curves labelled 'Decomposed' are obtained from Theorems 3.11 and 3.13, the lower bounds are derived from the mean system, and Theorem 3.10 is used to calculate the exact H_2-norm.

implemented and solved using the YALMIP modelling language (Löfberg, 2004). The resulting norm curves are shown in Fig. 3.1.

As expected, the norm bounds obtained from the decomposed and mean system conditions do not match the exact H_2-norm, but over- and underestimate it, respectively. The gap between the upper and lower bound does, however, remain narrow even at the worst probability. For $p \to 0$, the estimates of both norms increase drastically, tending towards infinity. This mirrors the observation of Section 3.3.3 that the consensus protocol (2.9) fails to converge the agents for $p = 0$, since this is the critical probability of the system. Observe that the mean system is equivalent to the MJLS for $p = 1$, such that the bound becomes exact in the limit. In contrast, the upper bounds obtained from Theorems 3.11 and 3.13 are conservative regardless of the transmission probability.

3.6.2. Scalability to Large Multiagent Systems

The premise of our second example is to study the scalability of the various analysis conditions to IS with many subsystems. For some conditions, such as the mean-square stability test Theorem 3.6 or the H_∞-norm bound of Theorem 3.13, this does not have to be evaluated as the underlying SDPs are of constant complexity independent of N. In contrast, the original MJLS analysis conditions of Theorems 3.1, 3.10, and 3.12 require enumeration of all modes and are hence exponential in the number of edges m. As such, we start by analysing a set of graphs with few edges, namely $\mathcal{G}_N^\circ$ with $N \leq 12$. The resulting computation times of Theorems 3.10 to 3.12 are shown on the left of Fig. 3.2.

While Theorem 3.11 shows no growth in its computation time, the SDPs of Theorems 3.10 and 3.12 have taken several hours to construct and solve, even for the small networks of at most twelve agents and edges. Moreover, the H_∞-norm calculation of Theorem 3.12 is orders of magnitudes more expensive than the H_2 condition, since

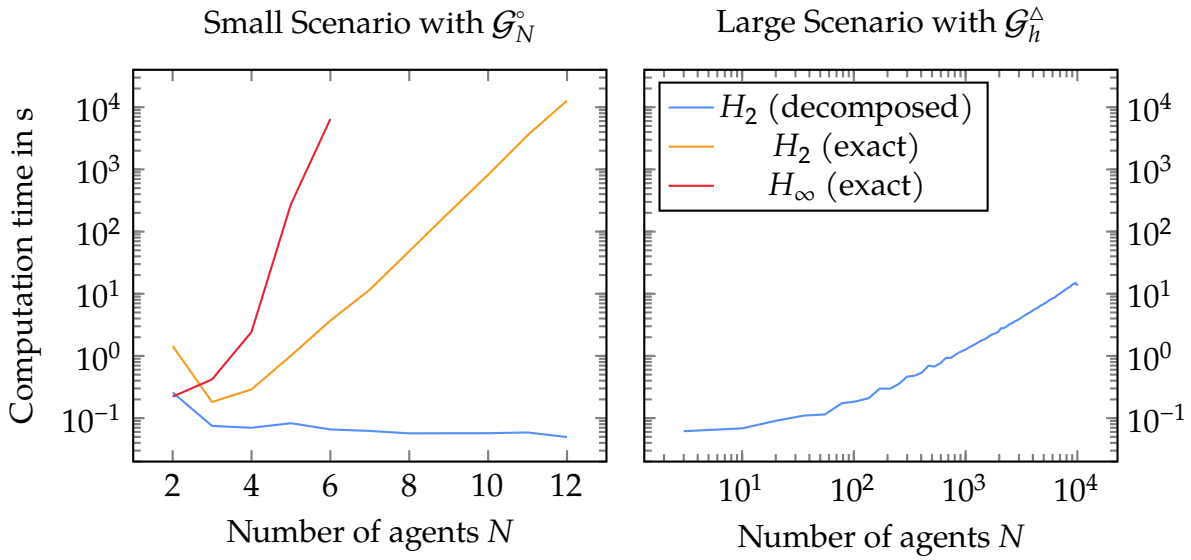

Figure 3.2.: Computation times of Theorems 3.10 to 3.12 with increasing number of subsystems. The exact norm computations are only performed for the small scenario due to their exponential complexity scaling.

in addition to enumerating all modes during construction, it requires one auxiliary variable and one LMI constraint per mode, rendering not only its construction but also the problem size exponential in m.

In the right half of Fig. 3.2, we have repeated the same calculation for large triangle grid graphs $\mathcal{G}_h^\triangle$ with up to 10 000 subsystems. Due to the exponential growth in complexity for the exact norms, this is only tractable for the decomposed analysis condition of Theorem 3.11. Although the figure indicates that the decomposed condition requires more time than before to analyse these large-scale systems, the growth is approximately linear such that the condition stays fast to evaluate relative to the size of the IS. Note, however, that this assumes the spectrum of the nominal Laplacian to be known, which is a non-trivial task by itself for graphs of this size.

Finally, let us study how the conservatism of the norm bound changes if the number of agents is increased by comparing them against the mean system. As such, Fig. 3.3 visualizes the norms obtained for the large scenario above, with graphs $\mathcal{G}_h^\triangle$ and fixed transmission probability $p = 0.5$. While the gap between the upper bound and the mean system is constant on a logarithmic scale for the H_2-norm, the H_∞-norm estimates are drifting apart fast. Since the exact norm must lie between the two bounds, we can therefore conclude for the first-order consensus example that the conservatism in the H_2-norm is moderate and nearly independent of the number of subsystems and on the other hand that the H_∞-norm estimates are mostly meaningless for large systems, since the two bounds are two orders of magnitude apart.

3.6.3. Influence of the Eigenvalue Bounds

Finally, the third scenario concerns the influence of the eigenvalues λ_2 and λ_N on the norm bounds of Theorems 3.11 and 3.13, respectively. In case of the H_2-norm, this presumes that $Z_i = Z$ for all $i \in \{2, \dots, N\}$ is chosen, since it is necessary to evaluate the

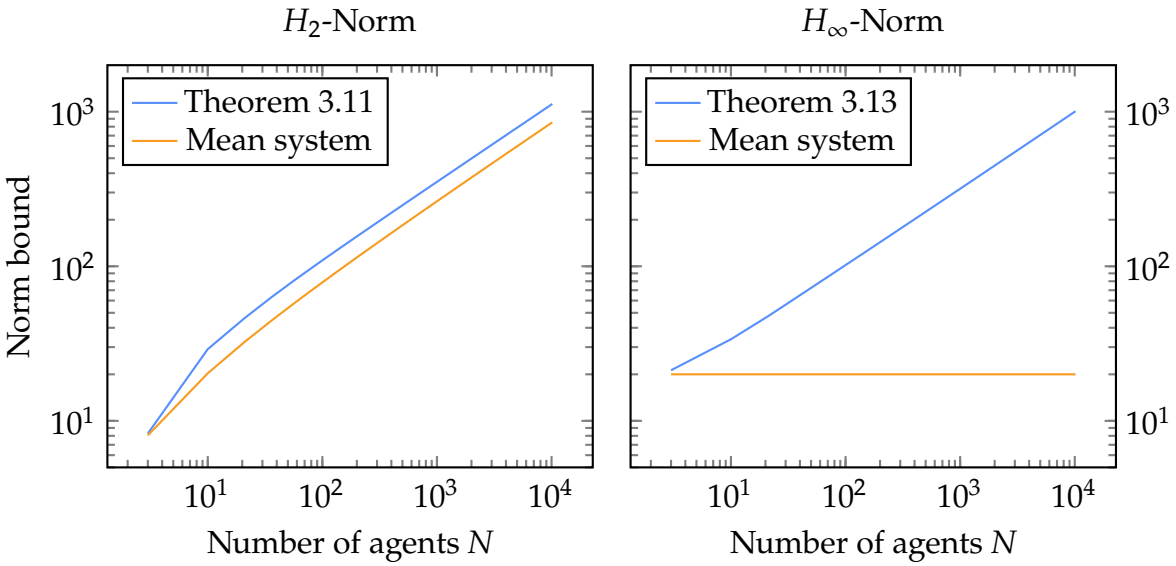

Figure 3.3.: Best upper bounds on the H_2- and H_∞-norm for the first-order consensus problem with $p = 0.5$ and increasing size of the communication graph $\mathcal{G}_h^\Delta$.

full spectrum of the Laplacian otherwise. The example has originally been discussed by Hespe and Werner (2023a) without the H_∞-norm results.

First, consider the H_2-norm of an IS consisting of $N = 20$ first-order integrators as introduced in Example 3.1. For such a network, the range of possible Laplacian eigenvalues is $0 < \lambda_2 \leq \lambda_N \leq N$ (Brouwer & Haemers, 2012, Section 3.9), where we assume that the underlying graph is undirected and connected. With fixed transmission probability $p = 0.5$, we can then utilize Theorem 3.11 to calculate an upper bound on the H_2-norm as a function of the eigenvalue bounds λ_2 and λ_N. Similarly, we apply Theorem 3.11 on the adjoint consensus problem with state-space matrices

$$\mathcal{A}_\mathrm{d} = 1, \qquad \mathcal{A}_\mathrm{c} = -\kappa, \qquad \mathcal{B}_\mathrm{p} = 1, \qquad C_\mathrm{d} = 1,$$

i.e. swapped inputs and outputs compared to Example 3.1. The contour lines of the resulting two-dimensional functions are shown in Figs. 3.4 and 3.5, respectively.

From the discussion of Section 3.4.2, we know that the primal and the adjoint consensus problem must have the same H_2-norm since their communication adheres to the Bernoulli packet loss model. In contrast, their H_2-norm bounds as obtained from Theorem 3.11 are entirely different, even though they are bounding the same underlying function. While the bound on Example 3.1 is essentially independent of λ_2 and close to linear in λ_N, Fig. 3.5 shows that the adjoint bound depends strongly on both the smallest and largest non-zero eigenvalue. This validates the suggestion given in Section 3.4.2 of evaluating the H_2-norm in terms of both the primal and adjoint system in order to obtain the best possible bound. Note, however, that the adjoint bound is strictly worse for all eigenvalue pairs (λ_2, λ_N) in this particular example.

In addition, we perform the same type of analysis on the H_∞-norm of the (primal) consensus problem. Varying the smallest and largest non-zero eigenvalue in the range $0 < \lambda_2 \leq \lambda_N \leq N$, the norm bound of Theorem 3.13 is evaluated as a function thereof and the resulting contour lines are shown in Fig. 3.6. Like the adjoint H_2-bound above,

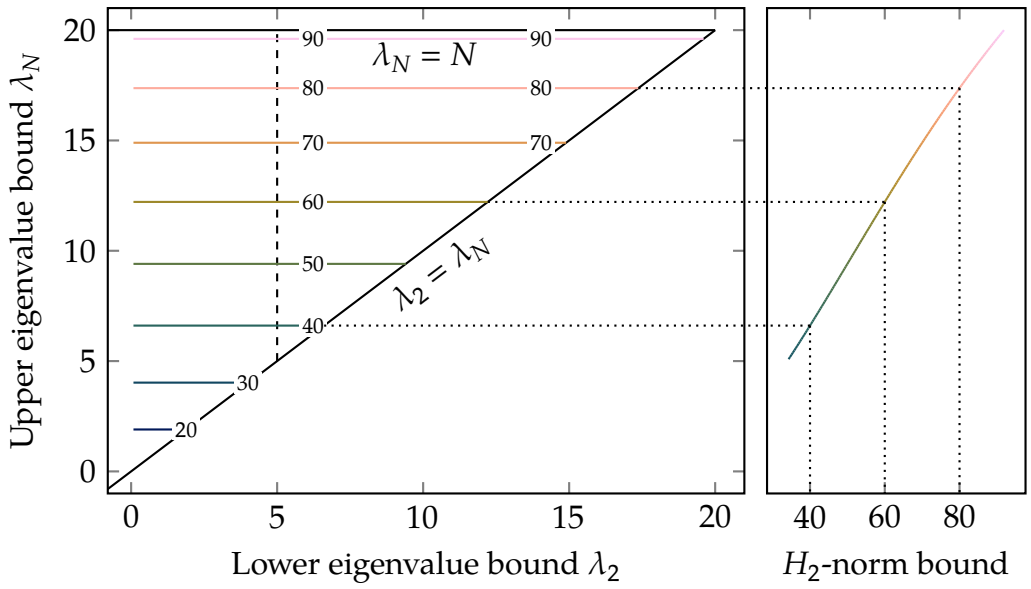

Figure 3.4.: Contour plot of the best upper bound on the H_2-norm of the consensus problem with $p = 0.5$ that can be obtained from Theorem 3.11 for different values of the eigenvalue bounds. The second plot shows a slice of the H_2-norm bound for fixed $\lambda_2 = 5$. (Hespe & Werner, 2023a)

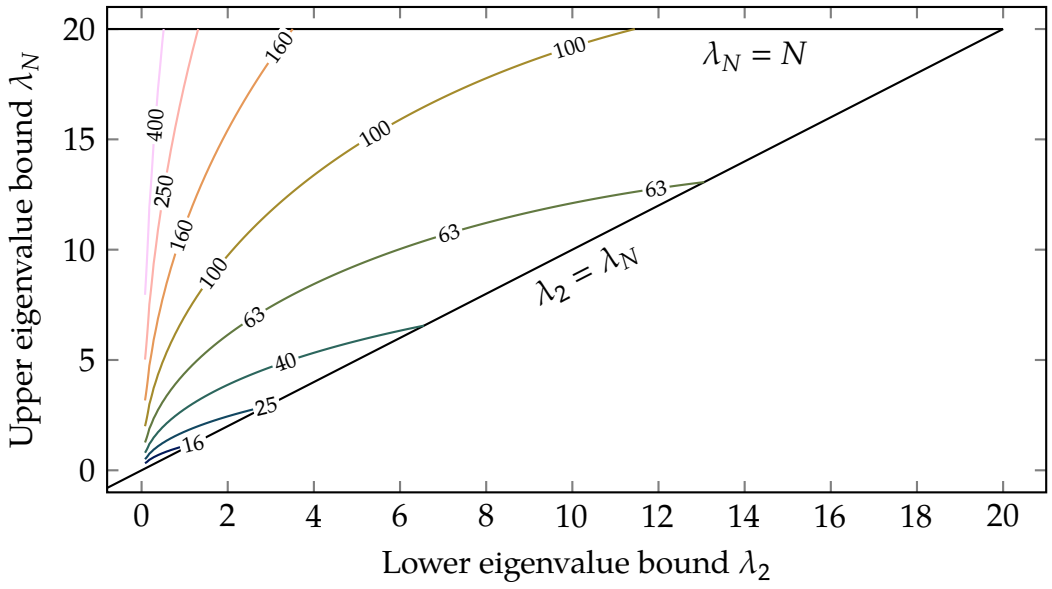

Figure 3.5.: Contour plot with logarithmically-spaced levels of the best upper bound on the H_2-norm of the adjoint consensus problem with $p = 0.5$ that can be obtained from Theorem 3.11 for different values of the eigenvalue bounds. (Hespe & Werner, 2023a)

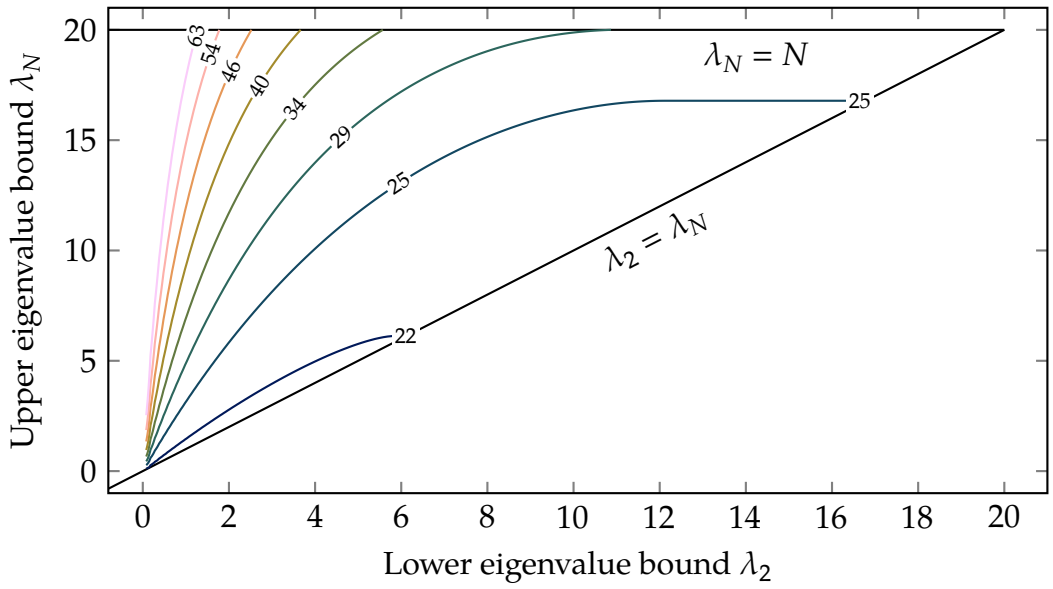

Figure 3.6.: Contour plot with logarithmically-spaced levels of the best upper bound on the H_∞-norm of the consensus problem with $p = 0.5$ that can be obtained from Theorem 3.13 for different values of the eigenvalue bounds.

the H_∞-bound depends on both λ_2 and λ_N. In particular, we observe a similar steep increase in the bound for small λ_2, which is to be expected since the connectivity of the underlying graphs degrades. Furthermore, the H_∞-norm bound is approximately constant along paths of equal ratio between λ_2 and λ_N, *i.e.* lines passing through the origin, for small eigenvalues, before starting to increase eventually. We emphasize, however, that these observations describe the norm *bound* as obtained by Theorem 3.13 and *not* the exact H_∞-norm of any particular system.

In conclusion, we see that Theorems 3.11 and 3.13 can be successfully employed even if only the boundary of the Laplacian spectrum is known. As expected, the norm bounds increase as the interval of admissible eigenvalues is enlarged, since the uncertainty in the underlying graph grows. Nonetheless, both theorems remain applicable and return useful norm bounds for the whole range of Laplacian eigenvalues.

Distributed Controller Synthesis for Stochastic Interconnections

4

In the previous chapter, we have seen how the framework of decomposable MJLS can be used to analyse the effect of stochastic communication in networked IS in a scalable manner. However, instead of merely appraising the influence of packet dropouts, it is desirable to design controllers that can mitigate the impact of random topology switching. Chapter 4 thus revolves around the derivation of synthesis conditions for (sub)optimal distributed state- and output-feedback controllers accounting for stochastic packet loss.

Accordingly, the focus lies on the open-loop MJLS

$$T\colon \begin{cases} x_{k+1} = A_{\sigma_k} x_k + B^w_{\sigma_k} w_k \ + B^u_{\sigma_k} u_k \\ z_k = C^z_{\sigma_k} x_k + D^{zw}_{\sigma_k} w_k + D^{zu}_{\sigma_k} u_k \\ y_k = C^y_{\sigma_k} x_k + D^{yw}_{\sigma_k} w_k \end{cases} \tag{4.1}$$

with state $x_k \in \mathbb{R}^{Nn_x}$ and the extra signals $u_k \in \mathbb{R}^{Nn_u}$ and $y_k \in \mathbb{R}^{Nn_y}$ that are the control input and measured output, respectively. All three signals are composites, consisting of signals $x^i_k \in \mathbb{R}^{n_x}$, $u^i_k \in \mathbb{R}^{n_u}$, and $y^i_k \in \mathbb{R}^{n_y}$. The stochastic switching process $\{\sigma_k\}$ and the performance in- and output w and z remain as they are defined for the closed loop in Section 2.4. Moreover, we introduce the controller K, which is a system that maps y into u and can be either static (Section 4.1) or dynamic (Section 4.2). A closed-loop system in the form of $\mathcal{T}$ is subsequently obtained by interconnecting the plant T and K through the signals u and y as shown in Fig. 4.1. Note that there is no direct feedthrough from u_k to y_k in the plant, but that there is no such assumption on the controller K. Even though this is a non-restrictive assumption since any physical system has a low-pass characteristic, it ensures that the closed-loop system is well-posed (*cf.* Scherer, 2000).

In general, the procedure to synthesize controllers through LMI-based system analysis conditions is well known: By treating the state-space model of the controller K as an optimization variable, we obtain a parametric representation of the closed-loop system that can be analysed through Theorems 3.11 and 3.13 for the H_2- and H_∞-norm, respectively. The main difficulty, however, lies in solving the resulting SDP. Since there are products of the Lyapunov matrix $\mathcal{X}$ with the closed-loop state-space matrices

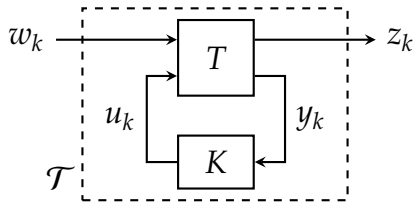

Figure 4.1.: Closed-loop system $\mathcal{T}$ consisting of the plant T and controller K

(and thus also with the state-space representation of K), it is necessary to perform a linearizing change of variables to solve the optimization problem efficiently (see Boyd et al., 1994; Gahinet, 1996, for state- and output-feedback versions thereof). In the realm of decomposable systems, similar transformations have been proposed by Massioni and Verhaegen (2009) to obtain distributed controllers as considered in this chapter. It is therefore the application of those known linearizing transformations to IS with stochastic communication that substantiates the novelty of the methods below.

The H_2-norm based synthesis conditions for state- and output-feedback controllers discussed in this chapter were originally derived in (Hespe et al., 2023).

4.1. Suboptimal Static State-Feedback Control

The first and simplest kind of control we are considering for this chapter are static state-feedback controllers that take the form

$$K\colon \quad u_k = D^{\mathrm{K}}_{\sigma_k} x_k = \left(I_N \otimes D^{\mathrm{K}}_{\mathrm{d}} + S_{\sigma_k} \otimes D^{\mathrm{K}}_{\mathrm{c}} + S^0 \otimes D^{\mathrm{K}}_{\mathrm{p}}\right) x_k \tag{4.2}$$

with matrix components $D^{\mathrm{K}}_{\mathrm{d}}$, $D^{\mathrm{K}}_{\mathrm{c}}$, and $D^{\mathrm{K}}_{\mathrm{p}}$ for the decoupled, stochastically coupled, and deterministically coupled channels, respectively. Note that this requires a specific structure in the plant T in which the measured output y corresponds to the state, *i.e.* $C^y_i = I_{Nn_x}$ and $D^{yw}_i = 0$ for all $i \in \mathcal{K}$. By inserting (4.2) into T, we obtain a closed-loop system with the same dynamic order as the plant and model matrices

$$\begin{aligned} \mathcal{A}_i &= A_i + B^u_i D^{\mathrm{K}}_i, & \mathcal{B}_i &= B^w_i, \\ \mathcal{C}_i &= C^z_i + D^{zu}_i D^{\mathrm{K}}_i, & \mathcal{D}_i &= D^{zw}_i \end{aligned}$$

such that the controller only appears in the system and output matrix and *not* in the input and feedthrough terms.

4.1.1. State-Feedback with H_2 Optimization

In order to apply the analysis results of Chapter 3, it has to be ensured that the closed loop of T and K is a decomposable MJLS matching the specification (2.14). First and foremost, this implies that the plant itself has to be decomposable, such that

$$C^z_i = I_N \otimes C^z_{\mathrm{d}} + S_i \otimes C^z_{\mathrm{c}} + S^0 \otimes C^z_{\mathrm{p}}$$

and similarly for all other terms of its state-space realization. However, because of the products $B^u_i D^{\mathrm{K}}_i$ and $D^{zu}_i D^{\mathrm{K}}_i$ in the closed-loop matrices above, this condition alone is not sufficient. It becomes apparent in the expanded product

$$\begin{aligned} B^u_i D^{\mathrm{K}}_i = I_N \otimes \left(B^u_{\mathrm{d}} D^{\mathrm{K}}_{\mathrm{d}}\right) + S_i \otimes \left(B^u_{\mathrm{d}} D^{\mathrm{K}}_{\mathrm{c}} + B^u_{\mathrm{c}} D^{\mathrm{K}}_{\mathrm{d}}\right) \\ + S^0 \otimes \left(B^u_{\mathrm{d}} D^{\mathrm{K}}_{\mathrm{p}} + B^u_{\mathrm{p}} D^{\mathrm{K}}_{\mathrm{d}}\right) + \left(S_i S_i\right) \otimes \left(B^u_{\mathrm{c}} D^{\mathrm{K}}_{\mathrm{c}}\right) \\ + \left(S^0 S_i\right) \otimes \left(B^u_{\mathrm{p}} D^{\mathrm{K}}_{\mathrm{c}}\right) + \left(S_i S^0\right) \otimes \left(B^u_{\mathrm{c}} D^{\mathrm{K}}_{\mathrm{p}}\right) + \left(S^0 S^0\right) \otimes \left(B^u_{\mathrm{p}} D^{\mathrm{K}}_{\mathrm{p}}\right) \end{aligned}$$

that the terms involving multiple interconnected components, *i.e.* B_{c}^{u}, B_{p}^{u}, $D_{\mathrm{c}}^{\mathrm{K}}$, and $D_{\mathrm{p}}^{\mathrm{K}}$, have to vanish since those belong to products of the pattern matrices which have no correspondence in $\mathcal{T}$. As such, the orthogonality constraints

$$B_{\mathrm{c}}^{u} D_{\mathrm{c}}^{\mathrm{K}} = B_{\mathrm{p}}^{u} D_{\mathrm{c}}^{\mathrm{K}} = B_{\mathrm{c}}^{u} D_{\mathrm{p}}^{\mathrm{K}} = B_{\mathrm{p}}^{u} D_{\mathrm{p}}^{\mathrm{K}} = 0 \tag{4.3a}$$

$$D_{\mathrm{c}}^{zu} D_{\mathrm{c}}^{\mathrm{K}} = D_{\mathrm{p}}^{zu} D_{\mathrm{c}}^{\mathrm{K}} = D_{\mathrm{c}}^{zu} D_{\mathrm{p}}^{\mathrm{K}} = D_{\mathrm{p}}^{zu} D_{\mathrm{p}}^{\mathrm{K}} = 0 \tag{4.3b}$$

have to be imposed on the controller parametrization during synthesis.

Even though these constraints are motivated from a purely algebraic standpoint, they have a very desirable *real-world* consequence when applied to MAS with Laplacian patterns. If the closed-loop system involved terms with products of pattern matrices, information could pass to the second-order neighbours, requiring either a two-hop communication scheme or multiple rounds of communication per time step to implement. The orthogonality constraints are therefore asserting that the network model introduced in Section 2.3 remains suitable for the closed loop.

Taking everything together, we are ready to state our H_2-norm based state-feedback synthesis condition. Due to its complexity, the theorem is stated in an abbreviated form below. The full statement and its proof can be found on page 143 in Appendix B.1.

Theorem 4.1.: H_2 State-Feedback Synthesis (Hespe et al., 2023)

Let T be a decomposable MJLS with L^0 and L_σ as patterns, an undirected nominal graph $\mathcal{G}^0$, and packet loss satisfying Assumption 3.4. There exists a state-feedback controller (4.2) *such that the closed loop is mean-square stable and has H_2-norm less than $\gamma > 0$ if there exist a symmetric X, a triple $\boldsymbol{N} \coloneqq (N_{\mathrm{d}}, N_{\mathrm{c}}, N_{\mathrm{p}})$ satisfying the orthogonality constraints*

$$B_{\mathrm{c}}^{u} N_{\mathrm{c}} = B_{\mathrm{p}}^{u} N_{\mathrm{c}} = B_{\mathrm{c}}^{u} N_{\mathrm{p}} = B_{\mathrm{p}}^{u} N_{\mathrm{p}} = 0, \tag{4.4a}$$

$$D_{\mathrm{c}}^{zu} N_{\mathrm{c}} = D_{\mathrm{p}}^{zu} N_{\mathrm{c}} = D_{\mathrm{c}}^{zu} N_{\mathrm{p}} = D_{\mathrm{p}}^{zu} N_{\mathrm{p}} = 0, \tag{4.4b}$$

and symmetric Z_i with $\sum_{i=1}^{N} \operatorname{tr} Z_i < \gamma^2$ that solve the LMIs

$$\mathrm{LMI}_{i,p}(X, \boldsymbol{N}) \succ 0 \qquad \text{(B.1a, abbreviated)}$$

$$\mathrm{LMI}_{i,p}(X, Z_i) \succ 0 \qquad \text{(B.1b, abbreviated)}$$

for all $i \in \{1, \dots, N\}$. Moreover, it is sufficient to validate (B.1a) *for $i \in \{1, N\}$.*

The synthesis conditions in Theorem 4.1 are affine in all variables, that is X, Z_i and the triple $(N_{\mathrm{d}}, N_{\mathrm{c}}, N_{\mathrm{p}})$, such that they can be implemented as an SDP with LMI constraints, and it is thus possible to optimize over the trace of Z_i. In addition, even though Theorem 4.1 just stipulates the *existence* of a norm bounding controller, the minimizing state-feedback gains are straightforward to recover from the optimized solution of the SDP as $D_{\mathrm{d}}^{\mathrm{K}} = N_{\mathrm{d}} X^{-1}$, $D_{\mathrm{c}}^{\mathrm{K}} = N_{\mathrm{c}} X^{-1}$, and $D_{\mathrm{p}}^{\mathrm{K}} = N_{\mathrm{p}} X^{-1}$. Note, however, that even though the resulting X is positive definite and thus non-singular, it might become ill-conditioned. For some cases, it is therefore be preferable to solve for the controller matrices by applying a numerically stable method instead of inverting X. A full procedure for synthesizing H_2-suboptimal state-feedback controllers is given by Algorithm 4.1.

Algorithm 4.1.: H_2 State-Feedback Synthesis

Require: Plant T, Laplacian L^0, Transmission probability p

1: Determine the eigenvalues λ_i of the Laplacian L^0.
2: Enforce the orthogonality constraints (4.4), *e.g.* by setting $N_\mathrm{c} = 0$ or $N_\mathrm{p} = 0$.
3: Solve the SDP

$$\begin{aligned} \min_{X, Z_i, \boldsymbol{N}} \quad & \sum_{i=1}^{N} \operatorname{tr} Z_i \\ \text{s.t.} \quad & \text{(B.1a)} \quad \forall\, i \in \{1, N\} \\ & \text{(B.1b)} \quad \forall\, i \in \{1, \dots, N\} \end{aligned}$$

4: Recover the controller through $D_\mathrm{d}^\mathrm{K} = N_\mathrm{d} X^{-1}$, $D_\mathrm{c}^\mathrm{K} = N_\mathrm{c} X^{-1}$, and $D_\mathrm{p}^\mathrm{K} = N_\mathrm{p} X^{-1}$.

4.1.2. Synthesizing H_∞ State-Feedback Controllers

In the same way as for the H_2-based controller synthesis in the previous section, the H_∞ analysis theorem can be employed to design state-feedback controllers that minimize the upper bound on the MJLS H_∞-norm. A major difference from the previous derivation is, however, that it is not only required that the closed-loop system is decomposable, but that there must not be any coupling in its input channel in order to satisfy Assumption 3.6. Since the state-feedback controller considered in this section does not appear in the input or feedthrough matrix of the closed-loop state-space realization, this can be assured based entirely on the open-loop system T through the following assumption:

Assumption 4.1.: Decoupled Performance Inputs

The decomposable MJLS T is input-decoupled on the performance channel, *i.e.* it holds that $B_\mathrm{c}^w = B_\mathrm{p}^w = 0$, $D_\mathrm{c}^{zw} = D_\mathrm{p}^{zw} = 0$, and $D_\mathrm{c}^{yw} = D_\mathrm{p}^{yw} = 0$.

The assumption that D_i^{yw} does not contain any coupling terms is redundant in the state-feedback case because $D_i^{yw} = 0$ for all $i \in \mathcal{K}$. However, this property is required for the H_∞-based output-feedback synthesis in Section 4.2.2, for which the controller parametrization does also influence the input and feedthrough terms. Together with the orthogonality constraints (4.3), Assumption 4.1 guarantees that the closed loop satisfies the preconditions of Theorem 3.13, leading to the following synthesis result. In the same way as for Theorem 4.1 above, the full statement and its proof have been moved into Appendix B.1 and can be found on page 144.

Theorem 4.2.: H_∞ State-Feedback Synthesis

Let T be a decomposable MJLS fulfilling Assumption 4.1 with L^0 and L_σ as patterns, an undirected nominal graph $\mathcal{G}^0$, and packet loss satisfying Assumption 3.4. There exists a state-feedback controller (4.2) *such that the closed loop is mean-square stable and has H_∞-norm less than $\gamma > 0$ if there exist a symmetric X and a triple $\boldsymbol{N} := (N_\mathrm{d}, N_\mathrm{c}, N_\mathrm{p})$ satisfying the orthogonality constraints* (4.4) *that solve the LMI*

$$\mathrm{LMI}_{i,p}(X, \boldsymbol{N}, \gamma) \succ 0 \qquad \text{(B.2, abbreviated)}$$

for $i \in \{1, N\}$.

Algorithm 4.2.: H_∞ State-Feedback Synthesis

Require: Plant T, Laplacian L^0, Transmission probability p

1: Determine the largest eigenvalue λ_N of the Laplacian L^0.
2: Enforce the orthogonality constraints (4.4), *e.g.* by setting $N_\mathrm{c} = 0$ or $N_\mathrm{p} = 0$.
3: Solve the SDP

$$\begin{aligned} \min_{X,\boldsymbol{N},\gamma} \quad & \gamma \\ \text{s.t.} \quad & \text{(B.2)} \quad \forall\, i \in \{1, N\} \end{aligned}$$

4: Recover the controller through $D_\mathrm{d}^\mathrm{K} = N_\mathrm{d} X^{-1}$, $D_\mathrm{c}^\mathrm{K} = N_\mathrm{c} X^{-1}$, and $D_\mathrm{p}^\mathrm{K} = N_\mathrm{p} X^{-1}$.

Since (B.2) is affine in γ, X, and the controller triple $(N_\mathrm{d}, N_\mathrm{c}, N_\mathrm{p})$, Theorem 4.2 can be posed as an SDP with the objective of minimizing γ in order to find the state-feedback controller with the best upper bound on the H_∞-norm. This procedure is outlined in Algorithm 4.2.

A common feature of both Theorems 4.1 and 4.2 is their excellent scalability to IS with many subsystems. For the H_2 result, the number of matrix variables and LMI constraints grows linearly with N while their size is constant. Even better, the H_∞ synthesis conditions of Theorem 4.2 are completely independent of the number of subsystems, leading to a constant computational complexity independent of N. This is a result of formulating the conditions with uniform X for all modal constraints as proposed in Section 3.1.2 to help with expressing the generalized variance and comes at the cost of suboptimal controllers. In contrast, the analysis of decomposable LTI systems is not restricted to a uniform Lyapunov matrix for all modal subsystems, and it is therefore possible to apply the more flexible linearizing change of variables proposed by de Oliveira et al. (1999). Nonetheless, synthesizing a controller with the desired decomposable structure necessitates imposing artificial constraints on the matrix variables, leading to conservative controllers even for the LTI synthesis of Massioni and Verhaegen (2009), albeit less so than for the conditions above.

4.2. Dynamic Output-Feedback Synthesis

Having outlined the general procedure for synthesizing suboptimal controllers for IS subject to stochastic communication effects, dynamic output-feedback controllers are investigated next. As such, this section deals with controllers K that take the form

$$K\colon \begin{cases} \eta_{k+1} = A_{\sigma_k}^\mathrm{K} \eta_k + B_{\sigma_k}^\mathrm{K} y_k, \\ u_k = C_{\sigma_k}^\mathrm{K} \eta_k + D_{\sigma_k}^\mathrm{K} y_k, \end{cases} \tag{4.5}$$

with controller state $\eta_k \in \mathbb{R}^{N n_\eta}$ and input and output corresponding to the measured *output* and control *input*, respectively. In the same way as the plant state, η_k is a composite signal consisting of the states $\eta_k^1, \eta_k^2, \ldots, \eta_k^N \in \mathbb{R}^{n_\eta}$ of the individual subsystems. For this dissertation, only full-order synthesis with $n_\eta = n_x$ is considered, *i.e.* the controller to be designed has the same number of states as T.

Table 4.1.: Constraints on the controller structure for three classes of open-loop plants, together with the corresponding variable constraints. (Hespe et al., 2023)

Case	Plant Structure	Controller Constraints	Variable Constraints
i)	$B_{\mathrm{c}}^{u} = B_{\mathrm{p}}^{u} = 0$ $D_{\mathrm{c}}^{zu} = D_{\mathrm{p}}^{zu} = 0$	$B_{\mathrm{c}}^{\mathrm{K}} = B_{\mathrm{p}}^{\mathrm{K}} = 0$ $D_{\mathrm{c}}^{\mathrm{K}} = D_{\mathrm{p}}^{\mathrm{K}} = 0$	$L_{\mathrm{c}} = L_{\mathrm{p}} = 0$ $N_{\mathrm{c}} = N_{\mathrm{p}} = 0$
ii)	$C_{\mathrm{c}}^{y} = C_{\mathrm{p}}^{y} = 0$ $D_{\mathrm{c}}^{yw} = D_{\mathrm{p}}^{yw} = 0$	$C_{\mathrm{c}}^{\mathrm{K}} = C_{\mathrm{p}}^{\mathrm{K}} = 0$ $D_{\mathrm{c}}^{\mathrm{K}} = D_{\mathrm{p}}^{\mathrm{K}} = 0$	$M_{\mathrm{c}} = M_{\mathrm{p}} = 0$ $N_{\mathrm{c}} = N_{\mathrm{p}} = 0$
iii)	All the above	None	None

By forming the interconnection of T and K as shown in Fig. 4.1 and stacking the plant and controller states, we obtain the closed-loop system

$$\begin{bmatrix} x_{k+1} \\ \eta_{k+1} \end{bmatrix} = \begin{bmatrix} A_{\sigma_k} + B_{\sigma_k}^{u} D_{\sigma_k}^{\mathrm{K}} C_{\sigma_k}^{y} & B_{\sigma_k}^{u} C_{\sigma_k}^{\mathrm{K}} \\ B_{\sigma_k}^{\mathrm{K}} C_{\sigma_k}^{y} & A_{\sigma_k}^{\mathrm{K}} \end{bmatrix} \begin{bmatrix} x_k \\ \eta_k \end{bmatrix} + \begin{bmatrix} B_{\sigma_k}^{w} + B_{\sigma_k}^{u} D_{\sigma_k}^{\mathrm{K}} D_{\sigma_k}^{yw} \\ B_{\sigma_k}^{\mathrm{K}} D_{\sigma_k}^{yw} \end{bmatrix} w_k$$

$$z_k = \begin{bmatrix} C_{\sigma_k}^{z} + D_{\sigma_k}^{zu} D_{\sigma_k}^{\mathrm{K}} C_{\sigma_k}^{y} & D_{\sigma_k}^{zu} C_{\sigma_k}^{\mathrm{K}} \end{bmatrix} \begin{bmatrix} x_k \\ \eta_k \end{bmatrix} + \left(D_{\sigma_k}^{zw} + D_{\sigma_k}^{zu} D_{\sigma_k}^{\mathrm{K}} D_{\sigma_k}^{yw} \right) w_k$$

with the desired performance inputs and outputs. However, the system does not match the structure of $\mathcal{T}$ since the pattern matrices cannot be pulled out as a left Kronecker factor, and the analysis results of Chapter 3 are therefore not applicable in its current form. For this reason, a permutation of the combined state has to be performed, such that the plant and controller states of the subsystems are stacked in alternating fashion, resulting in

$$\xi_k^{\top} = \begin{bmatrix} \left(x_k^1\right)^{\top} & \left(\eta_k^1\right)^{\top} & \left(x_k^2\right)^{\top} & \left(\eta_k^2\right)^{\top} & \dots & \left(x_k^N\right)^{\top} & \left(\eta_k^N\right)^{\top} \end{bmatrix}$$

for the closed loop, together with appropriately transformed $\mathcal{A}_i$, $\mathcal{B}_i$, and $\mathcal{C}_i$. The inputs and outputs, on the other hand, are not affected by the permutation.

4.2.1. Suboptimal H_2 Based Controller Design

Just like in the state-feedback scenario, it has to be ensured that all preconditions are met and thus that the closed-loop system is decomposable, before Theorem 3.11 can be applied for synthesis. However, it is impractical to enforce this property through orthogonality constraints like (4.3) as the number of matrix combinations would be drastically higher in the output-feedback case. Instead, we opt to formulate the constraints for three different kinds of open-loop plants, where there is no coupling in either i) the control input channel (B_i^u, D_i^{zu}), ii) the measured output channel (C_i^y, D_i^{yw}), iii) or both. For all three cases, the implications for the controller K, and subsequently the optimization variables to be introduced below, are shown in Table 4.1. The table shows that the constraints follow a straightforward pattern: If the plant is interconnected in its output (and thus the first case is relevant) the controller may not be interconnected in its input and *vice versa*. Similar albeit less restrictive constraints are put in place by Massioni and Verhaegen (2009) in their synthesis conditions for IS *without* stochastic networking

effects. Although the restrictiveness is exacerbated by the need of Theorems 3.11 and 3.13 for closed-loop systems that are affine in the patterns, the issue of having to artificially constrain the controller is therefore not unique to decomposable MJLS but a requirement for synthesizing controllers with the same structure as the plant.

The general approach to convert Theorem 3.11 into an output-feedback synthesis condition is analogous to the derivations in Section 4.1 for the state-feedback case. First it has to be ensured that no products between model matrices occur, then the closed-loop system is inserted, and finally a linearizing change of variables is applied to obtain an LMI that can be used to optimize over the parametrized controller. However, the linearizing change of variables that has been applied in Section 4.1 is not viable in the current scenario because of the sophisticated controller parametrization. Instead, we rely on the linearization technique proposed by Gahinet (1996) and Scherer et al. (1997). Due to its complexity, the theorem is stated in an abbreviated form below. The full statement and its proof can be found on page 145 in Appendix B.2.

Theorem 4.3.: H_2 Output-Feedback Synthesis (Hespe et al., 2023)

Let T be a decomposable MJLS matching one of the three cases in Table 4.1 that has L^0 and L_σ as patterns, an undirected nominal graph $\mathcal{G}^0$, and packet loss satisfying Assumption 3.4. There exists an output-feedback controller (4.5) *such that the closed loop is mean-square stable and has H_2-norm less than $\gamma > 0$ if there exist symmetric P, Q, triples $\boldsymbol{K} \coloneqq (K_\mathrm{d}, K_\mathrm{c}, K_\mathrm{p})$, $\boldsymbol{L} \coloneqq (L_\mathrm{d}, L_\mathrm{c}, L_\mathrm{p})$, $\boldsymbol{M} \coloneqq (M_\mathrm{d}, M_\mathrm{c}, M_\mathrm{p})$, $\boldsymbol{N} \coloneqq (N_\mathrm{d}, N_\mathrm{c}, N_\mathrm{p})$ satisfying one of the constraints of Table 4.1, and symmetric Z_i with $\sum_{i=1}^{N} \operatorname{tr} Z_i < \gamma^2$ that solve the LMIs*

$$\mathrm{LMI}_{i,p}(P, Q, \boldsymbol{K}, \boldsymbol{L}, \boldsymbol{M}, \boldsymbol{N}) \succ 0 \qquad \text{(B.3a, abbreviated)}$$

$$\mathrm{LMI}_{i,p}(P, Q, Z_i, \boldsymbol{L}, \boldsymbol{N}) \succ 0 \qquad \text{(B.3b, abbreviated)}$$

for all $i \in \{1, \dots, N\}$. Moreover, it is sufficient to validate (B.3a) *for $i \in \{1, N\}$.*

By itself, Theorem 4.3 is only an existence result, *i.e.* its feasibility establishes that there must exist a controller in the form of (4.5) that achieves the desired closed-loop H_2-norm. However, similar to the state-feedback case, its proof is constructive, and the desired controller can be reconstructed from the solution of the underlying SDP. Having obtained P and Q from Theorem 4.3, the first step is to solve $UV^\top = I - QP$ for a pair U, V of non-singular matrices. Starting at $D_\mathrm{d}^\mathrm{K} = N_\mathrm{d}$ and $D_\bullet^\mathrm{K} = N_\bullet$, the controller matrices can then be recovered in reverse order as

$$C_\mathrm{d}^\mathrm{K} = (M_\mathrm{d} - D_\mathrm{d}^\mathrm{K} C_\mathrm{d}^y P) V^{-\top}, \qquad C_\bullet^\mathrm{K} = (M_\bullet - D_\bullet^\mathrm{K} C_\mathrm{d}^y P - D_\mathrm{d}^\mathrm{K} C_\bullet^y P) V^{-\top}, \tag{4.6a}$$

$$B_\mathrm{d}^\mathrm{K} = U^{-1}(L_\mathrm{d} - Q B_\mathrm{d}^u D_\mathrm{d}^\mathrm{K}), \qquad B_\bullet^\mathrm{K} = U^{-1}(L_\bullet - Q B_\bullet^u D_\mathrm{d}^\mathrm{K} - Q B_\mathrm{d}^u D_\bullet^\mathrm{K}) \tag{4.6b}$$

for the input and output terms and finally

$$\begin{aligned} A_\mathrm{d}^\mathrm{K} &= U^{-1}\Big(K_\mathrm{d} - Q(A_\mathrm{d} + B_\mathrm{d}^u D_\mathrm{d}^\mathrm{K} C_\mathrm{d}^y) P\Big) V^{-\top} - B_\mathrm{d}^\mathrm{K} C_\mathrm{d}^y P V^{-\top} - U^{-1} Q B_\mathrm{d}^u C_\mathrm{d}^\mathrm{K}, \\ A_\bullet^\mathrm{K} &= U^{-1}\Big(K_\bullet - Q(A_\bullet + B_\bullet^u D_\mathrm{d}^\mathrm{K} C_\mathrm{d}^y + B_\mathrm{d}^u D_\bullet^\mathrm{K} C_\mathrm{d}^y + B_\mathrm{d}^u D_\mathrm{d}^\mathrm{K} C_\bullet^y) P\Big) V^{-\top} \\ &\quad - (B_\bullet^\mathrm{K} C_\mathrm{d}^y + B_\mathrm{d}^\mathrm{K} C_\bullet^y) P V^{-\top} - U^{-1} Q (B_\bullet^u C_\mathrm{d}^\mathrm{K} + B_\mathrm{d}^u C_\bullet^\mathrm{K}) \end{aligned} \tag{4.6c}$$

for the system matrices, where the subscript $\bullet$ is a placeholder for either 'c' or 'p'. The complete synthesis procedure is described in Algorithm 4.3.

Algorithm 4.3.: H_2 Output-Feedback Synthesis

Require: Plant T, Laplacian L^0, Transmission probability p

1: Determine the eigenvalues λ_i of the Laplacian L^0.
2: Determine which case of Table 4.1 applies for T.
3: Enforce the respective constraints of Table 4.1 on $(L_\mathrm{c}, L_\mathrm{p})$, $(M_\mathrm{c}, M_\mathrm{p})$, and $(N_\mathrm{c}, N_\mathrm{p})$.
4: Solve the SDP

$$\begin{aligned} \min_{\substack{P,Q,Z_i,\\ \boldsymbol{K},\boldsymbol{L},\boldsymbol{M},\boldsymbol{N}}} \quad & \sum_{i=1}^{N} \operatorname{tr} Z_i \\ \text{s.t.} \quad & \text{(B.3a)} \quad \forall\, i \in \{1, N\} \\ & \text{(B.3b)} \quad \forall\, i \in \{1, \dots, N\} \end{aligned}$$

5: Solve $UV^\top = I - QP$ for non-singular U and V, *e.g.* by singular value decomposition.
6: Recover the controller through (4.6).

A problem with this explicit construction is that the term $I - QP$ tends to be ill-conditioned for optimized solutions of (B.3). For this reason, an augmented optimization procedure with heuristic regulation terms is proposed in Section 4.2.2 of Scherer and Weiland (2015), who furthermore suggest using a numerically stable equation solver instead of the explicit expressions for the controller matrices given above.

4.2.2. H_∞ Synthesis for Input-Decoupled Interconnected Systems

Analogous conditions for output-feedback synthesis with respect to the H_∞-norm can be derived in similar fashion. Since the linearizing change of variables of Gahinet (1996) applies in the same way as before, we have to be mostly concerned about ensuring that the closed loop is input-decoupled according to Assumption 3.6. Contrasting the state-feedback case, Assumption 4.1 alone is insufficient as the input and feedthrough matrix of $\mathcal{T}$ are parametrized on the controller. However, in view of the constraints in Table 4.1 that are required to guarantee that the closed loop is decomposable, the desired structure can be imposed by combining Case i) with Assumption 4.1. The following result is therefore limited to IS that are connected through their measured output. As for Theorems 4.1 to 4.3 above, the synthesis conditions are given in abbreviated form and the full statement has been moved together with its proof to Appendix B.2 on page 146 due to its complexity. The corresponding synthesis procedure is described by Algorithm 4.4.

Theorem 4.4.: H_∞ Output-Feedback Synthesis

Let T be a decomposable MJLS fulfilling Assumption 4.1 in conjunction with Case i) of Table 4.1 that has L^0 and L_σ as patterns, an undirected nominal graph $\mathcal{G}^0$, and packet loss satisfying Assumption 3.4. There exists an output-feedback controller (4.5) such that the closed loop is mean-square stable and has H_∞-norm less than $\gamma > 0$ if there exist symmetric P, Q, triples $\boldsymbol{K} \coloneqq (K_\mathrm{d}, K_\mathrm{c}, K_\mathrm{p})$, $\boldsymbol{M} \coloneqq (M_\mathrm{d}, M_\mathrm{c}, M_\mathrm{p})$, and matrices L_d, N_d that solve

$$\mathrm{LMI}_{i,p}(P, Q, \boldsymbol{K}, L_\mathrm{d}, \boldsymbol{M}, N_\mathrm{d}, \gamma) \succ 0 \qquad \text{(B.4, abbreviated)}$$

for $i \in \{1, N\}$.

Algorithm 4.4.: H_∞ Output-Feedback Synthesis

Require: Plant T, Laplacian L^0, Transmission probability p

1: Determine the largest eigenvalue λ_N of the Laplacian L^0.

2: Solve the SDP

$$\begin{aligned} \min_{\substack{P,Q,\gamma,\\ \boldsymbol{K},L_\mathrm{d},\boldsymbol{M},N_\mathrm{d}}} \quad & \gamma \\ \text{s.t.} \quad & \text{(B.4)} \quad \forall\, i \in \{1, N\} \end{aligned}$$

3: Solve $UV^\top = I - QP$ for non-singular U and V, *e.g.* by singular value decomposition.

4: Recover the controller through (4.6).

Imposing the required structure by setting $L_\mathrm{c} = L_\mathrm{p} = 0$ and $N_\mathrm{c} = N_\mathrm{p} = 0$ in the proof of Theorem 4.4 reveals a general problem with enforcing additional constraints on the controller: Because of the linearizing change of variables, constraints cannot be asserted on the controller directly, but have to be applied through the respective optimization variables instead. For an example where this becomes an issue, consider how a practical distributed implementation of the synthesized output-feedback controllers would look like, and in particular what the mode-independent interconnected components A_p^K, B_p^K, C_p^K, and D_p^K entail. Conflicting the premise that all communication takes place over a stochastic network, these components mandate the existence of an ideal communication channel, and it is thus essential to zero all four terms during synthesis. However, enforcing this condition via the substituted variables K_p, L_p, M_p, and N_p is possible only if A_p, B_p^u, and C_p^y are zero as well, *i.e.* the deterministic component is used exclusively on the performance channel. In all other cases, the change of variables necessitates that the controller inherits the structure of the plant.

4.3. Application Examples

Similar to Chapter 3, the discussion on the suboptimal controller synthesis is closed by considering four examples to demonstrate the applicability of the results.

4.3.1. Optimized Consensus Gains

The first example is revisiting the integrators with inputs that were introduced in Example 3.1. Whereas the previous chapter only analysed the consensus problem with fixed gain $\kappa = 0.1$, the newly derived synthesis conditions create the possibility to tune the consensus protocol for better control performance in terms of the system norms. Note, however, that the protocol is not immediately in the required form for state-feedback synthesis, as shown by Fig. 4.2: A direct translation of (2.9) places the stochastic Laplacian between the integrators and the consensus gain κ, which corresponds to a static output-feedback control problem. Instead, we take advantage of the equivalent reformulation shown in Fig. 4.2b, which can be obtained by applying the commutation property of the Kronecker product (see Section 2.2.2). Even though this is trivial for the scalar consensus gain, the same technique can be utilized for higher order systems.

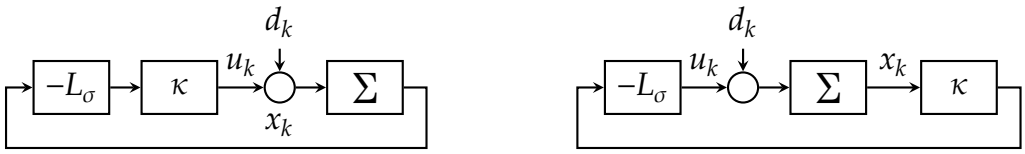

(a) Direct protocol representation (b) Rewritten to state-feedback form

Figure 4.2.: Block diagram representation of the first-order consensus problem. The left figure is a direct translation of the consensus protocol (2.9), the right figure is an equivalent reformulation that is suitable for state-feedback synthesis.

Based on Fig. 4.2, we formulate a generalized plant for controller synthesis with performance input $w_k = d_k$ through the disturbance and performance output $z_k = L^0 x_k + u_k$ as the sum of the consensus error and the input signal for regularization. In terms of the decomposable open-loop MJLS T, this results in the matrices

$$A_\mathrm{d} = 1, \qquad B_\mathrm{d}^w = 1, \qquad B_\mathrm{c}^u = -1, \qquad C_\mathrm{p}^z = \begin{bmatrix} 1 \\ 0 \end{bmatrix}, \qquad D_\mathrm{c}^{zu} = \begin{bmatrix} 0 \\ 1 \end{bmatrix},$$

where the control input u_k is deliberately passed to the performance channel through the stochastically interconnected component D_c^{zu} since the input is only applied by the agents if it is successfully received. The agents are then interconnected through the graph $\mathcal{G}_5^{\triangle}$ such that there are 15 agents in total with $\lambda_2 = 0.75$ and $\lambda_N = 7.66$. Sweeping over the transmission probability p with both Theorems 4.1 and 4.2, we obtain the optimized consensus gains visualized in Fig. 4.3.

The general trend indicated by the figure for both the H_2- and the H_∞-norm is that the consensus gain should be increased if the transmission probability is small. Intuitively, this is explained by the decreased loop gain due to the loss of information, such that the controller gain can be increased to compensate. Observe in particular that the optimized gains for small transmission probabilities are above the convergence threshold for ideal communication. Accordingly, while Proposition 3.9 has shown that gains stabilizing the ideal scenario with $p = 1$ continue to work for all non-zero probabilities, the converse is not necessarily true. For example, if the gains are chosen to optimize the performance at $p = 0.2$, the closed loop will become unstable for probabilities p close to 1.

4.3.2. Output-Feedback Synthesis for Second-Order Models

After discussing an example for the state-feedback synthesis of Theorems 4.1 and 4.2, the following scenarios are concerned with *distributed* output-feedback controllers. As such, we introduce a dynamic agent model that still has a single input and output but is subject to inertia, in contrast to the kinematic first-order integrators considered above.

Example 4.1.: Second-Order Friction Model

Consider a collective of decoupled masses moving along a one-dimensional space with linear velocity-dependent friction. This is described by the ordinary differential equation

$$\begin{bmatrix} \dot{s}^i(t) \\ \dot{v}^i(t) \end{bmatrix} = \begin{bmatrix} 0 & 1 \\ 0 & -b/M \end{bmatrix} \begin{bmatrix} s^i(t) \\ v^i(t) \end{bmatrix} + \begin{bmatrix} 0 \\ 1/M \end{bmatrix} f^i(t),$$

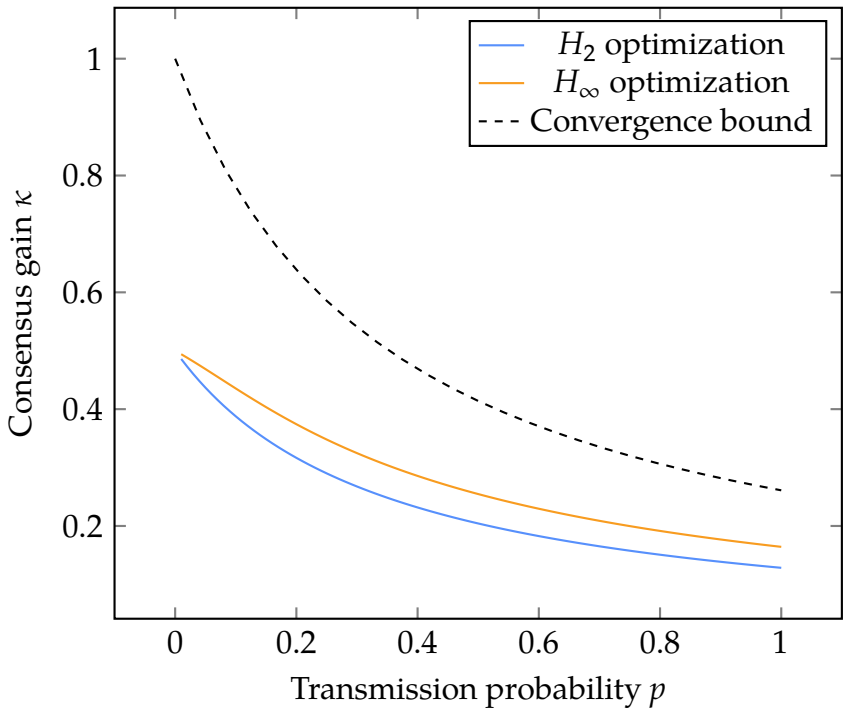

Figure 4.3.: Consensus gain κ tuned with respect to the H_2- and H_∞-norm depending on the transmission probability p. The dashed line indicates the upper bound on κ to ensure convergence as obtained by Proposition 3.9.

where $s^i(t)$, $v^i(t)$, and $f^i(t)$ are the position, velocity, and force input of mass i, respectively. Assuming a mass of $M = 1\,\mathrm{kg}$ and a damping coefficient $b = 4\,\mathrm{kg/s}$, an exact zero-order hold discretization with 1 s sampling time leads to a discrete-time agent model of

$$\begin{bmatrix} s^i_{k+1} \\ v^i_{k+1} \end{bmatrix} = \begin{bmatrix} 1 & 0.25 \\ 0 & 0.018 \end{bmatrix} \begin{bmatrix} s^i_k \\ v^i_k \end{bmatrix} + \begin{bmatrix} 0.19 \\ 0.25 \end{bmatrix} f^i_k. \tag{4.7}$$

The force f^i_k is determined by the control input u^i_k and a disturbance w^i_k as $f^i_k = u^i_k + w^i_k$, and the position is measured for feedback, *i.e.* $y^i_k = s^i_k$.

The task at hand is now to find a distributed controller to drive the network of agents into consensus in terms of their position. More specifically, we consider a feedback loop as shown in Fig. 4.4, where a collective of dynamically decoupled agents is controlled by identical controllers K that not only receive the consensus error e_k but furthermore locally exchange their states η_k. This leads to the distributed difference equation

$$\begin{aligned} \eta^i_{k+1} &= \mathcal{A}^{\mathrm{K}}_{\mathrm{d}} \eta^i_k + \sum_{j \in \mathcal{N}_i^-} \phi^{ij}_k \Big[A^{\mathrm{K}}_{\mathrm{c}} \big(\eta^i_k - \eta^j_k \big) - B^{\mathrm{K}}_{\mathrm{d}} \big(y^i_k - y^j_k \big) \Big] \\ u^i_k &= C^{\mathrm{K}}_{\mathrm{d}} \eta^i_k + \sum_{j \in \mathcal{N}_i^-} \phi^{ij}_k \Big[C^{\mathrm{K}}_{\mathrm{c}} \big(\eta^i_k - \eta^j_k \big) - D^{\mathrm{K}}_{\mathrm{d}} \big(y^i_k - y^j_k \big) \Big] \end{aligned}$$

for the controller of the ith agent that can be evaluated locally by the agent.

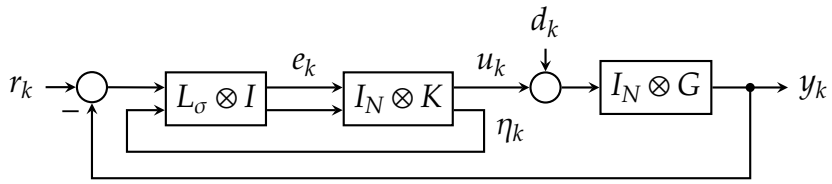

Figure 4.4.: Block diagram of dynamically decoupled agents with distributed dynamic output-feedback controllers. Note that the agents are not only exchanging their own measured states y_k, but in addition their local controller states η_k. (Hespe et al., 2023)

For the first scenario, we are comparing H_2-suboptimal controllers: one controller obtained from Theorem 4.3 for *fixed* transmission probability $p = 0.3$, and the second synthesized by applying Theorem 15 of Massioni and Verhaegen (2009) under the assumption of ideal communication. In both cases, additional constraints placed on the controller variables ensure that it can be implemented in a distributed fashion with a single exchange of information per time step, corresponding to the first case of Table 4.1 for Theorem 4.3 and Case 2 of Table 1 in Massioni and Verhaegen (2009). Furthermore, as discussed below Theorem 4.4, it has to be enforced that A_p^K, B_p^K,C_p^K, and D_p^K are zero by restricting the associated controller variables in Theorem 4.3.

The performance of both controllers is evaluated for IS with communication networks that adhere to the homogeneous Bernoulli packet loss model with varying transmission probabilities by calculating the H_2-norm using Theorem 3.12. As such, we are severely restricted in the number of agents we can consider due to scalability of the underlying SDP (see Section 3.6.2) and can only discuss the controllers for interconnections on the graph $\mathcal{G}_3^\triangle$. In the following, it is important to distinguish between the transmission probability of the communication network and the design parameter used during synthesis. Even though both are typically related, treating p as a free parameter creates additional degrees of freedom in the design. Figure 4.5 shows the resulting closed-loop norms, where we emphasize that a single controller is designed with Theorem 4.3 (with *design parameter* $p = 0.3$), but that this controller is tested on the whole range of probabilities.

As indicated by the figure, neither of the controllers is superior to the other for the entire range of transmission probabilities. For probabilities larger than 0.55, the reference controller of Massioni and Verhaegen (2009) outperforms the proposed solution, which does not stabilize the closed loop for networks with $p > 0.8$. On the other hand, the proposed method results in a 10 % improvement in closed-loop norm at the design probability of $p = 0.3$, demonstrating that the packet loss induced performance degradation can be partially compensated. Finally, both controllers fail to stabilize the system for $p \to 0$ since exchanging information becomes almost impossible.

4.3.3. Simulated Performance Evaluation Based on the SINR

The first evaluation scenario has shown that the proposed synthesis approach can lead to controllers with improved closed-loop H_2-norm for systems subject to packet loss following the homogeneous Bernoulli model of Assumption 3.4. However, as discussed in Chapter 3, this model does not accurately describe physical reality and is employed for mathematical tractability. For the second scenario, taken from Hespe et al. (2023), the

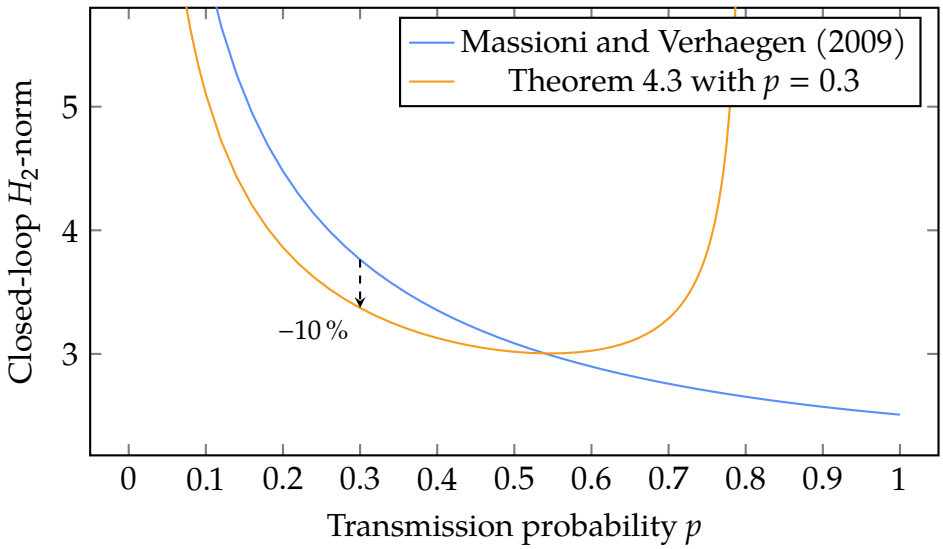

Figure 4.5.: Closed-loop H_2-norm of the second-order friction model with two different controllers plotted over the transmission probability. A nominal controller designed using the synthesis conditions of Massioni and Verhaegen (2009) is compared to a controller derived from Theorem 4.3 with $p = 0.3$.

idea is hence to evaluate controllers designed with Theorem 4.3 outside their specification in a communication network model that is closer to reality.

One kind of model that can represent stochastic packet loss in networked IS more accurately is based on calculating the SINR for each attempted transmission. Since analysing this kind of model is tractable only for specific cases such as the first-order consensus problem considered by Schneider and Frey (2020), we opt to rely on Monte-Carlo simulations instead, which are implemented in the WiMAS simulation environment described in Appendix A. This works well for the H_2-norm, since it is defined in terms of the expected output energy as the response to a known and fixed input signal, the discrete-time unit impulse. As such, the norm can be approximated by repeatedly simulating the same system for different realization of the switching process $\{\sigma_k\}$. In contrast, the H_∞-norm requires finding the worst-case *stochastic* input signal w, and Monte-Carlo simulations would therefore only result in lower bounds on the norm.

As before, we evaluate two kinds of output-feedback controllers: a nominal controller obtained from the approach of Massioni and Verhaegen (2009), and controllers synthesized using Theorem 4.3 for different values of the *synthesis parameter* p. The controllers are tasked with bringing a network of 25 masses as described in Example 4.1 into a line with 1 m distance between agents, representing a formation of approximated vehicle models. It is assumed that the scenario takes place underwater, and WiMAS is therefore configured to simulate an acoustic underwater modem called Marlin as described by Sendra et al. (2016). Transmitting at a carrier frequency of 23 kHz with a bandwidth of 14 kHz, the capacity of the communication channel is severely limited compared to radio frequency communication, reaching only 480 bit/s. Since the simulation is set up to slightly exceed this threshold, the channel quality degrades and transmissions become unreliable. Furthermore, the communication topology is restricted to a two-hop line graph resembling the targeted formation to localize the computation required at the

Table 4.2.: Parameters of the WiMAS simulation used in Section 4.3.3. See Appendix A and (Hespe et al., 2023) for a description of the parameters.

Parameter Name	Value	Unit
Nakagami shape parameter	2	
Path loss coefficient	2.5	
Carrier frequency	23	kHz
Channel bandwidth	14	kHz
Transmission power	10	mW
Package size	96	bit
Number of agents	25	
Number of transmission slots	10	

agent level, even though the acoustic modem is inherently broadcasting. On overview of the WiMAS simulation parameters that are used in this section can be found in Table 4.2. For reference, the same set of controllers is tested with idealized communication, where the exact H_2-norm can be computed efficiently since the closed loops are decomposable LTI systems. This results in two sets of closed-loop H_2-norms, estimated for the SINR case and exact for the idealized one, which are visualized in Fig. 4.6.

As expected, the reference controller based on the approach of Massioni and Verhaegen (2009) achieves a lower closed-loop H_2-norm than Theorem 4.3 applied with $p = 1$, since their technique is based on a less conservative linearizing change of variables. However, the best achievable H_2-norm under the structural constraints on the controller is unknown since neither approach results in an optimal controller. Coincidentally, this leads to a small range of synthesis parameters around $p \approx 0.5$ for which controllers derived from Theorem 4.3 are marginally improving on the reference implementation. On the other hand, the closed-loop H_2-norm of the reference controller increases from 5.90 to 7.11 under SINR-based packet loss, showing how the closed-loop control performance is affected by the network properties. In contrast, the controllers synthesized from Theorem 4.3 are less affected by the stochastic switching and achieve a best-case H_2-norm of 6.59, recovering 43 % of the packet loss induced performance degradation.

4.3.4. Mixed-Objective Synthesis

For our final controller synthesis example, we consider a mixed-objective controller synthesis problem that involves both the H_2- and the H_∞-norm. More specifically, the H_2-norm is kept as the performance criterion in the same way as for the previous examples, and a bound is placed on the closed-loop H_∞-norm to guarantee robust stability using the *small-gain theorem* (Todorov & Fragoso, 2009, 2012). As such, consider a version of the difference equation (4.7) that is affected by the uncertainty $\delta^i \in \mathbb{R}$ as

$$\begin{bmatrix} s_k^i \\ v_k^i \end{bmatrix} = \begin{bmatrix} 1 & 0.1 \\ 0 & 0.1 + \delta^i \end{bmatrix} \begin{bmatrix} s_k^i \\ v_k^i \end{bmatrix} + \begin{bmatrix} 0 \\ 1 \end{bmatrix} f_k^i$$
$$y_k^i = \begin{bmatrix} 1 & 0 \end{bmatrix} \begin{bmatrix} s_k^i \\ v_k^i \end{bmatrix},$$

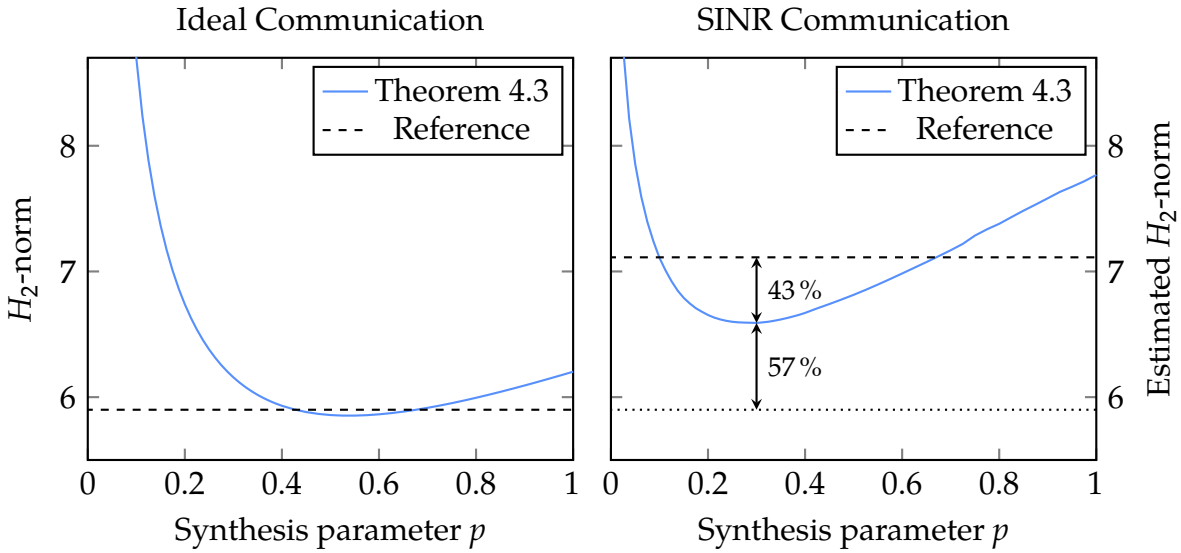

Figure 4.6.: Estimated H_2-norm for controller synthesized by Theorem 4.3 for different values of the synthesis parameter p with either ideal communication or an underwater SINR-based packet loss model. The performance of a controller synthesized by the technique of Massioni and Verhaegen (2009) is included for reference.

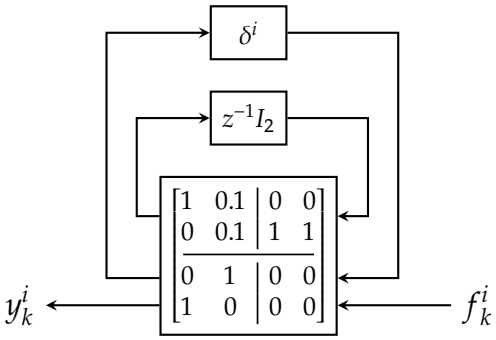

Figure 4.7.: Visualization of the LFT (4.8) representing a single uncertain subsystem, where z^{-1} represent the discrete-time one-step delay operator.

i.e. has uncertain damping. Applying a linear fractional transformation (LFT), this can be rewritten into

$$\begin{bmatrix} s_k^i \\ v_k^i \end{bmatrix} = \begin{bmatrix} 1 & 0.1 \\ 0 & 0.1 \end{bmatrix} \begin{bmatrix} s_k^i \\ v_k^i \end{bmatrix} + \begin{bmatrix} 0 \\ 1 \end{bmatrix} w_k^{\delta,i} + \begin{bmatrix} 0 \\ 1 \end{bmatrix} f_k^i \tag{4.8a}$$

$$z_k^{\delta,i} = \begin{bmatrix} 0 & 1 \end{bmatrix} \begin{bmatrix} s_k^i \\ v_k^i \end{bmatrix} \tag{4.8b}$$

$$y_k^i = \begin{bmatrix} 1 & 0 \end{bmatrix} \begin{bmatrix} s_k^i \\ v_k^i \end{bmatrix} \tag{4.8c}$$

with scalar uncertainty channel $w_k^{\delta,i} = \delta^i z_k^{\delta,i}$. A visual representation of the transformed loop is shown in Fig. 4.7. For the combined MAS, this results in the block-diagonal uncertainty $\Delta := \operatorname{diag}(\delta^1, \delta^2, \dots, \delta^N)$ with norm bound $\|\Delta\| = \max_i |\delta^i|$. According to the

small-gain theorem, a controller is therefore robustly stabilizing the uncertain system if the H_∞-norm of the channel $w^\delta \to z^\delta$ is less than $1/\|\Delta\|$.

In order to solve the resulting control problem, we follow the approach proposed by Scherer et al. (1997) of searching for a common Lyapunov function for both performance criteria. Therefore, the LMI constraints of Theorems 4.3 and 4.4 are imposed with shared variables P and Q, and the controller is recovered with the same transformation as described in Section 4.2.1. This is a known conservative choice, leading to worse bounds on the norms, but allows to directly take advantage of the individual synthesis conditions in a straightforward way. A less conservative technique that supports different Lyapunov functions for each norm constraint has been introduced by de Oliveira et al. (1999), requiring extra coupling variables with a more extensive linearization and subsequently different LMI constraints.

For evaluation, this technique is applied to an IS with $N = 9$ subsystems that are interconnected using the graph $\mathcal{G}_3^\Delta$ and subject to homogeneous Bernoulli distributed packet loss. In order to study the effect of a growing uncertainty, we synthesize output-feedback controllers for varying loss probabilities and different norm bounds on the uncertainties δ^i. Therefore, the design objective is to minimize the closed-loop H_2-norm bound while guaranteeing that the $w^\delta \to z^\delta$ channel has a H_∞-norm of less than $1/\|\Delta\|$. The resulting H_2-norm bounds are visualized in Fig. 4.8 for five different values of $\|\Delta\|$. As expected, the H_2-norm bound increases as the uncertainty in δ^i grows. Furthermore, the same holds for the smallest transmission probability for which the synthesis procedure is able to find a stabilizing controller. While the ideal case ($\delta^i = 0$) can be stabilized even with p below 0.1, the procedure fails to synthesize controllers for probabilities less than 0.7 in the worst scenario ($|\delta^i| < 0.2$).

Finally, we consider the closed-loop H_∞-norm of the uncertainty channel $w^\delta \to z^\delta$. During the mixed-objective synthesis, the minimization of the H_2-norm leads to an increase in the H_∞-norm bound up to the small-gain condition, *i.e.* that the H_∞-norm is less than $1/\|\Delta\|$. However, since the procedure is conservative, the actual closed-loop H_∞-norm is generally smaller, such that larger uncertainties can be tolerated. Therefore, we apply Theorem 3.13 and the alternative BRL described in Section 3.4.4 in order to obtain improved H_∞-norm bounds. The resulting curve for the case with uncertainty norm bound $|\delta^i| < 0.2$ is visualized in Fig. 4.9.

Both improved norm bounds stay far below the small-gain limit of 20 that follows from $\|\Delta\| < 0.05$ with more than an order of magnitude difference for some transmission probabilities, highlighting the conservatism of the synthesis procedure. As discussed by de Oliveira et al. (1999) and Scherer et al. (1997), the issue lies in using a shared Lyapunov function for both the H_2- and H_∞-norm bounds and can be partially avoided by applying a different linearizing change of variables in the derivation of the synthesis LMIs. In addition, Fig. 4.9 demonstrates that the bound obtained from the BRL in Section 3.4.4 is significantly smaller than the norm-bound provided by Theorem 3.13. However, since Section 3.4.4 is restricted to deterministic input signals and z^δ (and hence also w^δ) is stochastic, it is invalid to use this bound in the context of the small-gain theorem. Note that computing the actual H_∞-norm of the $w^\delta \to z^\delta$ channel using Theorem 3.12 is computationally intractable, such that the bound obtained from Theorem 3.13 is the best available estimate.

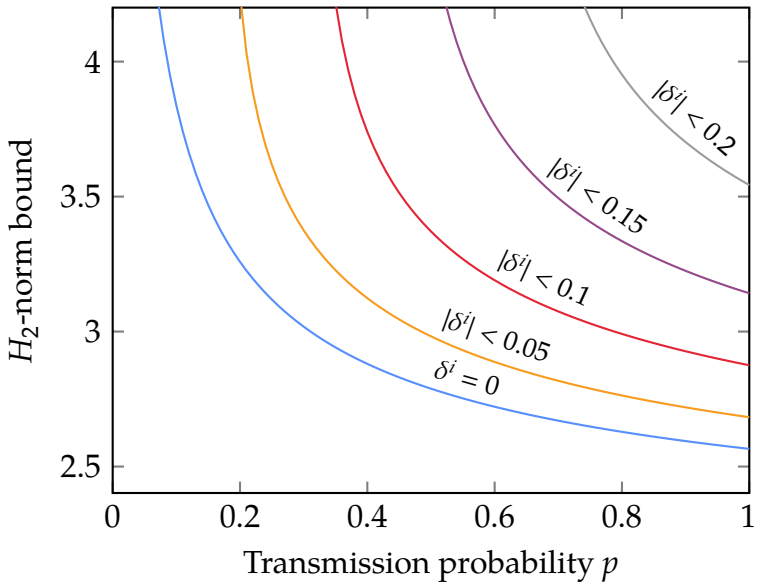

Figure 4.8.: Bounds on the closed-loop H_2-norm as obtained during synthesis for different transmission probabilities p and bounds on the norm of the uncertainty δ^i.

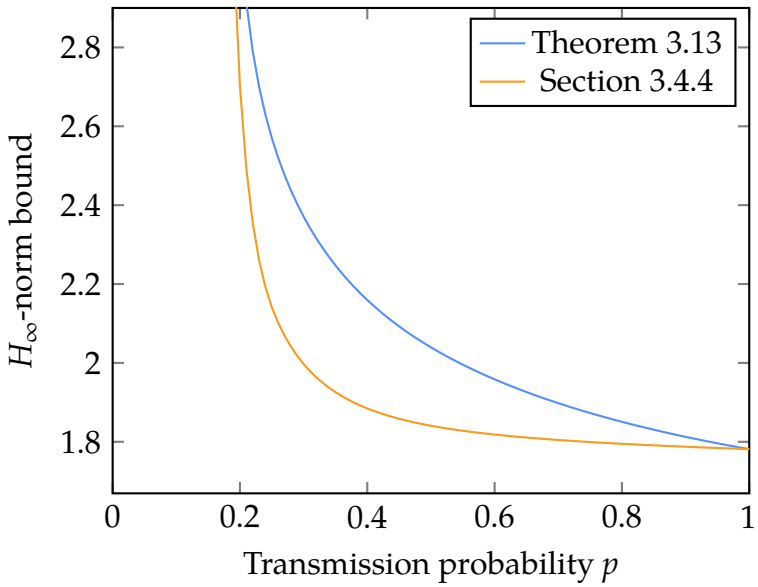

Figure 4.9.: Closed-loop H_∞-norm bounds as obtained from Theorem 3.13 and the alternative BRL as described in Section 3.4.4 for varying transmission probability p and with uncertainty norm bound $|\delta^i| < 0.05$.

5 Going Beyond Homogeneous Bernoulli Distributions

Up to this point, the control theoretic results of this dissertation have revolved around two central assumptions:

1) All preceding results, whether they are formulated in general terms for the patterns S_i and S^0 or specialized to the Laplacian, rely on the assumption that the switching process $\{\sigma_k\}$ is independent in time.

2) The results that are specialized to the Laplacian require spatial independence for the edge-wise loss processes and a homogeneous transmission probability.

However, as discussed in Section 2.3, these assumptions are made for reasons of mathematical tractability and only serve as an idealized approximation of the communication process. For accurately modelled wireless broadcast networks, the distribution of the edge loss processes $\{\phi_k^{ij}\}$ depends on the location of the transmitter and receiver, and the loss probabilities are therefore heterogeneous. Furthermore, networking components such as medium access control, routing, or congestion control have an influence on the distributions and are potentially introducing spatial dependencies between transmission links (Lee & Messerschmitt, 2002; Schneider & Frey, 2020). (See also Goldsmith, 2012; Tse & Viswanath, 2005, for a general overview.)

Despite the empirical evidence of Section 4.3.3 that controllers tuned with respect to the idealized Bernoulli networking model are performing well even if run outside their specification, the discussion above implies that the analytic guarantees that were obtained in the preceding chapters are invalid for most practically relevant scenarios. The aim of this chapter is therefore to challenge the assumptions one by one, gradually softening them. At first, Section 5.1 is removing the assumption of having a known transmission probability by treating the parameter p as an uncertainty and falling back to tools from robust control. Building on these ideas, Section 5.2 presents an alternative decomposition of the analysis conditions that remains applicable for communication networks with heterogeneous but symmetric transmission probabilities. Finally, Section 5.3 develops a geometric argument to show that the stability and performance analysis is distributionally robust, even against small spatio-temporal dependencies between transmission links. The majority of the results discussed below were reported before in (Hespe & Werner, 2023b) and (Hespe, Datar & Werner, 2024).

5.1. Uncertain Homogeneous Transmission Probabilities

As mentioned in the introduction to the current chapter, our first step is to consider the homogeneous transmission probability p as an uncertain parameter of the system.

Importantly, however, we assume that there are known bounds on the probability in the sense that $p \in [\rho_\mathrm{l}, \rho_\mathrm{u}]$ with constants $0 \leq \rho_\mathrm{l} \leq \rho_\mathrm{u} \leq 1$, where the trivial bound $\rho_\mathrm{l} = 0$ and $\rho_\mathrm{u} = 1$ is permissible but corresponds to a scenario without any information on the probability. Moreover, p is considered to be constant, *i.e.* while only partial knowledge about its value is available, it is guaranteed not to change. In view of the mean-square stability and performance analysis conditions of Chapter 3, the question is therefore whether the feasibility of the corresponding SDPs can be established not only for a single probability, but rather all $p \in [\rho_\mathrm{l}, \rho_\mathrm{u}]$, which by nature is an infinite-dimensional constraint. Finding a suitable formulation for each of the problems is therefore essential to arrive at computationally tractable conditions. In order to present the core ideas concisely, the discussion is focussed on robust mean-square stability in the following, and the question of robust performance is postponed to Section 5.2.

5.1.1. Obtaining Polynomial Uncertainties Through Parameter Lifting

The first question to answer involves the parametrization of the Lyapunov matrix Y. Since mean-square stability can be verified separately for each transmission probability as p is assumed to be constant, the feasibility of the LMI (3.7) does not have to be checked with uniform Y for all $p \in [\rho_\mathrm{l}, \rho_\mathrm{u}]$, but different $Y(p)$ are admissible. Compared to searching for a single Y, this has the potential to drastically reduce the incurred conservatism (see Hoffmann & Werner, 2015a; Wu et al., 1996, for discussions in the context of LPV systems), but the resulting infinite-dimensional optimization variables need to be suitably parametrized in order to obtain computationally tractable conditions. As an example, de Oliveira et al. (2009) suggest parametrizing $Y(p)$ as a homogeneous polynomial of fixed degree in order to solve a robust stabilization problem for general uncertain MJLS. However, as the primary objective of this section is to develop the fundamental techniques required to analyse heterogeneous loss models, we will limit our considerations to the case of a constant Y for the sake of simplicity.

Inspired by the convexity argument in the proof of Theorem 3.6, a particularly simple result could be obtained if the left-hand side of

$$\bar{\mathcal{A}}_i^\mathsf{T} Y \bar{\mathcal{A}}_i + 2p(1-p)\lambda_i \mathcal{A}_\mathrm{c}^\mathsf{T} Y \mathcal{A}_\mathrm{c} \prec Y \qquad \text{(3.7, restated)}$$

is a convex matrix-valued polynomial in p. As shown in Lemma 8 of Hespe, Saadabadi et al. (2024), this is the case if and only if all non-zero eigenvalues of the nominal Laplacian L^0 are greater than or equal to two (with the elementary hypothesis of $\mathcal{A}_\mathrm{c} \neq 0$). Unfortunately, all undirected planar graphs adhere to the bound

$$\lambda_2 \leq \frac{8}{N} \max_i d_i$$

provided by Theorem 3.3 of Spielman and Teng (2007). Because the number of vertices N is typically much larger than the maximum vertex degree d_i, the convexity argument is therefore only applicable in exceptional cases.

Instead, we propose to isolate the uncertainty by applying an LFT (Zhou et al., 1996). The first step is to rewrite (3.7) as

$$\begin{bmatrix} I_{n_\xi} \\ \mathcal{A}_\mathrm{d} + p\lambda_i \mathcal{A}_\mathrm{c} + \lambda_i \mathcal{A}_\mathrm{p} \\ \sqrt{2p(1-p)\lambda_i}\mathcal{A}_\mathrm{c} \end{bmatrix}^\mathsf{T} \begin{bmatrix} -Y & & \\ & Y & \\ & & Y \end{bmatrix} \begin{bmatrix} I_{n_\xi} \\ \mathcal{A}_\mathrm{d} + p\lambda_i \mathcal{A}_\mathrm{c} + \lambda_i \mathcal{A}_\mathrm{p} \\ \sqrt{2p(1-p)\lambda_i}\mathcal{A}_\mathrm{c} \end{bmatrix} \prec 0, \qquad (5.1)$$

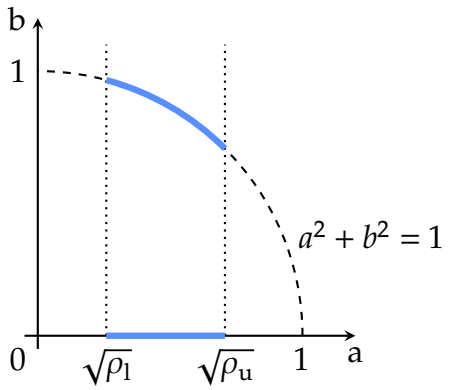

Figure 5.1.: Visualization of the described parameter lifting technique. The one-dimensional interval $[\rho_l, \rho_u]$ is lifted onto the two-dimensional unit circle, resulting in a non-convex uncertainty set.

separating the model matrices in the left and right factors from the Lyapunov matrix Y and exposing an issue with the current parametrization of the uncertainty. Because of their structure, LFTs are only applicable to rational parametric uncertainties, while the outer factors contain radicals of the parameter. Therefore, it is necessary to introduce a parameter transformation, embedding the one-dimensional uncertainty in a two-dimensional parameter space as shown in Fig. 5.1. As such, we define two new parameters $a := \sqrt{p}$ and $b := \sqrt{1-p}$, *i.e.* we project the uncertainty set onto the unit circle since a and b satisfy $a^2 + b^2 = 1$ by definition. Observe that $p = a^2$ and $\sqrt{p(1-p)} = ab$ such that the uncertainty is a homogeneous polynomial in the lifted parametrization, resulting in the LMI

$$\begin{bmatrix} I_{n_\xi} \\ \mathcal{A}_d + a^2\lambda_i\mathcal{A}_c + \lambda_i\mathcal{A}_p \\ \sqrt{2\lambda_i}ab\mathcal{A}_c \end{bmatrix}^\top \begin{bmatrix} -Y & & \\ & Y & \\ & & Y \end{bmatrix} \begin{bmatrix} I_{n_\xi} \\ \mathcal{A}_d + a^2\lambda_i\mathcal{A}_c + \lambda_i\mathcal{A}_p \\ \sqrt{2\lambda_i}ab\mathcal{A}_c \end{bmatrix} \prec 0. \tag{5.2}$$

However, this comes at the price of a non-convex lifted uncertainty set, trading ease of representation against unfavourable set properties.

5.1.2. Equivalent Conditions Through the Full-Block S-Procedure

Having converted the uncertainty into a polynomial form, an LFT can be applied to split the outer matrix factors of (5.2) into a nominal and an uncertain part. The idea is to introduce an *uncertainty channel*, passing the required signals through a matrix-valued uncertainty

$$\Delta \in \boldsymbol{\Delta} := \left\{ \begin{bmatrix} a & 0 \\ b & 0 \\ 0 & a \end{bmatrix} \middle| \begin{array}{l} a, b \geq 0 \\ a^2 \in [\rho_l, \rho_u] \\ b^2 = 1 - a^2 \end{array} \right\} \tag{5.3}$$

before being added to the known components. This process is visualized in Fig. 5.2, which shows how the uncertainty Δ (adjusted to match the vector dimension) is interconnected with the known matrices in an *upper LFT*. By solving for the output 'channels',

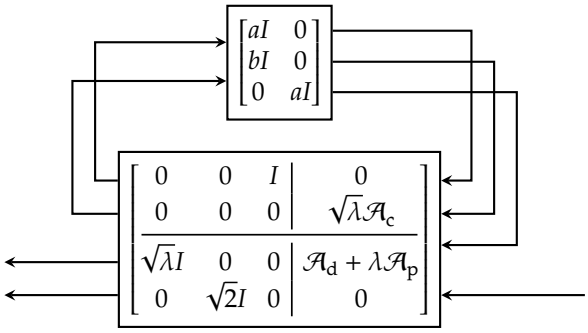

Figure 5.2.: Visualization of an upper LFT that separates the uncertainty Δ from the known components of the outer factors. The input and output channels do *not* correspond to specific signals of the underlying MJLS. Instead, the interconnection represents a $2n_\xi \times n_\xi$ matrix parametrized by the transmission probability p.

the algebraic loop can be converted into a matrix inverse, resulting in

$$\begin{bmatrix} \mathcal{A}_\mathrm{d} + a^2\lambda_i\mathcal{A}_\mathrm{c} + \lambda_i\mathcal{A}_\mathrm{p} \\ \sqrt{2\lambda_i}ab\mathcal{A}_\mathrm{c} \end{bmatrix} = \begin{bmatrix} \mathcal{A}_\mathrm{d} + \lambda_i\mathcal{A}_\mathrm{p} \\ 0 \end{bmatrix} + \begin{bmatrix} \sqrt{\lambda_i}I_{n_\xi} & 0 & 0 \\ 0 & \sqrt{2}I_{n_\xi} & 0 \end{bmatrix} \left(I_{3n_\xi} - \Delta_{(n_\xi)} \begin{bmatrix} 0 & 0 & I_{n_\xi} \\ 0 & 0 & 0 \end{bmatrix} \right)^{-1} \Delta_{(n_\xi)} \begin{bmatrix} 0 \\ \sqrt{\lambda_i}\mathcal{A}_\mathrm{c} \end{bmatrix} \tag{5.4}$$

for the outer factors of (5.2). Note that invertibility of the central term is ensured by the internal structure of Δ and the feedthrough term of the algebraic loop.

With the LFT reformulation of the outer matrix factors, we can apply the full block S-procedure (FBSP) as proposed by Scherer (2000, 2001) to isolate the uncertainty in the probability p from the LMI constraint (3.7). The idea is to introduce the multiplier set

$$\mathcal{P}_d := \left\{ P = P^\top \;\middle|\; \begin{bmatrix} \Delta \otimes I_d \\ I_{2d} \end{bmatrix}^\top P \begin{bmatrix} \Delta \otimes I_d \\ I_{2d} \end{bmatrix} \succ 0 \;\; \forall \Delta \in \boldsymbol{\Delta} \right\} \tag{5.5}$$

that captures the uncertainty $\boldsymbol{\Delta}$, where the index d denotes the dimension of the exchanged signals. Finally, this leads to the following equivalence result:

Proposition 5.1.: Equivalent Multiplier Condition

A matrix Y solves the LMI (3.7) for all $p \in [\rho_\mathrm{l}, \rho_\mathrm{u}]$ if and only if there exists a multiplier $P \in \mathcal{P}_{n_\xi}$ such that

$$\left[\begin{array}{cc} I_{n_\xi} & 0 \\ \mathcal{A}_\mathrm{d} + \lambda_i\mathcal{A}_\mathrm{p} & \sqrt{\lambda_i}\mathcal{I}_1 \\ 0 & \sqrt{2}\mathcal{I}_2 \\ \hline 0 & I_{3n_\xi} \\ 0 & \mathcal{I}_3 \\ \sqrt{\lambda_i}\mathcal{A}_\mathrm{c} & 0 \end{array}\right]^\top \left[\begin{array}{ccc|c} -Y & & & \\ & Y & & \\ & & Y & \\ \hline & & & P \end{array}\right] \left[\begin{array}{cc} I_{n_\xi} & 0 \\ \mathcal{A}_\mathrm{d} + \lambda_i\mathcal{A}_\mathrm{p} & \sqrt{\lambda_i}\mathcal{I}_1 \\ 0 & \sqrt{2}\mathcal{I}_2 \\ \hline 0 & I_{3n_\xi} \\ 0 & \mathcal{I}_3 \\ \sqrt{\lambda_i}\mathcal{A}_\mathrm{c} & 0 \end{array}\right] \prec 0 \tag{5.6}$$

holds, where $\mathcal{I}_j$ is the jth block-row of $I_3 \otimes I_{n_\xi}$.

Proof. The equivalence is a direct consequence of the FBSP, applied in the same way as for Theorem 10.2 of Scherer (2000). ■

Even though both of the conditions of Proposition 5.1 are infinite-dimensional, there is a decisive advantage of the reformulated constraints: While the LMI (3.7) involves square-roots of the uncertain transmission probability p and is therefore difficult to evaluate for all $p \in [\rho_\mathrm{l}, \rho_\mathrm{u}]$, the multiplier condition (5.5) is a quadratic form in the matrix uncertainty Δ. As such, there exist a variety of techniques resulting in inner approximations of the set $\mathcal{P}_d$ that can be described in a computationally tractable way. Among the simplest approaches is ensuring that the involved quadratic form is concave in Δ by forcing the top-left block of the multiplier P to be negative semidefinite. Since this implies that the multiplier condition is satisfied on the convex hull of the tested points, it would be sufficient to test as few as three carefully chosen pairs (a_i, b_i). More refined techniques include D- and D/G-scalings (Apkarian & Gahinet, 1995; Scorletti & Ghaoui, 1998), as well as Pólya or sum-of-squares relaxations (Scherer, 2005, 2006; Veenman et al., 2016), where the relaxations can be tuned for either exactness or low computational demand and are known to be asymptotically exact. Finally, the *ad hoc* approach of gridding the uncertainty set $\boldsymbol{\Delta}$ is often applied in the context of LPV systems even though this leads to an outer approximation of $\mathcal{P}_d$ and is therefore not providing theoretical guarantees (Hoffmann & Werner, 2015a).

5.2. From Homogeneous to Heterogeneous Transmission Probabilities

The previous section has shown how to utilize tools from robust control, namely LFTs and the FBSP, together with a lifted uncertainty representation in order to guarantee mean-square stability over a range of *homogeneous* transmission probabilities. A logical next step is therefore to study how these techniques can be generalized to networks of uncertain *heterogeneous* probabilities p^{ij} while preserving the favourable scalability properties of the previously developed conditions.

5.2.1. An Alternative Factorization of the Expected Laplacian

For all stability and performance results presented in the preceding chapters, system analysis and controller synthesis alike, Lemma 3.4 on page 36 has played a pivotal role in ensuring that the underlying SDP can be decomposed and thus solved in a scalable manner. This is because all the aforementioned results are based on the fundamental concept of simultaneously diagonalizing the fixed pattern matrix S^0 and the stochastic moments $\mathbb{E}[S_\sigma]$ and $\Xi_I[S_\sigma]$ of the switched pattern. However, for heterogeneous transmission probabilities, *i.e.* without Assumption 3.4, simultaneous diagonalizability of these terms is no longer guaranteed, and an alternative strategy for decomposing the SDP has to be devised. This necessitates the following generalization of Assumption 3.4 to heterogeneous probabilities:

Assumption 5.1.: Probabilistic Communication Symmetry

In addition to Assumptions 3.1 and 3.3, the nominal communication graph $\mathcal{G}^0$ is undirected, and the transmission *probabilities* are symmetric, that is

$$\mathbb{P}\left(\phi_k^{ij} = 1\right) = p^{ij} = p^{ji} = \mathbb{P}\left(\phi_k^{ji} = 1\right)$$

for all $k \in \mathbb{N}_0$ and edges $(i, j) \in \mathcal{E}^0$.

Assumption 5.1 is not strong enough to ensure simultaneous diagonalizability of the three pattern terms as discussed above, but preserves another important property of the Laplacian, its symmetry. Even though it is not guaranteed that the graph process $\{\mathcal{G}_{\sigma_k}\}$ is undirected for any specific step k such that a sampled Laplacian L_{σ_k} may generally be non-symmetric, Lemma 3.3 and Assumption 5.1 imply that its expectation and variance are symmetrically weighted Laplacians of the nominal graph $\mathcal{G}^0$. Motivated by this observation, we define the stochastic process

$$\Phi_k \coloneqq \operatorname{diag}\left(\phi_k^{ij} \,\middle|\, (i, j) \in \tilde{\mathcal{E}}^0\right)$$

taking values in $\mathbb{R}^{\tilde{m} \times \tilde{m}}$ as the diagonal concatenation of the edge processes, where $\tilde{\mathcal{E}}^0$ denotes the set of edges as chosen for the incidence matrix $\Psi(\mathcal{G}^0)$, $|\tilde{\mathcal{E}}^0| = \tilde{m} = m/2$ since $\mathcal{G}^0$ is undirected, and the order of diagonal elements matches the columns of $\Psi(\mathcal{G}^0)$. Since we will only be referring to the incidence matrix of the nominal graph, we are using the shorthand notation $\Psi \coloneqq \Psi(\mathcal{G}^0)$ in the following. Finally, the key result of this section is obtained via straightforward calculations:

Lemma 5.2.: Incidence Factorization (Hespe & Werner, 2023b)

Given a nominal communication graph $\mathcal{G}^0$ and packet loss satisfying Assumption 5.1, the expectation and variance of the switched Laplacian are given by

$$\mathbb{E}[L_\sigma] = \Psi\, \mathbb{E}[\Phi] \Psi^\top,$$
$$\operatorname{Var}[L_\sigma] = \Psi \operatorname{Var}[\Phi] \Psi^\top.$$

Proof. Both $\mathbb{E}[L_\sigma]$ and $\operatorname{Var}[L_\sigma]$ are weighted Laplacians of the nominal graph $\mathcal{G}^0$, with edge weights equal to the expectation and variance of the corresponding stochastic process. Since the probabilities of the involved Bernoulli processes are identical for opposing edges according to Assumption 5.1, the weights are symmetric, and it is therefore possible to use (2.1) plus diagonal weighting matrices to factor the stochastic moments of L_σ. ■

In essence, Lemma 5.2 serves as a replacement for the diagonalization Lemma 3.4 under the weaker hypotheses of Assumption 5.1 instead of the homogeneous Bernoulli model of Chapter 3. Its crucial feature is the separation of the structure of the nominal graph $\mathcal{G}^0$ (captured by its incidence matrix Ψ) from the stochastic properties of the communication links described by the first two moments of the edge processes in Φ_k. In the context of treating the transmission probabilities p^{ij} as constant uncertainties, we can therefore replace the uncertainties $\mathbb{E}[L_\sigma]$ and $\operatorname{Var}[L_\sigma]$ by larger but diagonal $\mathbb{E}[\Phi]$ and $\operatorname{Var}[\Phi]$ together with a known graph structure in the incidence matrix.

5.2.2. Decomposing Structured Multiplier Constraints

Based on the factorization of expectation and variance of the Laplacian, it is now possible to retrace the steps of Section 5.1 in order to extend the robust stability analysis to the heterogeneous case. Since Assumption 3.4 is invalidated, the derivation cannot be built on the decomposed LMI conditions of Theorem 3.6 but has to be developed from the general mean-square stability test of Theorem 3.1. Nonetheless, the subsequent steps follow similarly as before: Starting from the LMI (3.4), we impose the structure $\mathcal{X} \coloneqq I_N \otimes Y$, and by Lemmas 3.3 and 5.2 we can factor the inequality as

$$\begin{bmatrix} * \\ * \\ * \end{bmatrix}^\top \begin{bmatrix} I_N \otimes (-Y) & & \\ & I_N \otimes Y & \\ & & I_{\tilde{m}} \otimes Y \end{bmatrix} \begin{bmatrix} I_N \otimes I_{n_\xi} \\ I_N \otimes \mathcal{A}_\mathrm{d} + \mathbb{E}[L_\sigma] \otimes \mathcal{A}_\mathrm{c} + L^0 \otimes \mathcal{A}_\mathrm{p} \\ \left(\sqrt{2}\,\mathrm{Var}[\Phi]^{1/2}\Psi^\top\right) \otimes \mathcal{A}_\mathrm{c} \end{bmatrix} \prec 0 \tag{5.7}$$

with symmetric left and right factors, which is the heterogeneous analogue to (5.1) with matrix valued diagonal uncertainties and the role of λ_N taken by the Laplacian and the incidence matrix. Note that the third block of the centre matrix has a dimension different from the first two because it has been pushed through the incidence matrix Ψ according to the mixed-product rule (*cf.* Lemma 2.3).

Next, observe that the diagonal structure of $\mathbb{E}[\Phi]$ and $\mathrm{Var}[\Phi]$ implies that there is no coupling in the uncertainties of different edges, which is a consequence of Assumption 3.3. As such, the parameter lifting technique that has been utilized for the homogeneous case with scalar uncertainty can be applied on a per-edge basis, leading to the block-diagonal uncertainty

$$\bar{\Delta} \coloneqq \mathrm{diag}\Big(\Delta^{ij} \,\Big|\, (i,j) \in \tilde{\mathcal{E}}^0\Big) \quad \text{with} \quad \Delta^{ij} \coloneqq \begin{bmatrix} a^{ij} & 0 \\ b^{ij} & 0 \\ 0 & a^{ij} \end{bmatrix},$$

where each block represents one particular edge of the graph. Even though each transmission probability p^{ij} may be different, we only consider a single *uniform* uncertainty set $\boldsymbol{\Delta}$ as described by (5.3) such that $\Delta^{ij} \in \boldsymbol{\Delta}$ for all edges $(i,j) \in \tilde{\mathcal{E}}^0$ (which trivially exists with $\rho_\mathrm{l} = 0$ and $\rho_\mathrm{u} = 1$). Similarly, the LFT visualized in Fig. 5.2 generalizes to the heterogeneous scenario through appropriate use of Kronecker products on the channels, resulting in the fractional representation

$$\begin{aligned} \begin{bmatrix} I_N \otimes \mathcal{A}_\mathrm{d} + \mathbb{E}[L_\sigma] \otimes \mathcal{A}_\mathrm{c} + L^0 \otimes \mathcal{A}_\mathrm{p} \\ \left(\sqrt{2}\,\mathrm{Var}[\Phi]^{1/2}\Psi^\top\right) \otimes \mathcal{A}_\mathrm{c} \end{bmatrix} &= \begin{bmatrix} I_N \otimes \mathcal{A}_\mathrm{d} + L^0 \otimes \mathcal{A}_\mathrm{p} \\ 0 \end{bmatrix} \\ &+ \begin{bmatrix} \Psi \otimes \begin{bmatrix} I_{n_\xi} & 0 & 0 \end{bmatrix} \\ I_{\tilde{m}} \otimes \begin{bmatrix} 0 & \sqrt{2} I_{n_\xi} & 0 \end{bmatrix} \end{bmatrix} \left(I_{3\tilde{m}n_\xi} - \bar{\Delta}_{(n_\xi)} \left(I_{\tilde{m}} \otimes \begin{bmatrix} 0 & 0 & I_{n_\xi} \\ 0 & 0 & 0 \end{bmatrix} \right) \right)^{-1} \bar{\Delta}_{(n_\xi)} \left(\Psi^\top \otimes \begin{bmatrix} 0 \\ \mathcal{A}_\mathrm{c} \end{bmatrix} \right) \end{aligned} \tag{5.8}$$

with clear resemblance of the homogeneous equivalent (5.4). As before, well-posedness of the interconnection is implied by the structure of $\bar{\Delta}$ and the nature of the algebraic loop. Ultimately, a sufficient stability condition is obtained by application of the FBSP:

Theorem 5.3.: Heterogeneous Mean-Square Stability (Hespe & Werner, 2023b)

A decomposable MJLS $\mathcal{T}$ with L^0 and L_σ as patterns, an interconnection structure satisfying Assumption 5.1, and transmission probabilities bounded as $p^{ij} \in [\rho_\mathrm{l}, \rho_\mathrm{u}]$ for all edges $(i,j) \in \mathcal{E}^0$ is mean-square stable if there exist a $Y \succ 0$ and a multiplier $P \in \mathcal{P}_{n_\xi}$ that solve the LMIs

$$\mathcal{A}_\mathrm{d}^\top Y \mathcal{A}_\mathrm{d} \prec Y \tag{5.9a}$$

$$\left[\begin{array}{cc} I_{n_\xi} & 0 \\ \mathcal{A}_\mathrm{d} + \lambda \mathcal{A}_\mathrm{p} & \sqrt{\lambda} \mathcal{I}_1 \\ 0 & \sqrt{2} \mathcal{I}_2 \\ \hline 0 & I_{3n_\xi} \\ 0 & \mathcal{I}_3 \\ \sqrt{\lambda} \mathcal{A}_\mathrm{c} & 0 \end{array}\right]^\top \left[\begin{array}{ccc|c} -Y & & & \\ & Y & & \\ & & Y & \\ \hline & & & P \end{array}\right] \left[\begin{array}{cc} I_{n_\xi} & 0 \\ \mathcal{A}_\mathrm{d} + \lambda \mathcal{A}_\mathrm{p} & \sqrt{\lambda} \mathcal{I}_1 \\ 0 & \sqrt{2} \mathcal{I}_2 \\ \hline 0 & I_{3n_\xi} \\ 0 & \mathcal{I}_3 \\ \sqrt{\lambda} \mathcal{A}_\mathrm{c} & 0 \end{array}\right] \prec 0 \tag{5.9b}$$

for the smallest and largest non-zero eigenvalue λ of the nominal Laplacian L^0, where $\mathcal{I}_i$ denotes the ith block-row of $I_3 \otimes I_{n_\xi}$.

Proof. Following the steps outlined above, the existence of a $Y \succ 0$ that solves (5.7) for all combinations of $p^{ij} \in [\rho_\mathrm{l}, \rho_\mathrm{u}]$ is a sufficient condition for mean-square stability of the MJLS $\mathcal{T}$. Taking advantage of the fractional representation (5.8), the FBSP proves that this condition is equivalent to finding a multiplier

$$\bar{P} \in \bar{\mathcal{P}} := \left\{ \bar{P} = \bar{P}^\top \;\middle|\; \begin{bmatrix} \bar{\Delta} \otimes I_{n_\xi} \\ I_{2\tilde{m}} \otimes I_{n_\xi} \end{bmatrix}^\top \bar{P} \begin{bmatrix} \bar{\Delta} \otimes I_{n_\xi} \\ I_{2\tilde{m}} \otimes I_{n_\xi} \end{bmatrix} \succ 0 \;\; \forall \bar{\Delta} \in \boldsymbol{\Delta} \times \cdots \times \boldsymbol{\Delta} \right\}$$

such that Y and $\bar{P}$ solve the LMI

$$\begin{aligned} \begin{bmatrix} * & * \\ * & * \\ * & * \end{bmatrix}^\top \begin{bmatrix} I_N \otimes (-Y) & & \\ & I_N \otimes Y & \\ & & I_{\tilde{m}} \otimes Y \end{bmatrix} \begin{bmatrix} I_N \otimes I_{n_\xi} & 0 \\ I_N \otimes \mathcal{A}_\mathrm{d} + L^0 \otimes \mathcal{A}_\mathrm{p} & \Psi \otimes \mathcal{I}_1 \\ 0 & \sqrt{2} I_{\tilde{m}} \otimes \mathcal{I}_2 \end{bmatrix} \\ + \begin{bmatrix} * & * \\ * & * \end{bmatrix}^\top \bar{P} \begin{bmatrix} 0 & I_{\tilde{m}} \otimes I_{3n_\xi} \\ \Psi^\top \otimes \begin{bmatrix} 0 \\ \mathcal{A}_\mathrm{c} \end{bmatrix} & I_{\tilde{m}} \otimes \begin{bmatrix} \mathcal{I}_3 \\ 0 \end{bmatrix} \end{bmatrix} \prec 0. \end{aligned} \tag{5.10}$$

Even though there is no coupling between different Δ^{ij}, the multiplier $\bar{P}$ is generally fully populated. In light of the goal to decompose the analysis conditions, we therefore impose

$$\bar{P} = \begin{bmatrix} I_{\tilde{m}} \otimes Q & I_{\tilde{m}} \otimes S \\ I_{\tilde{m}} \otimes S^\top & I_{\tilde{m}} \otimes R \end{bmatrix} \quad \text{and define} \quad P := \begin{bmatrix} Q & S \\ S^\top & R \end{bmatrix},$$

where $Q = Q^\top \in \mathbb{R}^{3n_\xi \times 3n_\xi}$, $S \in \mathbb{R}^{3n_\xi \times 2n_\xi}$, and $R = R^\top \in \mathbb{R}^{2n_\xi \times 2n_\xi}$ are arbitrary matrices. Observe that this restriction means that $\bar{P} \in \bar{\mathcal{P}}$ is implied by $P \in \mathcal{P}_{n_\xi}$ with the set defined in (5.5), such that the multiplier condition only has to be evaluated for a single link.

The next step is to decompose (5.10) into an equivalent set of smaller LMI constraints. Therefore, consider the singular value decomposition $\Psi = U \Sigma V^\top$ of the incidence matrix, where U and V are orthogonal matrices and Σ is a non-square diagonal matrix

containing its singular values. Furthermore, because $\mathcal{G}^0$ is undirected by assumption, it holds that $L^0 = \Psi\Psi^\top = U\Sigma\Sigma^\top U^\top = U\Lambda U^\top$ with diagonal Λ containing its eigenvalues. As such, the matrix $\operatorname{diag}(U \otimes I_{n_\xi}, V \otimes I_{3n_\xi})$ can be applied as a congruence transformation, leading to the equivalent but decomposed LMI

$$\begin{bmatrix} * & * \\ * & * \\ * & * \end{bmatrix}^\top \begin{bmatrix} I_N \otimes (-Y) & & \\ & I_N \otimes Y & \\ & & I_{\tilde{m}} \otimes Y \end{bmatrix} \begin{bmatrix} I_N \otimes I_{n_\xi} & 0 \\ I_N \otimes \mathcal{A}_\mathrm{d} + \Lambda \otimes \mathcal{A}_\mathrm{p} & \Sigma \otimes \mathcal{I}_1 \\ 0 & \sqrt{2} I_{\tilde{m}} \otimes \mathcal{I}_2 \end{bmatrix} + \begin{bmatrix} * & * \\ * & * \end{bmatrix}^\top \bar{P} \begin{bmatrix} 0 & I_{\tilde{m}} \otimes I_{3n_\xi} \\ \Sigma^\top \otimes \begin{bmatrix} 0 \\ \mathcal{A}_\mathrm{c} \end{bmatrix} & I_{\tilde{m}} \otimes \begin{bmatrix} \mathcal{I}_3 \\ 0 \end{bmatrix} \end{bmatrix} \prec 0,$$

where we have used the commutation property of the Kronecker product to preserve the structure of the central matrix and the multiplier. Since all blocks have diagonal shape, the condition can be permuted into smaller decoupled LMIs, resulting in (5.9a) for all zero eigenvalues, (5.9b) for the $\tilde{N}$ non-zero eigenvalues λ, and $\tilde{m} - \tilde{N}$ copies of

$$2\mathcal{I}_2^\top Y \mathcal{I}_2 + \begin{bmatrix} I_{3n_\xi} \\ \mathcal{I}_3 \\ 0 \end{bmatrix}^\top P \begin{bmatrix} I_{3n_\xi} \\ \mathcal{I}_3 \\ 0 \end{bmatrix} \prec 0 \tag{5.11}$$

that exist due to extra columns of Σ if there are more edges than non-zero eigenvalues. Note that (5.11) is implied by the bottom-right block of (5.9b) for any positive λ, and that the only graph with no positive eigenvalue is the null graph with $\mathcal{E}^0 = \varnothing$ and thus $\tilde{m} = \tilde{N} = 0$, such that it is redundant to verify (5.11).

Finally, we have to show that it is sufficient to verify (5.9b) for the smallest and largest eigenvalue only. Since this LMI is only considered for positive λ, $\operatorname{diag}\left(I_{n_\xi}, \sqrt{\lambda} I_{3n_\xi}\right)$ constitutes a valid congruence transformation if applied from the left and right. After the transformation, the resulting LMI is a quadratic polynomial in λ with coefficient

$$\begin{bmatrix} \mathcal{A}_\mathrm{p}^\top Y \mathcal{A}_\mathrm{p} & \mathcal{A}_\mathrm{p}^\top Y \mathcal{I}_1 \\ \mathcal{I}_1^\top Y \mathcal{A}_\mathrm{p} & \mathcal{I}_1^\top Y \mathcal{I}_1 \end{bmatrix} = \begin{bmatrix} \mathcal{A}_\mathrm{p}^\top \\ \mathcal{I}_1^\top \end{bmatrix} Y \begin{bmatrix} \mathcal{A}_\mathrm{p}^\top \\ \mathcal{I}_1^\top \end{bmatrix}^\top \geq 0$$

for λ^2 and thus convex. Therefore, if Y and P solve (5.9b) for the smallest and largest non-zero eigenvalue of L^0, they satisfy the transformed LMI for these λ, and thus also all other non-zero eigenvalues by convexity. In turn, this guarantees that the original condition (5.9b) holds for all non-zero eigenvalues. ■

With Theorem 5.3, there is now an LMI-based condition for testing mean-square stability of decomposable MJLS without having to rely on Assumption 3.4 but only the weaker Assumption 5.1. Remarkably, the condition remains scalable in the sense that the number of variables and constraints is constant, and their dimension depends on neither N nor m but only on the state dimension n_ξ, even though the network properties are no longer homogeneous. The proof reveals that this is because of the homogeneous *bounds* on the transmission probabilities, which together with the structure imposed on $\bar{P}$ means that it is sufficient to implement the small multiplier condition (5.5).

Another important observation is that (5.6), the LMI condition for robust stability in the homogeneous case, is identical to (5.9b), but that the two stability results couple their

conditions in different ways. While Proposition 5.1 is purely an equivalence result for two LMI constraints such that we could employ separate multipliers $P_1, P_2, \dots, P_N \in \mathcal{P}_{n_\xi}$ for the eigenvalues λ_i, Theorem 5.3 requires a uniform multiplier that solves the LMI for all eigenvalues at once.

5.2.3. Extended Uncertainty Channels for Performance Analysis

Many of the ideas discussed above require only minor adjustments to become applicable for performance analysis problems. Most importantly, a factorization of the analysis LMIs similar to (5.7) has to be found such that LFTs can be employed to isolate the uncertain transmission probabilities.

Robustly Bounding the H_2-Norm

In case of the H_2-norm, we thus start at the LMI (3.16) that is based on the structured Lyapunov matrix $\mathcal{X} = I_N \otimes Y$ but no other restrictive assumptions. After reducing the generalized variance using Lemma 3.3 and separating the incidence matrix with Lemma 5.2, the LMI can be factorized as

$$\begin{bmatrix} * \\ [*] \\ [*] \end{bmatrix}^\top \begin{bmatrix} I_N \otimes (-Y) & & \\ & I_N \otimes \left[\begin{smallmatrix} Y & \\ & I_{n_z} \end{smallmatrix}\right] & \\ & & I_{\tilde{m}} \otimes \left[\begin{smallmatrix} Y & \\ & I_{n_z} \end{smallmatrix}\right] \end{bmatrix} \begin{bmatrix} I_N \otimes I_{n_\xi} \\ I_N \otimes \left[\begin{smallmatrix} \mathcal{A}_\mathrm{d} \\ C_\mathrm{d} \end{smallmatrix}\right] + \mathbb{E}[L_\sigma] \otimes \left[\begin{smallmatrix} \mathcal{A}_\mathrm{c} \\ C_\mathrm{c} \end{smallmatrix}\right] + L^0 \otimes \left[\begin{smallmatrix} \mathcal{A}_\mathrm{p} \\ C_\mathrm{p} \end{smallmatrix}\right] \\ \left(\sqrt{2}\,\mathrm{Var}[\Phi]^{1/2}\Psi^\top\right) \otimes \left[\begin{smallmatrix} \mathcal{A}_\mathrm{c} \\ C_\mathrm{c} \end{smallmatrix}\right] \end{bmatrix} \prec 0,$$

where the system and output matrix have been stacked to resemble (5.7) as close as possible. This reveals that the first of the two H_2-LMIs is essentially an augmented variant of the mean-square stability condition and that the results of Section 5.2.2 are directly applicable. Accordingly, a fractional representation of the outer factors is obtained from (5.8) by replacing $\mathcal{A}_\mathrm{d}$, $\mathcal{A}_\mathrm{c}$, and $\mathcal{A}_\mathrm{p}$ by the stacked augmented matrices and increasing the dimension of the uncertainty channel to $n_\xi + n_z$, resulting in

$$\begin{aligned} \begin{bmatrix} I_N \otimes \left[\begin{smallmatrix} \mathcal{A}_\mathrm{d} \\ C_\mathrm{d} \end{smallmatrix}\right] + \mathbb{E}[L_\sigma] \otimes \left[\begin{smallmatrix} \mathcal{A}_\mathrm{c} \\ C_\mathrm{c} \end{smallmatrix}\right] + L^0 \otimes \left[\begin{smallmatrix} \mathcal{A}_\mathrm{p} \\ C_\mathrm{p} \end{smallmatrix}\right] \\ \left(\sqrt{2}\,\mathrm{Var}[\Phi]^{1/2}\Psi^\top\right) \otimes \left[\begin{smallmatrix} \mathcal{A}_\mathrm{c} \\ C_\mathrm{c} \end{smallmatrix}\right] \end{bmatrix} &= \begin{bmatrix} I_N \otimes \left[\begin{smallmatrix} \mathcal{A}_\mathrm{d} \\ C_\mathrm{d} \end{smallmatrix}\right] + L^0 \otimes \left[\begin{smallmatrix} \mathcal{A}_\mathrm{p} \\ C_\mathrm{p} \end{smallmatrix}\right] \\ 0 \end{bmatrix} \\ &\quad + \begin{bmatrix} \Psi \otimes \left[\begin{smallmatrix} I_{n_\xi+n_z} & 0 & 0 \end{smallmatrix}\right] \\ I_{\tilde{m}} \otimes \left[\begin{smallmatrix} 0 & \sqrt{2} I_{n_\xi+n_z} & 0 \end{smallmatrix}\right] \end{bmatrix} \left(I - \bar{\Delta}_{(n_\xi+n_z)} \left(I_{\tilde{m}} \otimes \begin{bmatrix} 0 & 0 & I_{n_\xi+n_z} \\ 0 & 0 & 0 \end{bmatrix} \right) \right)^{-1} \bar{\Delta}_{(n_\xi+n_z)} \left(\Psi^\top \otimes \left[\begin{smallmatrix} 0 \\ \mathcal{A}_\mathrm{c} \\ C_\mathrm{c} \end{smallmatrix}\right] \right) \end{aligned}$$

with $\bar{\Delta}$ as defined in Section 5.2.2. A fractional representation of the second H_2-LMI can be derived analogously by stacking the input and feedthrough terms. In the same way as for Theorem 5.3, a decomposed robust performance bound follows by application of the FBSP. The full theorem and its proof can be found in Appendix B.3 on page 146.

Theorem 5.4.: Heterogeneous H_2-Norm Bound (Hespe & Werner, 2023b)

A decomposable MJLS $\mathcal{T}$ with L^0 and L_σ as patterns, an interconnection satisfying Assumption 5.1, and transmission probabilities bounded as $p^{ij} \in [\rho_\mathrm{l}, \rho_\mathrm{u}]$ for all edges $(i,j) \in \mathcal{E}^0$ is mean-square stable and has H_2-norm less than $\gamma > 0$ if there exist a $Y \succ 0$, symmetric Z_i

with $\sum_{i=1}^{N} \operatorname{tr} Z_i < \gamma^2$*, and multipliers* $P_1, P_2 \in \mathcal{P}_{n_\xi + n_z}$ *that solve the LMIs*

$$\mathcal{A}_\mathrm{d}^\top Y \mathcal{A}_\mathrm{d} + C_\mathrm{d}^\top C_\mathrm{d} \prec Y \tag{5.12a}$$
$$\mathcal{B}_\mathrm{d}^\top Y \mathcal{B}_\mathrm{d} + \mathcal{D}_\mathrm{d}^\top \mathcal{D}_\mathrm{d} \prec Z_i \tag{5.12b}$$

for all i *such that* $\lambda_i = 0$ *and furthermore satisfy*

$$\mathrm{LMI}_{\lambda_i}(Y, P_1) \prec 0 \qquad \text{(B.5a, abbreviated)}$$
$$\mathrm{LMI}_{\lambda_i}(Y, Z_i, P_2) \prec 0 \qquad \text{(B.5b, abbreviated)}$$

for all non-zero λ_i*, where* λ_i *are the eigenvalues of* L^0*. Moreover, it is sufficient to validate* (B.5a) *for the smallest and largest non-zero eigenvalue.*

Remark. Note that Theorem 5.4 imposes uniform multipliers for all eigenvalues of the Laplacian. This is generally a conservative assumption, but necessary to decompose the multiplier-based matrix inequalities. In contrast, a robust bound on the H_2-norm for uncertain but homogeneous transmission probabilities as considered in Section 5.1 would allow for a different multiplier for each eigenvalue, since the LMIs are decomposed before the multipliers are introduced.

Bounding the H_∞-Norm for Input-Decoupled Systems

Formulating a robust upper bound on the H_∞-norm from Theorem 3.12 can be approached in similar fashion but requires more in-depth modifications. To start, we impose Assumption 3.6, *i.e.* that the IS is input-decoupled, and obtain the matrix inequality (3.20) as a basis for the following derivation. In contrast to Section 3.4.3, the condition cannot be decomposed at this point since that would require Assumption 3.4 to hold, but it is still possible to retrace the repeated Schur complements in the proof of Theorem 3.13. After applying the transformations except for the final one, the resulting negative definite left-hand side of the LMI can be split into a central matrix

$$\operatorname{diag}\Big(I_N \otimes (-Y), I_N \otimes (-\gamma^2 I_{n_w}), I_{\tilde{m}} \otimes (-\gamma^2 I_{n_w}), I_N \otimes \begin{bmatrix} Y \\ & I_{n_z} \end{bmatrix}, I_{\tilde{m}} \otimes \begin{bmatrix} Y \\ & I_{n_z} \end{bmatrix}\Big),$$

the corresponding right factor

$$\begin{bmatrix} I_N \otimes I_{n_\xi} & 0 & 0 \\ 0 & I_N \otimes I_{n_w} & 0 \\ 0 & 0 & I_{\tilde{m}} \otimes I_{n_w} \\ I_N \otimes \begin{bmatrix} \mathcal{A}_\mathrm{d} \\ C_\mathrm{d} \end{bmatrix} + \mathbb{E}[L_\sigma] \otimes \begin{bmatrix} \mathcal{A}_\mathrm{c} \\ C_\mathrm{c} \end{bmatrix} + L^0 \otimes \begin{bmatrix} \mathcal{A}_\mathrm{p} \\ C_\mathrm{p} \end{bmatrix} & I_N \otimes \begin{bmatrix} \mathcal{B}_\mathrm{d} \\ \mathcal{D}_\mathrm{d} \end{bmatrix} & 0 \\ \left(\sqrt{2}\operatorname{Var}[\Phi]^{1/2}\Psi^\top\right) \otimes \begin{bmatrix} \mathcal{A}_\mathrm{c} \\ C_\mathrm{c} \end{bmatrix} & 0 & I_{\tilde{m}} \otimes \begin{bmatrix} \mathcal{B}_\mathrm{d} \\ \mathcal{D}_\mathrm{d} \end{bmatrix} \end{bmatrix},$$

and its transpose on the left. Note that while all four matrices of the state-space representation are present in the outer factor, only the stacked $\mathcal{A}_\mathrm{c}$ and C_c terms are multiplied with the uncertainty, and they are only present in the first block-column of the matrix.

As such, the fractional representation

$$\begin{bmatrix} I_N \otimes \left[\begin{smallmatrix} \mathcal{A}_\mathrm{d} \\ C_\mathrm{d} \end{smallmatrix}\right] + L^0 \otimes \left[\begin{smallmatrix} \mathcal{A}_\mathrm{p} \\ C_\mathrm{p} \end{smallmatrix}\right] & I_N \otimes \left[\begin{smallmatrix} \mathcal{B}_\mathrm{d} \\ \mathcal{D}_\mathrm{d} \end{smallmatrix}\right] & 0 \\ 0 & 0 & I_{\tilde{m}} \otimes \left[\begin{smallmatrix} \mathcal{B}_\mathrm{d} \\ \mathcal{D}_\mathrm{d} \end{smallmatrix}\right] \end{bmatrix} + \begin{bmatrix} \Psi \otimes \left[\begin{smallmatrix} I_{n_\xi+n_z} & 0 & 0 \end{smallmatrix}\right] \\ I_{\tilde{m}} \otimes \left[\begin{smallmatrix} 0 & \sqrt{2} I_{n_\xi+n_z} & 0 \end{smallmatrix}\right] \end{bmatrix}$$
$$\cdot \left(I - \bar{\Delta}_{(n_\xi+n_z)} \left(I_{\tilde{m}} \otimes \begin{bmatrix} 0 & 0 & I_{n_\xi+n_z} \\ 0 & 0 & 0 \end{bmatrix} \right) \right)^{-1} \bar{\Delta}_{(n_\xi+n_z)} \begin{bmatrix} \Psi^\top \otimes \left[\begin{smallmatrix} 0 \\ \mathcal{A}_\mathrm{c} \\ C_\mathrm{c} \end{smallmatrix}\right] & 0 & 0 \end{bmatrix}$$

of the outer factor is obtained from the H_2-case by concatenating its input term with zero columns and adding the stacked known matrices $\mathcal{B}_\mathrm{d}$ and $\mathcal{D}_\mathrm{d}$ in the feedthrough of appropriately increased dimension. The dimension of the uncertainty channel itself remains unchanged in comparison to its H_2 analogue above. Finally, the FBSP leads to the following decomposed H_∞-norm bound, where the full statement has again been moved into Appendix B.3 on page 147.

Theorem 5.5.: Heterogeneous H_∞-Norm Bound

A decomposable MJLS $\mathcal{T}$ fulfilling Assumption 3.6 with L^0 and L_σ as patterns, an interconnection satisfying Assumption 5.1, and transmission probabilities bounded as $p^{ij} \in [\rho_\mathrm{l}, \rho_\mathrm{u}]$ for all edges $(i,j) \in \mathcal{E}^0$ is mean-square stable and has H_∞-norm less than $\gamma > 0$ if there exists a $Y \succ 0$ and a multiplier $P \in \mathcal{P}_{n_\xi+n_z}$ that solve the LMI

$$\begin{bmatrix} \mathcal{A}_\mathrm{d}^\top Y \mathcal{A}_\mathrm{d} - Y & \mathcal{A}_\mathrm{d}^\top Y \mathcal{B}_\mathrm{d} & C_\mathrm{d}^\top \\ \mathcal{B}_\mathrm{d}^\top Y \mathcal{A}_\mathrm{d} & \mathcal{B}_\mathrm{d}^\top Y \mathcal{B}_\mathrm{d} - \gamma^2 I_{n_w} & \mathcal{D}_\mathrm{d}^\top \\ C_\mathrm{d} & \mathcal{D}_\mathrm{d} & -I_{n_z} \end{bmatrix} \prec 0 \tag{5.13}$$

and furthermore satisfy

$$\mathrm{LMI}_\lambda(Y, P, \gamma) \prec 0 \qquad \text{(B.6, abbreviated)}$$

for the smallest and largest non-zero eigenvalue λ of L^0.

Due to their similar structure, Theorems 5.4 and 5.5 inherit the favourable scalability properties of Theorem 5.3. Note that while the number of matrix variables and LMI constraints in Theorem 5.4 scales linearly with N in the current formulation, the condition can be reduced to a constant number of constraints and variables at the cost of additional conservatism. More specifically, restricting the condition to two Z_i, namely Z_1 for $\lambda_i = 0$ and Z_2 for all positive eigenvalues, it is sufficient to validate (B.5b) for the smallest and largest positive eigenvalue.

5.2.4. Robust Conditions for Consensus-Type Problems

All the above theorems contain a nominal condition that corresponds to $\lambda_i = 0$ and involves only the decoupled components $\mathcal{A}_\mathrm{d}, \mathcal{B}_\mathrm{d}, C_\mathrm{d}$, and $\mathcal{D}_\mathrm{d}$. As discussed in Section 3.3.1, this is an issue for specific kinds of distributed control problems, *e.g.* consensus problems or formation control, since their decoupled components are marginally stable and the nominal conditions thus infeasible. However, it is possible to consider a partially decoupled system as introduced in Sections 3.3.1 and 3.4.5 to isolate the eigenvalue

associated with the agreement space. The issue of marginal stability on the agreement space can then be averted by focussing on the bottom-right subsystem, neglecting $\lambda_1 = 0$. Utilizing $\Xi_{\Pi}[L_\sigma] \preceq \Xi_{I_N}[L_\sigma]$ before applying Lemma 5.2, the remaining steps follow as above with the exception that the decoupling congruence transformations have to be changed to

$$\operatorname{diag}\left(I_{N-1} \otimes I_{n_\xi}, V \otimes I_{3n_\xi}\right),$$
$$\operatorname{diag}\left(I_{N-1} \otimes I_{n_\xi}, V \otimes I_{3(n_\xi+n_z)}\right), \text{ and}$$
$$\operatorname{diag}\left(I_{N-1} \otimes I_{n_\xi}, I_{N-1} \otimes I_{n_w}, V \otimes I_{n_w}, V \otimes I_{3(n_\xi+n_z)}\right)$$

for Theorem 5.3, Theorem 5.4, and Theorem 5.5, respectively. Due to the reduced transformation $\tilde{U}$ (defined in (3.9) on on page 39), this results in *exactly one* less copy of the nominal constraint each. The above theorems can therefore be applied to consensus and formation control problems by neglecting (5.9a), (5.12), and (5.13) if $\mathcal{G}^0$ is connected such that there is precisely one Laplacian eigenvalue at 0.

5.3. General Dependencies Between Communication Links

With the results of the first sections of Chapter 5, two of the three simplifying assumptions mentioned in the beginning have been softened without giving up on the requirement of scalability. Next on the list is therefore the combination of Assumptions 3.1 and 3.3, imposing spatio-temporal independence on the stochastic edge processes which is unrealistic for wireless networks. In contrast to the previous sections, introducing stochastic dependencies between communication links means that the edge processes cannot be studied in isolation, but that their joint distribution has to be considered instead. For this reason, we will first study how to analyse MJLS with general uncertain TPMs, before specializing the approach for IS.

5.3.1. Robust Analysis of Markov Jump Linear Systems

In the framework of MJLS that has been outlined in Section 2.4, it is an implicit assumption that the TPM of the associated Markov chain is precisely known. Of course, this is idealizing real-world circumstances, and it is merited to study techniques for robust stability or performance of MJLS with uncertain transition probabilities. As such, this section considers MJLS for which the TPM is not known precisely but only in form of the inclusion $\Theta \in \boldsymbol{\Theta}$ for some known uncertainty set $\boldsymbol{\Theta}$ of row-stochastic matrices. In addition, there is a set $\boldsymbol{t}$ of probability vectors that constrains the initial distribution as $t \in \boldsymbol{t}$. Note that convex combinations of row-stochastic matrices are also row-stochastic, and convex combinations of probability vectors are still probability vectors (de Oliveira et al., 2009), such that all elements in the convex hulls of $\boldsymbol{\Theta}$ and $\boldsymbol{t}$ can be considered as distributions for the MJLS.

In order to analyse these MJLS with uncertain probabilities, it has to be shown that the SDPs guaranteeing mean-square stability or bounded norm remain feasible for all $\Theta \in \boldsymbol{\Theta}$, similar to the discussion of Section 5.1. Since Θ is uncertain but constant, the subproblems for different Θ are independent, and parameter-dependent solutions are permissible. For a specific kind of model uncertainty that is obtained if $\boldsymbol{\Theta}$ and $\boldsymbol{t}$ are

convex polytopes with finitely many vertices as proposed by Costa et al. (1997, 1999), this approach is taken by de Oliveira et al. (2009) and Morais et al. (2013, 2015). Formulating the uncertainty in terms of the simplex $\mathcal{S}_{n_\Theta - 1}$, where n_Θ is the number of vertices, they parametrize the Lyapunov variables $\mathcal{X}_i(\nu)$ as homogeneous polynomials in $\nu \in \mathcal{S}_{n_\Theta - 1}$ and apply Pólya relaxations of increasing degree to obtain asymptotically exact estimates. On the other hand, a simpler but potentially conservative choice is to search for uniform solutions $\mathcal{X}_i$ that are independent of the parameter. Since all involved LMIs are affine in Θ, this reduces the problem to be evaluated on the vertices (Gonçalves et al., 2012). In contrast, the number of matrix variables grows like n_Θ^d if a Pólya relaxation of degree d is used, quickly becoming computationally intractable for MJLS with high-dimensional uncertainty sets.

Proposition 5.6.: Analysis of MJLS with Uncertain Transition Probabilities

The matrix inequalities (2.12), (3.15), *and* (3.19) *are affine in* Θ *and* t*, respectively. In particular, given* $\gamma > 0$*, the MJLS* $\mathcal{T}$

i) *is mean-square stable for all* $\Theta \in \operatorname{conv} \boldsymbol{\Theta}$ *if there exist* $\mathcal{X}_i > 0$ *that solve* (2.12) *for all* $i \in \mathcal{K}$ *and* $\Theta \in \boldsymbol{\Theta}$*.*

ii) *is mean-square stable and satisfies* $\|\mathcal{T}\|_{H_2} < \gamma$ *for all* $\Theta \in \operatorname{conv} \boldsymbol{\Theta}$ *and* $t \in \operatorname{conv} \boldsymbol{t}$ *if there exist* $\mathcal{X}_i > 0$ *and a symmetric* $\mathcal{Z}$ *with* $\operatorname{tr} \mathcal{Z} < \gamma^2$ *that solve* (3.15) *for all* $i \in \mathcal{K}$*,* $\Theta \in \boldsymbol{\Theta}$*, and* $t \in \boldsymbol{t}$*.*

iii) *is mean-square stable and satisfies* $\|\mathcal{T}\|_{H_\infty} < \gamma$ *for all* $\Theta \in \operatorname{conv} \boldsymbol{\Theta}$ *if there exist* $\mathcal{X}_i > 0$ *that solve* (3.19) *for all* $i \in \mathcal{K}$ *and* $\Theta \in \boldsymbol{\Theta}$*.*

Proof. Pick any two pairs $\Theta^{(1)}, \Theta^{(2)} \in \boldsymbol{\Theta}$ and $t^{(1)}, t^{(2)} \in \boldsymbol{t}$, and define

$$\Theta(\tau) \coloneqq \tau\Theta^{(1)} + (1-\tau)\Theta^{(2)} \qquad\qquad t(\tau) \coloneqq \tau t^{(1)} + (1-\tau)t^{(2)}$$

such that $\theta_{ij}(\tau) = \tau\theta_{ij}^{(1)} + (1-\tau)\theta_{ij}^{(2)}$. Referring to Theorem 2.5, we obtain

$$\sum_{j\in\mathcal{K}} \theta_{ij}(\tau)\mathcal{A}_j^\top \mathcal{X}_j \mathcal{A}_j - \mathcal{X}_i = \tau\left(\sum_{j\in\mathcal{K}} \theta_{ij}^{(1)}\mathcal{A}_j^\top \mathcal{X}_j \mathcal{A}_j - \mathcal{X}_i\right) + (1-\tau)\left(\sum_{j\in\mathcal{K}} \theta_{ij}^{(2)}\mathcal{A}_j^\top \mathcal{X}_j \mathcal{A}_j - \mathcal{X}_i\right) \prec 0$$

for all $i \in \mathcal{K}$ and $\tau \in [0,1]$ since $\Theta^{(1)}$ and $\Theta^{(2)}$ satisfy (2.12) by assumption. Analogously, the statements on the H_2- and H_∞-norm follow by inserting the parametrized probabilities into Theorems 3.10 and 3.12 because the LMIs are affine in Θ and t. ■

Proposition 5.6 generalizes the vertex argument of Gonçalves et al. (2012) to non-convex and non-polyhedral sets, and the original statement is recovered if $\boldsymbol{\Theta}$ is a finite set since this makes $\operatorname{conv} \boldsymbol{\Theta}$ a convex polytope. Another way to represent non-convex uncertainties is the *multi-simplex* uncertainty model proposed by Morais et al. (2013, 2015). The idea is to introduce separate simplices for the rows of Θ, eliminating the inherent convexity of the single simplex model described above. However, the techniques discussed in the following section are designed to take advantage of the convex hull argument. The multi-simplex would thus be an unjustified complication.

5.3.2. Analysis with Independent Vertex Distributions

Although only a subset of the uncertainty set has to be evaluated, the LMIs (2.12), (3.15), and (3.19) are too expensive to verify for large IS because of the high dimensionality of the uncertainty (recall that $|\mathcal{K}| = 2^m$). The next step is therefore to relate the stability and performance conditions of Proposition 5.6 with the techniques of Section 5.2 to improve their scalability. Since the analysis conditions are verified only on $\boldsymbol{\Theta}$ but result in guarantees for all of conv $\boldsymbol{\Theta}$, the goal of the current section is to construct and exploit sets of computationally advantageous probability distributions. Whether these sets actually provide the desired distributional robustness is discussed in Section 5.3.3 below.

More specifically, the idea is to rely on subsets that satisfy the independence and symmetry assumption of Section 5.2 such that Theorems 5.3 to 5.5 become applicable. Naturally, this comes at the cost of a reduced set of available probability distributions to form the desired uncertainty set $\boldsymbol{\Theta}$. However, due to the shape of the resulting manifold, their convex hull can still contain distributions with dependencies between edges.

Example 5.1.: Independence Model of Binary Random Variables

Consider a pair of binary random variables X_1 and X_2. In combination, the pair has four outcomes, and its joint probability distribution is therefore a point in the three-dimensional simplex $\mathcal{S}_3$ shown in Fig. 5.3 (one dimension is lost to the constraint that the joint probabilities have to sum up to 1). However, if X_1 and X_2 are assumed to be independent, we obtain

$$\begin{bmatrix} \mathbb{P}(X_1 = 0, X_2 = 0) \\ \mathbb{P}(X_1 = 1, X_2 = 0) \\ \mathbb{P}(X_1 = 0, X_2 = 1) \\ \mathbb{P}(X_1 = 1, X_2 = 1) \end{bmatrix} = \begin{bmatrix} (1 - \mathbb{P}(X_1 = 1))(1 - \mathbb{P}(X_2 = 1)) \\ \mathbb{P}(X_1 = 1)(1 - \mathbb{P}(X_2 = 1)) \\ (1 - \mathbb{P}(X_1 = 1))\,\mathbb{P}(X_2 = 1) \\ \mathbb{P}(X_1 = 1)\,\mathbb{P}(X_2 = 1) \end{bmatrix}$$

and are thus left with only two degrees of freedom. This is called the *independence model* of binary random variables (Montúfar Cuartas, 2013) and covers a two-dimensional manifold embedded in the three-dimensional simplex, which is visualized by the blue mesh in Fig. 5.3.

Based on the independence model discussed in Example 5.1, a generalization of the joint distribution to d independent binary random variables is obtained as the function

$$f_d \colon \mathbb{R}^d \to \mathbb{R}^{2^d}, \qquad f_d(p) \coloneqq \begin{bmatrix} 1 - p_d \\ p_d \end{bmatrix} \otimes \begin{bmatrix} 1 - p_{d-1} \\ p_{d-1} \end{bmatrix} \otimes \cdots \otimes \begin{bmatrix} 1 - p_1 \\ p_1 \end{bmatrix} \tag{5.14}$$

through concatenated Kronecker products, where p_i is the probability that the ith variable is 1 and the p_i are stacked into a d-dimensional vector p. Accordingly, the heterogeneous packet loss distributions of Section 5.2 are described by the set

$$\hat{\boldsymbol{\theta}}_d \coloneqq \left\{ \theta = f_d(p) \,\middle|\, p \in \mathbb{R}^d, p_i \in [\rho_\mathrm{l}, \rho_\mathrm{u}] \right\} \subset \mathcal{S}_{2^d - 1}$$

with uniform bounds $0 \leq \rho_\mathrm{l} \leq \rho_\mathrm{u} \leq 1$ for all variables. Note that $\hat{\boldsymbol{\theta}}_2$ is precisely the blue manifold shown in Fig. 5.3 if $\rho_\mathrm{l} = 0$ and $\rho_\mathrm{u} = 1$, and subsets thereof if smaller intervals are considered. In addition, we define

$$\hat{\boldsymbol{\Theta}}_d \coloneqq \left\{ \Theta = \begin{bmatrix} \theta^{(1)} & \theta^{(2)} & \dots & \theta^{(2^d)} \end{bmatrix}^\top \,\middle|\, \theta^{(i)} \in \hat{\boldsymbol{\theta}}_d \right\} \subset \mathbb{T}_d$$

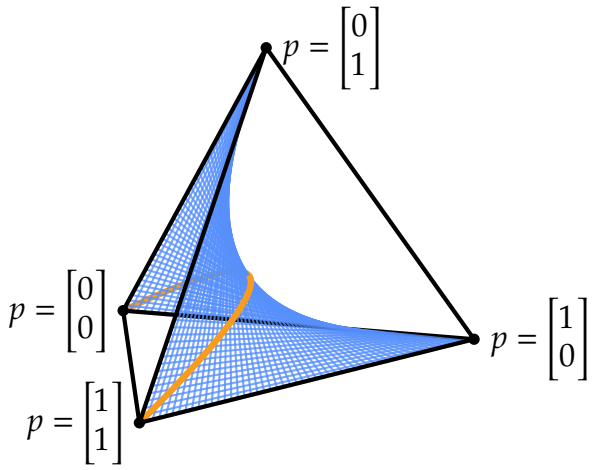

Figure 5.3.: 3-Simplex $\mathcal{S}_3$ describing all admissible joint probability distributions for a pair of binary random variables. The blue mesh is the manifold of probability distributions with independent variables and the labelled points represent its four limiting cases. The orange line is its submanifold with $p_1 = p_2$.

as the set of all TPMs that can be assembled from probability vectors of independent binary random variables, where $\mathbb{T}_d$ is the set of all 2^d dimensional probability matrices. Essentially, $\hat{\boldsymbol{\Theta}}_d$ can be associated with $\hat{\boldsymbol{\theta}}_d \times \cdots \times \hat{\boldsymbol{\theta}}_d$ with 2^d factors of $\hat{\boldsymbol{\theta}}_d$, and analogously for $\mathbb{T}_d$ and $\mathcal{S}_{2^d-1} \times \cdots \times \mathcal{S}_{2^d-1}$.

Next to independence of the edge processes, Assumption 5.1 also imposes that the transmission probabilities in the network have to be symmetric, *i.e.* $p^{ij} = p^{ji}$ for all edges $(i,j) \in \mathcal{E}^0$. In the definition of $\hat{\boldsymbol{\theta}}_d$, this restriction halves the available degrees of freedom, and thus also the dimension of the resulting manifold, since there have to be pairs of p_i with equal value. For the two random variables in Example 5.1, this is visualized by the orange line in Fig. 5.3. Notice that the submanifold is entirely contained in a two-dimensional affine subspace, while the full manifold and the probability simplex are both three-dimensional. In order to be distributionally robust, we therefore have to reduce the dimension of the probability simplex by only considering one stochastic process for each pair of edges connecting the same vertices:

Assumption 5.2.: Instantaneous Communication Symmetry

The nominal communication graph $\mathcal{G}^0$ is undirected, and the edge *processes* are symmetric such that

$$\phi_k^{ij} = \phi_k^{ji} \quad \forall\, k \in \mathbb{N}_0$$

holds for all edges $(i,j) \in \mathcal{E}^0$.

Since $\mathcal{G}_{\sigma_k}$ is undirected for all $k \in \mathbb{N}_0$ by Assumption 5.2, it is sufficient to consider a direction agnostic edge enumeration function $\tilde{\alpha}$ with $\tilde{\alpha}(i,j) \equiv \tilde{\alpha}(j,i)$ for all edges $(i,j) \in \mathcal{E}^0$ and therefore $\tilde{\alpha} : \mathcal{E}^0 \to \{1, 2, \dots, m/2\}$ (*cf.* Section 2.3). The stochastic networking model can therefore be associated with the independence model discussed above by matching p_l with p^{ij} such that $\tilde{\alpha}(i,j) = l$. As a corollary of Theorem 5.3 and Proposition 5.6, we

then obtain the following distributionally robust mean-square stability test in terms of the constructed uncertainty set $\hat{\boldsymbol{\Theta}}_d$:

Corollary 5.7.: Distributionally Robust Stability (Hespe, Datar & Werner, 2024)

A decomposable MJLS $\mathcal{T}$ with L^0 and L_σ as patterns and an interconnection satisfying Assumption 5.2 is mean-square stable for all $\Theta \in \operatorname{conv} \hat{\boldsymbol{\Theta}}_{m\!/2}$ if there exist a $Y \succ 0$ and a multiplier $P \in \mathcal{P}_{n_\xi}$ satisfying to the conditions of Theorem 5.3.

Proof. First, note that the structure of $\hat{\boldsymbol{\theta}}_d$ and Assumption 5.2 imply that all $\theta \in \hat{\boldsymbol{\theta}}_{m\!/2}$ satisfy Assumption 5.1, such that Lemma 5.2 remains applicable. By Theorem 5.3, it then follows that there exists an $X \succ 0$ that solves

$$\sum_{j \in \mathcal{K}} \theta_j \mathcal{A}_j^\top X \mathcal{A}_j \prec X$$

for all probability vectors $\theta \in \hat{\boldsymbol{\theta}}_{m\!/2}$. Furthermore, since the matrices of $\hat{\boldsymbol{\Theta}}_d$ are assembled row-wise from probability vectors in $\hat{\boldsymbol{\theta}}_d$, this implies that $X_i = X$ solve (2.12) for all $i \in \mathcal{K}$ and TPMs $\Theta \in \hat{\boldsymbol{\Theta}}_{m\!/2}$. Finally, we conclude that $\mathcal{T}$ is mean-square stable for all $\Theta \in \operatorname{conv} \hat{\boldsymbol{\Theta}}_{m\!/2}$ by Proposition 5.6. ■

Corollary 5.7 shows that the LMIs of Theorem 5.3 provide stability guarantees for two different scenarios: Either the packet loss is considered to be spatio-temporally independent but may be asymmetric (Assumption 5.1), or stochastic dependencies between links are permitted and dropouts are always symmetric (Assumption 5.2). Importantly, the guarantee extends to the convex hull of $\hat{\boldsymbol{\Theta}}_{m\!/2}$ instead of just stabilizing the MJLS for probability vectors from the set $\hat{\boldsymbol{\theta}}_{m\!/2}$ in the second case. Analogously, this fact also extends to the H_2- and H_∞-norm bounds of Theorems 5.4 and 5.5.

Corollary 5.8.: Distributionally Robust Performance

Given $\gamma > 0$, a decomposable MJLS $\mathcal{T}$ with L^0 and L_σ as patterns and an interconnection satisfying Assumption 5.2 is mean-square stable and

i) $\|\mathcal{T}\|_{H_2} < \gamma$ for all $\Theta \in \operatorname{conv} \hat{\boldsymbol{\Theta}}_{m\!/2}$ and $t \in \operatorname{conv} \hat{\boldsymbol{\theta}}_{m\!/2}$ if there exist a $Y \succ 0$, symmetric Z_i, and multipliers $P_1, P_2 \in \mathcal{P}_{n_\xi + n_z}$ according to the conditions of Theorem 5.4.

ii) $\|\mathcal{T}\|_{H_\infty} < \gamma$ for all $\Theta \in \operatorname{conv} \hat{\boldsymbol{\Theta}}_{m\!/2}$ if $\mathcal{T}$ satisfies Assumption 3.6 and there exist a $Y \succ 0$ and a multiplier $P \in \mathcal{P}_{n_\xi + n_z}$ according to the conditions of Theorem 5.5.

5.3.3. Characterizing the Uncertainty Set

Even though both $\boldsymbol{\Theta}$ and $\hat{\boldsymbol{\Theta}}_d$ are sets of uncertain probability distributions, their interpretation is different. For $\boldsymbol{\Theta}$, and thus Proposition 5.6, the uncertainty set is part of the system description, *i.e.* the question of robust stability or performance is only meaningful for the MJLS in combination with its corresponding $\boldsymbol{\Theta}$. On the other hand, the set $\hat{\boldsymbol{\Theta}}_{m\!/2}$ in Corollaries 5.7 and 5.8 is constructed in a computationally favourable way and is not intrinsically linked to any MJLS. Moreover, it is unclear which TPMs are contained in

conv $\hat{\boldsymbol{\Theta}}_d$ and whether stabilizing or bounding the IS for all $\Theta \in \operatorname{conv} \hat{\boldsymbol{\Theta}}_d$ provides non-trivial distributional robustness. As such, this section is studying geometric properties of conv $\hat{\boldsymbol{\theta}}_d$ and conv $\hat{\boldsymbol{\Theta}}_d$, with a focus on which elements lie in their interior.

To start, note that the properties of $\hat{\boldsymbol{\theta}}_d$ and $\hat{\boldsymbol{\Theta}}_d$ are intricately linked to the function f_d as defined in (5.14) since both sets are based on applying f_d to the compact interval $[\rho_\mathrm{l}, \rho_\mathrm{u}]$. For example, both sets are compact since f_d is continuous (Rudin, 2008, Theorem 4.14). It is therefore instrumental to study f_d to understand the geometry of the uncertainty. The first step is to prove that the function f_d is injective, *i.e.* that it maps distinct points into distinct points, which can be established using the mixed-product property.

Lemma 5.9.: Injectivity of f

The function f_d is injective for all $d \in \mathbb{N}$.

Proof. We prove that f_d is injective by constructing a left-inverse. First, observe that f_d attains a specific pattern if the canonical basis vectors e_i are used as its argument like

$$f_d\left(\tfrac{e_i+\mathbf{1}_d}{2}\right) = \begin{bmatrix}0.5\\0.5\end{bmatrix} \otimes \cdots \otimes \begin{bmatrix}0\\1\end{bmatrix} \otimes \cdots \otimes \begin{bmatrix}0.5\\0.5\end{bmatrix} = \frac{1}{2^{d-1}} \left(\begin{bmatrix}1\\1\end{bmatrix} \otimes \cdots \otimes \begin{bmatrix}0\\1\end{bmatrix} \otimes \cdots \otimes \begin{bmatrix}1\\1\end{bmatrix}\right).$$

By the mixed-product property of the Kronecker product (Lemma 2.3), it follows that

$$f_d\left(\tfrac{e_i+\mathbf{1}_d}{2}\right)^\top f_d(p) = \frac{1}{2^{d-1}} \left(\begin{bmatrix}1\\1\end{bmatrix}^\top \begin{bmatrix}1-p_d\\p_d\end{bmatrix}\right) \cdots \left(\begin{bmatrix}0\\1\end{bmatrix}^\top \begin{bmatrix}1-p_i\\p_i\end{bmatrix}\right) \cdots \left(\begin{bmatrix}1\\1\end{bmatrix}^\top \begin{bmatrix}1-p_1\\p_1\end{bmatrix}\right) = \frac{p_i}{2^{d-1}},$$

i.e. a specific p_i can be extracted by the basis vector e_i. Finally, $Kf_d(p) = p$, where

$$K \coloneqq 2^{d-1} \begin{bmatrix} f_d\left(\tfrac{e_1+\mathbf{1}_d}{2}\right) & f_d\left(\tfrac{e_2+\mathbf{1}_d}{2}\right) & \dots & f_d\left(\tfrac{e_d+\mathbf{1}_d}{2}\right) \end{bmatrix}^\top. \qquad \blacksquare$$

A second important property of the function f_d is of geometric nature: Given a line, *i.e.* a one-dimensional affine set, that is aligned with one of the canonical basis vectors, the image of the line under f_d is also a line, although not necessarily aligned with the basis of its codomain. However, in contrast to affine functions, this property does not extend to arbitrary lines that f_d is applied on. This weakening of the property is essential for our purpose, as affine functions would map $\mathbb{R}^d$ into a d-dimensional hyperplane, such that we would not be able to span the probability simplex.

Lemma 5.10.: Canonical Line Invariance

The function f_d is preserving lines along the canonical basis vectors for all $d \in \mathbb{N}$, i.e.

$$f_d\big(\tau p + (1-\tau)p'\big) = \tau f_d(p) + (1-\tau) f_d(p')$$

holds for points $p, p' \in [0,1]^d$ that differ in at most a single coordinate and $\tau \in \mathbb{R}$.

Proof. Since f_d is defined in terms of the Kronecker product, we can rely on its associativity and distributivity. Inserting points along the basis vectors, we obtain

$$\begin{aligned} f_d\big(\tau p + (1-\tau)p'\big) &= \begin{bmatrix} 1-p_d \\ p_d \end{bmatrix} \otimes \cdots \otimes \begin{bmatrix} 1-\big(\tau p_i + (1-\tau)p_i'\big) \\ \tau p_i + (1-\tau)p_i' \end{bmatrix} \otimes \cdots \otimes \begin{bmatrix} 1-p_1 \\ p_1 \end{bmatrix} \\ &= \begin{bmatrix} 1-p_d \\ p_d \end{bmatrix} \otimes \cdots \otimes \left(\tau \begin{bmatrix} 1-p_i \\ p_i \end{bmatrix} + (1-\tau) \begin{bmatrix} 1-p_i' \\ p_i' \end{bmatrix} \right) \otimes \cdots \otimes \begin{bmatrix} 1-p_1 \\ p_1 \end{bmatrix} \\ &= \tau f_d(p) + (1-\tau) f_d(p'). \end{aligned}$$

■

Our final lemma on f_d involves another geometric property of its image, which for sets $\mathcal{M} \subseteq [0,1]^d$ is defined as $f_d(\mathcal{M}) \coloneqq \{f_d(p) \mid p \in \mathcal{M}\}$. Figuratively speaking, the question is whether f_d 'takes advantage' of all available output dimensions even though the input is of much lower dimension ($\mathbb{R}^d$ compared to $\mathbb{R}^{2^d}$). More precisely, we show that the dimension of aff $f_d(\mathcal{M})$ is non-trivially bounded from below for specific sets $\mathcal{M}$.

Lemma 5.11.: Minimal Affine Set (Hespe, Datar & Werner, 2024)

For all $d \in \mathbb{N}$, there exists no affine set of dimension $2^d - 2$ that contains $f_d(\{\rho_\mathrm{l}, \rho_\mathrm{u}\}^d)$ if $\rho_\mathrm{l} < \rho_\mathrm{u}$.

Proof. Arrange the vectors in $f_d(\{\rho_\mathrm{l}, \rho_\mathrm{u}\}^d)$ as

$$M = \begin{bmatrix} f_d\big(p^{(1)}\big) & f_d\big(p^{(2)}\big) & \dots & f_d\big(p^{(2^d-1)}\big) & f_d\big(p^{(2^d)}\big) \end{bmatrix} \tag{5.15}$$

where $p^{(r)} \coloneqq \rho_\mathrm{l}\mathbf{1}_d + (\rho_\mathrm{u} - \rho_\mathrm{l})\bar{\beta}(r-1)$ and $\bar{\beta}(n) \coloneqq [\beta(n,1), \dots, \beta(n,d)]^\top$ maps integers to their base-2 representation (see Section 2.3). Note that $M = \tilde{M} \otimes \cdots \otimes \tilde{M}$ with d factors of

$$\tilde{M} = \begin{bmatrix} 1-\rho_\mathrm{l} & 1-\rho_\mathrm{u} \\ \rho_\mathrm{l} & \rho_\mathrm{u} \end{bmatrix}$$

and that $\det \tilde{M} = \rho_\mathrm{u} - \rho_\mathrm{l}$. By the rules for determinants of Kronecker product (see (2.7) on page 17), $\det M > 0$ follows, which implies that $M\nu = 0$ only if $\nu = 0$. This guarantees that the points in $f_d(\{\rho_\mathrm{l}, \rho_\mathrm{u}\}^d)$ are affinely independent and that there exists no $2^d - 2$ dimensional affine set that contains $f_d(\{\rho_\mathrm{l}, \rho_\mathrm{u}\}^d)$ (Rockafellar, 1970, Section 1). ■

Note that Lemma 5.11 implies that aff $f_d(\{\rho_\mathrm{l}, \rho_\mathrm{u}\}^d) = \operatorname{aff} \mathcal{S}_{2^d-1}$ as long as we allow for some uncertainty in the probability, *i.e.* $0 \leq \rho_\mathrm{l} < \rho_\mathrm{u} \leq 1$, since the affine hull of finite sets with d elements is at most $d-1$ dimensional and the inclusion $f_d(\{\rho_\mathrm{l}, \rho_\mathrm{u}\}^d) \subseteq \hat{\boldsymbol{\theta}}_d \subset \mathcal{S}_{2^d-1}$ holds. This means that the uncertainty is rich enough to impact all available degrees of freedom of the probabilistic network model. Combining the lemmas, we obtain a useful identity for the function f_d in terms of the extreme points of its image and pre-image.

Proposition 5.12.: Extreme Point Identity (Hespe, Datar & Werner, 2024)

Let $\mathbb{B} = [\rho_\mathrm{l}, \rho_\mathrm{u}]^d$ with $d \in \mathbb{N}$ and $0 \leq \rho_\mathrm{l} < \rho_\mathrm{u} \leq 1$. Then f_d satisfies the identity

$$\mu\big(\operatorname{conv} f_d(\mathbb{B})\big) = f_d\big(\mu(\mathbb{B})\big),$$

where μ is the set of extreme points as introduced in Section 2.5.

Proof. Suppose for some $\theta \in \operatorname{conv} f_d(\mathbb{B})$ there exists no $p \in \mathbb{B}$ such that $\theta = f_d(p)$ and thus $\theta \in (\operatorname{conv} f_d(\mathbb{B})) \setminus f_d(\mathbb{B})$. Because the extreme points of $\operatorname{conv} \mathcal{M}$ must be in $\mathcal{M}$ (Rockafellar, 1970, Corollary 18.3.1), it follows that $\theta \notin \mu(\operatorname{conv} f_d(\mathbb{B}))$. On the other hand, suppose there exists a $p \in \mathbb{B}$ with $\theta = f_d(p)$ but $p \notin \mu(\mathbb{B})$. Since $\mathbb{B}$ is axis-aligned, there exist a $\tau \in (0,1)$ and $p', p'' \in \mathbb{B}$ that differ in exactly one coordinate such that $p = \tau p' + (1-\tau)p''$. It therefore follows from Lemma 5.10 that $\theta = f_d(p) = \tau f_d(p') + (1-\tau) f_d(p'')$, where Lemma 5.9 implies $f_d(p') \neq f_d(p'')$ and thus that $\theta \notin \mu(\operatorname{conv} f_d(\mathbb{B}))$ and $\mu(\operatorname{conv} f_d(\mathbb{B})) \subseteq f_d(\mu(\mathbb{B}))$.

For the converse, note that $|\mu(\mathbb{B})| = 2^d$ since $\rho_\mathrm{l} < \rho_\mathrm{u}$. Furthermore, Lemma 5.11 implies that there exists no $2^d - 2$ dimensional affine set containing $f_d(\mathbb{B})$. Now, suppose there exists a $p \in \mu(\mathbb{B})$ for which $f_d(p) \notin \mu(\operatorname{conv} f_d(\mathbb{B}))$ and thus the first half of the proof implies $\left|\mu(\operatorname{conv} f_d(\mathbb{B}))\right| \leq 2^d - 1$. However, every finite set with $2^d - 1$ elements is contained in some $2^d - 2$ dimensional affine set, contradicting the statement above since $f_d(\mathbb{B})$ is compact (Rockafellar, 1970, Corollary 18.5.1). ■

Essentially, Lemma 5.11 and Proposition 5.12 together imply that f_d is distorting hypercubes into simplices with non-empty interior, and that there is a one-to-one correspondence between their vertices. This by itself demonstrates that Corollaries 5.7 and 5.8 provide non-trivial distributional robustness, but does not show *which* probability distributions are guaranteed to be in the interior and thus robustly stabilized. In addition, it would be useful to know whether increasing the size of the interval $[\rho_\mathrm{l}, \rho_\mathrm{u}]$ is guaranteed to monotonically increase the set of distributions that are considered, and if there are distributions that are never included in the uncertainty set even for the limiting case of $\rho_\mathrm{l} = 0$ and $\rho_\mathrm{u} = 1$. These questions are answered by Theorem 5.13, which is the main result of this section.

Theorem 5.13.: Spatial Robustness (Hespe, Datar & Werner, 2024)

Let $0 \leq \rho'_\mathrm{l} \leq \rho_\mathrm{l} < \rho_\mathrm{u} \leq \rho'_\mathrm{u} \leq 1$ *with corresponding sets* $\hat{\boldsymbol{\theta}}_d$ *and* $\hat{\boldsymbol{\theta}}'_d$. *Then for all* $d \in \mathbb{N}$

i) $\operatorname{conv} \hat{\boldsymbol{\theta}}_d = \mathcal{S}_{2^d-1}$ *if* $\rho_\mathrm{l} = 0$ *and* $\rho_\mathrm{u} = 1$,

ii) $\operatorname{conv} \hat{\boldsymbol{\theta}}_d \subset \operatorname{conv} \hat{\boldsymbol{\theta}}'_d$ *if* $\rho'_\mathrm{l} < \rho_\mathrm{l}$ *or* $\rho_\mathrm{u} < \rho'_\mathrm{u}$, *and*

iii) $f(p) \in \operatorname{ri}(\operatorname{conv} \hat{\boldsymbol{\theta}}_d)$ *for all* $p \in (\rho_\mathrm{l}, \rho_\mathrm{u})^d$.

Proof. An elementary fact that follows from Proposition 5.12 and the Krein-Milman Theorem (Rockafellar, 1970, Corollary 18.5.1) is that

$$\operatorname{conv} \hat{\boldsymbol{\theta}}_d = \operatorname{conv} f_d\left([\rho_\mathrm{l}, \rho_\mathrm{u}]^d\right) = \operatorname{conv} f_d\left(\mu([\rho_\mathrm{l}, \rho_\mathrm{u}]^d)\right) = \operatorname{conv} f_d\left(\{\rho_\mathrm{l}, \rho_\mathrm{u}\}^d\right).$$

We can therefore study the sets in terms of the vertices of the hypercube.

i) With $\rho_\mathrm{l} = 0$ and $\rho_\mathrm{u} = 1$, we have $f_d(\{0,1\}^d) = \{e_i \mid 1 \leq i \leq 2^d\}$ with the canonical basis vectors e_i, which are the vertices of $\mathcal{S}_{2^d-1}$ (see Fig. 5.3).

ii) It follows from the assumptions that $[\rho_\mathrm{l}, \rho_\mathrm{u}] \subset [\rho'_\mathrm{l}, \rho'_\mathrm{u}]$, which implies $\hat{\boldsymbol{\theta}}_d \subset \hat{\boldsymbol{\theta}}'_d$ and furthermore $\operatorname{conv} \hat{\boldsymbol{\theta}}_d \subseteq \operatorname{conv} \hat{\boldsymbol{\theta}}'_d$ since f_d is injective (Lemma 5.9). Additionally, both intervals have non-empty interior, such that Proposition 5.12 leads to $\mu(\operatorname{conv} \hat{\boldsymbol{\theta}}_d) \neq \mu(\operatorname{conv} \hat{\boldsymbol{\theta}}'_d)$ and therefore $\operatorname{conv} \hat{\boldsymbol{\theta}}_d \neq \operatorname{conv} \hat{\boldsymbol{\theta}}'_d$.

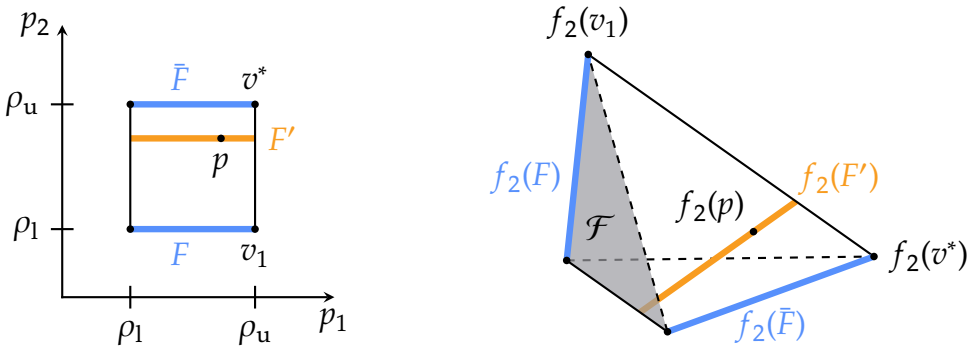

(a) Hypercube $[\rho_l, \rho_u]^2$ (b) Projected uncertainty set conv $\hat{\boldsymbol{\theta}}_2$

Figure 5.4.: Visualization of the relevant points and sets in the proof of Theorem 5.13 for a two-dimensional example. The left figure shows the uncertainty in terms of the edge-wise probabilities p_1 and p_2, and the right figure contains a projected view of the matching sets in the probability simplex $\mathcal{S}_3$. (Hespe, Datar & Werner, 2024)

iii) We proceed by induction. For $d = 1$, there exists a scalar $\tau \in (0,1)$ that satisfies $p = \tau\rho_l + (1-\tau)\rho_u$, which by Lemma 5.10 implies

$$f_1(p) = f_1\big(\tau\rho_l + (1-\tau)\rho_u\big) = \tau f_1(\rho_l) + (1-\tau) f_1(\rho_u)$$

and thus $f_1(p)$ is in ri(conv $\hat{\boldsymbol{\theta}}_1$).

Next, assume the statement holds for some $d \geq 1$ and consider the problem for $d+1$. From the hypercube $[\rho_l, \rho_u]^{d+1}$, chose an arbitrary pair of opposing facets F and $\bar{F}$ and any vertex v^* such that $v^* \in \mu(\bar{F})$. We denote by $V \subset \mu(F) \times \mu(\bar{F})$ the 2^d pairs of vertices (v_1, v_2) such that $\tau v_1 + (1-\tau)v_2$ with $\tau \in [0,1]$ is an edge of $[\rho_l, \rho_u]^{d+1}$. Finally, introduce the facet $\mathcal{F} := \operatorname{conv} f_{d+1}(\{\rho_l, \rho_u\}^{d+1} \setminus \{v^*\})$ of the uncertainty simplex, where $f_{d+1}(F) \subset \mathcal{F}$ but $f_{d+1}(\bar{F}) \not\subset \mathcal{F}$ by construction independent of the choice of v^*. A visualization of the points and sets for $d = 2$ can be found in Fig. 5.4.

By Lemma 5.11, $f_{d+1}(v^*) \notin \operatorname{aff} \mathcal{F}$ as $\mathcal{F}$ is at most $2^{d+1} - 2$ dimensional, and there exists a unique $v_1 \in \mu(F)$ such that $(v_1, v^*) \in V$. Since the edges of the hypercube are axis-aligned for all pairs in V, we therefore have

$$f_{d+1}\big(\tau v_1 + (1-\tau)v^*\big) = \tau f_{d+1}(v_1) + (1-\tau) f_{d+1}(v^*) \notin \mathcal{F}$$

for all $\tau \in [0,1)$ by Lemma 5.10. Now, consider $\tau' \in (0,1)$ such that

$$p \in F' := \operatorname{conv}\Big\{\tau' v_1 + (1-\tau')v_2 \;\Big|\; (v_1, v_2) \in V\Big\},$$

where τ' is guaranteed to exist by assumption. Furthermore, $p \in \operatorname{ri} F'$, which by the induction hypothesis implies $f_{d+1}(p) \in \operatorname{ri}(\operatorname{conv} f_{d+1}(F'))$ since F' is a d-dimensional hypercube and axis-aligned. On the other hand, it follows from $f_{d+1}(\tau' v_1 + (1-\tau')v^*) \notin \mathcal{F}$ that $f_{d+1}(\mu(F')) \not\subset \mathcal{F}$ and therefore, because the choice of the vertex v^* was arbitrary, that there is no facet that contains $f_{d+1}(\mu(F'))$. As such, conv $f_{d+1}(F')$ is not entirely contained in the relative boundary of conv $\hat{\boldsymbol{\theta}}_{d+1}$, and we conclude

$$f_{d+1}(p) \in \operatorname{ri}(\operatorname{conv} f_{d+1}(F')) \subseteq \operatorname{ri}(\operatorname{conv} \hat{\boldsymbol{\theta}}_{d+1})$$

by application of Lemma 2.7. ■

According to Theorem 5.13, the vector-valued uncertainty set conv $\hat{\boldsymbol{\theta}}_d$ is monotonically growing with the bounds on the edge probabilities, can cover the set $\mathcal{S}_{2^d-1}$ of all probability vectors in the limit, and contains distributions of spatially-independent communication links in its interior. Note, however, that while the last property guarantees distributional robustness with respect to spatial dependencies between links, the results of Theorem 5.13 are insufficient to discuss temporal dependencies as they have to be modelled by probability *matrices* instead of *vectors*. The final step is therefore to extend the above statements to the set conv $\hat{\boldsymbol{\Theta}}_d$ of uncertain TPMs, which can be achieved as a direct corollary of Lemma 2.6 and Theorem 5.13.

Corollary 5.14.: Spatio-Temporal Robustness (Hespe, Datar & Werner, 2024)

Let $0 \leq \rho_\mathrm{l}' \leq \rho_\mathrm{l} < \rho_\mathrm{u} \leq \rho_\mathrm{u}' \leq 1$ *with corresponding sets* $\hat{\boldsymbol{\Theta}}_d$ *and* $\hat{\boldsymbol{\Theta}}_d'$. *Then for all* $d \in \mathbb{N}$

i) conv $\hat{\boldsymbol{\Theta}}_d = \mathbb{T}_d$ *if* $\rho_\mathrm{l} = 0$ *and* $\rho_\mathrm{u} = 1$,

ii) conv $\hat{\boldsymbol{\Theta}}_d \subset$ conv $\hat{\boldsymbol{\Theta}}_d'$ *if* $\rho_\mathrm{l}' < \rho_\mathrm{l}$ *or* $\rho_\mathrm{u} < \rho_\mathrm{u}'$, *and*

iii) $\begin{bmatrix} f\left(p^{(1)}\right) & f\left(p^{(2)}\right) & \dots & f\left(p^{(2^d)}\right) \end{bmatrix}^\top \in \mathrm{ri}\left(\mathrm{conv}\, \hat{\boldsymbol{\Theta}}_d\right)$ *for all* $p^{(i)} \in (\rho_\mathrm{l}, \rho_\mathrm{u})^d$.

Proof. Since the convex hull and the relative interior distribute over the Cartesian product by Lemma 2.6, we obtain

$$\mathrm{conv}\left(\hat{\boldsymbol{\theta}}_d \times \cdots \times \hat{\boldsymbol{\theta}}_d\right) = \mathrm{conv}(\hat{\boldsymbol{\theta}}_d) \times \cdots \times \mathrm{conv}(\hat{\boldsymbol{\theta}}_d)$$

and

$$\mathrm{ri}\left(\mathrm{conv}(\hat{\boldsymbol{\theta}}_d \times \cdots \times \hat{\boldsymbol{\theta}}_d)\right) = \mathrm{ri}(\mathrm{conv}\, \hat{\boldsymbol{\theta}}_d) \times \cdots \times \mathrm{ri}(\mathrm{conv}\, \hat{\boldsymbol{\theta}}_d).$$

Accordingly, Statement i) follows by Theorem 5.13 since $\hat{\boldsymbol{\Theta}}_d$ is associated with $\hat{\boldsymbol{\theta}}_d \times \cdots \times \hat{\boldsymbol{\theta}}_d$ and $\mathbb{T}_d$ is with $\mathcal{S}_{2^d-1} \times \cdots \times \mathcal{S}_{2^d-1}$. Furthermore, conv $\hat{\boldsymbol{\theta}}_d \subset$ conv $\hat{\boldsymbol{\theta}}_d'$ implies that also conv $\hat{\boldsymbol{\theta}}_d \times \cdots \times$ conv $\hat{\boldsymbol{\theta}}_d$ is a proper subset of conv $\hat{\boldsymbol{\theta}}_d' \times \cdots \times$ conv $\hat{\boldsymbol{\theta}}_d'$, proving Statement ii). Finally, the nested relative interior and convex hull lead to Statement iii) since $f_d(p^{(i)}) \in$ ri(conv $\hat{\boldsymbol{\theta}}_d$) by Theorem 5.13. ■

Corollary 5.14 proves that stabilizing (or bounding either system norm) for all conv $\hat{\boldsymbol{\Theta}}_d$ as formulated in Corollaries 5.7 and 5.8 is indeed providing distributional robustness. In particular, for TPMs with rows of spatially independent communication links of bounded probability, there exists no small perturbation pushing them out of conv $\hat{\boldsymbol{\Theta}}_d$. Since the affine hull of $\hat{\boldsymbol{\Theta}}_d$ and $\mathbb{T}_d$ are identical by Lemmas 2.6 and 5.11, this includes spatio-temporal dependencies between edges. Remarkably, this is the case even though Theorems 5.3 to 5.5 consider only independent (both spatially and temporally) distributions. However, Theorem 5.13 and Corollary 5.14 provide no quantification of the robustness, *i.e.* there are no bounds on the magnitude of perturbation that can be tolerated, and as such small errors might lead to instability.

5.4. Application Examples

Before closing Chapter 5, we will use this final section to discuss three examples that demonstrate the applicability of the proposed methods. The first scenario revisits the

first-order consensus problem with the generalized packet loss model, followed by a discussion on the conservatism of the norm bounds and an example for real-world TPMs that are encompassed by the parametrized uncertainty model.

5.4.1. Integrator Convergence Revisited

In Section 3.3.3, it has been shown that the first-order consensus problem is guaranteed to converge under the homogeneous Bernoulli packet loss model if the gain κ is chosen sufficiently small. Importantly, the gain bound is monotonically growing if the transmission probability is reduced, such that gains that stabilize the deterministic variant with $p = 1$ are admissible for all non-zero probabilities. Based on Theorem 5.3, the same statement can now be made for the more general heterogeneous Bernoulli and Markov loss models discussed in the current chapter.

Proposition 5.15.: Heterogeneous Mean-Square First-Order Consensus

Proposition 3.9 continues to hold if Assumption 3.4 is replaced by Assumption 5.1 and there exists a $\rho_l > 0$ such that the transmission probabilities are bounded as $\rho_l \leq p^{ij} \leq 1$ for all $(i,j) \in \mathcal{E}^0$.

Proof. We proceed by constructing a solution $Y \succ 0$ and $P \in \mathcal{P}_1$ to the LMI (5.9b) that is valid for all $0 < \rho_l \leq \rho_u = 1$. First, choose the multiplier as

$$P = \begin{bmatrix} Q & S \\ S^\top & R \end{bmatrix} \qquad \text{with} \qquad S^\top = \begin{bmatrix} 0 & 0 & -1 \\ 1 & 0 & 0 \end{bmatrix}$$

and diagonal matrices $Q = \operatorname{diag}(Q_{11}, Q_{22}, Q_{33})$ and $R = \operatorname{diag}(R_{11}, R_{22})$. Subsequently, the multiplier constraint (5.5) simplifies to the scalar inequalities $\rho Q_{11} + (1-\rho)Q_{22} + R_{11} \geq 0$ and $\rho Q_{33} + R_{22} \geq 0$ for $\rho \in [\rho_l, 1]$. Furthermore, choosing $Y = \kappa$, (5.9b) decouples into $R_{22} < 0$, $Q_{11} + \lambda\kappa < 0$, $Q_{22} + 2\kappa < 0$, and $Q_{33} + R_{11} < 2$ for $\lambda \in \{\lambda_2, \lambda_N\}$. Finally, all scalar inequalities are satisfied by the solution

$$\begin{aligned} Q_{11} = Q_{22} &= -\kappa\lambda_N - \varepsilon & R_{11} &= \kappa\lambda_N + 2\varepsilon \\ Q_{33} &= 2 - \kappa\lambda_N - 3\varepsilon & R_{22} &= \rho_l(\kappa\lambda_N - 2 + 4\varepsilon) \end{aligned}$$

for any ε with $0 < \varepsilon < \frac{2-\kappa\lambda_N}{4}$ which exists by assumption, since $\lambda_N \geq 2$ for non-trivial graphs by Proposition 2.1. ■

Alternatively, since Corollary 5.7 relies on the same LMI conditions as Theorem 5.3, the statement can also be posed in terms of communication networks that satisfy Assumption 5.2. As such, the first-order consensus problem converges even for packet loss with spatio-temporal dependencies if each edge has a non-zero transmission probability.

5.4.2. Conservatism Estimated for Small and Large Networks

For the second example, the goal is to study how conservative the robust analysis conditions for the heterogeneous Bernoulli (and by Corollary 5.8 also the symmetric Markov) model are at different transmission probabilities and network sizes. We therefore go back

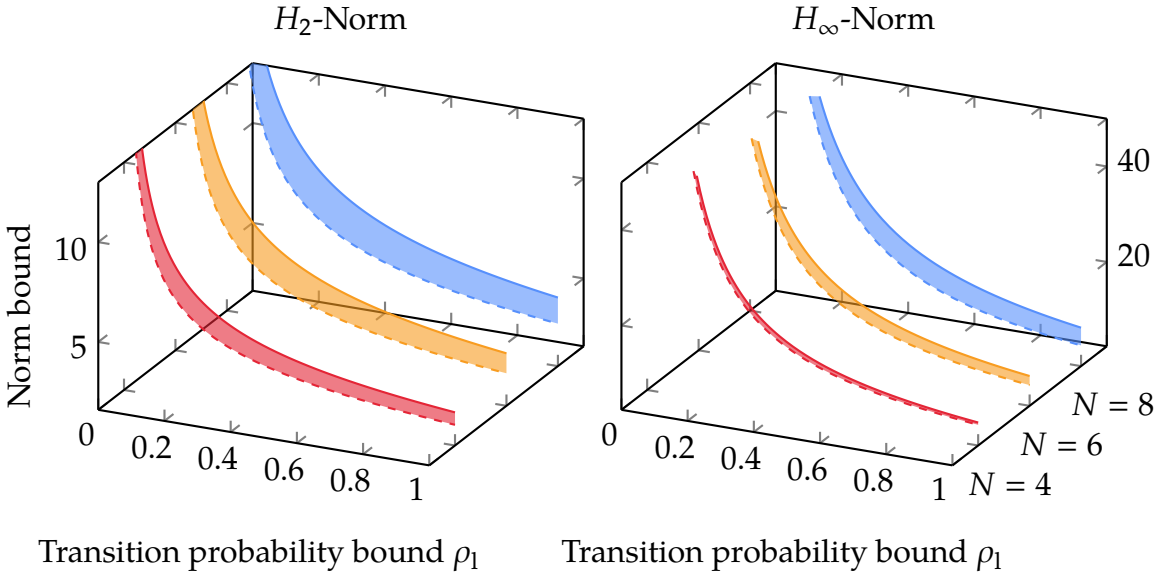

Figure 5.5.: Best upper bounds that can be obtained from Theorems 5.4 and 5.5 for transition probabilities in the interval $[\rho_1, 1]$ with $N \in \{4, 6, 8\}$. For comparison, lower bounds are obtained from evaluating the mean system for all combinations of $p^{ij} \in \{\rho_1, 1\}$, and the filled areas indicate the potential conservatism.

to the masses with friction of Example 4.1, but instead of designing an output-feedback controller, the masses are interconnected through the consensus protocol

$$u_k^i = \kappa \sum_{j \in \mathcal{N}_i^-} \phi_k^{ij} \left(y_k^j - y_k^i \right)$$

with gain $\kappa > 0$. Similar to Section 3.6, this leads to a closed-loop system of the collective MAS in form of a decomposable MJLS with the Laplacian as pattern matrix,

$$\mathcal{A}_\mathrm{d} = \begin{bmatrix} 1 & 0.25 \\ 0 & 0.018 \end{bmatrix}, \qquad \mathcal{A}_\mathrm{c} = -\kappa \begin{bmatrix} 0.19 & 0 \\ 0.25 & 0 \end{bmatrix}, \qquad \mathcal{B}_\mathrm{d} = \begin{bmatrix} 0.19 \\ 0.25 \end{bmatrix}, \qquad C_\mathrm{p} = \begin{bmatrix} 1 & 0 \end{bmatrix},$$

and all other terms zero.

As the first step, consider groups of masses interconnected through circular graphs $\mathcal{G}_N^\circ$ as introduced in Example 2.1 with fixed upper probability bound $\rho_\mathrm{u} = 1$, and let the lower bound ρ_l vary between 0 and 1. By analysing these systems with four, six, and eight agents using Theorems 5.4 and 5.5, we obtain robust upper bounds that depend on the size of the uncertainty interval $[\rho_\mathrm{l}, 1]$ and are shown in Fig. 5.5. In addition, the figure contains lower bounds on the system norms that are obtained by analysing the mean system (*cf.* Section 3.5) for all possible packet loss distributions such that p^{ij} is either ρ_l or 1. Note that this estimate is exact for $\rho_\mathrm{l} = 1$, since this corresponds to the idealized scenario.

For both norms, the robust bounds are monotonically increasing for decreasing ρ_l, which is to be expected because the uncertainty is growing. Furthermore, the gap between the upper and lower bounds is increased for larger networks especially for the H_∞-norm bounds, indicating that the analysis is more conservative the more subsystems there are, paralleling the observations of Section 3.6.2.

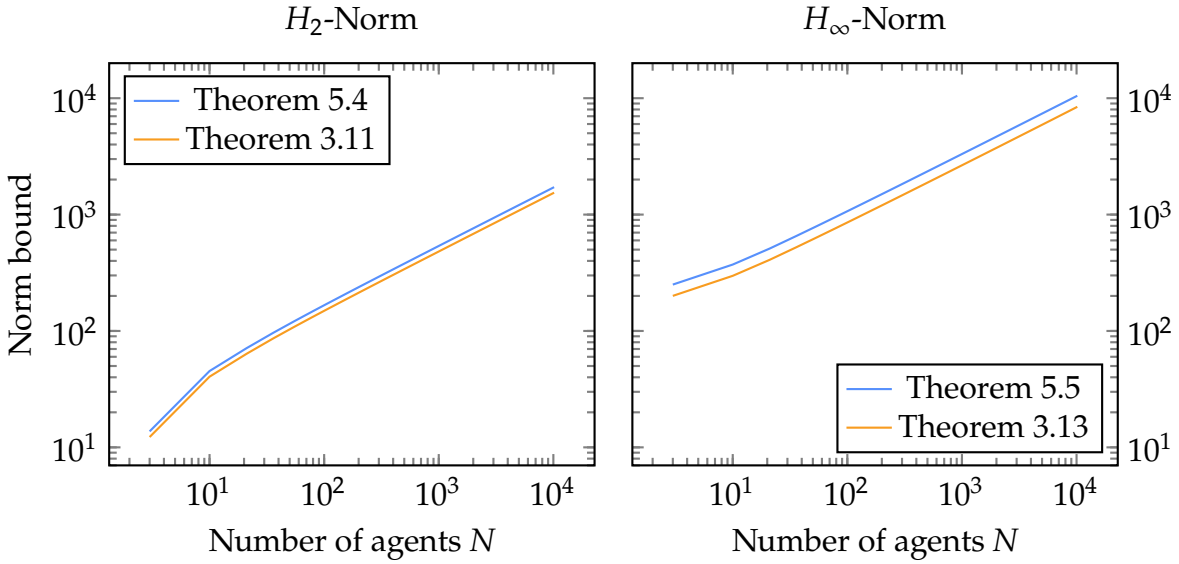

Figure 5.6.: Comparison of performance bounds for networks with heterogeneous transmission probabilities $p^{ij} \in [0.4, 0.6]$ (Theorems 5.4 and 5.5) with networks of homogeneous probability $p = 0.5$ (Theorems 3.11 and 3.13).

Since the previous systems were limited in size due to the combinatorial analysis performed on the mean system, the second step is to study how the conservatism evolves for large-scale IS. Starting at $h = 2$ (and thus $N = 3$), we therefore apply Theorems 5.4 and 5.5 on systems interconnected by triangular grid graphs $\mathcal{G}_h^{\triangle}$ (see Example 2.2) and transmission probabilities $p^{ij} \in [0.4, 0.6]$. For comparison, the same systems are furthermore analysed using Theorems 3.11 and 3.13 with fixed *homogeneous* transmission probability $p = 0.5$ such that the gap indicates the increase of the norm bound due to the uncertainty. Both sets of curves are visualized in Fig. 5.6.

Regardless of which norm we consider, the gap between the robust and homogeneous norms is approximately constant on a logarithmic scale, which translates into having a constant ratio between the bounds independent of network size. In terms of computational effort, the longest time required to solve the underlying SDP in case of the robust H_2-norm bound was in the order of a few minutes, such that bounding the norms of even the largest IS considered is sufficiently fast.

5.4.3. Fitting Data of Vehicle-To-Vehicle Networks

With the previous section, we have shown how the robust analysis LMIs behave for increasing size of the IS or uncertainty, but the uncertainty set $\hat{\boldsymbol{\Theta}}_d$ remains rather abstract. Even though Section 5.3.3 has shown that the set has non-empty interior, it is still an open question whether the uncertainty encompasses typical TPMs of real-world scenarios. The idea behind this final example is therefore to take data from vehicle-to-vehicle networks to fit non-trivial sets $\hat{\boldsymbol{\Theta}}_d$, demonstrating that the uncertainty description is rich enough to model realistic communication behaviour.

The general idea for fitting an uncertainty set to the available data relies on the fact that a convex polytope can be defined as the convex hull of its vertices. As such, a probability vector θ is in conv $\hat{\boldsymbol{\theta}}_d$ for fixed $0 \leq \rho_l \leq \rho_u \leq 1$ if and only if there exists a $\nu \in \mathcal{S}_{2^d-1}$ such

Table 5.1.: Smallest intervals such that the TPMs are contained in conv $\hat{\boldsymbol{\Theta}}_d$ for six platooning scenarios from Razzaghpour et al. (2022) that differ in terms of the traffic density and inter packet gap (IPG). (Hespe, Datar & Werner, 2024)

Scenario		Probability Interval		
Traffic Density	IPG in ms	ρ_l	ρ_u	$\rho_\mathrm{u} - \rho_\mathrm{l}$
Low	0 – 100	0.23	0.97	0.74
Low	200 – 300	0.18	0.68	0.50
Medium	0 – 100	0.23	0.92	0.69
Medium	200 – 300	0.11	0.56	0.45
High	0 – 100	0.34	0.98	0.64
High	200 – 300	0.13	0.57	0.45

that $\theta = Mv$, where M is as defined in (5.15) and contains the vertices of the uncertainty set. Moreover, this condition extends to TPMs by stacking the constraints row-wise. Thus, the existence of a solution $V \in \mathbb{R}^{2^d \times 2^d}$ to the linear feasibility problem

$$VM^\top = \Theta \tag{5.16a}$$
$$V\mathbf{1}_{2^d} = \mathbf{1}_{2^d} \tag{5.16b}$$
$$V \geq 0 \tag{5.16c}$$

is equivalent to $\Theta \in \operatorname{conv} \hat{\boldsymbol{\Theta}}_d$, where (5.16c) is an element-wise inequality. We can therefore obtain non-trivial intervals $[\rho_\mathrm{l}, \rho_\mathrm{u}]$ such that $\Theta \in \operatorname{conv} \hat{\boldsymbol{\Theta}}_d$ by iteratively checking the feasibility of (5.16).

The dataset which we are fitting the uncertainty set on has been obtained by Razzaghpour et al. (2022) through high-fidelity simulations of vehicle platooning scenarios. The dataset is parametrized by two quantities, the traffic density and the inter packet gap, which describes the time between two successful transmissions, but the number of vehicles in the platoon is fixed at six. After the minimization procedure outlined above, we obtain the intervals as shown in Table 5.1. In each of the six cases, the procedure results in a non-trivial interval, demonstrating that the uncertainty description by the sets $\hat{\boldsymbol{\Theta}}_d$ is rich enough to convey real-world TPMs through convex combinations of fixed probability vectors.

6 Stability and Performance with Time-Varying Topologies

Many of the results in the preceding chapters offer some form of inherent or deliberate robustness. For example, the stability and performance analysis conditions of Theorems 3.6, 3.11, and 3.13 in Chapter 3 only require checking the boundary of the Laplacian spectrum. As such, the results are not restricted to a specific nominal graph $\mathcal{G}^0$ but cover all graphs whose spectrum is contained in the tested interval, such that stability can be guaranteed even if the underlying topology is uncertain. However, in contrast to analogous results for IS *without* stochastic communication effects (*e.g.* Pilz et al., 2009), the current modelling framework does not permit to reason about time-varying *nominal* topologies (as opposed to random switching due to packet loss). Motivated by this discrepancy, the current chapter is not aimed at deriving new stability and performance tests, but rather at providing a suitable framework to prove that the existing conditions extend seamlessly to time-varying nominal graphs.

In order to encompass time-varying graphs, the framework outlined below requires further weakening the assumptions underlying the techniques of Chapters 3 and 4. Specifically, while we continue to assume that the transmission links are spatio-temporally independent, their distribution is switched based on whether the underlying nominal graph has an edge for that link at time k or not. As such, Assumption 2.4 is invalidated, and is therefore explicitly *not* imposed throughout this chapter. The following developments are based on (Hespe & Werner, 2023a) and are presented in revised form to match the general framework discussed in this dissertation.

6.1. Modelling Time-Varying Communication Networks

Let us first discuss how to extend the general modelling framework for stochastic packet loss that has been introduced in Section 2.3 to cover time-varying nominal topologies. Instead of considering a single nominal graph $\mathcal{G}^0$, there is now a whole family $\{\mathcal{G}_l^0 \mid l \in \mathcal{K}^0\}$ of nominal interconnections, where $\mathcal{K}^0 := \{1, 2, \dots, |\mathcal{K}^0|\}$ is a finite index set. We assume that all switched nominal graphs share the same vertex set, resulting in graphs $\mathcal{G}_l^0 = (\mathcal{V}^0, \mathcal{E}_l^0)$ for all $l \in \mathcal{K}^0$ and ensuring that the underlying state-space has constant dimension. Furthermore, $\mathcal{E}^0$ is now understood as $\mathcal{E}^0 = \bigcup_{l \in \mathcal{K}^0} \mathcal{E}_l^0$, the set of edges that are present in at least one of the nominal topologies, and L_l^0 denotes $L(\mathcal{G}_l^0)$. Based on this family of graphs, the time dependency of the nominal interconnection is described by $\mathcal{G}_{v_k}^0$, where $v \colon \mathbb{N}_0 \to \mathcal{K}^0$ is a deterministic switching sequence, and therefore $\mathcal{E}_{v_k}^0$ is the set of *potentially* transmitting edges at step k. Note that v_k is considered to be unknown in the following, which is conservative in case knowledge about the switching is available, *e.g.* in case of proximity graphs, but required for the framework to be developed below.

For the topology of the networked IS, this means that the stochastic switching due to packet loss and deterministic switching of the nominal interconnection structure are superimposed. Nonetheless, the stochastic processes $\{\phi_k^{ij}\}$ are still interpreted as before with $\phi_k^{ij} = 1$ indicating a successful transmission across the edge $(i,j) \in \mathcal{E}^0$ at time k, which implies that their distribution must depend on v_k since transmissions are only possible if $(i,j) \in \mathcal{E}^0_{v_k}$. Analogous to Section 2.3, the edge processes are then condensed into a single network-wide process

$$\sigma_k = 1 + \sum_{(i,j)\in\mathcal{E}^0} \phi_k^{ij} 2^{\alpha(i,j)-1} \qquad \text{taking values in} \qquad \mathcal{K} = \left\{1, 2, \dots, 2^{|\mathcal{E}^0|}\right\},$$

and the graph process $\{\mathcal{G}_{\sigma_k}\}$ determines which topology is implemented at a particular time step k. The definitions of the subgraphs $\mathcal{G}_i$ and edge sets $\mathcal{E}_i$ remain unchanged.

For the same reason as in Chapter 3, allowing $\{\sigma_k\}$ to be a general Markov chain on finite state-space $\mathcal{K}$ is computationally intractable, such that simplifying assumptions have to be imposed. Most importantly, it is still assumed that the edge processes are spatio-temporally independent in the sense of Assumptions 3.1 and 3.3 if applied to each instance of the switched distribution. Moreover, all edges in the *current* nominal graph are assumed to have a homogeneous transmission probability, which leads to the following generalization of Assumption 3.4:

Assumption 6.1.: Switched Homogeneous Bernoulli Packet Loss Model

In addition to Assumptions 3.1 and 3.3, the processes $\{\phi_k^{ij}\}$ have homogeneous probability $p \in [0,1]$ if they are present in the graph $\mathcal{G}^0_{v_k}$ and zero otherwise, *i.e.*

$$\mathbb{P}\left(\phi_k^{ij} = 1\right) = \begin{cases} p & \text{if } (i,j) \in \mathcal{E}^0_{v_k}, \\ 0 & \text{else} \end{cases}$$

holds for all edges $(i,j) \in \mathcal{E}^0$ and all $k \in \mathbb{N}_0$.

The packet loss model of Assumption 6.1 is *not* time-homogeneous and therefore violates Assumption 2.4, in contrast to all models presented before. Importantly, however, $\{\sigma_k\}$ is independent in time, and many results of the preceding chapters can therefore be applied by considering the switching sequence v as a constant. For example, by combining Lemmas 3.3 and 5.2, we obtain

$$\Xi_{I_N}\left[L_{\sigma_k}\right] = 2p(1-p)L^0_{v_k} \tag{6.1}$$

as the generalized variance of the Laplacian with switching nominal topology if all nominal graphs $\mathcal{G}^0_l$ are undirected.

6.2. Switched Markov Jump Linear Systems

For standard MJLS as introduced in Section 2.4, it is an essential assumption that the underlying Markov chain is homogeneous and its TPM therefore time-invariant. In addition, said Markov chain is their only source of switching, and no secondary *deterministic*

switching sequence is permitted. Both of these issues prevent capturing the kind of network model discussed in the previous section, such that more general jump systems have to be devised.

A class of systems that encompasses both stochastic and deterministic switching and time-varying transition probabilities are so-called *switched Markov jump linear systems* that take the form

$$\mathcal{T}\colon \begin{cases} \xi_{k+1} = \mathcal{A}_{\sigma_k,\upsilon_k}\xi_k + \mathcal{B}_{\sigma_k,\upsilon_k}w_k, \\ z_k = \mathcal{C}_{\sigma_k,\upsilon_k}\xi_k + \mathcal{D}_{\sigma_k,\upsilon_k}w_k, \end{cases} \tag{6.2}$$

where $\sigma_k \in \mathcal{K}$ is the state of a Markov chain with initial distribution $\mathbb{P}(\sigma_0 = i) = t_i^{\upsilon_0}$ and transition probabilities

$$\mathbb{P}(\sigma_{k+1} = j \mid \sigma_k = i) = \theta_{ij}^{\upsilon_k},$$

and $\upsilon_k \in \mathcal{K}^0$ is an exogenous switching signal. Multiple variants of this kind of system have been discussed in the literature before. For example, Bolzern et al. (2010) study stability properties of continuous-time switched MJLS for which the distribution of $\{\sigma_k\}$ is independent of υ_k, and an extension that includes such dependencies has been reported by Song et al. (2016). In a discrete-time setting, such questions were discussed by Qu et al. (2018), including the switching probability distribution. On the performance side, Bolzern et al. (2015) and Zhang et al. (2011) propose a BRL for switched MJLS, which they apply for H_∞-norm based controller synthesis, and Hou et al. (2013) treat the generalized H_2-norm. However, none of the aforementioned works have considered the special case of switched MJLS whose Markov chain has no dependencies between time steps and therefore satisfies $\theta_{ij}^{l} = \theta_{j}^{l}$ for all $i, j \in \mathcal{K}$ and $l \in \mathcal{K}^0$. Given the potential for significant simplification of the analysis for this kind of MJLS (see Fioravanti et al., 2012, 2013), this will be the focus of the following discussion.

6.2.1. Mean-Square Stability for Switched Jump Systems

Similar to our discussion on standard MJLS in Chapter 3, the first property of $\mathcal{T}$ to discuss is its stability. Generally, the exogenous switching sequence υ is treated as an adversarial signal, and therefore all conclusions have to be drawn with respect to its worst-case instance. As such, the concepts of mean-square and almost sure stability as introduced in Definition 2.5 remain valid, though their convergence conditions have to hold not only for all initial condition but also all switching sequences υ.

The essential idea behind the analysis discussed below is that stochastic quadratic forms can be bounded in expectation if their central matrix term is independent of the outer factors and bounded in expectation itself. As such, the central matrix can be constrained by an LMI in order to infer properties of the quadratic form as a whole without having to calculate its expectation. This is formalized by the following lemma:

Lemma 6.1.: Expectation Bounded Quadratic Form (Hespe & Werner, 2023a)

Let v and M be a random vector and a symmetric random matrix taking values in $\mathbb{R}^n$ and $\mathbb{R}^{n\times n}$, respectively. Assume furthermore that v and M are independent. Then

$$\mathbb{E}\left[v^\top M v\right] \leq \mathbb{E}\left[v^\top W v\right] \tag{6.3}$$

follows for symmetric W with $\mathbb{E}[M] \preceq W$.

Proof. For symmetric matrices A and W with $A \preceq W$ and an arbitrary $B \succeq 0$ we have

$$A \preceq W \;\Rightarrow\; B^{1/2}AB^{1/2} \preceq B^{1/2}WB^{1/2} \;\Rightarrow\; \operatorname{tr}(AB) = \operatorname{tr}\left(B^{1/2}AB^{1/2}\right) \leq \operatorname{tr}\left(B^{1/2}WB^{1/2}\right) = \operatorname{tr}(WB),$$

where $B^{1/2}$ denotes the matrix square root. Furthermore, the independence of v and M as well as the linearity of expectation and trace imply that

$$\mathbb{E}\left[v^\top Mv\right] = \mathbb{E}\left[\operatorname{tr}(v^\top Mv)\right] = \mathbb{E}\left[\operatorname{tr}(Mvv^\top)\right] = \operatorname{tr}\left(\mathbb{E}[Mvv^\top]\right) = \operatorname{tr}\left(\mathbb{E}[M]\,\mathbb{E}[vv^\top]\right),$$

such that in combination taking $A = \mathbb{E}[M]$ and $B = \mathbb{E}[vv^\top]$ results in

$$\mathbb{E}\left[v^\top Mv\right] = \operatorname{tr}\left(\mathbb{E}[M]\,\mathbb{E}[vv^\top]\right) \leq \operatorname{tr}\left(W\,\mathbb{E}[vv^\top]\right) = \mathbb{E}\left[\operatorname{tr}(Wvv^\top)\right] = \mathbb{E}\left[v^\top Wv\right]. \qquad \blacksquare$$

Even though the matrix W is arbitrary in Lemma 6.1, we are mostly interested in the special case with identity bound $W = cI_n$. For this choice of W, the right-hand side of (6.3) turns into $\mathbb{E}\left[v^\top Wv\right] = c\,\mathbb{E}\left[\|v\|^2\right]$, *i.e.* a norm bound on the original quadratic form. With this, we are now ready to state and prove Theorem 6.2, a generalization of Theorem 3.1 to switched MJLS with the caveat that only sufficiency is established.

Theorem 6.2.: Switched Mean-Square Stability

A switched MJLS $\mathcal{T}$ satisfying Assumption 3.1 is mean-square stable if there exists an $\mathcal{X} > 0$ that solves the LMI

$$\sum_{j\in\mathcal{K}} \theta_j^l \mathcal{A}_{j,l}^\top \mathcal{X} \mathcal{A}_{j,l} \prec \mathcal{X} \tag{6.4}$$

for all $l \in \mathcal{K}^0$.

Proof. It follows from the LMI (6.4) that there are $\varepsilon_l > 0$ for $l \in \mathcal{K}^0$ such that

$$\mathbb{E}\left[\mathcal{A}_{\sigma_k,v_k}^\top \mathcal{X} \mathcal{A}_{\sigma_k,v_k}\right] - \mathcal{X} \preceq -\varepsilon_{v_k} I_{Nn_\xi} \preceq -\bar{\varepsilon} I_{Nn_\xi} \prec 0 \tag{6.5}$$

holds for all $k \in \mathbb{N}_0$ regardless of v, where $\bar{\varepsilon} := \min_{l\in\mathcal{K}^0} \varepsilon_l$ is guaranteed to exist because $\mathcal{K}^0$ is finite. Next, introduce the Lyapunov function candidate $V(\xi) = \xi^\top \mathcal{X} \xi$ and its increment $\Delta V_k := V(\xi_{k+1}) - V(\xi_k)$. Since $\mathcal{X} > 0$, V satisfies $V(0) = 0$ and $0 < V(\xi) \leq c\|\xi\|^2$ by definition if $\xi \neq 0$ with $c := \|\mathcal{X}\|$. Furthermore, Lemma 6.1 and (6.5) imply that

$$\mathbb{E}\left[\Delta V_k\right] = \mathbb{E}\left[\xi_k^\top (\mathcal{A}_{\sigma_k,v_k}^\top \mathcal{X} \mathcal{A}_{\sigma_k,v_k} - \mathcal{X})\xi_k\right] \leq -\bar{\varepsilon}\,\mathbb{E}\left[\|\xi_k\|^2\right]$$

as ξ_k and σ_k are independent by Assumption 3.1. Now, chose any final time $T \in \mathbb{N}_0$ and initial condition ξ_0, and calculate the telescoping sum

$$\sum_{k=0}^{T} \mathbb{E}\left[\Delta V_k\right] = \mathbb{E}\left[V(\xi_{T+1})\right] - V(\xi_0) \leq -\bar{\varepsilon} \sum_{k=0}^{T} \mathbb{E}\left[\|\xi_k\|^2\right]$$

to conclude that

$$\mathbb{E}\left[\|\xi_T\|^2\right] \leq \sum_{k=0}^{T} \mathbb{E}\left[\|\xi_k\|^2\right] \leq \frac{1}{\bar{\varepsilon}}\left(V(\xi_0) - \mathbb{E}[V(\xi_{T+1})]\right) \leq \frac{1}{\bar{\varepsilon}} V(\xi_0) \leq \frac{c}{\bar{\varepsilon}}\|\xi_0\|^2$$

because $V(\xi_{T+1}) \geq 0$, which implies that the state is bounded in mean-square. Finally, in the limit we obtain

$$\lim_{T\to\infty} \sum_{k=0}^{T} \mathbb{E}\left[\|\xi_k\|^2\right] \leq \frac{c}{\varepsilon}\|\xi_0\|^2 < \infty,$$

which implies that the series converges since $\|\xi_k\|^2 \geq 0$ and therefore $\lim_{k\to\infty} \mathbb{E}\left[\|\xi_k\|^2\right] = 0$, proving that the system is mean-square stable. ■

In the same way as Theorem 3.1, its generalization consists of a single matrix variable $\mathcal{X}$ independent of the cardinality of $\mathcal{K}$ and $\mathcal{K}^0$. It is however necessary to enumerate all modes of the Markov chain and check (6.4) for all $l \in \mathcal{K}^0$, which may lead to tractability issues if either of the two sets is large. Nonetheless, this results in a significant reduction in computational complexity compared to the general case without Assumption 3.1 which requires evaluating LMIs for all $l \in \mathcal{K}^0$ *and* $i \in \mathcal{K}$ (Qu et al., 2018).

6.2.2. Worst-Case H_2-Norm Calculations

The approach introduced above to prove mean-square stability can be applied in similar fashion to obtain bounds on the performance of switched MJLS. Since no information is available about the exogenous switching sequence, the bounds have to be formulated in a worst-case sense with respect to υ, in contrast to the switching caused by $\{\sigma_k\}$ where the known transition probabilities can be taken into account. The H_2-norm is therefore redefined for switched MJLS as follows:

Definition 6.2.: Switched MJLS H_2-Norm
The H_2-norm of the mean-square stable switched MJLS $\mathcal{T}$ is given by

$$\|\mathcal{T}\|_{H_2} \coloneqq \sup_{\upsilon} \sqrt{\sum_{i\in\mathcal{K}} \sum_{s=1}^{Nn_w} t_i^{\upsilon_0} \|z^{\upsilon,s,i}\|_{\ell_2}^2},$$

where $z^{\upsilon,s,i}$ is the response of $\mathcal{T}$ to the input $w_k = e_s\delta_k$ with initial condition $\xi_0 = 0$, $\sigma_0 = i$, and switching sequence υ, and δ_k, e_s are the unit impulse and sth canonical basis vector as introduced in Definition 2.7.

Based on Lemma 6.1, we can then state a set of LMI constraints that guarantee an upper bound on this worst-case H_2-norm.

Theorem 6.3.: Switched H_2-Norm Bound (Hespe & Werner, 2023a)

A switched MJLS $\mathcal{T}$ satisfying Assumption 3.1 is mean-square stable and has H_2-norm less than $\gamma > 0$ if there exist an $\mathcal{X} \succ 0$ and symmetric $\mathcal{Z}_l$ with $\operatorname{tr} \mathcal{Z}_l < \gamma^2$ *that solve the LMIs*

$$\sum_{j\in\mathcal{K}} \theta_j^l \left(\mathcal{A}_{j,l}^\top \mathcal{X} \mathcal{A}_{j,l} + \mathcal{C}_{j,l}^\top \mathcal{C}_{j,l}\right) \prec \mathcal{X}, \tag{6.6a}$$

$$\sum_{j\in\mathcal{K}} t_j^l \left(\mathcal{B}_{j,l}^\top \mathcal{X} \mathcal{B}_{j,l} + \mathcal{D}_{j,l}^\top \mathcal{D}_{j,l}\right) \prec \mathcal{Z}_l \tag{6.6b}$$

for all $l \in \mathcal{K}^0$.

Proof. The proof is adapted from a result of Duan and Xiang (2013) for deterministically switched two-dimensional linear systems. First and foremost, note that (6.6a) implies (6.4) and therefore mean-square stability of $\mathcal{T}$. Furthermore, introduce the storage function $V(\xi) = \xi^\top \mathcal{X} \xi$, which has the same properties as the Lyapunov function in the proof of Theorem 6.2.

For bounding the H_2-norm, let ξ^s denote the stochastic state-sequence if a unit impulse is applied at the sth input for some sequence v and take $\mathcal{B}^s_{j,l}$ and $\mathcal{D}^s_{j,l}$ as the sth column of $\mathcal{B}_{j,l}$ and $\mathcal{D}_{j,l}$, respectively. This results in $\xi^s_0 = 0$, $\xi^s_1 = \mathcal{B}^s_{\sigma_0,v_0}$, and $\xi^s_{k+1} = \mathcal{A}_{\sigma_k,v_k}\xi^s_k$ for all $k \in \mathbb{N}$. Taking $\Delta V^s_k \coloneqq V(\xi^s_{k+1}) - V(\xi^s_k)$ as the storage function increment corresponding to ξ^s and choosing any $T \in \mathbb{N}_0$ results in the telescoping sum

$$\sum_{k=0}^{T} \mathbb{E}\Big[\Delta V^s_k\Big] = \mathbb{E}\Big[V(\xi^s_{T+1})\Big] - V(\xi^s_0) = \mathbb{E}\Big[V(\xi^s_{T+1})\Big],$$

where it follows from mean-square stability that $\lim_{T\to\infty} \mathbb{E}\Big[V(\xi^s_{T+1})\Big] = 0$. On the other hand, the above values for ξ^s give

$$\sum_{k=0}^{\infty} \mathbb{E}\Big[\Delta V^s_k\Big] = \mathbb{E}\Big[(\mathcal{B}^s_{\sigma_0,v_0})^\top \mathcal{X} \mathcal{B}^s_{\sigma_0,v_0}\Big] + \sum_{k=1}^{\infty} \mathbb{E}\Big[(\xi^s_k)^\top (\mathcal{A}^\top_{\sigma_k,v_k} \mathcal{X} \mathcal{A}_{\sigma_k,v_k} - \mathcal{X})\xi^s_k\Big]$$

such that the mean output energy for a specific switching sequence v is

$$\begin{aligned}
\|z^{v,s,\sigma_0}\|^2_{\ell_2} &= \mathbb{E}\Big[(\mathcal{D}^s_{\sigma_0,v_0})^\top \mathcal{D}^s_{\sigma_0,v_0}\Big] + \sum_{k=1}^{\infty} \mathbb{E}\Big[(\xi^s_k)^\top \mathcal{C}^\top_{\sigma_k,v_k} \mathcal{C}_{\sigma_k,v_k} \xi^s_k\Big] \\
&= \mathbb{E}\Big[(\mathcal{B}^s_{\sigma_0,v_0})^\top \mathcal{X} \mathcal{B}^s_{\sigma_0,v_0} + (\mathcal{D}^s_{\sigma_0,v_0})^\top \mathcal{D}^s_{\sigma_0,v_0}\Big] \\
&\qquad + \sum_{k=1}^{\infty} \mathbb{E}\Big[(\xi^s_k)^\top (\mathcal{A}^\top_{\sigma_k,v_k} \mathcal{X} \mathcal{A}_{\sigma_k,v_k} + \mathcal{C}^\top_{\sigma_k,v_k} \mathcal{C}_{\sigma_k,v_k} - \mathcal{X})\xi^s_k\Big] \\
&\leq \mathbb{E}\Big[(\mathcal{B}^s_{\sigma_0,v_0})^\top \mathcal{X} \mathcal{B}^s_{\sigma_0,v_0} + (\mathcal{D}^s_{\sigma_0,v_0})^\top \mathcal{D}^s_{\sigma_0,v_0}\Big],
\end{aligned}$$

where in the second equality we added $0 = \sum_{k=0}^{\infty} \mathbb{E}\Big[\Delta V^s_k\Big]$ and the inequality follows from Lemma 6.1 and (6.6a) since ξ^s_k and σ_k are independent by Assumption 3.1. Finally, the H_2-norm is obtained as

$$\begin{aligned}
\|\mathcal{T}\|^2_{H_2} = \sup_{v} \sum_{s=1}^{Nn_w} \|z^{v,s,\sigma_0}\|^2_{\ell_2} &\leq \max_{v_0} \sum_{s=1}^{Nn_w} \mathbb{E}\Big[(\mathcal{B}^s_{\sigma_0,v_0})^\top \mathcal{X} \mathcal{B}^s_{\sigma_0,v_0} + (\mathcal{D}^s_{\sigma_0,v_0})^\top \mathcal{D}^s_{\sigma_0,v_0}\Big] \\
&= \max_{v_0} \operatorname{tr} \mathbb{E}\Big[\mathcal{B}^\top_{\sigma_0,v_0} \mathcal{X} \mathcal{B}_{\sigma_0,v_0} + \mathcal{D}^\top_{\sigma_0,v_0} \mathcal{D}_{\sigma_0,v_0}\Big] \\
&< \max_{l \in \mathcal{K}^0} \operatorname{tr} \mathcal{Z}_l < \gamma^2,
\end{aligned}$$

where the penultimate inequality follows from (6.6b). ∎

Analogous to the relation between Theorems 3.1 and 6.2 for analysing mean-square stability, Theorem 6.3 is generalizing Theorem 3.10 to switched MJLS. Essentially, the norm-bound LMIs (3.15) are evaluated for all admissible values of the switching sequence v with uniform matrix variable $\mathcal{X}$, resulting in a bound that is robust against the unknown switching imposed by v. Of course, this implies that the set $\mathcal{K}^0$ has to be enumerated, potentially leading to scalability issues for systems with large codomains for their exogenous switching function in the same way as discussed for Theorem 6.2.

6.2.3. Evaluating Quadratic Performance Specifications

The extension of the H_2-norm bound to switched MJLS begs the question of whether the H_∞-norm condition of Theorem 3.12 can be generalized with the same technique. However, before directly discussing H_∞-norm bounds, we first introduce a general quadratic performance specification adapted from Scherer (2000), who considers a similar criterion for robust analysis of LPV systems.

Definition 6.3.: Quadratic Performance Specification

Let $Q = Q^\top$, S and $R \geq 0$ be fixed matrices. A switched MJLS complies with the *quadratic performance* specification if there exists an $\varepsilon > 0$ such that

$$\sum_{k=0}^{\infty} \mathbb{E}\left[\begin{bmatrix} w_k \\ z_k \end{bmatrix}^\top \begin{bmatrix} Q & S \\ S^\top & R \end{bmatrix} \begin{bmatrix} w_k \\ z_k \end{bmatrix}\right] \leq -\varepsilon \|w\|_{\ell_2}^2 \tag{6.7}$$

holds for any trajectory of the system with $\xi_0 = 0$.

The quadratic performance specification encompasses two important special cases: On the one hand, the choice $Q = -\gamma^2 I_{Nn_w}$, $S = 0$, and $R = I_{Nn_z}$ leads to a BRL-type result with bounded ℓ_2-gain $\|w\|_{\ell_2} < \gamma \|z\|_{\ell_2}$. Moreover, the matrices $Q = R = 0$ and $S = -I_{n_w}$ result in a certificate of strict passivity, or positive realness (Scherer, 2000, 2022). However, in order to obtain a computational test for the quadratic performance specification similar to Theorems 6.2 and 6.3 for mean-square stability and the H_2-norm, we have to work under the hypothesis that the input signal w is independent of the Markov chain $\{\sigma_k\}$, leading to the following proposition:

Proposition 6.4.: Switched Quadratic Performance

A switched MJLS $\mathcal{T}$ satisfying Assumption 3.1 is mean-square stable and complies with the quadratic performance specification for all input signals $w \in \ell_2^{Nn_w}$ that are independent of $\{\sigma_k\}$ *if there exists an $\mathcal{X} > 0$ that solves the LMI*

$$\sum_{j \in \mathcal{K}} \theta_j^l \left[\begin{array}{cc} I_{Nn_\xi} & 0 \\ \mathcal{A}_{j,l} & \mathcal{B}_{j,l} \\ \hline 0 & I_{Nn_w} \\ C_{j,l} & \mathcal{D}_{j,l} \end{array}\right]^\top \left[\begin{array}{cc|cc} -\mathcal{X} & & & \\ & \mathcal{X} & & \\ \hline & & Q & S \\ & & S^\top & R \end{array}\right] \left[\begin{array}{cc} I_{Nn_\xi} & 0 \\ \mathcal{A}_{j,l} & \mathcal{B}_{j,l} \\ \hline 0 & I_{Nn_w} \\ C_{j,l} & \mathcal{D}_{j,l} \end{array}\right] \prec 0 \tag{6.8}$$

for all $l \in \mathcal{K}^0$.

Proof. The proof is based on a similar result of Scherer (2000) for LPV systems. First, note that the LMI (6.8) is a 2×2 block matrix inequality and the top-left block reads

$$\sum_{j \in \mathcal{K}} \theta_j^l \left(\mathcal{A}_{j,l}^\top \mathcal{X} \mathcal{A}_{j,l} + C_{j,l}^\top R C_{j,l} \right) \prec \mathcal{X},$$

which together with $R \succeq 0$ implies (6.4) and therefore mean-square stability. Furthermore, since $\mathcal{K}^0$ is a finite set, there exists an $\varepsilon > 0$ such that

$$\mathbb{E}\left[\begin{bmatrix} * & * \\ * & * \end{bmatrix}^\top \begin{bmatrix} -\mathcal{X} & \\ & \mathcal{X} \end{bmatrix} \begin{bmatrix} I_{Nn_\xi} & 0 \\ \mathcal{A}_{\sigma_k,\upsilon_k} & \mathcal{B}_{\sigma_k,\upsilon_k} \end{bmatrix} + \begin{bmatrix} * & * \\ * & * \end{bmatrix}^\top \begin{bmatrix} Q & S \\ S^\top & R \end{bmatrix} \begin{bmatrix} 0 & I_{Nn_w} \\ C_{\sigma_k,\upsilon_k} & \mathcal{D}_{\sigma_k,\upsilon_k} \end{bmatrix}\right] \preceq -\varepsilon \begin{bmatrix} 0 & \\ & I_{Nn_w} \end{bmatrix}$$

holds for all $k \in \mathbb{N}_0$ and all switching sequences υ (see the proof of Theorem 6.2).

Next, introduce the storage function $V(\xi) \coloneqq \xi^\top \mathcal{X} \xi$ and supply rate (Scherer, 2022)

$$s(w, z) \coloneqq -\begin{bmatrix} w \\ z \end{bmatrix}^\top \begin{bmatrix} Q & S \\ S^\top & R \end{bmatrix} \begin{bmatrix} w \\ z \end{bmatrix},$$

where the storage function increment is given by $\Delta V_k \coloneqq V(\xi_{k+1}) - V(\xi_k)$. For a specific $k \in \mathbb{N}_0$, the expected change in storage is

$$\begin{aligned} &\mathbb{E}\Big[\Delta V_k - s(w_k, z_k)\Big] \\ &\quad = \mathbb{E}\left[\begin{bmatrix} \xi_k \\ w_k \end{bmatrix}^\top \left(\begin{bmatrix} * & * \\ * & * \end{bmatrix}^\top \begin{bmatrix} -\mathcal{X} & \\ & \mathcal{X} \end{bmatrix} \begin{bmatrix} I_{Nn_\xi} & 0 \\ \mathcal{A}_{\sigma_k,\upsilon_k} & \mathcal{B}_{\sigma_k,\upsilon_k} \end{bmatrix} + \begin{bmatrix} * & * \\ * & * \end{bmatrix}^\top \begin{bmatrix} Q & S \\ S^\top & R \end{bmatrix} \begin{bmatrix} 0 & I_{Nn_w} \\ C_{\sigma_k,\upsilon_k} & \mathcal{D}_{\sigma_k,\upsilon_k} \end{bmatrix}\right) \begin{bmatrix} \xi_k \\ w_k \end{bmatrix}\right] \\ &\quad \leq -\varepsilon\, \mathbb{E}\Big[\|w_k\|^2\Big], \end{aligned}$$

where the inequality follows from Lemma 6.1 and the non-strict LMI above because ξ_k and w_k are independent of σ_k by assumption. Summing over k up to $T \in \mathbb{N}_0$ results in

$$\sum_{k=0}^{T} \mathbb{E}\Big[\Delta V_k - s(w_k, z_k)\Big] = \mathbb{E}\Big[V(\xi_{T+1})\Big] - \sum_{k=0}^{T} \mathbb{E}\Big[s(w_k, z_k)\Big] \leq -\varepsilon \sum_{k=0}^{T} \mathbb{E}\Big[\|w_k\|^2\Big]$$

since $V(\xi_0) = 0$. In the limit for $T \to \infty$, this implies (6.7) because $\lim_{T\to\infty} \mathbb{E}\Big[V(\xi_{T+1})\Big] = 0$ by mean-square stability of $\mathcal{T}$. ■

The proof of Proposition 6.4 shows that the independence assumption on the input signal w is crucial, and that the current technique does not apply without it. Mirroring the discussion of Section 3.4.4, this potentially excludes the signals with worst-case gain, since they are derived from the state (ξ_k, σ_k). The ℓ_2-gain bounds derived from Proposition 6.4 are therefore *not* a generalization of Theorem 3.12 but rather the alternative BRL studied in Section 3.4.4 that is only applicable with deterministic inputs.

6.3. Decomposable Switched Jump Systems

Based on the results for general switched MJLS derived in the preceding section, the statements can now be specialized to decomposable jump systems, paralleling the developments of Chapter 3. We therefore introduce *decomposable switched MJLS* which are jump systems whose state-space representation is structured as

$$\begin{aligned} \mathcal{A}_{i,l} &= I_N \otimes \mathcal{A}_\mathrm{d} + S_i \otimes \mathcal{A}_\mathrm{c} + S_l^0 \otimes \mathcal{A}_\mathrm{p} \\ \mathcal{B}_{i,l} &= I_N \otimes \mathcal{B}_\mathrm{d} + S_i \otimes \mathcal{B}_\mathrm{c} + S_l^0 \otimes \mathcal{B}_\mathrm{p} \end{aligned}$$

$$C_{i,l} = I_N \otimes C_\mathrm{d} + S_i \otimes C_\mathrm{c} + S_l^0 \otimes C_\mathrm{p}$$
$$\mathcal{D}_{i,l} = I_N \otimes \mathcal{D}_\mathrm{d} + S_i \otimes \mathcal{D}_\mathrm{c} + S_l^0 \otimes \mathcal{D}_\mathrm{p}$$

with switched pattern matrices S_i and S_l^0 for $i \in \mathcal{K}$ and $l \in \mathcal{K}^0$. In particular, this chapter is focussed on systems with $S_i = L_i$ and $S_l^0 = L_l^0$, *i.e.* the switched Laplacian as pattern, and packet loss that satisfies Assumption 6.1. Additionally, the set of admissible nominal graphs is constrained by the following assumption:

Assumption 6.4.: Undirected and Connected Switched Graphs

The graphs $\mathcal{G}_l^0$ are undirected and connected for all $l \in \mathcal{K}^0$.

Because Assumption 6.4 stipulates that all switched nominal graphs are undirected, their Laplacians are necessarily symmetric. Consequently, the Laplacian eigenvalues are guaranteed to be real, and we can define

$$\lambda_1 \coloneqq \min_{l \in \mathcal{K}^0} \lambda_2\left(L_l^0\right) \qquad\qquad \lambda_\mathrm{u} \coloneqq \max_{l \in \mathcal{K}^0} \lambda_N\left(L_l^0\right)$$

as bounds on their joint spectrum. Note that the lower bound is minimized over the Fiedler eigenvalue λ_2 because λ_1 is trivially 0. In addition, Assumption 6.4 ensures all nominal graphs are connected such that $\lambda_1 > 0$ by Proposition 2.1. However, in contrast to the assumption of undirected nominal graphs, connectedness is imposed for notational convenience only and is not a prerequisite for establishing the results below.

6.3.1. Stability on Time-Varying Topologies

We start by considering the mean-square stability LMI of Theorem 6.2 for an arbitrary but fixed $l \in \mathcal{K}^0$. Importantly, notice that the condition is equivalent to the LMI (3.2) under this hypothesis, and that the simplifications proposed in Section 3.1 therefore remain applicable. In particular, by imposing the (conservative) structure $\mathcal{X} = I_N \otimes Y$ onto the Lyapunov variable, it is possible to isolate and eliminate the expectation $\sum_{j \in \mathcal{K}} \theta_j^l L_j = pL_l^0$ and generalized variance of the Laplacian given in (6.1) as the sole cause of randomness in the condition. For decomposable switched MJLS, we thus obtain

$$\begin{aligned}\left(I_N \otimes \mathcal{A}_\mathrm{d} + L_l^0 \otimes \left(p\mathcal{A}_\mathrm{c} + \mathcal{A}_\mathrm{p}\right)\right)^\top \left(I_N \otimes Y\right) \left(I_N \otimes \mathcal{A}_\mathrm{d} + L_l^0 \otimes \left(p\mathcal{A}_\mathrm{c} + \mathcal{A}_\mathrm{p}\right)\right) \\ + 2p(1-p)L_l^0 \otimes \left(\mathcal{A}_\mathrm{c}^\top Y \mathcal{A}_\mathrm{c}\right) \prec I_N \otimes Y \quad (6.9)\end{aligned}$$

as a sufficient condition for the LMI (6.4), which can be decoupled into modal constraints since there is only a single fixed pattern matrix involved. Finally, this leads to the following strengthening of Theorem 3.6:

Theorem 6.5.: Decomposed Switched Mean-Square Stability

A decomposable switched MJLS $\mathcal{T}$ with $L_{\upsilon_k}^0$ and L_{σ_k} as patterns and an interconnection topology that satisfies Assumptions 6.1 and 6.4 is mean-square stable if there exists a $Y \succ 0$ that solves the LMI (3.7) of Theorem 3.6 for $\lambda_i \in \{0, \lambda_\mathrm{u}\}$.

Proof. First, recall that the LMI (3.7) is convex in λ_i as outlined in the proof of Theorem 3.6, and therefore

$$\Big(\mathcal{A}_\mathrm{d} + \lambda(p\mathcal{A}_\mathrm{c} + \mathcal{A}_\mathrm{p})\Big)^\top Y \Big(\mathcal{A}_\mathrm{d} + \lambda(p\mathcal{A}_\mathrm{c} + \mathcal{A}_\mathrm{p})\Big) + 2p(1-p)\lambda\mathcal{A}_\mathrm{c}^\top Y\mathcal{A}_\mathrm{c} \prec Y \tag{6.10}$$

is satisfied for all $\lambda \in [0, \lambda_\mathrm{u}]$. Furthermore, by Assumptions 6.1 and 6.4 there exist orthogonal matrices U_l for $l \in \mathcal{K}^0$ which diagonalize the Laplacians L_l^0 as $U_l^\top L_l^0 U_l = \Lambda_l^0$, such that applying $U_l \otimes I_{n_\xi}$ as a congruence transformation to (6.9) decouples the LMI into modal constraint in the form of (6.10) with λ replaced by the eigenvalues of L_l^0. Since λ_u is an eigenvalue bound for all admissible Laplacians, this implies that $Y \succ 0$ solves (6.9) for all $l \in \mathcal{K}^0$, and thus by extension also (6.4), guaranteeing stability. ■

Theorem 6.5 establishes that the original decomposed mean-square stability condition of Theorem 3.6 is not only robust against uncertain constant nominal Laplacians L^0, but also covers IS with time-varying nominal topology that adheres to Assumption 6.4. Moreover, this extends to the mean-square consensus test of Theorem 3.7 if the LMI (3.8) is applied for λ_1 and λ_u instead of λ_2 and λ_N.

6.3.2. Calculating Robust H_2-Norm Bounds

In the same way as for the stability result above, the H_2-norm bound of Theorem 3.11 can be strengthened to encompass time-varying nominal topologies. The core idea is again to decompose the LMIs (6.6) for a fixed $l \in \mathcal{K}^0$ in tandem with using the convexity of the constraints to establish a solution for all admissible Laplacian eigenvalues.

Theorem 6.6.: Bounded Switched H_2-Norm (Hespe & Werner, 2023a)

A decomposable switched MJLS $\mathcal{T}$ with $L_{\upsilon_k}^0$ and L_{σ_k} as patterns and an interconnection topology that satisfies Assumptions 6.1 and 6.4 is mean-square stable and has H_2-norm less than $\gamma > 0$ if there exists a $Y \succ 0$ and symmetric Z_1, Z_2 with $\operatorname{tr} Z_1 + (N-1)\operatorname{tr} Z_2 < \gamma^2$ that solve the LMI (3.17a) of Theorem 3.11 for $\lambda_i \in \{0, \lambda_\mathrm{u}\}$ and furthermore satisfy the LMIs

$$\mathcal{B}_\mathrm{d}^\top Y \mathcal{B}_\mathrm{d} + \mathcal{D}_\mathrm{d}^\top \mathcal{D}_\mathrm{d} \prec Z_1 \tag{6.11a}$$

$$\bar{\mathcal{B}}_\lambda^\top Y \bar{\mathcal{B}}_\lambda + \bar{\mathcal{D}}_\lambda^\top \bar{\mathcal{D}}_\lambda + 2p(1-p)\lambda\Big(\mathcal{B}_\mathrm{c}^\top Y \mathcal{B}_\mathrm{c} + \mathcal{D}_\mathrm{c}^\top \mathcal{D}_\mathrm{c}\Big) \prec Z_2 \tag{6.11b}$$

with $\lambda \in \{\lambda_1, \lambda_\mathrm{u}\}$, where $\bar{\mathcal{B}}_\lambda$ denotes $\mathcal{B}_\mathrm{d} + \lambda(p\mathcal{B}_\mathrm{c} + \mathcal{B}_\mathrm{p})$, and analogously for $\bar{\mathcal{D}}_\lambda$.

Proof. As before, Assumptions 6.1 and 6.4 ensure that there exist orthogonal matrices U_l that diagonalize L_l^0 as $U_l^\top L_l^0 U_l = \Lambda_l^0$. Imposing the structure $\mathcal{X} = I_N \otimes Y$ into the Lyapunov variable, we repeat the simplification discussed in Section 3.4.1 for fixed $l \in \mathcal{K}^0$, followed by a congruence transformation with $U_l \otimes I_{n_\xi}$, to obtain

$$\begin{aligned}\Big(\mathcal{A}_\mathrm{d} + \lambda(p\mathcal{A}_\mathrm{c} + \mathcal{A}_\mathrm{p})\Big)^\top Y \Big(\mathcal{A}_\mathrm{d} + \lambda(p\mathcal{A}_\mathrm{c} + \mathcal{A}_\mathrm{p})\Big) \\ + \Big(C_\mathrm{d} + \lambda(pC_\mathrm{c} + C_\mathrm{p})\Big)^\top \Big(C_\mathrm{d} + \lambda(pC_\mathrm{c} + C_\mathrm{p})\Big) + 2p(1-p)\lambda\Big(\mathcal{A}_\mathrm{c}^\top Y \mathcal{A}_\mathrm{c} + C_\mathrm{c}^\top C_\mathrm{c}\Big) \prec Y\end{aligned}$$

for all eigenvalues λ of the Laplacian L_l^0 as a decomposed sufficient condition for the feasibility of (6.6a). Since this is a convex matrix-valued polynomial in λ (see the proof of

Theorem 3.11), (3.17a) ensures that Y solves the above LMI for all $\lambda \in [0, \lambda_u]$. Because l was arbitrary, $I_N \otimes Y$ therefore solves (6.6a) for all $l \in \mathcal{K}^0$. Furthermore, applying the same simplification on (6.6b) *without* imposing structure into $\mathcal{Z}_l$ results in

$$\begin{aligned}\left(I_N \otimes \mathcal{B}_d + L_l^0 \otimes \left(p\mathcal{B}_c + \mathcal{B}_p\right)\right)^\top \left(I_N \otimes Y\right) \left(I_N \otimes \mathcal{B}_d + L_l^0 \otimes \left(p\mathcal{B}_c + \mathcal{B}_p\right)\right) \\ + \left(I_N \otimes \mathcal{D}_d + L_l^0 \otimes \left(p\mathcal{D}_c + \mathcal{D}_p\right)\right)^\top \left(I_N \otimes \mathcal{D}_d + L_l^0 \otimes \left(p\mathcal{D}_c + \mathcal{D}_p\right)\right) \\ + 2p(1-p) L_l^0 \otimes \left(\mathcal{B}_c^\top Y \mathcal{B}_c + \mathcal{D}_c^\top \mathcal{D}_c\right) \prec \mathcal{Z}_l \quad (6.12)\end{aligned}$$

as a sufficient condition for (6.6b).

On the other hand, (6.11) imply that $\bar{\mathcal{Z}} \coloneqq \operatorname{diag}(Z_1, I_{N-1} \otimes Z_2)$ solves

$$\begin{aligned}\left(I_N \otimes \mathcal{B}_d + \Lambda \otimes \left(p\mathcal{B}_c + \mathcal{B}_p\right)\right)^\top \left(I_N \otimes Y\right) \left(I_N \otimes \mathcal{B}_d + \Lambda \otimes \left(p\mathcal{B}_c + \mathcal{B}_p\right)\right) \\ + \left(I_N \otimes \mathcal{D}_d + \Lambda \otimes \left(p\mathcal{D}_c + \mathcal{D}_p\right)\right)^\top \left(I_N \otimes \mathcal{D}_d + \Lambda \otimes \left(p\mathcal{D}_c + \mathcal{D}_p\right)\right) \\ + 2p(1-p) \Lambda \otimes \left(\mathcal{B}_c^\top Y \mathcal{B}_c + \mathcal{D}_c^\top \mathcal{D}_c\right) \prec \bar{\mathcal{Z}}\end{aligned}$$

for all diagonal matrices Λ such that

$$\Lambda \in \boldsymbol{\Lambda} \coloneqq \left\{\Lambda = \operatorname{diag}(0, \lambda_2, \lambda_3, \dots, \lambda_N) \,\middle|\, \lambda_i \in [\lambda_l, \lambda_u]\right\},$$

since (6.11b) is convex in λ. Since $\Lambda_l^0 \in \boldsymbol{\Lambda}$ for all $l \in \mathcal{K}^0$, a congruence transformation with $U_l \otimes I_{n_w}$ shows that $\mathcal{Z}_l \coloneqq (U_l \otimes I_{n_w}) \bar{\mathcal{Z}} (U_l \otimes I_{n_w})^\top$ solve (6.12), and thus in extension also (6.6b). Finally, $\operatorname{tr} \mathcal{Z}_l = \operatorname{tr} \bar{\mathcal{Z}} < \gamma^2$ for all $l \in \mathcal{K}^0$ because the trace is invariant under orthogonal transformations. ■

Similar to the mean-square stability result above, Theorem 6.6 shows that solving the LMI (3.17b) with uniform Z for all non-zero eigenvalues does not only provide robustness against uncertain nominal topologies as contemplated in Chapter 3 but encompasses time-varying topologies as well. Furthermore, since there is exactly one eigenvalue at 0 for each L_l^0 by Assumption 6.4, the modal constraint for $\lambda_1 = 0$ does not have to be considered in a robust fashion, leading to separate Z_1 and Z_2.

In contrast, we are unable to establish an equivalent result for the H_∞-norm bound of Theorem 3.13, since the switched quadratic performance specification considered above does only hold for stochastically independent input signals w. Instead, one could consider an alternative BRL as discussed in Section 3.4.4 as a special case of Proposition 6.4.

6.4. Simulated Switching Topologies

Finally, let us discuss an example that demonstrates how switching nominal topologies influence the H_2-norm of networked IS. As such, consider a group of 20 first-order integrators with inputs as introduced in Example 3.1 which are connected through the consensus protocol (2.9) and subject to switched interconnection structures as shown in

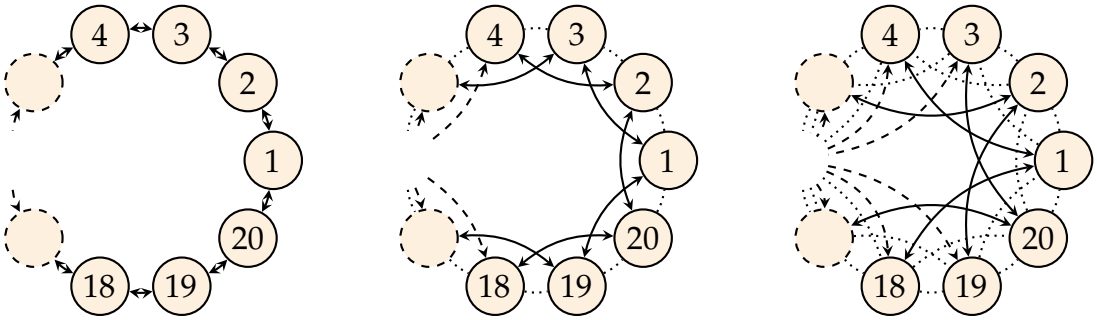

Figure 6.1.: Undirected circular graphs with $N = 20$ vertices and one, two, or three forward edges. The edges of the precursor graphs are dotted.

Fig. 6.1. Specifically, the nominal topology is switched between one of seven circular graphs, but in contrast to the graphs $\mathcal{G}_N^\circ$ that are presented in Section 2.1, each vertex has between one and seven forward and, due to the requirement that all graphs are undirected, an equal number of backward neighbours. The eigenvalue bounds for this set of topologies are $\lambda_l = 0.10$ and $\lambda_u = 18.24$.

To accurately assess the conservatism of Theorem 6.6, it is necessary to find the worst-case exogenous switching sequence v on the given set of graphs. Since this is a hard problem, we resort to estimating a lower bound on the H_2-norm instead by empirically approximating the performance of the closed-loop system for a variety of switching sequences through Monte-Carlo simulations. Among the selected v are those with constant value (and therefore constant topology), sequential switching between the graphs and randomly switched nominal graphs. This procedure is repeated for a grid of probabilities $p \in (0,1]$, and the span of norm bounds obtained in this way is shown in Fig. 6.2 together with the norm bound provided by Theorem 6.6. For each switching sequence and probability, ten realizations of the packet loss process are sampled in the Monte-Carlo simulation in order to estimate the H_2-norm.

The figure shows that the upper bound calculated via Theorem 6.6 approximates the best lower-bound obtained from the Monte-Carlo simulations reasonably well. A significant widening of the gap between the two bounds is only observed for transmission probability p close to 1. On the other hand, both bounds diverge for $p \to 0$, which mirrors the observation of Section 3.6.1 and is caused by the critical probability $p = 0$ at which the integrators cannot communicate and fail to converge.

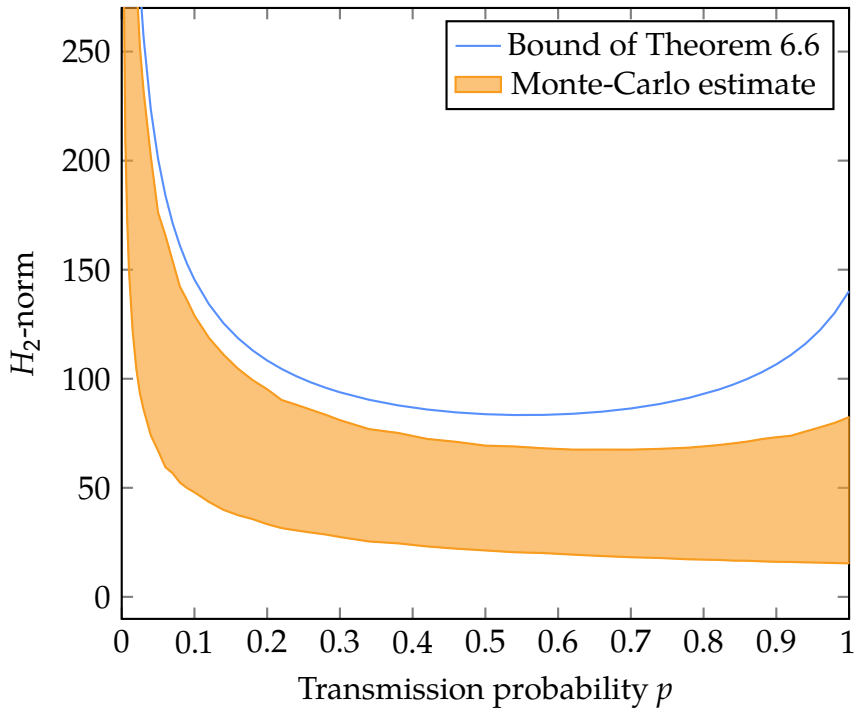

Figure 6.2.: H_2-Norm bounds for the first-order consensus problem with switching nominal topologies plotted over the transmission probability p. A robust upper bound is obtained from Theorem 6.6 and Monte-Carlo simulations are used to estimate the norm for different exogenous switching sequences v. (Hespe & Werner, 2023a)

A Note on Event-Triggered Control with Stochastic Communication

7

Given the digital nature of modern control architectures, sampled discrete-time systems, as considered in this dissertation, represent a logical choice of model (Chen & Francis, 1995). However, the regularly spaced sampling intervals with fixed rate studied above are not the only option for realizing a sampled control system. Instead, one can consider controllers that update in irregular intervals, leading to *aperiodic control*. A particular instance are the *event-triggered* controllers which we briefly review next.

In event-triggered control (ETC), the core idea is to update the controller only when necessary to preserve the desired performance criteria, and thus to reduce the number of samples taken. For this purpose, a trigger mechanism is implemented in addition to the controller, which determines the instances when an update is unavoidable. Early demonstrations of this concept were presented by Åarzén (1999) and Åström and Bernhardsson (1999) on simple linear control systems, with both works indicating that the event-based sampling leads to only minor reduction in closed-loop performance. This is especially relevant if the sensor, controller, and actuator are not co-located on the same device but rather connected through a communication network since the network bandwidth is often a scarce resource and reduced sampling does additionally lessen the demand for communication (Mazo & Tabuada, 2008). Nevertheless, it is not a given that event-triggered controllers will always outperform time-triggered ones. For example, Meister et al. (2022, 2023) show that periodic control is to be preferred for large networks of first-order integrators.

This general concept of ETC has since developed into a substantial body of literature. Importantly, there exist systematic tuning procedures for controllers meeting the desired criteria (*e.g.* Heemels et al., 2008; Tabuada, 2007) and techniques for co-design of controller and triggering mechanism (Abdelrahim et al., 2014; Meng & Chen, 2013). Furthermore, distributed event-triggers have been developed for integrators (Seyboth et al., 2013) as well as for general LTI (Hu & Liu, 2017) and LPV systems (Saadabadi & Werner, 2021), matching their controller counterpart. Evident questions that emerge in the context of this dissertation are therefore how ETC interacts with stochastic packet loss, and in particular how to combine both aspects during analysis to preserve previously obtained guarantees. Hence, the following sections study how these problems are approached in existing literature and investigate where difficulties arise compared to the periodic time-triggered case that has been considered before.

7.1. Fundamentals of Event-Triggered Control

Before discussing the interaction between the event-driven triggering mechanism and unreliable networks, let us first introduce the basic formalism that has been developed

to analyse ETC loops. In line with the rest of this dissertation, the focus will be on discrete-time LTI systems, and for the sake of simplicity only asymptotic stability is considered. A general introduction is provided by Heemels et al. (2012), but the most important concepts are reviewed below.

As such, consider an LTI system in the form of

$$x_{k+1} = Ax_k + Bu_k \qquad \forall\, k \in \mathbb{N}_0 \tag{7.1}$$

with state x_k and control input u_k, for which an event-triggered state-feedback controller is to be designed. Therefore, the state is sampled aperiodically by the controller at (yet to be determined) *trigger instants* $k_t \in \mathbb{N}_0$ such that $k_0 = 0$ and $k_{t+1} > k_t$, where $t \in \mathbb{N}_0$ is the triggering index. Between samples, the measurement is held constant, leading to

$$u_k = Kx_{k_t} \qquad \forall\, k \in \{k_t, \dots, k_{t+1} - 1\},\ \ t \in \mathbb{N}_0$$

with feedback matrix K. Next, define the *trigger error* e as

$$e_k \coloneqq x_{k_t} - x_k \qquad \forall\, k \in \{k_t, \dots, k_{t+1} - 1\},\ \ t \in \mathbb{N}_0,$$

which is a crucial element in the analysis of ETC schemes (Heemels et al., 2012). Inserting the control signal and the trigger error into the open-loop system (7.1), we obtain

$$x_{k+1} = Ax_k + BKx_{k_t} = \big(A + BK\big)x_k + BKe_k =: \mathcal{A}x_k + \mathcal{B}e_k$$

as the closed feedback loop, where $\mathcal{A}$ corresponds to the closed-loop under time-triggered control and the second term is a perturbation caused by the aperiodic triggering. Finally, a trigger mechanism is designed such that it ensures

$$\begin{bmatrix} x_k \\ e_k \end{bmatrix}^\top \Omega \begin{bmatrix} x_k \\ e_k \end{bmatrix} \leq 0 \qquad \text{with} \qquad \Omega = \begin{bmatrix} Q & S \\ S^\top & R \end{bmatrix} \qquad \text{and} \qquad Q \leq 0 \tag{7.2}$$

holds, *i.e.* the state is sampled at time k if the inequality would be violated otherwise, ensuring $e_k = 0$ and thus satisfaction of the condition (a rationale for the quadratic trigger mechanism is provided by Heemels et al., 2012). A particular choice of Ω is $Q = -\omega^2 I_{n_x}$, $S = 0$ and $R = I_{n_x}$, resulting in the condition $\|e_k\| \leq \omega \|x_k\|$ for all $k \in \mathbb{N}_0$.

Based on this formulation of the closed-loop system, asymptotic stability can now be proven by finding a valid Lyapunov function. Introducing the candidate function $V(x) = x^\top \mathcal{X} x$ with $\mathcal{X} > 0$, a sufficient stability condition is therefore that its increment

$$V(x_{k+1}) - V(x_k) = \begin{bmatrix} x_k \\ e_k \end{bmatrix}^\top \begin{bmatrix} \mathcal{A}^\top \mathcal{X} \mathcal{A} - \mathcal{X} & \mathcal{A}^\top \mathcal{X} \mathcal{B} \\ \mathcal{B} \mathcal{X} \mathcal{A} & \mathcal{B}^\top \mathcal{X} \mathcal{B} \end{bmatrix} \begin{bmatrix} x_k \\ e_k \end{bmatrix}$$

is negative along trajectories of the system, *i.e.* for all $x_k \neq 0$ and e_k such that (7.2) holds. Using the S-procedure (Boyd et al., 1994, p. 24), this is guaranteed if there exists a multiplier $\tau \geq 0$ such that

$$\begin{bmatrix} \mathcal{A}^\top \mathcal{X} \mathcal{A} - \mathcal{X} & \mathcal{A}^\top \mathcal{X} \mathcal{B} \\ \mathcal{B} \mathcal{X} \mathcal{A} & \mathcal{B}^\top \mathcal{X} \mathcal{B} \end{bmatrix} \prec \tau \Omega \tag{7.3}$$

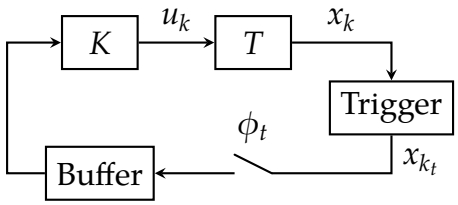

(a) Buffer only updated if the transmission is successful

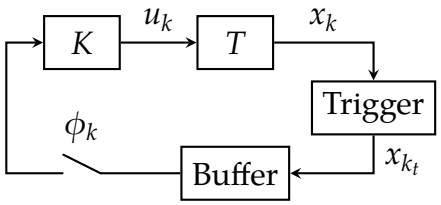

(b) Continuous retransmission of buffer contents

Figure 7.1.: Two different models that represent how ETC and an unreliable network interact. The output of the buffer is held constant until a new value is received.

holds, and we can furthermore absorb the multiplier in the Lyapunov matrix X by imposing $\tau > 0$. As such, the controller K with trigger mechanism (7.2) is asymptotically stabilizing the LTI system (7.1) if there exists an $X > 0$ that solves the LMI (7.3) with $\tau = 1$. Finally, as presented by Golabi et al. (2016) and Meng and Chen (2013), it is possible to derive a co-design procedure for K and the trigger mechanism along the lines of Section 4.1.

Although the preceding discussion refers to a specific form of ETC for LTI systems, the fundamental idea of imposing a weakened bound on the Lyapunov function increment as in (7.3) remains applicable in more general settings (Heemels et al., 2012). For example, Girard (2015) has shown that it is sufficient to enforce the invariant (7.2) in average instead of all $k \in \mathbb{N}_0$, leading to a dynamic trigger mechanism which can further reduce the number of required samples. Moreover, it is possible to substitute the state-based controller and trigger mechanism presented above by output-based versions (see Heemels et al., 2012, for a brief survey).

7.2. Triggering Mechanisms for Unreliable Networks

Having introduced the basic principles of ETC, we look at the difficulties that arise if an event-triggered controller is implemented over an unreliable communication network as shown in Fig. 7.1. Next to the trigger mechanism, there is a switching element controlled by the sequence ϕ, which can either be a deterministic signal or a stochastic process, and an explicit buffer that holds its output constant until a new input is received. Two distinct formulations regarding the interaction between the trigger and the network can be identified in the literature: The first formulation, illustrated in Fig. 7.1a, considers a scenario in which the trigger mechanism is not only responsible for determining sampling instances but also for when information is transmitted over the network. Consequently, if a transmission is lost, the buffer is held constant and the controller cannot be updated until the next trigger instant. Note that this implies that the controller cannot distinguish between time steps where the trigger decided not to sample and steps in which the state was sampled but the transmission failed. In Fig. 7.1b, on the other hand, the trigger mechanism does only control the sampling and the buffer contents are continuously transmitted. As such, the output of the controller is zeroed if a packet is lost, but the information is available in the next step $k \in \mathbb{N}_0$. Similar transmission modes are also known for time-triggered IS (Datar et al., 2018; Schenato, 2009).

Generally, the issues which occur due to the interplay of ETC and unreliable communication are that the trigger mechanism and controller can become desynchronized, *i.e.* the last *transmitted* signal might be different from the last *received* value, and that a controller update cannot be guaranteed even if an event is triggered. Of course, the characteristics of both issues depend on the kind of network model that is imposed, *i.e.* deterministic or stochastic losses, and also on whether the setup of Fig. 7.1a or Fig. 7.1b is considered. The following sections will therefore discuss several approaches that have been proposed in the literature for the respective kinds of models.

7.2.1. Deterministic Worst-Case Analysis

The first scenario we consider is of deterministic nature and follows the setup of Fig. 7.1a, *i.e.* information that fails to transmit is permanently lost. Because of the worst-case perspective that has to be taken during analysis in this case, it is necessary to impose a bound on the *maximum allowable number of successive packet dropouts* to ensure that the trigger mechanism is eventually able to communicate with the controller.

For systems with a single communication link, Dolk and Heemels (2017) consider two special cases within the given scenario. First, they assume that the controller is able to provide acknowledgements to the trigger mechanism for packets that have been successfully received, such that the trigger has perfect knowledge of the information available to the controller and can therefore accurately determine the current trigger error e_k. On the other hand, if no such acknowledgements are possible, the authors propose to simulate multiple scenarios for varying numbers of successively dropped packets, which can be done exhaustively because the number of admissible scenarios is bounded by assumption. Similarly, Guinaldo et al. (2012) and Zhao and Hua (2024) discuss MAS scenarios with acknowledgements, where the former approach relies on converting the unreliable transmissions into an artificial delay which is taken into account in the design of the controller and trigger mechanism, and the latter employs hybrid system modelling.

The main limitation of the above approaches lies in the bounded number of successively dropped packets. While this assumption is necessary for the worst-case analysis, it can be overly conservative since wireless communication networks are inherently random (see Section 2.3) and successful transmissions can therefore never be guaranteed. Consequently, the stochastic approaches that are discussed next are more suitable.

7.2.2. Stochastic Online Trigger Error Estimation

In accordance with the overarching theme of this dissertation, the second type of network model that will be considered is of a random nature, and the switching sequence $\{\phi_k\}$ is a stochastic process. As such, the worst-case stability guarantees that were outlined in the preceding section are superseded by weaker almost sure or mean-square stability results which take advantage of available knowledge about the loss distribution.

Generally speaking, the probabilistic approaches follow similar Lyapunov arguments as employed in Section 7.1 to prove asymptotic stability of the closed ETC loop. Given a candidate function $V(x) = x^\top \mathcal{X} x$ with $\mathcal{X} \succ 0$, mean-square stability follows if

$$\mathbb{E}\Big[V(x_{k+1}) - V(x_k)\Big] < 0$$

holds for all non-zero x_k. In order to establish a weakened convergence condition such as (7.3), it is therefore often sufficient to satisfy the trigger invariant (given by (7.2) in the example above) in expectation, rather than enforcing it for every admissible realization of the system trajectories. However, the trigger mechanism is only capable of measuring a single realization of the system trajectory since it is observing the physical plant, and thus estimating the mean-square trigger error $\mathbb{E}\left[\|e_k\|^2\right]$ presents a significant challenge.

One potential solution to this issue is to implement an *online* (meaning co-located with the trigger mechanism) estimator for the expected trigger error as presented by Viel et al. (2022) for MAS with homogeneous Bernoulli packet loss (see Assumption 3.4). Analogous to the multi-scenario simulations of Dolk and Heemels (2017) in the deterministic case above, they propose to estimate $\mathbb{E}\left[\|e_k\|^2\right]$ by predicting the state trajectory for different realizations of the loss process, and rely on acknowledgements to prune the resulting scenario tree. Importantly, the authors are able to bound the number of necessary simulated realizations despite imposing no bound on the number of successively lost transmissions, preventing potentially unbounded computational requirements.

Nevertheless, the online estimator leads to a significantly increased complexity of the trigger mechanism compared to the idealized lossless case. A much more desirable outcome would be controllers and trigger mechanisms that inherit the existing structure of their lossless counterparts but are retuned or augmented to account for the stochastic communication, just like the time-triggered controllers synthesized in Chapter 4.

7.3. Stochastic Offline Trigger Error Modelling

In addition to the techniques that have been discussed in Section 7.2, there exists a class of trigger mechanisms for unreliable networks that takes an entirely different approach. Instead of modifying the trigger to accommodate for lost information, the available knowledge about the transmission network is taken into account during synthesis to retune a standard ETC loop. This has the obvious advantage of requiring no extra *online* complexity in the controller or trigger mechanism, but poses challenges during the *offline* synthesis phase, especially if a network model as shown in Fig. 7.1a is considered.

7.3.1. Trigger Mechanisms with Continuous Retransmission

Let us first explore ETC loops in which the trigger mechanism only controls the sampling of the plant state but not the transmission network, which is the setup depicted in Fig. 7.1b. Since the buffer is directly adjacent to the trigger, it can be updated reliably and $\hat{x}_k = x_{k_t}$ for $k \in \{k_t, \dots, k_{t+1} - 1\}$, such that the fallible network only affects the controller itself. For systems with a single transmission link, this results in the control signal

$$u_k = \phi_k K \hat{x}_k = \phi_k K x_{k_t} \qquad \forall\, k \in \{k_t, \dots, k_{t+1} - 1\},\ \ t \in \mathbb{N}_0 \tag{7.4}$$

with the stochastic process $\{\phi_k\}$, such that we obtain the closed-loop system

$$x_{k+1} = Ax_k + \phi_k BK x_{k_t} = \big(A + \phi_k BK\big)x_k + \phi_k BK e_k$$

by recalling the definition of the trigger error e_k. Note that the closed loop corresponds to an MJLS with switching process $\sigma_k := \phi_k + 1$ and mode-dependent matrices

$$\mathcal{A}_1 = A \qquad \mathcal{A}_2 = A + BK \qquad \mathcal{B}_1 = 0 \qquad \mathcal{B}_2 = BK \tag{7.5}$$

if $\{\phi_k\}$ satisfies Assumptions 2.3 and 2.4, thereby enabling the extensive body of literature to be employed for analysis.

A proof of mean-square stability can now be approached along the lines of Section 7.1. With Lyapunov function candidate $V(x)$ as introduced above, the system is mean-square stable if there exist an $\mathcal{X} \succ 0$ such that

$$\mathbb{E}\Big[V(x_{k+1}) - V(x_k)\Big] = \mathbb{E}\left[\begin{bmatrix} x_k \\ e_k \end{bmatrix}^\top \begin{bmatrix} \mathcal{A}_{\sigma_k}^\top \mathcal{X} \mathcal{A}_{\sigma_k} - \mathcal{X} & \mathcal{A}_{\sigma_k}^\top \mathcal{X} \mathcal{B}_{\sigma_k} \\ \mathcal{B}_{\sigma_k} \mathcal{X} \mathcal{A}_{\sigma_k} & \mathcal{B}_{\sigma_k}^\top \mathcal{X} \mathcal{B}_{\sigma_k} \end{bmatrix} \begin{bmatrix} x_k \\ e_k \end{bmatrix}\right] \overset{\text{(a)}}{<} \mathbb{E}\left[\begin{bmatrix} x_k \\ e_k \end{bmatrix}^\top \Omega \begin{bmatrix} x_k \\ e_k \end{bmatrix}\right] \overset{\text{(b)}}{\leq} 0$$

holds for all non-zero x_k. Assuming that $\{\phi_k\}$ is a Bernoulli process, *i.e.* ϕ_k and $\phi_{k'}$ are independent if $k \neq k'$, σ_k is independent of all preceding samples and hence of x_k and e_k due to causality. Accordingly, Lemma 6.1 implies that inequality (a) is satisfied if $\mathcal{X}$ solves

$$\mathbb{E}\begin{bmatrix} \mathcal{A}_\sigma^\top \mathcal{X} \mathcal{A}_\sigma - \mathcal{X} & \mathcal{A}_\sigma^\top \mathcal{X} \mathcal{B}_\sigma \\ \mathcal{B}_\sigma \mathcal{X} \mathcal{A}_\sigma & \mathcal{B}_\sigma^\top \mathcal{X} \mathcal{B}_\sigma \end{bmatrix} \prec \Omega. \tag{7.6}$$

Furthermore, the trigger invariant (7.2) can be enforced for all realizations of $\{\phi_k\}$ due to the reliable buffer update, ensuring that the non-strict inequality (b) holds. Feasibility of the LMI (7.6) is therefore a sufficient condition for mean-square stability of the closed-loop system, closely resembling condition (7.3) from the lossless case with $\tau = 1$.

In the literature, ETC schemes that adhere to the communication model of Fig. 7.1b have been considered especially in the context of MAS. The simplest case is presented by Ma and Qiao (2016) and Wang et al. (2021), who assume that there exists a Bernoulli process $\{\phi_k\}$ that controls the status of the entire network, *i.e.* $\phi_k^{ij} = \phi_k$ for all edges $(i, j) \in \mathcal{E}^0$, and thus that all transmission either succeed or fail unanimously. In contrast, Chen et al. (2018) discuss a scenario in which there is one loss process *per agent* such that $\phi_k^{ij} = \phi_k^i$, but additionally impose that all processes have identical failure probability. Furthermore, Li et al. (2014) and Saadabadi et al. (2022) study event-triggered first-order consensus problems that are subject to homogeneous Bernoulli packet loss as described in Assumption 3.4, meaning that each edge can fail individually with uniform probability.

Ultimately, the disadvantage of the approach presented in this section lies in the limited applicability of the network model with continuous retransmission of the buffer contents as illustrated in Fig. 7.1b. Given that the fundamental objective of ETC is to conserve energy and optimize network usage, it would be more logical to utilize the trigger mechanism to determine both sampling instances *and* transmissions times, rather than reverting to a time-triggered scheme for the latter. Nevertheless, should periodic transmissions become necessary within a particular scenario, the aforementioned approaches offer compelling solutions since they require only minimal modifications compared to the lossless case.

7.3.2. Controller-Side Transmission Buffering

A superior model for ETC schemes with unreliable communication than continuous retransmission is to include a controller-side buffer as illustrated in Fig. 7.1a. This scenario has served as the foundation for all the approaches discussed in Section 7.2 but poses additional challenges when compared to the previously considered trigger-side buffer. Nevertheless, the first step is the same as before, namely to derive a suitable switched system description for the unreliable ETC loop which we adapt from the model proposed by Hu et al. (2021) and Zhao et al. (2022).

As such, we introduce a stochastic process $\{\phi_t\}$ taking values in $\{0,1\}$ which, different from above, is defined only at the trigger instants k_t since the network only attempts to transmit when the trigger detects an event. Furthermore, define a continuation $\{\bar{\phi}_k\}$ for $\{\phi_t\}$ that extends the previous process to all $k \in \mathbb{N}_0$ by persisting its value, *i.e.*

$$\bar{\phi}_k \coloneqq \phi_t \qquad \forall\, k \in \{k_t, \dots, k_{t+1} - 1\},\ \ t \in \mathbb{N}_0.$$

For the buffer, we assume that it has no information about the plant at the beginning and is therefore initialized with $\hat{x}_0 = 0$. Its update at the trigger instants k_t is then

$$\hat{x}_{k_t+1} = \phi_t x_{k_t} + (1 - \phi_t)\hat{x}_{k_t},$$

taking on the current state of the plant if the transmission is successful ($\phi_t = 1$) and keeping its previous value in case it failed ($\phi_t = 0$). At all other times k, the network will never transmit and the buffer is thus guaranteed to preserve its value, *i.e.* $\hat{x}_{k+1} = \hat{x}_k$ for all $k \in \mathbb{N}_0 \setminus \{k_0, k_1, \dots\}$. Combining both cases, the buffer dynamics are given by

$$\hat{x}_{k+1} = \bar{\phi}_k(x_k + e_k) + (1 - \bar{\phi}_k)\hat{x}_k$$

with trigger error e_k as introduced in Section 7.1. Note that even though $\hat{x}_k$ appears to change value for every k if $\bar{\phi}_k = 1$ because it depends on x_k, the definition of e_k ensures that the buffer stays constant between trigger instants.

Having described the buffer in sufficient detail, we are now able to close the loop through the state-feedback gain K. To avoid an artificial delay in the loop, we assume that the buffer is transparent to the controller, *i.e.* a successful transmission is passed to the controller immediately and the buffered signal is only used between trigger instants or if a transmission failed. This leads to the control input

$$u_k = \bar{\phi}_k K(x_k + e_k) + (1 - \bar{\phi}_k)K\hat{x}_k,$$

which has an extra term compared to (7.4) because of the controller-side buffering. Stacking the plant and buffer states as $\xi_k^\top \coloneqq \begin{bmatrix} x_k^\top & \hat{x}_k^\top \end{bmatrix}$, we obtain the closed-loop system

$$\xi_{k+1} = \begin{bmatrix} A + \bar{\phi}_k BK & (1 - \bar{\phi}_k)BK \\ \bar{\phi}_k I_{n_x} & (1 - \bar{\phi}_k)I_{n_x} \end{bmatrix} \xi_k + \begin{bmatrix} \bar{\phi}_k BK \\ \bar{\phi}_k I_{n_x} \end{bmatrix} e_k$$

with the trigger error e_k as input. In the same way as the unbuffered scenario above, this takes the form of a stochastic jump system $\xi_{k+1} = \mathcal{A}_{\sigma_k}\xi_k + \mathcal{B}_{\sigma_k}e_k$ with switching process $\{\sigma_k\}$ defined by $\sigma_k \coloneqq \bar{\phi}_k + 1$ and matrices

$$\mathcal{A}_1 = \begin{bmatrix} A & BK \\ 0 & I_{n_x} \end{bmatrix} \qquad \mathcal{A}_2 = \begin{bmatrix} A + BK & 0 \\ I_{n_x} & 0 \end{bmatrix} \qquad \mathcal{B}_1 = \begin{bmatrix} 0 \\ 0 \end{bmatrix} \qquad \mathcal{B}_2 = \begin{bmatrix} BK \\ I_{n_x} \end{bmatrix}. \tag{7.7}$$

Based on the similarity of the closed-loop system representations (7.5) and (7.7), one might expect that mean-square stability can be established by following the remaining steps of Section 7.3.1. However, there is a fundamental difference between the two cases due to the buffering: The continuation argument involving $\{\bar{\phi}_k\}$ implies that samples of $\{\sigma_k\}$ are generally *not* independent for different times k even if the underlying $\{\phi_k\}$ is assumed to be a Bernoulli process, contrasting the scenario of the preceding section (Hu et al., 2021). More specifically, all samples of $\{\sigma_k\}$ between two consecutive trigger instants are identical but independent of samples associated with the preceding or succeeding k_t. Consequently, $\{\sigma_k\}$ is a Markov chain that is not homogeneous, *i.e.* it violates Assumption 2.4. This is due to the fact that its transition probabilities

$$\mathbb{P}\big(\sigma_{k+1} = 2 \,\big|\, \sigma_k = 2\big) = \begin{cases} p & \text{if } \exists t \in \mathbb{N}_0 : k+1 = k_t, \\ 1 & \text{else,} \end{cases} \tag{7.8a}$$

$$\mathbb{P}\big(\sigma_{k+1} = 2 \,\big|\, \sigma_k = 1\big) = \begin{cases} p & \text{if } \exists t \in \mathbb{N}_0 : k+1 = k_t, \\ 0 & \text{else} \end{cases} \tag{7.8b}$$

and their respective complements are switched based on whether the next time step is a trigger instant k_t, as determined by the trigger mechanism.

The stochastic dependency of the switching process across time steps means that the approach of Chapter 6 and Section 7.3.1 cannot be applied since Lemma 6.1 requires the dynamic state ξ_k to be independent of the chain state σ_k. Instead, we employ a switched Lyapunov function candidate $V(\xi, i) = \xi^\top \mathcal{X}_i \xi$ on the joint dynamic and Markov chain state with $\mathcal{X}_i > 0$, $\xi \in \mathbb{R}^{n_\xi}$, and $i \in \mathcal{K} = \{1, 2\}$ as proposed by Seiler and Sengupta (2003). Using $\mathcal{F}_k$ to denote all information available about the stochastic processes up to time k, *i.e.* $\{\sigma_0, \sigma_1, \dots, \sigma_k\}$, the expected Lyapunov increment can be calculated as

$$\begin{aligned}
\mathbb{E}\big[\Delta V_k \,\big|\, \mathcal{F}_k\big] &= \mathbb{E}\big[V(\xi_{k+1}, \sigma_{k+1}) - V(\xi_k, \sigma_k) \,\big|\, \mathcal{F}_k\big] \\
&= \mathbb{E}\big[\xi_{k+1}^\top \mathcal{X}_{\sigma_{k+1}} \xi_{k+1} - \xi_k^\top \mathcal{X}_{\sigma_k} \xi_k \,\big|\, \mathcal{F}_k\big] \\
&= \mathbb{E}\big[(\mathcal{A}_{\sigma_k}\xi_k + \mathcal{B}_{\sigma_k} e_k)^\top \mathcal{X}_{\sigma_{k+1}} (\mathcal{A}_{\sigma_k}\xi_k + \mathcal{B}_{\sigma_k} e_k) - \xi_k^\top \mathcal{X}_{\sigma_k} \xi_k \,\big|\, \mathcal{F}_k\big] \\
&= \begin{bmatrix} \xi_k \\ e_k \end{bmatrix}^\top \begin{bmatrix} \mathcal{A}_{\sigma_k}^\top \mathbb{E}[\mathcal{X}_{\sigma_{k+1}} \,|\, \mathcal{F}_k] \mathcal{A}_{\sigma_k} - \mathcal{X}_{\sigma_k} & \mathcal{A}_{\sigma_k}^\top \mathbb{E}[\mathcal{X}_{\sigma_{k+1}} \,|\, \mathcal{F}_k] \mathcal{B}_{\sigma_k} \\ \mathcal{B}_{\sigma_k}^\top \mathbb{E}[\mathcal{X}_{\sigma_{k+1}} \,|\, \mathcal{F}_k] \mathcal{A}_{\sigma_k} & \mathcal{B}_{\sigma_k}^\top \mathbb{E}[\mathcal{X}_{\sigma_{k+1}} \,|\, \mathcal{F}_k] \mathcal{B}_{\sigma_k} \end{bmatrix} \begin{bmatrix} \xi_k \\ e_k \end{bmatrix},
\end{aligned}$$

and, based on the aforementioned switched transition probabilities, the expectation of the next Lyapunov matrix is given by

$$\mathbb{E}\big[\mathcal{X}_{\sigma_{k+1}} \,\big|\, \mathcal{F}_k\big] = \mathbb{E}\big[\mathcal{X}_{\sigma_{k+1}} \,\big|\, \sigma_k\big] = \begin{cases} \bar{\mathcal{X}} & \text{if } \exists t \in \mathbb{N}_0 : k+1 = k_t, \\ \mathcal{X}_{\sigma_k} & \text{else,} \end{cases}$$

where $\bar{\mathcal{X}} := (1-p)\mathcal{X}_1 + p\mathcal{X}_2$.

The remaining steps can then be applied in similar fashion as before. The essential idea is to ensure that the decrease condition $\mathbb{E}\big[\Delta V_k \,\big|\, \mathcal{F}_k\big] < 0$ holds for all $\xi_k \neq 0$, $\sigma_k \in \mathcal{K}$, and input signals e_k that satisfy the augmented trigger invariant

$$\begin{bmatrix} \xi_k \\ e_k \end{bmatrix}^\top \bar{\Omega} \begin{bmatrix} \xi_k \\ e_k \end{bmatrix} \leq 0 \qquad \text{with} \qquad \bar{\Omega} := \begin{bmatrix} Q & 0 & S \\ 0 & 0 & 0 \\ S^\top & 0 & R \end{bmatrix} \tag{7.9}$$

with Q, S, and R as defined for Ω in (7.2). Note that the zero pattern of $\bar{\Omega}$ ensures that the invariant can be enforced by the trigger mechanism since it does not have access to the state $\hat{x}_k$ of the buffer. Utilizing the S-procedure, a sufficient condition for the desired decrease is that $\mathcal{X}_i > 0$ solve the LMIs

$$\begin{bmatrix} \mathcal{A}_i^\top \bar{\mathcal{X}} \mathcal{A}_i - \mathcal{X}_i & \mathcal{A}_i^\top \bar{\mathcal{X}} \mathcal{B}_i \\ \mathcal{B}_i^\top \bar{\mathcal{X}} \mathcal{A}_i & \mathcal{B}_i^\top \bar{\mathcal{X}} \mathcal{B}_i \end{bmatrix} \prec \bar{\Omega} \qquad \begin{bmatrix} \mathcal{A}_i^\top \mathcal{X}_i \mathcal{A}_i - \mathcal{X}_i & \mathcal{A}_i^\top \mathcal{X}_i \mathcal{B}_i \\ \mathcal{B}_i^\top \mathcal{X}_i \mathcal{A}_i & \mathcal{B}_i^\top \mathcal{X}_i \mathcal{B}_i \end{bmatrix} \prec \bar{\Omega} \tag{7.10}$$

for $i \in \mathcal{K}$, where the first LMI corresponds to times $k+1$ that are trigger instants k_t and the second to $k+1$ that are not. Mean-square stability would then follow from the telescoping sum

$$\mathbb{E}\Big[V(\xi_{T+1})\Big] - V(\xi_0) = \sum_{k=0}^{T} \mathbb{E}\Big[\Delta V_k\Big] = \sum_{k=0}^{T} \mathbb{E}\Big[\mathbb{E}[\Delta V_k \mid \mathcal{F}_k]\Big] \leq -\varepsilon \sum_{k=0}^{T} \mathbb{E}\Big[\|\xi_k\|^2\Big]$$

for some $\varepsilon > 0$ (*cf.* Theorem 6.2) along admissible trajectories of the system.

Because the trigger instants k_t have been abstracted away in the closed-loop system (7.7), the LMIs (7.10) had to be formulated in a robust, trigger-agnostic manner. That is, regardless of whether the trigger mechanism detects an event at time $k+1$, the expected Lyapunov increment $\mathbb{E}\Big[\Delta V_k \,\Big|\, \mathcal{F}_k\Big]$ is guaranteed to be negative. However, this leads to a fundamental issue in the above LMIs, which becomes apparent by considering the scenario where the next step is *not* a trigger instant, *i.e.* $k+1 \neq k_t$, and the last transmission failed such that $\sigma_k = 1$. By inserting (7.7) into the right LMI of (7.10) with $i = 1$, we therefore obtain

$$\begin{bmatrix} \mathcal{A}_1^\top \mathcal{X}_1 \mathcal{A}_1 - \mathcal{X}_1 & 0 \\ 0 & 0 \end{bmatrix} \prec \bar{\Omega} \qquad \Rightarrow \qquad \mathcal{A}_1^\top \mathcal{X}_1 \mathcal{A}_1 - \mathcal{X}_1 \prec \begin{bmatrix} Q & 0 \\ 0 & 0 \end{bmatrix} \leq 0$$

from the Schur complement, such that any $\mathcal{X}_1$ that solves (7.10) must also satisfy the right-hand side LMI, which corresponds to the standard Lyapunov inequality (2.3) of Theorem 2.2. On the other hand, such a solution cannot exist since $\mathcal{A}_1$ has at least one eigenvalue at 1 due to the buffer, implying that the LMIs are infeasible regardless of which system, controller, trigger invariant, or transmission probability are considered. Furthermore, even if the buffer state is neglected, the plant is running in open loop within $\mathcal{A}_1$, rendering the method inapplicable for systems that require feedback for stabilization.

The core problem has already been identified in the preceding paragraph. Since the trigger mechanism has been abstracted away in the closed loop, the above analysis is stabilizing arbitrary trigger sequences including those with only finitely many trigger instants. This has not been an issue in previous setups where the control input u_k is derived directly from the sampled plant state x_{k_t} but is troublesome now due to the buffering, creating a scenario in which $\hat{x}_k$ is never updated again, and thus not asymptotically stable. These findings indicate that the trigger-agnostic approach of the derivation above is too conservative to yield a useful stability test for the ETC scheme with controller-side buffering.

7.3.3. A Critical View on Implicit Independence Assumptions

In the articles that originally proposed the reformulation of an unreliable ETC loop with controller-side buffering into the switched system (7.7), Hu et al. (2021) and Zhao et al.

(2022) suggest taking a different approach for analysing the closed-loop than described in the preceding section, which we will briefly discuss in the following.

Their proposal is to introduce the Lyapunov function candidate $V(\xi) = \xi^\top \mathcal{X} \xi$ that does not depend on the Markov chain state $i \in \mathcal{K}$, contrasting the candidate function of Section 7.3.2. To calculate the expected Lyapunov increment, it is then assumed that ξ_k and e_k are given (Hu et al., 2021, only consider ξ_k to be fixed), resulting in

$$\begin{aligned}\mathbb{E}\Big[\Delta V_k \,\Big|\, \xi_k, e_k\Big] &= \mathbb{E}\Big[V(\xi_{k+1}) - V(\xi_k) \,\Big|\, \xi_k, e_k\Big] \\ &= \mathbb{E}\Big[(\mathcal{A}_{\sigma_k}\xi_k + \mathcal{B}_{\sigma_k} e_k)^\top \mathcal{X}(\mathcal{A}_{\sigma_k}\xi_k + \mathcal{B}_{\sigma_k} e_k) - \xi_k^\top \mathcal{X} \xi_k \,\Big|\, \xi_k, e_k\Big] \\ &= \begin{bmatrix}\xi_k \\ e_k\end{bmatrix}^\top \mathbb{E}\left[\begin{bmatrix}\mathcal{A}_{\sigma_k}^\top \mathcal{X} \mathcal{A}_{\sigma_k} - \mathcal{X} & \mathcal{A}_{\sigma_k}^\top \mathcal{X} \mathcal{B}_{\sigma_k} \\ \mathcal{B}_{\sigma_k}^\top \mathcal{X} \mathcal{A}_{\sigma_k} & \mathcal{B}_{\sigma_k}^\top \mathcal{X} \mathcal{B}_{\sigma_k}\end{bmatrix} \middle| \, \xi_k, e_k\right] \begin{bmatrix}\xi_k \\ e_k\end{bmatrix} \end{aligned} \tag{7.11}$$

as a partial evaluation of the involved conditional expectation. Furthermore, notice that the switched matrices can be expressed as

$$\begin{aligned}\mathcal{A}_{\sigma_k} &= (2 - \sigma_k)\mathcal{A}_1 + (\sigma_k - 1)\mathcal{A}_2 \\ \mathcal{B}_{\sigma_k} &= (\sigma_k - 1)\mathcal{B}_2\end{aligned}$$

since $\mathcal{K}$ has only two elements, explicitly pulling out the switching process $\{\sigma_k\}$. The entries of the central matrix of (7.11) are thus given by

$$\begin{aligned}\mathbb{E}\Big[\mathcal{A}_{\sigma_k}^\top \mathcal{X} \mathcal{A}_{\sigma_k} - \mathcal{X} \,\Big|\, \xi_k, e_k\Big] = \mathbb{E}\Big[(2 - \sigma_k)^2 \,\Big|\, \xi_k, e_k\Big]\mathcal{A}_1^\top \mathcal{X} \mathcal{A}_1 + \mathbb{E}\Big[(\sigma_k - 1)^2 \,\Big|\, \xi_k, e_k\Big]\mathcal{A}_2^\top \mathcal{X} \mathcal{A}_2 \\ + \mathbb{E}\Big[(2 - \sigma_k)(\sigma_k - 1) \,\Big|\, \xi_k, e_k\Big]\Big(\mathcal{A}_1^\top \mathcal{X} \mathcal{A}_2 + \mathcal{A}_2^\top \mathcal{X} \mathcal{A}_1\Big) - \mathcal{X}\end{aligned}$$

for the top-left block, and

$$\begin{aligned}\mathbb{E}\Big[\mathcal{A}_{\sigma_k}^\top \mathcal{X} \mathcal{B}_{\sigma_k} \,\Big|\, \xi_k, e_k\Big] &= \mathbb{E}\Big[(2 - \sigma_k)(\sigma_k - 1) \,\Big|\, \xi_k, e_k\Big]\mathcal{A}_1^\top \mathcal{X} \mathcal{B}_2 + \mathbb{E}\Big[(\sigma_k - 1)^2 \,\Big|\, \xi_k, e_k\Big]\mathcal{A}_2^\top \mathcal{X} \mathcal{B}_2 \\ \mathbb{E}\Big[\mathcal{B}_{\sigma_k}^\top \mathcal{X} \mathcal{B}_{\sigma_k} \,\Big|\, \xi_k, e_k\Big] &= \mathbb{E}\Big[(\sigma_k - 1)^2 \,\Big|\, \xi_k, e_k\Big]\mathcal{B}_2^\top \mathcal{X} \mathcal{B}_2\end{aligned}$$

for the cross terms and the bottom-right component. Importantly, this formulation isolates the expectation from the system matrices such that only the switching process has to be taken into account.

The difficulty in calculating the Lyapunov increment lies therefore in evaluating the conditional expectations

$$\mathbb{E}\Big[(2 - \sigma_k)^2 \,\Big|\, \xi_k, e_k\Big], \quad \mathbb{E}\Big[(\sigma_k - 1)^2 \,\Big|\, \xi_k, e_k\Big], \quad \text{and} \quad \mathbb{E}\Big[(2 - \sigma_k)(\sigma_k - 1) \,\Big|\, \xi_k, e_k\Big],$$

which can be reduced to just $\mathbb{E}[\sigma_k | \xi_k]$ and $\mathbb{E}[\sigma_k^2 | \xi_k]$ since σ_k is independent of x_{k_t} if $k \geq k_t$. However, in the proof of (Hu et al., 2021, Theorem 1) the analogous expectations are implicitly replaced by the unconditional expectations $\mathbb{E}[\sigma_k]$ and $\mathbb{E}[\sigma_k^2]$, a modification that is in general only correct if σ_k and ξ_k are independent random variables. This is illustrated by the following example:

Example 7.1.: Independence of the Switching Process

Consider a stochastic jump system $\xi_{k+1} = \mathcal{A}_{\sigma_k}\xi_k + \mathcal{B}_{\sigma_k}e_k$ with the switching process $\{\sigma_k\}$ taking values in $\mathcal{K} = \{1, 2\}$ and model matrices given by $\mathcal{A}_1 = 0$, $\mathcal{B}_1 = 0$, $\mathcal{A}_2 = 1$, and $\mathcal{B}_2 = 1$. Spelling out the modes explicitly results in

$$\xi_{k+1} = \begin{cases} 0 & \text{if } \sigma_k = 1, \\ \xi_k + e_k & \text{if } \sigma_k = 2, \end{cases}$$

which corresponds to a first-order integrator that resets if $\sigma_k = 1$. As such, we can deduce from $\xi_k \neq 0$ that $\sigma_{k-1} = 2$ by shifting one step into the past, or in other words $\mathbb{P}(\sigma_{k-1} = 2 \mid \xi_k \neq 0) = 1$ and $\mathbb{P}(\sigma_{k-1} = 1 \mid \xi_k \neq 0) = 0$.
Now, consider a switching process $\{\sigma_k\}$ that is a Markov chain with transition probabilities described by (7.8) and thus expectation $\mathbb{E}[\sigma_k] = p + 1$. If k is *not* a trigger instant k_t as determined by the trigger mechanism, it follows that $\sigma_k = \sigma_{k-1}$ and therefore

$$\mathbb{E}\Big[\sigma_k \,\Big|\, \xi_k \neq 0\Big] = \mathbb{E}\Big[\sigma_{k-1} \,\Big|\, \xi_k \neq 0\Big] = 2$$

from the probabilities given above. This illustrates that the conditional expectation $\mathbb{E}[\sigma_k \mid \xi_k]$ is in general different from $\mathbb{E}[\sigma_k]$.

Example 7.1 highlights the consequences of the interaction between the trigger mechanism and the stochastic communication network: Even though all network transmissions are independent, the trigger condition is introducing artificial dependencies into the switching process $\{\sigma_k\}$, which have to be taken into account while calculating its expectation. Hence, failing to do so may induce misleading results and invalidate analytical guarantees that were obtained in this way. This is demonstrated in Example 7.2.

Example 7.2.: ETC for an Unstable First-Order System

Consider the unstable first-order system $x_{k+1} = 1.1x_k + u_k$ which shall be stabilized using an event-triggered controller as visualized in Fig. 7.1a with control input $u_k = K\hat{x}_k$ determined from the buffered state $\hat{x}_k$. The trigger mechanism is enforcing

$$\|e_k\|^2 < \varepsilon \|x_{k_t}\|^2$$

for some $\varepsilon > 0$, translating into $Q = -\varepsilon$, $S = -\varepsilon$, and $R = 1 - \varepsilon$ in terms of Ω as defined in (7.2). Note that Hu et al. (2021) include a noise input w_k in their model which we suppress by setting the state-dependent scaling factor to zero.
Following this setup, we determine a suitable controller and trigger level through Theorem 1 of Hu et al. (2021). Assuming a transmission probability of $p = 0.8$, choosing $K = -0.5$ for the controller gain and $\varepsilon = 0.3$ for the trigger level leads to a feasible solution of the required LMI given by $P_1 = 2$, $P_2 = 0.28$, $\lambda = 1$, and arbitrary $\lambda^* > 2$, resulting in the Lyapunov function

$$V(x, \hat{x}) = x^\top P_1 x + \hat{x}^\top P_2 \hat{x}.$$

Its evolution is visualized in the scenario tree of Fig. 7.2 for initial state $x_0 = 1$ (note that Hu et al. assume $\hat{x}_0 = 0$). The nodes contain closed-loop states of the system labelled with the associated value of V and a branch indicates that the trigger mechanism has been activated.

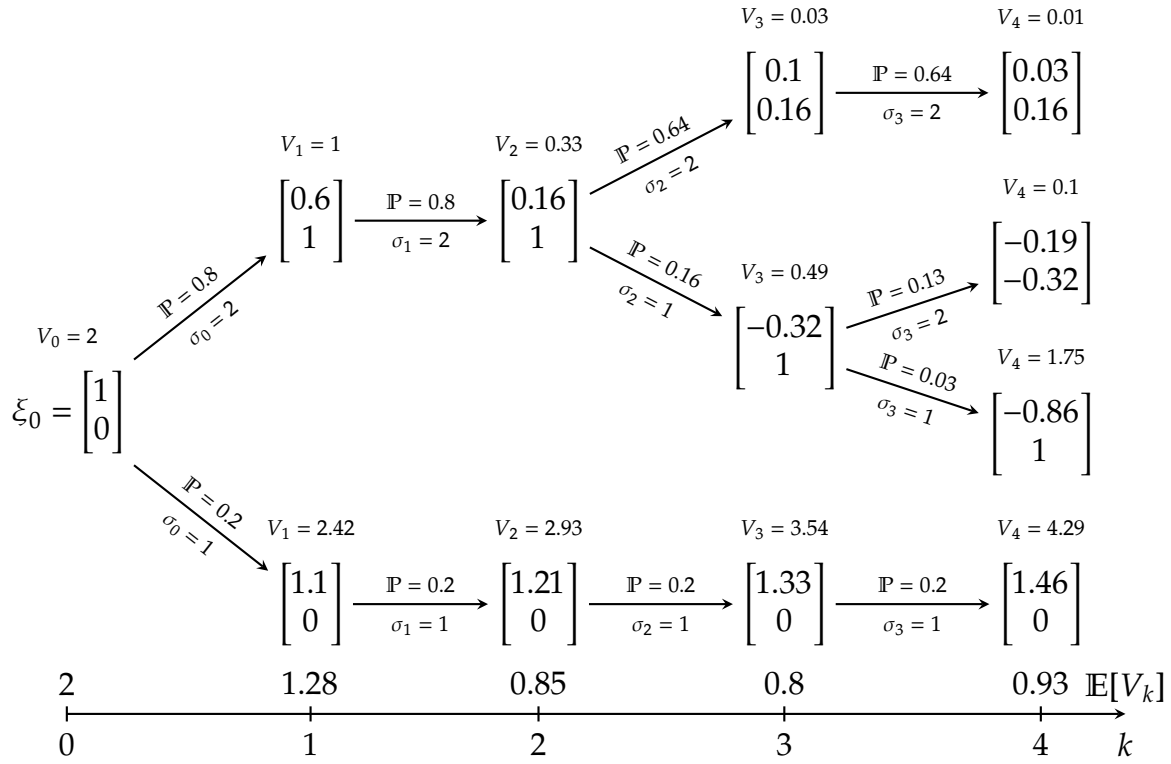

Figure 7.2.: Scenario tree of the first four steps of Example 7.2. The nodes visualize closed-loop states ξ_k which are labelled with the associated value of the Lyapunov function candidate V. The edges indicate possible state transitions, where branches are labelled with their realization of the stochastic process and its probability. At the bottom, the timeline shows the expected value of V_k at different times k.

According to Theorem 1 of Hu et al. (2021), the function V introduced in Example 7.2 is a mean-square Lyapunov function for the stochastically switched system. However, the scenario tree visualized in Fig. 7.2 shows that $\mathbb{E}[V_k]$ is *not* monotonically decreasing along the system trajectory for this particular initial condition, invalidating its application as a Lyapunov function. As such, Example 7.2 constitutes a counterexample for the stability theorem of Hu et al. (2021).

Unfortunately, calculating the expectations $\mathbb{E}[\sigma_k \mid \xi_k]$ and $\mathbb{E}[\sigma_k^2 \mid \xi_k]$ while taking the conditioning into account is difficult and will likely not result in a constant value independent of ξ_k such that correcting the problem is out of reach for this chapter. Moreover, the issue persists in the observer based extension of the approach by Zhao et al. (2022) since an analogous implicit assumption is imposed. As with the switched Lyapunov function candidate presented in Section 7.3.2, the alternative technique proposed by Hu et al. (2021) and Zhao et al. (2022) does therefore not provide an applicable stability or performance guarantee for the ETC loop with controller-side buffering.

7.4. Discussion

The preceding discourse on ETC schemes for unreliable networks has revealed that no universal solution currently exists. On the one hand, there are the approaches discussed

in Section 7.2 that employ modified trigger mechanisms specifically designed to handle failed transmissions, while the techniques of Section 7.3 on the other hand rely on offline analysis to guarantee closed-loop stability with standard state-feedback controllers and quadratic trigger mechanism.

From a conceptual standpoint, the offline analysis approach is particularly appealing because it enables existing event-triggered controllers to be retuned to compensate for the packet loss, which parallels the concept of the time-triggered controller synthesis of Chapter 4. However, the majority of existing ETC schemes of this kind adopt a specific network architecture that relies on continuous retransmission of the sampled plant state, impeding the objective of utilizing the trigger mechanism to reduce not only the computational demand of the controller but also the network load. Furthermore, for schemes that *do* consider a controller-side buffer, the interaction between the trigger mechanism and the stochastic transmissions leads to a non-homogeneous Markov chain as the switching process, rendering existing analysis techniques inapplicable.

In contrast, schemes that run a modified trigger mechanism online at the plant have access to more information, *e.g.* the timing of the preceding trigger instants k_t and the actual value of the trigger error e_k, which can be employed for estimating the impact of the unreliable network. It is evident that this leads to an elevated conceptual and computational complexity in comparison to standard ETC architectures, especially for networked IS where each subsystem has to implement one such estimator per neighbour. Nevertheless, their ability to analyse ETC loops with controller-side buffering demonstrates the effectiveness of online estimation triggering mechanisms.

An aspect which has only briefly been touched upon in this chapter is the availability of transmission acknowledgements by the controller to the trigger mechanism. It is pointed out by both Dolk and Heemels (2017) and Viel et al. (2022) that such acknowledgements form an essential component of their respective triggering schemes since they significantly improve quality of the involved error estimates. This mirrors similar observations for time-triggered schemes made by Schenato et al. (2007), who demonstrate a lack of acknowledgements makes stabilization and optimal control more difficult. On the other hand, none of the offline analysis schemes presented in Section 7.3 consider the potential of a feedback channel from the controller to the trigger to enhance the closed-loop performance. A possible avenue for further improvements of the closed-loop performance and towards an offline analysis of the controller-side buffer is therefore to integrate acknowledgements into the approaches outlined above.

8 Summary and Future Directions

The central theme of this dissertation are structured large-scale IS that are subject to stochastic communication effects, and in particular unreliable transmissions. After discussing its core aspect, the development of a general scalable analysis framework under simplifying assumptions on the communication network, the thesis introduces several extensions, covering suboptimal controller synthesis, robustness against switching topologies, and stochastic dependencies between transmissions. In this final chapter, the above results are summarized and put into context, before an outlook on promising future research directions is given.

8.1. Conclusions

By now, modelling and control of MAS and IS at large has been an active field of research for more than two decades. However, while numerous combinations of system architectures, subsystem models, and control approaches have been considered in the literature, this thesis studies the interplay between communication and control, a crucial aspect of networked systems that is frequently overlooked. In particular, the focus is on the adverse effects caused by intermittent transmission failures resulting from the inherently stochastic nature of communication networks. This naturally gives rise to a number of research questions that are answered throughout the chapters and are summarized broadly as follows:

1. How can the loss of information between subsystems be integrated into the dynamic model of the underlying IS?

2. What is an effective approach for analysing large-scale systems with stochastic communication? Is it feasible to derive a set of decoupled subproblems that can be solved independently, just like in the lossless case?

3. Is it possible to utilize the technique not just for analysing but even improving the closed-loop performance, *e.g.* by synthesizing purpose built controllers?

4. What is the minimal set of assumptions on the communication network such that the approach remains applicable?

After a general introduction in Chapter 1, the second chapter revolves around answering Question 1. Embedded within a brief review of the most important notions about LTI systems, decomposable systems as proposed by Massioni and Verhaegen (2009) are presented as the main modelling framework of the thesis. However, the subsequent discussion reveals that the stochastic nature of communication networks necessarily

leads to a random graph representation of the interconnection topology, and hence LTI systems are insufficient for modelling both dynamics and communication. In order to address this issue, Chapter 2 proposes to adapt the concept of decomposability within the broader context of MJLS, building the foundation for the remainder of the thesis.

Having found a suitable modelling framework, the question is how to derive appropriate analysis conditions for large-scale systems. Working under the hypothesis that the information loss on each communication link can be described by a Bernoulli process, Chapter 3 establishes that LMI-based decoupling techniques remain applicable for decomposable MJLS, culminating in the sufficient stability and performance conditions of Theorems 3.6, 3.11, and 3.13 given in terms of modal subproblems. A key element of the derivation are the stochastic moments of the graph Laplacian as provided by Lemma 3.3 which explicitly exposes their internal structure, contrasting a related result of Wu and Shi (2012). Different from existing methods, this allows to formulate the theorems in a decoupled manner, ensuring their applicability to large-scale systems even though the system itself cannot be decomposed due to its switching topology.

Building upon the previously derived analysis conditions, Chapter 4 studies distributed controller synthesis problems under the influence of stochastic packet loss. The chapter begins by applying established variable transformations to linearize the resulting optimization problems, thereby enabling the derivation of suboptimal synthesis conditions for static state-feedback controllers (Theorems 4.1 and 4.2) and their subsequent extension to dynamic output-feedback controllers by Theorems 4.3 and 4.4. The most intriguing property of the synthesized controllers is their ability to recover significant fractions of the packet loss induced performance degradation, not only with the network model they are tuned for but also a realistic, physically motivated model as implemented in the WiMAS simulation library. In light of the preceding observations, it can therefore be concluded that the answer to Question 3 is affirmative.

Question 4 presents a more complex issue that is explored in depth in three separate chapters. The first step is to challenge the hypotheses about the network model that were established in Chapter 3 for the sake of mathematical tractability. Removing one assumption at a time, the analysis is extended to uncertain distributions (Section 5.1), heterogeneous loss probabilities (Section 5.2), and spatio-temporal dependencies between communication links (Section 5.3). The central idea is to apply the FBSP in order to eliminate the transmission probabilities from the main LMI condition, leading to the scalable and distributionally robust stability and performance tests of Corollaries 5.7 and 5.8. Remarkably, Theorem 5.13 and Corollary 5.14 establish that the underlying abstract uncertainty set contains distributions with dependent links even though no such dependencies are considered during the analysis.

The second extension of the previous results is presented in Chapter 6 and deals with time-varying interconnection topologies, *i.e.* the neighbouring relation between subsystems changes even in the absence of packet loss. By expanding the considered system class to switched MJLS, Theorems 6.5 and 6.6 show that the mean-square stability and H_2-norm results of Chapter 3 prevail, paralleling similar results for LTI systems. In contrast, the proposed technique cannot be utilized to extend the H_∞-norm bound of Theorem 3.13 to the time-varying case due to a key stochastic independence assumption in Lemma 6.1, excluding the worst-case input signals.

Finally, Chapter 7 explores if an extension of the analysis to aperiodic control system is feasible. More specifically, the chapter studies a variety of ETC schemes for unreliable

networks with either deterministic and stochastic closed-loop guarantees, which are partitioned into two categories: 1.) schemes with modified trigger mechanisms and online error estimation, and 2.) schemes with an extended offline analysis. Unfortunately, none of the investigated strategies are able to conclusively solve the underlying control problem, suffering from either excessive complexity, inadequate modelling capabilities, or mathematical tractability issues. Consequently, ETC with stochastic packet loss remains a challenging problem.

8.2. Outlook

A multitude of avenues for further refinement and extension of the presented results exists throughout the thesis. The following paragraphs will discuss a number of specific instances from both categories.

Improvements on Existing Results

Different from its analogue for decomposable LTI systems as presented by Massioni and Verhaegen (2009), the decoupling LMI transformation proposed in Chapter 3 is not exact but introduces conservatism, especially for large IS. The cause lies in Lemma 3.3, which is restricted to generalized variances with identity weighting instead of arbitrary positive semidefinite matrices. Since this lemma constitutes the foundation for essentially all stability and performance results that follow, establishing a generalization would create many opportunities for further refinements throughout the thesis, *e.g.* exact norm calculations and improved controller synthesis conditions. An initial result with general weights has been reported by Wu and Shi (2012), but their calculations lack the necessary structure for applying a decoupling transformation.

Similarly, the robust analysis conditions of Chapter 5 are more conservative than necessary since only parameter-independent Lyapunov functions have been considered. Based on the analysis of Bliman (2004) and Bliman et al. (2006), the functions should instead be parametrized as matrix-valued homogeneous polynomials in the uncertainty, the same configuration as considered by de Oliveira et al. (2009) and Morais et al. (2013, 2015). These works suggest applying Pólya relaxations in order to obtain finite-dimensional SDPs which provide asymptotically exact bounds, but as discussed in Section 5.3.1 this is intractable for large IS. An alternative is provided by the parameter-dependent FBSP variant of Wu and Dong (2006), although preserving the decomposable structure likely requires restrictions on the admissible parametrization.

On the other hand, the incidence factorization introduced in Lemma 5.2 does not lead to conservatism in the analysis but imposes restrictive assumptions on the network model down the line since the product $\Psi\Psi^\top$ is inherently symmetric. In order to eliminate the need for Assumptions 5.1 and 5.2, it is therefore necessary to identify an alternative *asymmetric* factorization of the graph Laplacian. A first step towards a solution involves an augmented incidence representation that splits Ψ into two separate matrices, Ψ^- for incoming and Ψ^+ for outgoing edges, such that $\Psi = \Psi^- + \Psi^+$ (Xu et al., 2018; Zeng et al., 2015). However, while this representation permits encoding Laplacians for directed graphs, the diagonalizing singular value decomposition utilized in Section 5.2.2 is invalidated and no surrogate decoupling transformation is known.

Lastly, there exists one more issue in Chapter 5 that warrants special attention, namely the lack of a quantifiable robustness measure in Theorem 5.13 and Corollary 5.14. One potential solution could be to use the matrix determinant derived in Lemma 5.11 not only to prove invertibility but as a proportional factor to the simplex volume. For a fixed point in the interior of the simplex, it is then possible to derive a closed-form expression for its barycentric coordinates (Rockafellar, 1970, p. 7) through a rank-one update of the matrix M in (5.15), which assumes a particularly simple form if just the smallest coordinate is of interest. Nevertheless, this represents only a marginal improvement in comparison to Theorem 5.13, given that converting into Cartesian coordinates is currently intractable for non-trivial examples.

Extensions to Broader Contexts in Control

A key question in the context of interconnected feedback loops with unreliable communication is how to address the issue of lost information. Even though there are generally two options, neglecting the information entirely or reusing old information (Guo et al., 2013; Schenato, 2009), this thesis has disregarded the latter except for a brief discussion in Chapter 7 since introducing an additional switched memory state is incompatible with the notion of a decomposable MJLS as introduced in Section 2.4.3. However, since Datar et al. (2018) and Schenato (2009) demonstrate that either variant (or a mixture of both) can be superior depending on the scenario, it should be studied how a memory component can be integrated into decomposable MJLS.

Another opportunity for extension arises from the controller synthesis conditions presented in Chapter 4. Currently, the resulting controllers are optimized for a single fixed transmission probability p, which therefore has to be known during synthesis. Given that the probability is often uncertain and time-varying, it would be beneficial to design gain-scheduled controllers that adapt to the network instead, *e.g.* along the lines presented by Hoffmann and Werner (2015a) and Rugh and Shamma (2000). By means of simulation, El-nwegy (2022) demonstrates that such a generalization can improve the closed-loop performance, but the underlying theory demands further attention. In particular, it should be taken into account that the transmission probability cannot be measured but has to be estimated empirically (see Vaideshwaran, 2023), such that there exists a random scheduling mismatch between the controller and the network.

Finally, this dissertation is focussed solely on linear controller structures and is hence neglecting potentially valuable techniques. In the context of large-scale IS, a notable example are distributed model predictive controllers that can solve coupled optimal control problems with constraints through localized computations (see Maestre & Negenborn, 2014; Müller & Allgöwer, 2017; Stomberg et al., 2022). As demonstrated by Bensel (2023), such schemes are sensitive to unreliable communication and require method-specific adjustments to converge, justifying further investigations. However, an extension of the approach proposed in this thesis to the predictive case is hindered by the nonlinearity of the involved optimization algorithms. One promising direction could be to utilize the analysis of first-order optimization algorithms by Lessard et al. (2016) and Sundararajan et al. (2020) based on integral quadratic constraints which is extended to the stochastic case by Hu et al. (2017).

Appendix

A Brief Tour Through WiMAS

A

The availability of high fidelity simulation environments is an invaluable resource in modern research since it opens the door for rapid low-stakes exploration and validation without the need for time-consuming and expensive experiments. Of course, this also applies to the field of cyber-physical networks (CPN) that are at the intersection of system and control theory on the one hand and communication networks on the other. However, it is exactly this domain-spanning nature of CPN that renders them challenging to simulate, as knowledge of multiple fields has to be accrued to achieve accurate results. This has led to the development of WiMAS, a narrow-scoped simulation library for MAS that are subject to detrimental networking effects (Hespe, Schneider et al., 2024).

A.1. Scope of the Simulation Library

For the simulation of MAS and control systems in general on the one hand, and communication networks on the other, there exists a plethora of specialized tools to work with. On the communication side, it is commonplace to evaluate network architectures and communication protocols using discrete event-based simulators such as OMNeT++ (Varga & Hornig, 2008) and ns-3 (Riley & Henderson, 2010). While these tools natively support modelling simple movement, integrating complex agent dynamics is challenging. Moreover, there are rich multi-robot simulation environments like Gazebo (Koenig & Howard, 2004) and ARGoS (Pinciroli et al., 2012) that employ detailed physics-based simulations of dynamic systems, but do not have the capabilities to model the communication between agents. In order to accurately simulate all aspects of CPN, it has therefore been suggested to create co-simulation environments that combine the strong aspects of tools from both fields. For example, COPADRIVe (Vieira et al., 2019) and CORNET (Acharya et al., 2020) propose to combine Gazebo with either OMNeT++ or ns-3 for autonomous driving and general purpose robotic simulations. Furthermore, CoCPN (Rosenthal et al., 2019) and ULTRAS (Berling et al., 2023) integrate Matlab into an OMNeT++ driven simulation scenario to enhance its simulation capabilities.

However, creating the necessary environment for a physics-accurate simulation requires effort that hampers progress in situation for which approximations of physical reality are acceptable. In addition, it can be advantageous if the underlying mathematical models can be analysed in closed form, *e.g.* for the kind of performance verification performed in Section 4.3. Therefore, WiMAS has been developed with the intention to provide a collection of interpretable stochastic communication models that can be swapped at will, together with agent models in terms of arbitrary differential or difference equations. While it is the goal to provide the means for simulating networked MAS that are subject to stochastic communication effects such as random loss of information,

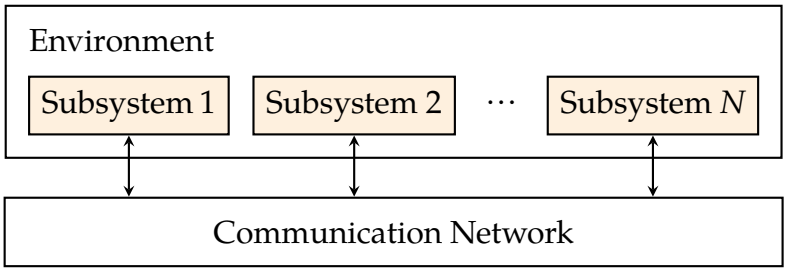

Figure A.1.: Schematic overview of a CPN

some aspects are opinionated with respect to its intended application and not geared towards being a general purpose simulation framework for MAS and CPN.

A.2. A Bird's-Eye View

From a high-level perspective, CPN as intended to be simulated by WiMAS have a common general structure as shown in Fig. A.1. The main component is the collective of N distinct subsystems that may implicitly interact through their shared environment. Furthermore, all subsystems have access to a communication network and can exchange information with distant peers. This structure has been directly transferred into the main components of WiMAS through the use of the object-oriented programming paradigm. Each subsystem is represented as an instance of a particular class, which determines its properties and dynamics. For convenience, a collection of basic vehicle models is provided, which includes simple linear models such as single and double integrators, a mass with friction as discussed in Example 4.1, and a linearized quadrotor model, but also nonlinear or nonholonomic models like a rolling disc and the HippoCampus (Dücker et al., 2018).

In the same way, the communication network is implemented as an object that is collecting and forwarding messages amongst the subsystems. The library provides implementations for four basic broadcasting networks, listed in order of increasing complexity:

1. An ideal scenario without stochastic effects, and optionally limited range.

2. An independent loss model that corresponds to the homogeneous or heterogeneous Bernoulli-type loss discussed in Chapters 3 and 5.

3. An implementation with spatially-independent Markov chains for each communication link, with no correspondence to the models discussed in this dissertation.

4. A physically motivated loss model based on the SINR, which has been employed in Section 4.3.3 and is further discussed below.

Except for the SINR-based network model, the entire library is implemented in Matlab, but the complex interaction rules for the physically motivated model pose a high computational demand and are thus implemented in C++.

A.3. Physically Motivated Packet Loss Modelling

For the first two stochastic network models listed above, the communication properties are entirely independent of the underlying MAS but has time-invariant and *a priori* fixed transmission (or transition, in the Markov case) probabilities. In contrast, the information loss of the SINR-based model depends on the distance between subsystems, and its probability distribution is therefore changing over time. Consequently, none of the closed-form communication models discussed in this dissertation is general enough to encompass the kind of packet loss. The precise model is discussed by Hespe et al. (2023), but a short overview is given below.

The SINR network abstraction of WiMAS implements a multi-layer model including Nakagami-m fast fading, binary phase-shift keying and slotted ALOHA medium access control (see Goldsmith, 2012, for a general introduction to these topics). Starting at the access control level, the slotted ALOHA protocol divides each sampling period into a fixed number of sections called *slots*. At every step, each subsystem picks a slot at random with equal probability and transmits with uniform transmission power P_{tx}. Importantly, it is assumed that transmission delays are negligible, and that transmission started in different slots do not overlap.

For a transmission from subsystem j to subsystem i, the received power P_{ij} is different from P_{tx} due to path loss and fading effects. The precise characteristics depend on the circumstances of the transmission, *e.g.* does it take place in free space, a densely developed area, or underwater, and as such WiMAS is configurable between different transmission modes, which broadly fall into two categories: Classical radio communication, such as intended for vehicle-to-vehicle networks, or acoustic underwater modems. Furthermore, all transmitted signals are received in superposition, and the reception of an individual transmission is therefore disturbed by interference and noise. This is modelled by the SINR, which is defined as

$$SINR(i,j) \coloneqq \frac{P_{ij}}{P_{\text{N}} + \sum_{l \in \mathcal{V}_{\text{S}} \setminus \{j\}} P_{il}},$$

where $\mathcal{V}_{\text{S}}$ is the set of subsystems that transmit in the same slot as subsystem j, *i.e.* the received power of the signal of interest is divided by the noise power P_{N} and the sum of all interfering signals received at the same time. Finally, the $SINR(i,j)$ is used to decide if the transmission from subsystem j to subsystem i has been successful. One possibility is to assume perfect modulation and derive an SINR threshold from Shannon's channel capacity formula (Goldsmith, 2012) using the bitrate of the transmitted signal and the available bandwidth. In that case, the transmission is considered to be received if $SINR(i,j)$ is above the threshold. On the other hand, binary phase-shift keying can be used for modulation, where the SINR is employed to calculate the bit error rate of the transmission and a reception probability is calculated. Note, however, that the transmission is random in either case, since the received power depends on the stochastic fading model.

Theorems and Proofs

B

This dissertation contains several results based on LMIs which are too involved to fit within the main text and are therefore summarized to only provide the core aspects. For reference, this appendix thus provides the full statements together with their proofs and any LMIs that were left out from the preceding chapters.

B.1. State-Feedback Controller Synthesis

Theorem 4.1.: H_2 State-Feedback Synthesis, (started on page 63)

Let T be a decomposable MJLS with L^0 and L_σ as patterns, an undirected nominal graph $\mathcal{G}^0$, and packet loss satisfying Assumption 3.4. There exists a state-feedback controller (4.2) *such that the closed loop is mean-square stable and has H_2-norm less than γ if there exist a symmetric X, a triple $(N_\mathrm{d}, N_\mathrm{c}, N_\mathrm{p})$ satisfying the orthogonality constraints*

$$B_\mathrm{c}^u N_\mathrm{c} = B_\mathrm{p}^u N_\mathrm{c} \;= B_\mathrm{c}^u N_\mathrm{p} \;= B_\mathrm{p}^u N_\mathrm{p} \;= 0, \tag{4.4a, restated}$$

$$D_\mathrm{c}^{zu} N_\mathrm{c} = D_\mathrm{p}^{zu} N_\mathrm{c} = D_\mathrm{c}^{zu} N_\mathrm{p} = D_\mathrm{p}^{zu} N_\mathrm{p} = 0, \tag{4.4b, restated}$$

and symmetric Z_i with $\sum_{i=1}^{N} \operatorname{tr} Z_i < \gamma^2$ that solve the LMIs

$$\begin{bmatrix} X & * & * & * & * \\ \bar{A}_i X + \bar{B}_i^u \bar{N}_i & X & * & * & * \\ \bar{C}_i^z X + \bar{D}_i^{zu} \bar{N}_i & 0 & I_{n_z} & * & * \\ \bar{\lambda}_i (A_\mathrm{c} X + B_\mathrm{d}^u N_\mathrm{c} + B_\mathrm{c}^u N_\mathrm{d}) & 0 & 0 & X & * \\ \bar{\lambda}_i (C_\mathrm{c}^z X + D_\mathrm{d}^{zu} N_\mathrm{c} + D_\mathrm{c}^{zu} N_\mathrm{d}) & 0 & 0 & 0 & I_{n_z} \end{bmatrix} \succ 0 \tag{B.1a}$$

$$\begin{bmatrix} Z_i & * & * & * & * \\ \bar{B}_i^w & X & * & * & * \\ \bar{D}_i^{zw} & 0 & I_{n_z} & * & * \\ \bar{\lambda}_i B_\mathrm{c}^w & 0 & 0 & X & * \\ \bar{\lambda}_i D_\mathrm{c}^{zw} & 0 & 0 & 0 & I_{n_z} \end{bmatrix} \succ 0 \tag{B.1b}$$

for all $i \in \{1, \dots, N\}$. In the LMIs, λ_i are the eigenvalues of L^0, $\bar{\lambda}_i := \sqrt{2p(1-p)\lambda_i}$, $\bar{A}_i$ denotes $A_\mathrm{d} + \lambda_i (p A_\mathrm{c} + A_\mathrm{p})$, and analogously for $\bar{B}_i^u$, $\bar{B}_i^w$, $\bar{C}_i^z$, $\bar{D}_i^{zu}$, $\bar{D}_i^{zw}$ and $\bar{N}_i$. Moreover, it is sufficient to validate (B.1a) *for the smallest and largest eigenvalue of L^0.*

Proof. The first step is to ensure that no products between the model matrices of the state-space realization of $\mathcal{T}$ occur in the LMI constraints. Therefore, a Schur complement is applied to (3.17), resulting in

$$\begin{bmatrix} Y^{-1} & * & * & * & * \\ \bar{\mathcal{A}}_N Y^{-1} & Y^{-1} & * & * & * \\ \bar{\mathcal{C}}_N Y^{-1} & 0 & I & * & * \\ \bar{\lambda}_N \mathcal{A}_\mathrm{c} Y^{-1} & 0 & 0 & Y^{-1} & * \\ \bar{\lambda}_N \mathcal{C}_\mathrm{c} Y^{-1} & 0 & 0 & 0 & I \end{bmatrix} \succ 0 \qquad \begin{bmatrix} Z_i & * & * & * & * \\ \bar{\mathcal{B}}_i & Y^{-1} & * & * & * \\ \bar{\mathcal{D}}_i & 0 & I & * & * \\ \bar{\lambda}_i \mathcal{B}_\mathrm{c} & 0 & 0 & Y^{-1} & * \\ \bar{\lambda}_i \mathcal{D}_\mathrm{c} & 0 & 0 & 0 & I \end{bmatrix} \succ 0,$$

where $\mathrm{diag}\left(Y^{-1}, I, I, I, I\right)$ has been used as a congruence transformation on the first inequality in the same step. Note that $Y^{-1} \succ 0$ and thus also $Y \succ 0$ are implied by the Schur complement. Introducing $X \coloneqq Y^{-1}$ and inserting the closed-loop model matrices derived above, we obtain (B.1a) and (B.1b) by the linearizing change of variables $N_\mathrm{d} \coloneqq D_\mathrm{d}^\mathrm{K} X$, $N_\mathrm{c} \coloneqq D_\mathrm{c}^\mathrm{K} X$, and $N_\mathrm{p} \coloneqq D_\mathrm{p}^\mathrm{K} X$. Finally, (4.3) and (4.4) are equivalent since X is non-singular, such that there exists a controller with bounded closed-loop H_2-norm for any solution of (B.1) by Theorem 3.11. ■

Theorem 4.2.: H_∞ State-Feedback Synthesis, (started on page 64)

Let T be a decomposable MJLS fulfilling Assumption 4.1 with L^0 and L_σ as patterns, an undirected nominal graph $\mathcal{G}^0$, and packet loss satisfying Assumption 3.4. There exists a state-feedback controller (4.2) *such that the closed loop is mean-square stable and has H_∞-norm less than γ if there exist a symmetric X and a triple $(N_\mathrm{d}, N_\mathrm{c}, N_\mathrm{p})$ satisfying the orthogonality constraints* (4.4) *that solve the LMI*

$$\begin{bmatrix} X & * & * & * & * & * & * \\ \bar{A}_i X + \bar{B}_i^u \bar{N}_i & X & B_\mathrm{d}^w & * & * & * & * \\ 0 & * & \gamma I_{n_w} & * & * & * & * \\ \bar{C}_i^z X + \bar{D}_i^{zu} \bar{N}_i & 0 & D_\mathrm{d}^{zw} & \gamma I_{n_z} & * & * & * \\ \bar{\lambda}_i (A_\mathrm{c} X + B_\mathrm{d}^u N_\mathrm{c} + B_\mathrm{c}^u N_\mathrm{d}) & 0 & 0 & 0 & X & B_\mathrm{d}^w & * \\ 0 & 0 & 0 & 0 & * & \gamma I_{n_w} & * \\ \bar{\lambda}_i (C_\mathrm{c}^z X + D_\mathrm{d}^{zu} N_\mathrm{c} + D_\mathrm{c}^{zu} N_\mathrm{d}) & 0 & 0 & 0 & 0 & D_\mathrm{d}^{zw} & \gamma I_{n_z} \end{bmatrix} \succ 0 \tag{B.2}$$

for $i \in \{1, N\}$. In the LMI, λ_i are the eigenvalues of L^0, $\bar{\lambda}_i \coloneqq \sqrt{2p(1-p)\lambda_i}$, $\bar{A}_i$ denotes $A_\mathrm{d} + \lambda_i(pA_\mathrm{c} + A_\mathrm{p})$, and analogously for $\bar{B}_i^u$, $\bar{C}_i^z$, $\bar{D}_i^{zu}$, and $\bar{N}_i$.

Proof. As for Theorem 4.1, it has to be ensured that no products between the model matrices occur. Accordingly, a Schur complement with respect to Y is applied to (3.21), resulting in

$$\begin{bmatrix} Y^{-1} & * & * & * & * & * & * \\ \bar{\mathcal{A}}_i Y^{-1} & Y^{-1} & \mathcal{B}_\mathrm{d} & * & * & * & * \\ 0 & * & \gamma I & * & * & * & * \\ \bar{\mathcal{C}}_i Y^{-1} & 0 & \mathcal{D}_\mathrm{d} & \gamma I & * & * & * \\ \bar{\lambda}_i \mathcal{A}_\mathrm{c} Y^{-1} & 0 & 0 & 0 & Y^{-1} & \mathcal{B}_\mathrm{d} & * \\ 0 & 0 & 0 & 0 & * & \gamma I & * \\ \bar{\lambda}_i \mathcal{C}_\mathrm{c} Y^{-1} & 0 & 0 & 0 & 0 & \mathcal{D}_\mathrm{d} & \gamma I \end{bmatrix} \succ 0$$

after a congruence transformation by $\operatorname{diag}\left(Y^{-1}, I, I, -I, I, I, -I\right)$. Again, $Y \succ 0$ is implied by the transformed condition. Inserting the controller-parametrized closed-loop system and defining $X \coloneqq Y^{-1}$, the LMI (B.2) is obtained by the same linearizing change of variables as above. Furthermore, Assumption 4.1 together with the orthogonality constraints (4.4) implies that the closed-loop is an input-decoupled decomposable MJLS, *i.e.* it satisfies Assumption 3.6. By Theorem 3.13, any solution to (B.2) therefore implies that there exists a controller that guarantees the desired H_∞-norm bound. ■

B.2. Output-Feedback Controller Synthesis

Theorem 4.3.: H_2 Output-Feedback Synthesis, (started on page 67)

Let T be a decomposable MJLS matching one of the three cases in Table 4.1 that has L^0 and L_σ as patterns, an undirected nominal graph $\mathcal{G}^0$, and packet loss satisfying Assumption 3.4. There exists an output-feedback controller (4.5) *such that the closed loop is mean-square stable and has H_2-norm less than γ if there exist symmetric P, Q, triples $(K_\mathrm{d}, K_\mathrm{c}, K_\mathrm{p})$, $(L_\mathrm{d}, L_\mathrm{c}, L_\mathrm{p})$, $(M_\mathrm{d}, M_\mathrm{c}, M_\mathrm{p})$, $(N_\mathrm{d}, N_\mathrm{c}, N_\mathrm{p})$ satisfying the constraints of Table 4.1, and symmetric Z_i with $\sum_{i=1}^{N} \operatorname{tr} Z_i < \gamma^2$ that solve the LMIs* (B.3) *for all $i \in \{1, \dots, N\}$. In the LMIs, λ_i are the eigenvalues of L^0, $\bar{\lambda}_i \coloneqq \sqrt{2p(1-p)\lambda_i}$, $\bar{A}_i$ denotes $A_\mathrm{d} + \lambda_i(pA_\mathrm{c} + A_\mathrm{p})$, and analogously for $\bar{B}_i^u$, $\bar{B}_i^w$, $\bar{C}_i^y$, $\bar{C}_i^z$, $\bar{D}_i^{yw}$, $\bar{D}_i^{zu}$ and $\bar{D}_i^{zw}$ as well as $\bar{K}_i$, $\bar{L}_i$, $\bar{M}_i$ and $\bar{N}_i$. Moreover, it is sufficient to validate* (B.3a) *for the smallest and largest eigenvalue of L^0.*

Proof. The derivation is based on the approach proposed by Gahinet (1996) in the formulation for decomposable LTI systems by Massioni and Verhaegen (2009). The general idea is to partition the Lyapunov matrix and its inverse into non-singular matrices P, Q, U, and V that satisfy $QP + UV^\top = I$. Linearizing substitutions are then given by

$$\begin{aligned} L_\mathrm{d} &\coloneqq UB_\mathrm{d}^\mathrm{K} + QB_\mathrm{d}^u D_\mathrm{d}^\mathrm{K}, & L_\bullet &\coloneqq UB_\bullet^\mathrm{K} + Q(B_\bullet^u D_\mathrm{d}^\mathrm{K} + B_\mathrm{d}^u D_\bullet^\mathrm{K}), \\ M_\mathrm{d} &\coloneqq C_\mathrm{d}^\mathrm{K} V^\top + D_\mathrm{d}^\mathrm{K} C_\mathrm{d}^y P, & M_\bullet &\coloneqq C_\bullet^\mathrm{K} V^\top + (D_\bullet^\mathrm{K} C_\mathrm{d}^y + D_\mathrm{d}^\mathrm{K} C_\bullet^y) P \end{aligned}$$

for the input and output channels,

$$\begin{aligned} K_\mathrm{d} &\coloneqq UA_\mathrm{d}^\mathrm{K} V^\top + Q(A_\mathrm{d} + B_\mathrm{d}^u D_\mathrm{d}^\mathrm{K} C_\mathrm{d}^y)P + UB_\mathrm{d}^\mathrm{K} C_\mathrm{d}^y P + QB_\mathrm{d}^u C_\mathrm{d}^\mathrm{K} V^\top, \\ K_\bullet &\coloneqq UA_\bullet^\mathrm{K} V^\top + Q(A_\mathrm{d} + B_\bullet^u D_\mathrm{d}^\mathrm{K} C_\mathrm{d}^y + B_\mathrm{d}^u D_\bullet^\mathrm{K} C_\mathrm{d}^y + B_\mathrm{d}^u D_\mathrm{d}^\mathrm{K} C_\bullet^y)P \\ &\quad + U(B_\bullet^\mathrm{K} C_\mathrm{d}^y + B_\mathrm{d}^\mathrm{K} C_\bullet^y)P + Q(B_\bullet^u C_\mathrm{d}^\mathrm{K} + B_\mathrm{d}^u C_\bullet^\mathrm{K}) V^\top \end{aligned}$$

for the main controller matrices, and $N_\mathrm{d} \coloneqq D_\mathrm{d}^\mathrm{K}$ and $N_\bullet \coloneqq D_\bullet^\mathrm{K}$ for the feedthrough terms. The subscript $\bullet$ denotes a placeholder for either 'c' or 'p'. As discussed in (Scherer et al., 1997), such a partition exists under the hypotheses of both Theorems 3.11 and 4.3, and the substitutions are therefore without loss of generality.

To move from (3.17) to (B.3) and back, apply the same Schur complements as for Theorem 4.1, followed by congruence transformations $\operatorname{diag}(\Pi_1, \Pi_2, I)$, $\operatorname{diag}(\Pi_1, \Pi_2, I, \Pi_2, I)$, and $\operatorname{diag}(I, \Pi_2, I, \Pi_2, I)$, respectively, where the transformations Π_1 and Π_2 are defined as

$$\Pi_1 \coloneqq \begin{bmatrix} P & I \\ V^\top & 0 \end{bmatrix} \quad \text{and} \quad \Pi_2 \coloneqq \begin{bmatrix} I & Q \\ 0 & U^\top \end{bmatrix} \quad \text{with} \quad \Pi_1^\top \Pi_2 = \begin{bmatrix} P & I \\ I & Q \end{bmatrix}.$$

The main difference from the existing results is that the variance terms must be considered. Since they feature the same internal structure as the standard LTI controller parametrization, we obtain analogous matrix identities as derived by Scherer et al. (1997). ■

Theorem 4.4.: H_∞ Output-Feedback Synthesis, (started on page 68)

Let T be a decomposable MJLS fulfilling Assumption 4.1 in conjunction with Case i) of Table 4.1 that has L^0 and L_σ as patterns, an undirected nominal graph $\mathcal{G}^0$, and packet loss satisfying Assumption 3.4. There exists an output-feedback controller (4.5) such that the closed loop is mean-square stable and has H_∞-norm less than γ if there exist symmetric P, Q, triples $(K_\mathrm{d}, K_\mathrm{c}, K_\mathrm{p})$, $(M_\mathrm{d}, M_\mathrm{c}, M_\mathrm{p})$, and matrices L_d, N_d that solve the LMI (B.4) for $i \in \{1, N\}$. In the LMI, λ_i are the eigenvalues of L^0, $\bar{\lambda}_i := \sqrt{2p(1-p)\lambda_i}$, $\bar{A}_i$ denotes $A_\mathrm{d} + \lambda_i(pA_\mathrm{c} + A_\mathrm{p})$, and analogously for $\bar{C}_i^y$, $\bar{C}_i^z$, and $\bar{D}_i^{zw}$ as well as $\bar{K}_i$ and $\bar{M}_i$.

Proof. Define the same partitioning of the Lyapunov matrix and the same substitutions for the controller parametrization as in the proof of Theorem 4.3 but note that $L_\mathrm{c} = L_\mathrm{p} = 0$ and $N_\mathrm{c} = N_\mathrm{p} = 0$ since Case i) holds. The LMI (B.4) is then obtained from (3.21) by applying the same Schur complement as for Theorem 4.1 followed by a congruence transformation with $\mathrm{diag}(\Pi_1, \Pi_2, I, -I, \Pi_2, I, -I)$. The variance terms are accounted for by the last three terms of the transformation and follow the same substitution rules as above. ■

B.3. Distributionally Robust System Analysis

Theorem 5.4.: Heterogeneous H_2-Norm Bound, (started on page 88)

A decomposable MJLS $\mathcal{T}$ with L^0 and L_σ as patterns, an interconnection satisfying Assumption 5.1, and transmission probabilities bounded as $p^{ij} \in [\rho_\mathrm{l}, \rho_\mathrm{u}]$ for all edges $(i,j) \in \mathcal{E}^0$ is mean-square stable and has H_2-norm less than γ if there exist a $Y \succ 0$, symmetric Z_i with $\sum_{i=1}^N \operatorname{tr} Z_i < \gamma^2$, and multipliers $P_1, P_2 \in \mathcal{P}_{n_\xi + n_z}$ that solve the LMIs

$$\mathcal{A}_\mathrm{d}^\top Y \mathcal{A}_\mathrm{d} + C_\mathrm{d}^\top C_\mathrm{d} \prec Y \qquad \text{(5.12a, restated)}$$
$$\mathcal{B}_\mathrm{d}^\top Y \mathcal{B}_\mathrm{d} + \mathcal{D}_\mathrm{d}^\top \mathcal{D}_\mathrm{d} \prec Z_i \qquad \text{(5.12b, restated)}$$

for all i such that $\lambda_i = 0$ and furthermore satisfy (B.5) for all non-zero λ_i, where $\mathcal{I}_j$ denotes the jth block-row of $I_3 \otimes I_{n_\xi + n_z}$ and λ_i are the eigenvalues of L^0. Moreover, it is sufficient to validate (B.5a) for the smallest and largest non-zero eigenvalue.

Proof. The two LMI constraints of Theorem 3.10 are considered separately. On the one hand, following the proof of Theorem 5.3 with the stacked system and input matrices, the existence of $Y \succ 0$ and $P_1 \in \mathcal{P}_{n_\xi + n_z}$ that solve (5.12a) and (B.5a) for all zero and non-zero eigenvalues of L^0, respectively, imply (3.15a). Furthermore, the argument of finding an LMI that is convex in λ_i and equivalent to (B.5a) for all *positive* eigenvalues

remains applicable, such that (B.5a) is solved for all positive eigenvalues if and only if it is solved for the smallest and largest positive λ_i.

On the other hand, employing the same proof once more with stacked input and feedthrough matrices shows that finding Z_i and $P_2 \in \mathcal{P}_{n_\xi+n_z}$ satisfying (5.12b) for all zero, and (B.5b) for all non-zero eigenvalues is a sufficient condition for (3.15b). ■

Theorem 5.5.: Heterogeneous H_∞-Norm Bound, (started on page 90)

A decomposable MJLS $\mathcal{T}$ fulfilling Assumption 3.6 with L^0 and L_σ as patterns, an interconnection satisfying Assumption 5.1, and transmission probabilities bounded as $p^{ij} \in [\rho_\mathrm{l}, \rho_\mathrm{u}]$ for all edges $(i,j) \in \mathcal{E}^0$ is mean-square stable and has H_∞-norm less than γ if there exists a $Y \succ 0$ and a multiplier $P \in \mathcal{P}_{n_\xi+n_z}$ that solve the LMI

$$\begin{bmatrix} \mathcal{A}_\mathrm{d}^\top Y \mathcal{A}_\mathrm{d} - Y & \mathcal{A}_\mathrm{d}^\top Y \mathcal{B}_\mathrm{d} & C_\mathrm{d}^\top \\ \mathcal{B}_\mathrm{d}^\top Y \mathcal{A}_\mathrm{d} & \mathcal{B}_\mathrm{d}^\top Y \mathcal{B}_\mathrm{d} - \gamma^2 I_{n_w} & \mathcal{D}_\mathrm{d}^\top \\ C_\mathrm{d} & \mathcal{D}_\mathrm{d} & -I_{n_z} \end{bmatrix} \prec 0 \qquad \text{(5.13, restated)}$$

and furthermore satisfy (B.6) *for the smallest and largest non-zero eigenvalue λ of L^0, where $\mathcal{I}_i$ denotes the ith block-row of $I_3 \otimes I_{n_\xi+n_z}$.*

Proof. The fractional representation derived above can be used in conjunction with the FBSP to obtain a multiplier based robust upper bound on the H_∞-norm in form of a coupled LMI constraint analogous to (5.10) from the mean-square stability result. After structuring the multiplier, applying $\operatorname{diag}(U \otimes I_{n_\xi}, U \otimes I_{n_w}, V \otimes I_{n_w}, V \otimes I_{3(n_\xi+n_z)})$ as a congruence transformation, where U and V are taken from the singular value decomposition $\Psi = U\Sigma V^\top$, diagonalizes the Laplacian and the incidence matrix and therefore decouples the LMI into modal constraints. By permutation, we obtain $\tilde{N}$ instances of (B.6) for the non-zero eigenvalues λ of L^0, $N - \tilde{N}$ versions of (5.13), and $\tilde{m} - \tilde{N}$ copies of

$$\begin{bmatrix} I_{n_w} & 0 \\ \mathcal{B}_\mathrm{d} & \sqrt{2}\mathcal{I}_2 \\ \mathcal{D}_\mathrm{d} & \end{bmatrix}^\top \begin{bmatrix} -\gamma^2 I_{n_w} & & \\ & Y & \\ & & I_{n_z} \end{bmatrix} \begin{bmatrix} I_{n_w} & 0 \\ \mathcal{B}_\mathrm{d} & \sqrt{2}\mathcal{I}_2 \\ \mathcal{D}_\mathrm{d} & \end{bmatrix} + \begin{bmatrix} 0 & I_{3(n_\xi+n_z)} \\ 0 & \mathcal{I}_3 \\ 0 & 0 \end{bmatrix}^\top P \begin{bmatrix} 0 & I_{3(n_\xi+n_z)} \\ 0 & \mathcal{I}_3 \\ 0 & 0 \end{bmatrix} \prec 0,$$

which is again implied by (B.6) for any $\lambda > 0$ and thus redundant (see the proof of Theorem 5.3). Finally, (B.6) can be convexified by the congruence transformation

$$\operatorname{diag}\left(I_{n_\xi}, I_{n_w}, \sqrt{\lambda} I_{n_w}, \sqrt{\lambda} I_{3(n_\xi+n_z)}\right),$$

and it is therefore sufficient to evaluate it for the extremal positive eigenvalues. ■

$$\begin{bmatrix}
P & * & * & * & * & * & * & * \\
I_{n_\xi} & Q & * & * & * & * & * & * \\
\bar{A}_i P + \bar{B}_i^u \bar{M}_i & \bar{A}_i + \bar{B}_i^u \bar{N}_i \bar{C}_i^y & P & * & * & * & * & * \\
\bar{K}_i & Q\bar{A}_i + \bar{L}_i \bar{C}_i^y & I_{n_\xi} & Q & * & * & * & * \\
\bar{C}_i^z P + \bar{D}_i^{zu} \bar{M}_i & \bar{C}_i^z + \bar{D}_i^{zu} \bar{N}_i \bar{C}_i^y & 0 & 0 & I_{n_z} & * & * & * \\
\bar{\lambda}_i (A_c P + B_d^u M_c + B_c^u M_d) & \bar{\lambda}_i (A_c + B_d^u N_d C_c^y + B_d^u N_c C_d^y + B_c^u N_d C_d^y) & 0 & 0 & 0 & P & * & * \\
\bar{\lambda}_i K_c & \bar{\lambda}_i (Q A_c + L_d C_c^y + L_c C_d^y) & 0 & 0 & 0 & I_{n_\xi} & Q & * \\
\bar{\lambda}_i (C_c^z P + D_d^{zu} M_c + D_c^{zu} M_d) & \bar{\lambda}_i (C_c^z + D_d^{zu} N_d C_c^y + D_d^{zu} N_c C_d^y + D_c^{zu} N_d C_d^y) & 0 & 0 & 0 & 0 & 0 & I_{n_z}
\end{bmatrix} \succ 0 \tag{B.3a}$$

$$\begin{bmatrix}
Z_i & * & * & * & * & * & * \\
\bar{B}_i^w + \bar{B}_i^u \bar{N}_i \bar{D}_i^{yw} & P & * & * & * & * & * \\
Q\bar{B}_i^w + \bar{L}_i \bar{D}_i^{yw} & I_{n_\xi} & Q & * & * & * & * \\
\bar{D}_i^{zw} + \bar{D}_i^{zu} \bar{N}_i \bar{D}_i^{yw} & 0 & 0 & I_{n_z} & * & * & * \\
\bar{\lambda}_i (B_c^w + B_d^u N_d D_c^{yw} + B_d^u N_c D_d^{yw} + B_c^u N_d D_d^{yw}) & 0 & 0 & 0 & P & * & * \\
\bar{\lambda}_i (Q B_c^w + L_d D_c^{yw} + L_c D_d^{yw}) & 0 & 0 & 0 & I_{n_\xi} & Q & * \\
\bar{\lambda}_i (D_c^{zw} + D_d^{zu} N_d D_c^{yw} + D_d^{zu} N_c D_d^{yw} + D_c^{zu} N_d D_d^{yw}) & 0 & 0 & 0 & 0 & 0 & I_{n_z}
\end{bmatrix} \succ 0 \tag{B.3b}$$

$$\begin{bmatrix}
P & I_{n_\xi} & * & * & * & * & * & * & * & * \\
I_{n_\xi} & Q & * & * & * & * & * & * & * & * \\
\bar{A}_i P + B_d^u \bar{M}_i & \bar{A}_i + B_d^u N_d \bar{C}_i^y & P & I_{n_\xi} & B_d^w + B_d^u N_d D_d^{yw} & * & * & * & * & * \\
\bar{K}_i & Q\bar{A}_i + L_d \bar{C}_i^y & I_{n_\xi} & Q & Q B_d^w + L_d D_d^{yw} & * & * & * & * & * \\
0 & 0 & * & * & \gamma I_{n_w} & * & * & * & * & * \\
\bar{C}_i^z P + D_d^{zu} \bar{M}_i & \bar{C}_i^z + D_d^{zu} N_d \bar{C}_i^y & 0 & 0 & D_d^{zw} + D_d^{zu} N_d D_d^{yw} & \gamma I_{n_z} & * & * & * & * \\
\bar{\lambda}_i (A_c P + B_d^u M_c) & \bar{\lambda}_i (A_c + B_d^u N_d C_c^y) & 0 & 0 & 0 & 0 & P & I_{n_\xi} & B_d^w + B_d^u N_d D_d^{yw} & * \\
\bar{\lambda}_i K_c & \bar{\lambda}_i (Q A_c + L_d C_c^y) & 0 & 0 & 0 & 0 & I_{n_\xi} & Q & Q B_d^w + L_d D_d^{yw} & * \\
0 & 0 & 0 & 0 & 0 & 0 & * & * & \gamma I_{n_w} & * \\
\bar{\lambda}_i (C_c^z P + D_d^{zu} M_c) & \bar{\lambda}_i (C_c^z + D_d^{zu} N_d C_c^y) & 0 & 0 & 0 & 0 & * & * & D_d^{zw} + D_d^{zu} N_d D_d^{yw} & \gamma I_{n_z}
\end{bmatrix} \succ 0 \tag{B.4}$$

$$\begin{bmatrix} I_{n_\xi} & 0 \\ \mathcal{A}_\mathrm{d}+\lambda_i\mathcal{A}_\mathrm{p} & \sqrt{\lambda_i}\mathcal{I}_1 \\ \mathcal{C}_\mathrm{d}+\lambda_i\mathcal{C}_\mathrm{p} & \\ 0 & \sqrt{2}\mathcal{I}_2 \\ 0 & \end{bmatrix}^\top \begin{bmatrix} -\mathcal{Y} & & & \\ & \mathcal{Y} & & \\ & & I_{n_z} & \\ & & & \mathcal{Y} \\ & & & & I_{n_z} \end{bmatrix} \begin{bmatrix} I_{n_\xi} & 0 \\ \mathcal{A}_\mathrm{d}+\lambda_i\mathcal{A}_\mathrm{p} & \sqrt{\lambda_i}\mathcal{I}_1 \\ \mathcal{C}_\mathrm{d}+\lambda_i\mathcal{C}_\mathrm{p} & \\ 0 & \sqrt{2}\mathcal{I}_2 \\ 0 & \end{bmatrix} + \begin{bmatrix} 0 & I_{3(n_\xi+n_z)} \\ 0 & \mathcal{I}_3 \\ 0 & \\ \sqrt{\lambda_i}\mathcal{A}_\mathrm{c} & 0 \\ \sqrt{\lambda_i}\mathcal{C}_\mathrm{c} & 0 \end{bmatrix}^\top P_1 \begin{bmatrix} 0 & I_{3(n_\xi+n_z)} \\ 0 & \mathcal{I}_3 \\ 0 & \\ \sqrt{\lambda_i}\mathcal{A}_\mathrm{c} & 0 \\ \sqrt{\lambda_i}\mathcal{C}_\mathrm{c} & 0 \end{bmatrix} \prec 0 \tag{B.5a}$$

$$\begin{bmatrix} I_{n_w} & 0 \\ \mathcal{B}_\mathrm{d}+\lambda_i\mathcal{B}_\mathrm{p} & \sqrt{\lambda_i}\mathcal{I}_1 \\ \mathcal{D}_\mathrm{d}+\lambda_i\mathcal{D}_\mathrm{p} & \\ 0 & \sqrt{2}\mathcal{I}_2 \\ 0 & \end{bmatrix}^\top \begin{bmatrix} -Z_i & & & \\ & \mathcal{Y} & & \\ & & I_{n_z} & \\ & & & \mathcal{Y} \\ & & & & I_{n_z} \end{bmatrix} \begin{bmatrix} I_{n_w} & 0 \\ \mathcal{B}_\mathrm{d}+\lambda_i\mathcal{B}_\mathrm{p} & \sqrt{\lambda_i}\mathcal{I}_1 \\ \mathcal{D}_\mathrm{d}+\lambda_i\mathcal{D}_\mathrm{p} & \\ 0 & \sqrt{2}\mathcal{I}_2 \\ 0 & \end{bmatrix} + \begin{bmatrix} 0 & I_{3(n_\xi+n_z)} \\ 0 & \mathcal{I}_3 \\ 0 & \\ \sqrt{\lambda_i}\mathcal{B}_\mathrm{c} & 0 \\ \sqrt{\lambda_i}\mathcal{D}_\mathrm{c} & 0 \end{bmatrix}^\top P_2 \begin{bmatrix} 0 & I_{3(n_\xi+n_z)} \\ 0 & \mathcal{I}_3 \\ 0 & \\ \sqrt{\lambda_i}\mathcal{B}_\mathrm{c} & 0 \\ \sqrt{\lambda_i}\mathcal{D}_\mathrm{c} & 0 \end{bmatrix} \prec 0 \tag{B.5b}$$

$$\begin{bmatrix} I_{n_\xi} & 0 & 0 & 0 \\ 0 & I_{n_w} & 0 & 0 \\ 0 & 0 & I_{n_w} & 0 \\ \mathcal{A}_\mathrm{d}+\lambda\mathcal{A}_\mathrm{p} & \mathcal{B}_\mathrm{d} & 0 & \sqrt{\lambda}\mathcal{I}_1 \\ \mathcal{C}_\mathrm{d}+\lambda\mathcal{C}_\mathrm{p} & \mathcal{D}_\mathrm{d} & 0 & \\ 0 & 0 & \mathcal{B}_\mathrm{d} & \sqrt{2}\mathcal{I}_2 \\ 0 & 0 & \mathcal{D}_\mathrm{d} & \end{bmatrix}^\top \begin{bmatrix} -\mathcal{Y} & & & & & \\ & -\gamma^2 I_{n_w} & & & & \\ & & -\gamma^2 I_{n_w} & & & \\ & & & \mathcal{Y} & & \\ & & & & I_{n_z} & \\ & & & & & \mathcal{Y} \\ & & & & & & I_{n_z} \end{bmatrix} \begin{bmatrix} I_{n_\xi} & 0 & 0 & 0 \\ 0 & I_{n_w} & 0 & 0 \\ 0 & 0 & I_{n_w} & 0 \\ \mathcal{A}_\mathrm{d}+\lambda\mathcal{A}_\mathrm{p} & \mathcal{B}_\mathrm{d} & 0 & \sqrt{\lambda}\mathcal{I}_1 \\ \mathcal{C}_\mathrm{d}+\lambda\mathcal{C}_\mathrm{p} & \mathcal{D}_\mathrm{d} & 0 & \\ 0 & 0 & \mathcal{B}_\mathrm{d} & \sqrt{2}\mathcal{I}_2 \\ 0 & 0 & \mathcal{D}_\mathrm{d} & \end{bmatrix} + \begin{bmatrix} 0 & 0 & 0 & I_{3(n_\xi+n_z)} \\ 0 & 0 & 0 & \mathcal{I}_3 \\ 0 & 0 & 0 & \\ \sqrt{\lambda}\mathcal{A}_\mathrm{c} & 0 & 0 & 0 \\ \sqrt{\lambda}\mathcal{C}_\mathrm{c} & 0 & 0 & 0 \end{bmatrix}^\top P \begin{bmatrix} 0 & 0 & 0 & I_{3(n_\xi+n_z)} \\ 0 & 0 & 0 & \mathcal{I}_3 \\ 0 & 0 & 0 & \\ \sqrt{\lambda}\mathcal{A}_\mathrm{c} & 0 & 0 & 0 \\ \sqrt{\lambda}\mathcal{C}_\mathrm{c} & 0 & 0 & 0 \end{bmatrix} \prec 0 \tag{B.6}$$

Bibliography

Åarzén, K.-E. (1999). A simple event-based PID controller. *IFAC Proceedings Volumes*, *32*(2), 8687–8692.

Abdelrahim, M., Postoyan, R., Daafouz, J., & Nešić, D. (2014). Co-design of output feedback laws and event-triggering conditions for linear systems. *Conference on Decision and Control*, 3560–3565.

Acharya, S., Bharadwaj, A., Simmhan, Y., Gopalan, A., Parag, P., & Tyagi, H. (2020). CORNET: A co-simulation middleware for robot networks. *International Conference on Communication Systems & Networks*, 245–251.

Apkarian, P., & Gahinet, P. (1995). A convex characterization of gain-scheduled H∞ controllers. *IEEE Transactions on Automatic Control*, *40*(5), 853–864.

Åström, K. J., & Bernhardsson, B. M. (1999). Comparison of periodic and event based sampling for first-order stochastic systems. *IFAC Proceedings Volumes*, *32*(2), 5006–5011.

Ballam, R. C., McFadyen, A., & Quevedo, D. E. (2022). H2 controller design for multi-agent systems with Markovian switching topologies. *Australian & New Zealand Control Conference*.

Ballam, R. C., McFadyen, A., & Quevedo, D. E. (2023). Local averaging for consensus over communication links with random dropouts. *IEEE Control Systems Letters*, *7*, 1387–1392.

Bensel, A. (2023, May 1). *Distributed predictive control with stochastic communication loss* [Master's thesis, Hamburg University of Technology] [Hespe, Christian and Werner, Herbert].

Berling, J., Hastedt, P., Wanniarachchi, S. T., Vieregg, A., Gertz, C., Turau, V., Werner, H., & Gollnick, V. (2023). A modular urban air mobility simulation toolchain with dynamic agent interaction. *Deutscher Luft- und Raumfahrtkongress*.

Bertsekas, D. P. (2009). *Convex optimization theory*. Athena Scientific.

Bliman, P.-A. (2004). An existence result for polynomial solutions of parameter-dependent LMIs. *Systems & Control Letters*, *51*(3–4), 165–169.

Bliman, P.-A., de Oliveira, R. C. d. L. F., Montagner, V. F., & Peres, P. L. D. (2006). Existence of homogeneous polynomial solutions for parameter-dependent linear matrix inequalities with parameters in the simplex. *Conference on Decision and Control*, 1486–1491.

Bolzern, P., Colaneri, P., & De Nicolao, G. (2004). On almost sure stability of discrete-time Markov jump linear systems. *Conference on Decision and Control*, 3204–3208.

Bolzern, P., Colaneri, P., & De Nicolao, G. (2010). Markov jump linear systems with switching transition rates: Mean square stability with dwell-time. *Automatica*, *46*(6), 1081–1088.

Bolzern, P., Colaneri, P., & De Nicolao, G. (2015). H∞ co-design for discrete-time dual switching linear systems. *European Control Conference*, 1742–1747.

Boyd, S., El Ghaoui, L., Feron, E., & Balakrishnan, V. (1994, January). *Linear matrix inequalities in system and control theory*. SIAM.

Brouwer, A. E., & Haemers, W. H. (2012). *Spectra of graphs*. Springer.

Bullo, F. (2018). *Lectures on network systems* (J. Cortés, F. Dörfler & S. Martínez, Eds.; 1.6). CreateSpace.

Capone, A., Jiao, J., Zarei, M., Zhang, S., & Hirche, S. (2023). Robust H∞ consensus for homogeneous multi-agent systems with parametric uncertainties. *American Control Conference*, 4191–4196.

Chen, G., Kang, Y., Zhang, C., & Chen, S. (2021). Consensus of discrete-time multi-agent systems over packet dropouts channels. *Journal of the Franklin Institute*, *358*(13), 6684–6704.

Chen, T., & Francis, B. A. (1995). *Optimal sampled-data control systems*. Springer London.

Chen, W., Ding, D., Wei, G., Zhang, S., & Li, Y. (2018). Event-based containment control for multi-agent systems with packet dropouts. *International Journal of Systems Science*, *49*(12), 2658–2669.

Cortés, J. (2006). Finite-time convergent gradient flows with applications to network consensus. *Automatica*, *42*(11), 1993–2000.

Cortés, J., & Egerstedt, M. (2017). Coordinated control of multi-robot systems: A survey. *SICE Journal of Control, Measurement, and System Integration*, *10*(6), 495–503.

Costa, O. L. d. V., de Assumpção Filho, E. O., Boukas, E.-K., & Marques, R. P. (1999). Constrained quadratic state feedback control of discrete-time Markovian jump linear systems. *Automatica*, *35*(4), 617–626.

Costa, O. L. d. V., do Val, J. B. R., & Geromel, J. C. (1997). A convex programming approach to H2 control of discrete-time Markovian jump linear systems. *International Journal of Control*, *66*(4), 557–580.

Costa, O. L. d. V., & Fragoso, M. D. (1993). Stability results for discrete-time linear systems with Markovian jumping parameters. *Journal of Mathematical Analysis and Applications*, *179*(1), 154–178.

Costa, O. L. d. V., & Marques, R. P. (1998). Mixed H_2/H_∞-control of discrete-time Markovian jump linear systems. *IEEE Transactions on Automatic Control*, *43*(1), 95–100.

Costa, O. L. d. V., Marques, R. P., & Fragoso, M. D. (2005). *Discrete-time Markov jump linear systems*. Springer London.

D'Andrea, R., & Dullerud, G. E. (2003). Distributed control design for spatially interconnected systems. *IEEE Transactions on Automatic Control*, *48*(9), 1478–1495.

Datar, A., Schneider, D., Mirali, F., Werner, H., & Frey, H. (2018). A memory weighted protocol for sampled-data systems subjected to packet dropouts. *American Control Conference*, 2485–2490.

De Caigny, J., Camino, J. F., de Oliveira, R. C. d. L. F., Peres, P. L. D., & Swevers, J. (2010). Gain-scheduled H2 and H∞ control of discrete-time polytopic time-varying systems. *IET Control Theory & Applications*, *4*(3), 362–380.

de Oliveira, M. C., Geromel, J. C., & Bernussou, J. (1999). An LMI optimization approach to multiobjective controller design for discrete-time systems. *Conference on Decision and Control*, 3611–3616.

de Oliveira, R. C. d. L. F., Vargas, A. d. N., do Val, J. B. R., & Peres, P. L. D. (2009). Robust stability, H2 analysis and stabilisation of discrete-time Markov jump linear systems with uncertain probability matrix. *International Journal of Control*, *82*(3), 470–481.

Diestel, R. (2017). *Graph theory*. Springer Berlin Heidelberg.

Dolk, V., & Heemels, W. P. M. H. (2017). Event-triggered control systems under packet losses. *Automatica*, *80*, 143–155.

Douc, R., Moulines, E., Priouret, P., & Soulier, P. (2018). *Markov chains*. Springer International Publishing.

do Val, J. B. R., Geromel, J. C., & Gonçalves, A. P. d. C. (2002). The H2-control for jump linear systems: Cluster observations of the Markov state. *Automatica*, *38*(2), 343–349.

Duan, Z., & Xiang, Z. (2013). H2 output feedback controller design for discrete-time 2D switched systems. *Transactions of the Institute of Measurement and Control*, *36*(1), 68–77.

Dücker, D.-A., Kreuzer, E., Maerker, G., & Solowjow, E. (2018). Parameter identification for micro underwater vehicles. *Proceedings in Applied Mathematics and Mechanics*, *18*(1).

Eichler, A., Hoffmann, C., & Werner, H. (2013). Robust stability analysis of interconnected systems with uncertain time-varying time delays via IQCs. *Conference on Decision and Control*, 2799–2804.

Elia, N. (2005). Remote stabilization over fading channels. *Systems & Control Letters*, *54*(3), 237–249.

El-nwegy, A. (2022, October 15). *Empirical studies of multi-agent formation control over stochastic communication networks* [research rep.]. Hamburg University of Technology [Hespe, Christian and Werner, Herbert].

Fagnani, F., & Zampieri, S. (2008). Randomized consensus algorithms over large scale networks. *IEEE Journal on Selected Areas in Communications*, *26*(4), 634–649.

Fagnani, F., & Zampieri, S. (2009). Average consensus with packet drop communication. *SIAM Journal on Control and Optimization*, *48*(1), 102–133.

Fang, H., & Antsaklis, P. J. (2008). Distributed control with integral quadratic constraints. *IFAC Proceedings Volumes*, *41*(2), 574–580.

Fang, Y., Loparo, K. A., & Feng, X. (1994). Almost sure and δ-moment stability of jump linear systems. *International Journal of Control*, *59*(5), 1281–1307.

Fax, J. A., & Murray, R. M. (2004). Information flow and cooperative control of vehicle formations. *IEEE Transactions on Automatic Control*, *49*(9), 1465–1476.

Fioravanti, A. R., Gonçalves, A. P. d. C., Deaecto, G. S., & Geromel, J. C. (2012). Equivalent LMI constraints: Applications to discrete-time MJLS and switched systems. *Conference on Decision and Control*, 1313–1318.

Fioravanti, A. R., Gonçalves, A. P. d. C., & Geromel, J. C. (2013). Optimal H2 and H∞ mode-independent filters for generalised Bernoulli jump systems. *International Journal of Systems Science*, *46*(3), 405–417.

Gahinet, P. (1996). Explicit controller formulas for LMI-based H∞ synthesis. *Automatica*, *32*(7), 1007–1014.

Gahinet, P., & Apkarian, P. (1994). A linear matrix inequality approach to H∞ control. *International Journal of Robust and Nonlinear Control*, *4*(4), 421–448.

Ghadami, R., & Shafai, B. (2010). Robust distributed control of decomposable systems with switching network topology. *Conference on Decision and Control*, 7238–7244.

Girard, A. (2015). Dynamic triggering mechanisms for event-triggered control. *IEEE Transactions on Automatic Control*, *60*(7), 1992–1997.

Golabi, A., Meskin, N., Tóth, R., Mohammadpour Velni, J., & Donkers, T. (2016). Event-triggered control for discrete-time linear parameter-varying systems. *American Control Conference*, 3680–3685.

Goldsmith, A. (2012). *Wireless communications*. Cambridge University Press.

Gonçalves, A. P. d. C., Fioravanti, A. R., & Geromel, J. C. (2012). H∞ robust and networked control of discrete-time MJLS through LMIs. *Journal of the Franklin Institute*, *349*(6), 2171–2181.

Grone, R., & Merris, R. (1994). The Laplacian spectrum of a graph II. *SIAM Journal on Discrete Mathematics*, *7*(2), 221–229.

Guinaldo, M., Lehmann, D., Sánchez, J. Á., Dormido, S., & Johansson, K. H. (2012). Distributed event-triggered control with network delays and packet losses. *Conference on Decision and Control*.

Guo, G., Lu, Z., & Shi, P. (2013). Event-driven actuators: To zero or to hold? *International Journal of Robust and Nonlinear Control*, *24*(17), 2761–2773.

Halder, K., Gillam, L., Dixit, S., Mouzakitis, A., & Fallah, S. (2022). Stability analysis with LMI based distributed H∞ controller for vehicle platooning under random multiple packet drops. *IEEE Transactions on Intelligent Transportation Systems*, *23*(12), 23517–23532.

Hatano, Y., & Mesbahi, M. (2005). Agreement over random networks. *IEEE Transactions on Automatic Control*, *50*(11), 1867–1872.

Heemels, W. P. M. H., Johansson, K. H., & Tabuada, P. (2012). An introduction to event-triggered and self-triggered control. *Conference on Decision and Control*, 3270–3285.

Heemels, W. P. M. H., Sandee, J. H., & Van Den Bosch, P. P. J. (2008). Analysis of event-driven controllers for linear systems. *International Journal of Control*, *81*(4), 571–590.

Hespanha, J. P. (2009). *Linear systems theory*. Princeton University Press.

Hespe, C., Datar, A., Schneider, D., Saadabadi, H., Werner, H., & Frey, H. (2023). Distributed H_2 controller synthesis for multi-agent systems with stochastic packet loss. *American Control Conference*, 4197–4202.

Hespe, C., Datar, A., & Werner, H. (2024). Robust stability for multiagent systems with spatio-temporally correlated packet loss. *European Control Conference*, 2946–2951.

Hespe, C., Saadabadi, H., Datar, A., Werner, H., & Tang, Y. (2024). A decomposition approach to multiagent systems with Bernoulli packet loss. *IEEE Transactions on Control of Network Systems*, *11*(1), 210–220.

Hespe, C., Schneider, D., Datar, A., Werner, H., & Frey, H. (2024). *WiMAS: Wireless multi-agent simulations* (comp. software). Zenodo.

Hespe, C., & Werner, H. (2023a). Robust performance analysis for time-varying multi-agent systems with stochastic packet loss. *IFAC-PapersOnLine*, *56*(2), 8809–8814.

Hespe, C., & Werner, H. (2023b). A scalable approach for analysing multi-agent systems with heterogeneous stochastic packet loss. *Conference on Decision and Control*, 3396–3401.

Hoffmann, C., Eichler, A., & Werner, H. (2013). Distributed control of linear parameter-varying decomposable systems. *American Control Conference*, 2380–2385.

Hoffmann, C., Eichler, A., & Werner, H. (2014). Control of heterogeneous groups of LPV systems interconnected through directed and switching topologies. *American Control Conference*, 5156–5161.

Hoffmann, C., & Werner, H. (2015a). A survey of linear parameter-varying control applications validated by experiments or high-fidelity simulations. *IEEE Transactions on Control Systems Technology*, *23*(2), 416–433.

Hoffmann, C., & Werner, H. (2015b). Control of heterogeneous LPV subsystems interconnected through arbitrary and switching directed topologies. *Conference on Decision and Control*, 3633–3638.

Horn, R. A., & Johnson, C. R. (2017). *Matrix analysis* (2nd ed.). Cambridge University Press.

Hou, L., Zong, G., Zheng, W., & Wu, Y. (2013). Exponential l2–l∞ control for discrete-time switching Markov jump linear systems. *Circuits, Systems, and Signal Processing*, *32*(6), 2745–2759.

Hu, B., Seiler, P., & Rantzer, A. (2017). A unified analysis of stochastic optimization methods using jump system theory and quadratic constraints. *Conference on Learning Theory*, *65*, 1157–1189.

Hu, W., & Liu, L. (2017). Cooperative output regulation of heterogeneous linear multi-agent systems by event-triggered control. *IEEE Transactions on Cybernetics*, *47*(1), 105–116.

Hu, Z., Shi, P., Zhang, J., & Deng, F. (2021). Control of discrete-time stochastic systems with packet loss by event-triggered approach. *IEEE Transactions on Systems, Man, and Cybernetics: Systems*, *51*(2), 755–764.

Janson, S., Łuczak, T., & Rucinski, A. (2000, February). *Random graphs*. Wiley.

Ji, Y., & Chizeck, H. J. (1990). Jump linear quadratic gaussian control: Steady-state solution and testable conditions. *Control-Theory and Advanced Technology*, *6*(3), 289–319.

Ji, Y., Chizeck, H. J., Feng, X., & Loparo, K. A. (1991). Stability and control of discrete-time jump linear systems. *Control-Theory and Advanced Technology*, *7*(2), 247–270.

Klenke, A. (2013). *Wahrscheinlichkeitstheorie*. Springer Berlin Heidelberg.

Koenig, N., & Howard, A. (2004). Design and use paradigms for Gazebo, an open-source multi-robot simulator. *International Conference on Intelligent Robots and Systems*.

Kouba, O., & Bernstein, D. S. (2020). What is the adjoint of a linear system? *IEEE Control Systems Magazine*, *40*(3), 62–70.

Langbort, C., Chandra, R. S., & D'Andrea, R. (2004). Distributed control design for systems interconnected over an arbitrary graph. *IEEE Transactions on Automatic Control*, *49*(9), 1502–1519.

Lee, E. A., & Messerschmitt, D. G. (2002). *Digital communication* (2nd ed.). Kluwer Academic Publ.

Leonard, N. E., & Fiorelli, E. (2001). Virtual leaders, artificial potentials and coordinated control of groups. *Conference on Decision and Control*, 2968–2973.

Lessard, L., Recht, B., & Packard, A. (2016). Analysis and design of optimization algorithms via integral quadratic constraints. *SIAM Journal on Optimization*, *26*(1), 57–95.

Li, Q.-Q., Wang, Y.-W., Xiao, J.-W., & Yi, J.-W. (2014). Event triggered control for multi-agent systems with packet dropout. *International Conference on Control & Automation*, 1180–1185.

Löfberg, J. (2004). YALMIP: A toolbox for modeling and optimization in MATLAB. *International Conference on Robotics and Automation*, 284–289.

Ma, C., & Qiao, H. (2016). Event-triggered consensus and passification co-design for multi-agent systems over unreliable communication networks. *American Control Conference*, 3716–3721.

Ma, J., Yu, X., & Lan, W. (2020). Distributed consensus of linear multi-agent systems with nonidentical random packet loss. *Conference on Decision and Control*, 4374–4379.

Maestre, J. M., & Negenborn, R. R. (Eds.). (2014). *Distributed model predictive control made easy* (Vols. 69). Springer Netherlands.

Massioni, P. (2014). Distributed control for alpha-heterogeneous dynamically coupled systems. *Systems & Control Letters*, *72*, 30–35.

Massioni, P., & Verhaegen, M. (2009). Distributed control for identical dynamically coupled systems: A decomposition approach. *IEEE Transactions on Automatic Control*, *54*(1), 124–135.

Massioni, P., & Verhaegen, M. (2010). A full block S-procedure application to distributed control. *American Control Conference*, 2338–2343.

Matei, I., Martins, N., & Baras, J. S. (2008). Almost sure convergence to consensus in Markovian random graphs. *Conference on Decision and Control*, 3535–3540.

Mazo, M., & Tabuada, P. (2008). On event-triggered and self-triggered control over sensor/actuator networks. *Conference on Decision and Control*.

Meister, D., Aurzada, F., Lifshits, M. A., & Allgöwer, F. (2022). Analysis of time-versus event-triggered consensus for a single-integrator multi-agent system. *Conference on Decision and Control*, 441–446.

Meister, D., Dürr, F., & Allgöwer, F. (2023). Shared network effects in time-versus event-triggered consensus of a single-integrator multi-agent system. *IFAC-PapersOnLine*, *56*(2), 5975–5980.

Meng, X., & Chen, T. (2013). Event detection and control co-design of sampled-data systems. *International Journal of Control*, *87*(4), 777–786.

Mesbahi, M., & Egerstedt, M. (2010). *Graph theoretic methods in multiagent networks*. Princeton University Press.

Mirali, F., & Werner, H. (2020). A dynamic quasi-Taylor approach for distributed consensus problems with packet loss. *American Control Conference*, 701–706.

Molinari, F., Agrawal, N., Stańczak, S., & Raisch, J. (2021). Max-consensus over fading wireless channels. *IEEE Transactions on Control of Network Systems*, *8*(2), 791–802.

Montúfar Cuartas, G. F. (2013). Mixture decompositions of exponential families using a decomposition of their sample spaces. *Kybernetika*, *49*(1), 23–39.

Morais, C. d. F., Braga, M. F., de Oliveira, R. C. d. L. F., & Peres, P. L. D. (2015). H∞ state feedback control for MJLS with uncertain probabilities. *Automatica*, *52*, 317–321.

Morais, C. d. F., Braga, M. F., de Oliveira, R. C. d. L. F., & Peres, P. L. D. (2013). H2 control of discrete-time Markov jump linear systems with uncertain transition probability matrix: Improved linear matrix inequality relaxations and multi-simplex modelling. *IET Control Theory & Applications*, *7*(12), 1665–1674.

Müller, M. A., & Allgöwer, F. (2017). Economic and distributed model predictive control: Recent developments in optimization-based control. *SICE Journal of Control, Measurement, and System Integration*, *10*(2), 39–52.

Murray, R. M. (2007). Recent research in cooperative control of multivehicle systems. *Journal of Dynamic Systems, Measurement, and Control*, *129*(5), 571–583.

Nakamura, M., Ishii, H., & Dibaji, S. M. (2018). Maximum-based consensus and its resiliency. *IFAC-PapersOnLine*, *51*(23), 283–288.

Olfati-Saber, R. (2005). Distributed kalman filter with embedded consensus filters. *Conference on Decision and Control*, 8179–8184.

Olfati-Saber, R. (2006). Flocking for multi-agent dynamic systems: Algorithms and theory. *IEEE Transactions on Automatic Control*, *51*(3), 401–420.

Olfati-Saber, R., Fax, J. A., & Murray, R. M. (2007). Consensus and cooperation in networked multi-agent systems. *Proceedings of the IEEE*, *95*(1), 215–233.

Olfati-Saber, R., & Murray, R. M. (2003). Consensus protocols for networks of dynamic agents. *American Control Conference*.

Olfati-Saber, R., & Murray, R. M. (2004). Consensus problems in networks of agents with switching topology and time-delays. *IEEE Transactions on Automatic Control*, *49*(9), 1520–1533.

Pan, Y.-J., Werner, H., Huang, Z., & Bartels, M. (2017). Distributed cooperative control of leader–follower multi-agent systems under packet dropouts for quadcopters. *Systems & Control Letters*, *106*, 47–57.

Patterson, S., Bamieh, B., & El Abbadi, A. (2010). Convergence rates of distributed average consensus with stochastic link failures. *IEEE Transactions on Automatic Control*, *55*(4), 880–892.

Pecora, L. M., & Carroll, T. L. (1998). Master stability functions for synchronized coupled systems. *Physical Review Letters*, *80*(10), 2109–2112.

Pilz, U., Popov, A. P., & Werner, H. (2009). Robust controller design for formation flight of quad-rotor helicopters. *Conference on Decision and Control*.

Pinciroli, C., Trianni, V., O'Grady, R., Pini, G., Brutschy, A., Brambilla, M., Mathews, N., Ferrante, E., Di Caro, G., Ducatelle, F., Birattari, M., Gambardella, L. M., & Dorigo, M. (2012). ARGoS: A modular, parallel, multi-engine simulator for multi-robot systems. *Swarm Intelligence*, *6*(4), 271–295.

Popov, A., & Werner, H. (2012). Robust stability of a multi-agent system under arbitrary and time-varying communication topologies and communication delays. *IEEE Transactions on Automatic Control*, *57*(9), 2343–2347.

Qu, H., Hu, J., Song, Y., & Yang, T. (2018). Mean square stabilization of discrete-time switching Markov jump linear systems. *Optimal Control Applications and Methods*, *40*(1), 141–151.

Razzaghpour, M., Datar, A., Schneider, D., Zaman, M., Werner, H., Frey, H., Mohammadpour Velni, J., & Fallah, Y. P. (2022). Finite state Markov modeling of C-V2X erasure links for performance and stability analysis of platooning applications. *International Systems Conference*.

Ren, W., & Beard, R. W. (2005). Consensus seeking in multiagent systems under dynamically changing interaction topologies. *IEEE Transactions on Automatic Control*, *50*(5), 655–661.

Ren, W., & Beard, R. W. (2008). *Distributed consensus in multi-vehicle cooperative control: Theory and applications*. Springer London.

Riley, G. F., & Henderson, T. R. (2010). The ns-3 network simulator. In *Modeling and tools for network simulation* (pp. 15–34). Springer Berlin Heidelberg.

Rockafellar, R. T. (1970, December). *Convex analysis*. Princeton University Press.

Rosenthal, F., Jung, M., Zitterbart, M., & Hanebeck, U. D. (2019). CoCPN - towards flexible and adaptive cyber-physical systems through cooperation. *Consumer Communications & Networking Conference*.

Rudin, W. (2008). *Principles of mathematical analysis* (3rd ed.). McGraw-Hill.

Rugh, W. J., & Shamma, J. S. (2000). Research on gain scheduling. *Automatica*, *36*(10), 1401–1425.

Saadabadi, H., Hespe, C., & Werner, H. (2022). Distributed event-triggered consensus with non-identical Bernoulli packet dropout. *European Control Conference*, 1818–1823.

Saadabadi, H., & Werner, H. (2021). Event-triggered ℓ2-optimal formation control for agents modeled as LPV systems. *Conference on Decision and Control*, 1256–1262.

Schenato, L. (2009). To zero or to hold control inputs with lossy links? *IEEE Transactions on Automatic Control*, *54*(5), 1093–1099.

Schenato, L., Sinopoli, B., Franceschetti, M., Poolla, K., & Sastry, S. S. (2007). Foundations of control and estimation over lossy networks. *Proceedings of the IEEE*, *95*(1), 163–187.

Scherer, C. W. (2000, January). Robust mixed control and linear parameter-varying control with full block scalings. In *Advances in linear matrix inequality methods in control* (pp. 187–207). SIAM.

Scherer, C. W. (2001). LPV control and full block multipliers. *Automatica*, *37*(3), 361–375.

Scherer, C. W. (2005). Relaxations for robust linear matrix inequality problems with verifications for exactness. *SIAM Journal on Matrix Analysis and Applications*, *27*(2), 365–395.

Scherer, C. W. (2006). LMI relaxations in robust control. *European Journal of Control*, *12*(1), 3–29.

Scherer, C. W. (2022). Dissipativity and integral quadratic constraints: Tailored computational robustness tests for complex interconnections. *IEEE Control Systems Magazine*, *42*(3), 115–139.

Scherer, C. W., Gahinet, P., & Chilali, M. (1997). Multiobjective output-feedback control via LMI optimization. *IEEE Transactions on Automatic Control*, *42*(7), 896–911.

Scherer, C. W., & Weiland, S. (2015, January). Linear matrix inequalities in control [Lecture Notes].

Schneider, D., & Frey, H. (2020). Analytical derivation of outage correlation in random media access with application to average consensus in wireless networks. *International Symposium on Personal, Indoor and Mobile Radio Communications*.

Schug, A.-K., & Werner, H. (2017). Active vibration control of an aluminum beam — an experimental testbed for distributed vs. centralized control. *Conference on Decision and Control*, 1876–1881.

Scorletti, G., & Ghaoui, L. E. (1998). Improved LMI conditions for gain scheduling and related control problems. *International Journal of Robust and Nonlinear Control*, *8*(10), 845–877.

Seiler, P. J. (2001). *Coordinated control of unmanned aerial vehicles* [Doctoral dissertation, University of California].

Seiler, P. J., & Sengupta, R. (2003). A bounded real lemma for jump systems. *IEEE Transactions on Automatic Control*, *48*(9), 1651–1654.

Seiler, P. J., & Sengupta, R. (2005). An H∞ approach to networked control. *IEEE Transactions on Automatic Control*, *50*(3), 356–364.

Sendra, S., Lloret, J., Jiménez, J. M., & Parra, L. (2016). Underwater acoustic modems. *IEEE Sensors Journal*, *16*(11), 4063–4071.

Seyboth, G. S., Dimarogonas, D. V., & Johansson, K. H. (2013). Event-based broadcasting for multi-agent average consensus. *Automatica*, *49*(1), 245–252.

Seyboth, G. S., Schmidt, G. S., & Allgöwer, F. (2012). Cooperative control of linear parameter-varying systems. *American Control Conference*, 2407–2412.

Skogestad, S., & Postlethwaite, I. (2010). *Multivariable feedback control: Analysis and design* (2nd ed.). Wiley.

Song, Y., Dong, H., Yang, T., & Fei, M. (2014). Almost sure stability of discrete-time Markov jump linear systems. *IET Control Theory & Applications*, *8*(11), 901–906.

Song, Y., Yang, J., Yang, T., & Fei, M. (2016). Almost sure stability of switching Markov jump linear systems. *IEEE Transactions on Automatic Control*, *61*(9), 2638–2643.

Spielman, D. A., & Teng, S.-H. (2007). Spectral partitioning works: Planar graphs and finite element meshes. *Linear Algebra and its Applications*, *421*(2–3), 284–305.

Steeb, W.-H. (1991). *Kronecker product of matrices and applications*. BI-Wissenschaftsverlag.

Stomberg, G., Engelmann, A., & Faulwasser, T. (2022). A compendium of optimization algorithms for distributed linear-quadratic MPC. *at - Automatisierungstechnik*, *70*(4), 317–330.

Sundararajan, A., Van Scoy, B., & Lessard, L. (2020). Analysis and design of first-order distributed optimization algorithms over time-varying graphs. *IEEE Transactions on Control of Network Systems*, *7*(4), 1597–1608.

Tabuada, P. (2007). Event-triggered real-time scheduling of stabilizing control tasks. *IEEE Transactions on Automatic Control*, *52*(9), 1680–1685.

Tahbaz-Salehi, A., & Jadbabaie, A. (2008). A necessary and sufficient condition for consensus over random networks. *IEEE Transactions on Automatic Control*, *53*(3), 791–795.

Todorov, M. G., & Fragoso, M. D. (2009). Robust stability and stabilization of discrete-time infinite Markov jump linear systems. *European Control Conference*, 3239–3244.

Todorov, M. G., & Fragoso, M. D. (2012). New results on the robustness of discrete-time Markov jump linear systems. *Conference on Decision and Control*, 1331–1336.

Tse, D., & Viswanath, P. (2005, May). *Fundamentals of wireless communication*. Cambridge University Press.

Tsitsiklis, J. N., Bertsekas, D., & Athans, M. (1986). Distributed asynchronous deterministic and stochastic gradient optimization algorithms. *IEEE Transactions on Automatic Control*, *31*(9), 803–812.

Vaideshwaran, V. (2023, December 20). *Investigations on local loss rate estimation for cooperative formation control* [research rep.]. Hamburg University of Technology [Hespe, Christian and Werner, Herbert].

Varga, A., & Hornig, R. (2008). An overview of the OMNeT++ simulation environment. *Conference on Simulation Tools and Techniques for Communications Networks and Systems*.

Veenman, J., Scherer, C. W., & Köroğlu, H. (2016). Robust stability and performance analysis based on integral quadratic constraints. *European Journal of Control*, *31*, 1–32.

Vieira, B., Severino, R., Filho, E. V., Koubaa, A., & Tovar, E. (2019). COPADRIVe - a realistic simulation framework for cooperative autonomous driving applications. *International Conference on Connected Vehicles and Expo*.

Viel, C., Kieffer, M., Piet-Lahanier, H., & Bertrand, S. (2022). Distributed event-triggered formation control for multi-agent systems in presence of packet losses. *Automatica*, *141*.

Wang, F., Wen, G., Peng, Z., Huang, T., & Yu, Y. (2021). Event-triggered consensus of general linear multiagent systems with data sampling and random packet losses. *IEEE Transactions on Systems, Man, and Cybernetics: Systems*, *51*(2), 1313–1321.

Wang, J., Duan, Z., Zhao, Y., Qin, G., & Yan, Y. (2013). H∞ and H2 control of multi-agent systems with transient performance improvement. *International Journal of Control*, *86*(12), 2131–2145.

Wu, C. W., & Chua, L. O. (1995). Synchronization in an array of linearly coupled dynamical systems. *IEEE Transactions on Circuits and Systems I: Fundamental Theory and Applications*, *42*(8), 430–447.

Wu, F., & Dong, K. (2006). Gain-scheduling control of LFT systems using parameter-dependent lyapunov functions. *Automatica*, *42*(1), 39–50.

Wu, F., Yang, X. H., Packard, A., & Becker, G. (1996). Induced L2-norm control for LPV systems with bounded parameter variation rates. *International Journal of Robust and Nonlinear Control*, *6*(9–10), 983–998.

Wu, J., & Shi, Y. (2012). Average consensus in multi-agent systems with time-varying delays and packet losses. *American Control Conference*, 1579–1584.

Xu, L., Mo, Y., & Xie, L. (2020). Distributed consensus over Markovian packet loss channels. *IEEE Transactions on Automatic Control*, *65*(1), 279–286.

Xu, L., Zheng, J., Xiao, N., & Xie, L. (2018). Mean square consensus of multi-agent systems over fading networks with directed graphs. *Automatica*, *95*, 503–510.

Zelazo, D., & Mesbahi, M. (2011). Edge agreement: Graph-theoretic performance bounds and passivity analysis. *IEEE Transactions on Automatic Control*, *56*(3), 544–555.

Zeng, Z., Wang, X., & Zheng, Z. (2015). Convergence analysis using the edge Laplacian: Robust consensus of nonlinear multi-agent systems via ISS method. *International Journal of Robust and Nonlinear Control*, *26*(5), 1051–1072.

Zhang, L., Wang, W., & Zhang, H. (2024). Mean-square consensus for heterogeneous multi-agent systems with packet losses. *IEEE Transactions on Circuits and Systems II: Express Briefs*, *71*(5), 2779–2783.

Zhang, L., Leng, Y., Chen, L., & Zhao, Y. (2011). A BRL for a class of discrete-time Markov jump linear system with piecewise-constant tps. *IFAC Proceedings Volumes*, *44*(1), 8699–8704.

Zhang, S., Li, Z., & Wang, X. (2021). Robust H2 consensus for multi-agent systems with parametric uncertainties. *IEEE Transactions on Circuits and Systems II: Express Briefs*, *68*(7), 2473–2477.

Zhang, W., Tang, Y., Huang, T., & Kurths, J. (2017). Sampled-data consensus of linear multi-agent systems with packet losses. *IEEE Transactions on Neural Networks and Learning Systems*, *28*(11), 2516–2527.

Zhang, Y., & Tian, Y.-P. (2009). Consentability and protocol design of multi-agent systems with stochastic switching topology. *Automatica*, *45*(5), 1195–1201.

Zhang, Y., & Tian, Y.-P. (2012). Maximum allowable loss probability for consensus of multi-agent systems over random weighted lossy networks. *IEEE Transactions on Automatic Control*, *57*(8), 2127–2132.

Zhao, G., & Hua, C. (2024). Hybrid event-triggered cooperative output regulation of multiagent systems with unreliable communication link. *IEEE Transactions on Cybernetics*, *54*(3), 1782–1793.

Zhao, N., Shi, P., Xing, W., & Lim, C. P. (2022). Event-triggered control for networked systems under denial of service attacks and applications. *IEEE Transactions on Circuits and Systems I: Regular Papers*, *69*(2), 811–820.

Zheng, J., Xu, L., Xie, L., & You, K. (2019). Consensusability of discrete-time multiagent systems with communication delay and packet dropouts. *IEEE Transactions on Automatic Control*, *64*(3), 1185–1192.

Zhou, K., Doyle, J. C., & Glover, K. (1996). *Robust and optimal control* (J. C. Doyle, Ed.). Prentice Hall.

Symbols and Acronyms

Acronyms

BRL	Bounded real Lemma
CPN	Cyber-physical network
ETC	Event-triggered control
FBSP	Full block S-procedure
IS	Interconnected system
LFT	Linear fractional transformation
LMI	Linear matrix inequality
LPV	Linear parameter-varying
LTI	Linear time-invariant
MAS	Multiagent system
MJLS	Markov jump linear system
SDP	Semidefinite program
SINR	Signal-to-interference-plus-noise ratio
TPM	Transition probability matrix

Sets and Spaces

$\mathbb{N}$	Set of natural numbers
$\mathbb{N}_0$	Set of natural numbers including 0
$\mathbb{R}$, $\mathbb{R}^n$, $\mathbb{R}^{n\times m}$	Set of real numbers
$\mathcal{M}_1 \subset \mathcal{M}_2$	$\mathcal{M}_1$ is proper subset of $\mathcal{M}_2$
$\mathcal{M}_1 \subseteq \mathcal{M}_2$	$\mathcal{M}_1$ is non-strict subset of $\mathcal{M}_2$
$\lvert\mathcal{M}\rvert$	Cardinality of the set $\mathcal{M}$
$\mathbb{1}_{\mathcal{M}}(x)$	Set-membership indicator function for the set $\mathcal{M}$
$\mathcal{S}_d$	Unit d-simplex
$\mathcal{M}_1 \times \mathcal{M}_2$	Cartesian set product
aff $\mathcal{M}$	Affine hull of the set $\mathcal{M}$
conv $\mathcal{M}$	Convex hull of the set $\mathcal{M}$
ri $\mathcal{M}$	Relative interior of the set $\mathcal{M}$
$\mu(\mathcal{M})$	Set of extreme points for convex sets $\mathcal{M}$

Linear Algebra

$\lvert x\rvert$	Absolute value
$\lVert x\rVert$	Vector 2-norm
$\lVert M\rVert$	Induced matrix 2-norm, spectral norm
$M^\top, M^{-1}, M^{-\top}$	Matrix transpose, inverse, and inverse transpose
$M \succ 0, M \succeq 0$	Positive (semi-)definite matrix
$M \prec 0, M \preceq 0$	Negative (semi-)definite matrix
$M_1 \otimes M_2$	Kronecker matrix product
$M_1 \circ M_2$	Hadamard matrix product
I_n	$n \times n$ identity matrix
$\mathbf{1}_n$	n-dimensional vector of all ones
Π	Projection onto the disagreement space
$\lambda_i(M)$	ith eigenvalue of matrix M
$\det M$	Determinant of matrix M
$\operatorname{tr} M$	Trace of matrix M
$\operatorname{diag}(x_1, \dots, x_n)$	Diagonal (block-)concatenation of scalars or matrices
$M_{(d)}$	Kronecker dimension matching, $M_{(d)} \coloneqq M \otimes I_d$

Systems and Signals

k	Discrete time index
t, k_t	Trigger index, trigger instants
T	Open-loop system
$\mathcal{T}$	Closed-loop system
$\bar{\mathcal{T}}$	Mean system
$\mathcal{T}^*$	Adjoint system
K	Controller, static or dynamic
$V(\xi)$	Lyapunov, storage function candidate, $\mathbb{R}^{n_\xi} \to \mathbb{R}$
A, B, C, D	Open-loop state-space matrices
$\mathcal{A}, \mathcal{B}, \mathcal{C}, \mathcal{D}$	Closed-loop state-space matrices
S^0, S_i	Generic pattern matrices
x_k, ξ_k	Open-loop, closed-loop system state
η_k	Controller state
v_k	Exogenous switching signal
u_k, y_k	Controlled input, measured output signal
w_k, z_k	Performance input, output
δ_k	Discrete unit impulse
e_k	Trigger error
Ω	Trigger weighting matrix
$\lVert z\rVert_{\ell_2}$	Stochastic signal ℓ_2-norm
$\lVert\mathcal{T}\rVert_{H_2}$	H_2-Norm of system $\mathcal{T}$
$\lVert\mathcal{T}\rVert_{H_\infty}$	H_∞-Norm of system $\mathcal{T}$

Graph Theory

$\mathcal{G}, \mathcal{G}^0$	Graph with $\mathcal{G} = (\mathcal{V}, \mathcal{E})$, nominal graph
$\mathcal{G}_N^\circ, \mathcal{G}_h^\triangle$	Circular and triangular lattice graphs
$\mathcal{G}^\top$	Transposed graph, inverted edge directions
$\mathcal{V}$	Vertex set $\mathcal{V} = \{1, 2, \dots, N\}$
$\mathcal{E}, \mathcal{E}^0$	Edge set with $\mathcal{E} \subset \mathcal{V} \times \mathcal{V}$, nominal edge set
N	Number of vertices $N \coloneqq \lvert\mathcal{V}\rvert$
m	Number of edges $m \coloneqq \lvert\mathcal{E}\rvert$
$\mathcal{N}_i^-$	In-neighbourhood of vertex i
$\mathcal{N}_i^+$	Out-neighbourhood of vertex i
d_i^-	In-degree of vertex i, $d_i^- \coloneqq \lvert\mathcal{N}_i^-\rvert$
d_i^+	Out-degree of vertex i, $d_i^+ \coloneqq \lvert\mathcal{N}_i^+\rvert$
$L(\mathcal{G}), L^0, L_i$	Laplacian of graph $\mathcal{G}$, nominal Laplacian, switched Laplacian
$\Psi(\mathcal{G})$	Incidence matrix of graph $\mathcal{G}$
$\alpha(i,j)$	Enumeration function, $\mathcal{E}^0 \to \mathbb{N}$
$\beta(n,i)$	Function to extract ith binary digit of n, $\mathbb{N}_0 \times \mathbb{N} \to \{0,1\}$
$\{\phi_k^{ij}\}$	Binary loss process for edge $(i,j) \in \mathcal{E}^0$
$\{\Phi_k\}$	Diagonal concatenation of edge processes, $\Phi_k \coloneqq \operatorname{diag}\left(\phi_k^{ij}\right)$

Probability Theory

$\mathbb{P}$	Probability measure
$\mathbb{E}[X]$	Expectation of the random variable X
$\operatorname{Var}[X]$	Element-wise variance of the random variable X
$\Xi_Q[X]$	Generalized weighted variance of the random matrix X
$\{\sigma_k\}$	Switching process, Markov chain
$\mathcal{K}$	Markov chain state space
Θ	Transition probability matrix
θ_{ij}	Transition probability from mode i to mode j
t_i	Initial distribution of the Markov chain $\{\sigma_k\}$

Robust Analysis and Multipliers

$P \in \mathcal{P}_d$	FBSP multiplier and its associated multiplier set
$\Delta \in \boldsymbol{\Delta}$	Edge-based uncertainty and its associated uncertainty set
$f(p)$	Joint probability distribution map, $[0,1]^m \to \mathcal{S}_{2^m-1}$
$\boldsymbol{\theta}, \hat{\boldsymbol{\theta}}_d$	Sets of uncertain probability vectors
$\boldsymbol{\Theta}, \hat{\boldsymbol{\Theta}}_d$	Sets of uncertain transition probability matrices
$\mathbb{T}_d$	Set of all transition probability matrices

Sub- and Superscripts

$_K$	Controller variable
$_{cg}$	Centre of gravity component of concatenated vector
$_\delta$	Disagreement component of concatenated vector
$_d$	Decoupled component of a matrix or system
$_c$	Stochastically coupled component of a matrix or system
$_p$	Deterministically coupled component of a matrix or system
$_l$	Lower bound
$_u$	Upper bound